Universidade de Aveiro
2014
Departamento de Química

Sandra Maria Semedo Carvalho Freire

Caracterização da matéria orgânica solúvel em água de aerossóis urbanos

Characterization of water-soluble organic matter from urban aerosols

DOCUMENTO PROVISÓRIO

Universidade de Aveiro
2014

Departamento de Química

Sandra Maria Semedo Carvalho Freire

Caracterização da matéria orgânica solúvel em água de aerossóis urbanos

Characterization of water-soluble organic matter from urban aerosols

Tese apresentada à Universidade de Aveiro para cumprimento dos requisitos necessários à obtenção do grau de Doutor em Química, realizada sob a orientação científica do Doutor Armando da Costa Duarte, Professor Catedrático do Departamento de Química da Universidade de Aveiro, e da Doutora Regina Maria Brandão de Oliveira Duarte, Investigadora Auxiliar do Centro de Estudos do Ambiente e do Mar (CESAM) da Universidade de Aveiro.

Apoio Financeiro do

Instituto Português de Apoio

ao Desenvolvimento (IPAD)

Ao meu filho Rúben,

Aos meus Pais e Irmãos

o júri

presidente

Doutor Carlos Manuel Martins da Costa
professor catedrático do Departamento de Economia, Gestão e Engenharia Industrial da Universidade de Aveiro

Doutor Armando da Costa Duarte
professor catedrático do Departamento de Química da Universidade de Aveiro

Doutora Maria Isabel Almeida Ferra
professora catedrática do Departamento de Química da Faculdade de Ciências da Universidade da Beira Interior

Doutora Maria Eduarda da Cunha Pereira
professora associada do Departamento de Química da Universidade de Aveiro

Doutora Teresa Alexandra Peixoto da Rocha-Santos
professora associada do Instituto Superior de Estudos Interculturais e Transdisciplinares (ISEIT) de Viseu, Instituto Piaget

Doutor Carlos Manuel de Melo Pereira
professor auxiliar com agregação do Departamento de Química e Bioquímica da Faculdade de Ciências da Universidade do Porto

agradecimentos

Meus sinceros agradecimentos a todas as pessoas que contribuíram para a realização deste trabalho:

Ao Prof. Doutor Armando da Costa Duarte quero manifestar o meu agradecimento pelo incentivo, e pelo empenho demonstrados ao longo do desenvolvimento deste trabalho, agradeço a amizade e compreensão reflectidas na sua preocupação para com o meu bem-estar nos momentos mais delicados deste processo.

À Doutora Regina Maria Brandão de Oliveira Duarte quero expressar a minha admiração pelas suas qualidades científicas, pelo seu profissionalismo, pela seriedade e por todo o tempo dedicado no processo de realização desta tese. O seu entusiasmo por esta pesquisa foi contagiante e deu-me a inspiração para continuar.

Aos meus colegas e amigos de trabalho, Patrícia Santos, Patrícia Silva, Pedro Pato, Cláudia Lopes, Cláudia Mieiro, Pedro Coelho, Ana Teresa, Luciana, António, Bruno, João Matos e Andreia Paula, meus agradecimentos pela agradável convivência e amizade.

Um agradecimento especial à Anabela e à Celine pelo seu companheirismo; pelo acolhimento, pela simpatia e pelo carinho demonstrados ao longo destes anos.

À Universidade de Aveiro, agradeço igualmente o acolhimento e as condições disponibilizadas para a concretização desta tese.

Ao IPAD meus agradecimentos pelo apoio financeiro através da concessão de uma bolsa de Doutoramento, que possibilitou as despesas inerentes ao processo de investigação. Ainda, à Fundação Portuguesa para a Ciência e Tecnologia (FCT) através do projeto ORGANOSOL (FCOMP-01-0124-FEDER-019913; PTDC/CTE-ATM/118551/2010) e ao Centro de Estudos do Ambiente e do Mar (CESAM, Universidade de Aveiro, Portugal), meus agradecimentos pelo apoio financeiro.

Ao Djoy, João, Mário e à Dos Anjos pelo incentivo à realização deste trabalho, e ainda pelo companheirismo demonstrado durante o período deste estudo.

Agradeço a estes e a todos os meus amigos que estiveram sempre presentes e que com as suas palavras de apoio encorajaram-me a continuar.

Aos meus pais e irmãos, meu porto seguro, quero aqui expressar o meu profundo reconhecimento pelo amor e pelo apoio incondicional e por toda a paciência e compreensão nestes anos de ausência.

Ao Ruben, meu filho querido, agradeço a sua existência, agradeço os momentos em que, mesmo à distância a sua meiga voz deu-me mais coragem e vontade de lutar. E peço-te desculpas, meu amor, pela minha ausência em momentos que foram tão especiais para nós.

À Universidade de Cabo Verde, os meus agradecimentos pelas autorizações de dispensa de trabalho concedidas durante a realização do meu Doutoramento.

palavras-chave

Aerossóis atmosféricos, área urbana, material carbonáceo, matéria orgânica solúvel em água, composição elementar, caracterização estrutural, espectroscopia, cromatografia líquida bidimensional abrangente.

resumo

A matéria orgânica solúvel em água (MOSA) de aerossóis atmosféricos é composta por um conjunto complexo de estruturas moleculares que influenciam as propriedades físico-químicas das partículas atmosféricas e, por conseguinte, desempenham um importante papel em diversos processos atmosféricos globalmente relevantes, afectando o clima e a saúde pública. Devido a uma ampla variedade de fontes e processos de formação, é ainda escasso o conhecimento acerca da composição estrutural da MOSA e do respectivo efeito nas propriedades dos aerossóis atmosféricos.

Assim, esta tese pretende fornecer novas perspetivas sobre a composição molecular da MOSA presente na fracção fina de partículas atmosféricas características de uma área urbana (Aveiro, Portugal). Para o efeito, numa primeira fase do trabalho, foi avaliada a ocorrência de eventuais fenómenos de adsorção de compostos orgânicos semi-voláteis nos filtros de fibra de quartzo utilizados na colheita das amostras de partículas atmosféricas. Posteriormente, e na mesma área urbana, foi efectuada a colheita de amostras de aerossóis atmosféricos, durante um período de 15 meses, numa base de amostragem semanal e em contínuo. Foram efectuados balanços mássicos que permitiram descrever a importância das fracções de carbono elementar, MOSA e matéria orgânica insolúvel em água, na massa total de aerossóis atmosféricos recolhidos na zona urbana de Aveiro, tendo-se dado especial relevo ao estudo dos efeitos de diferentes condições meteorológicas.

Na tentativa de entender a complexidade da MOSA de aerossóis urbanos, foram efectuados estudos de caracterização estrutural com recurso às espectroscopias de infravermelho com transformadas de Fourier (FTIR) acoplada a um sistema de reflectância total atenuada (ATR, sigla inglesa de *Attenuated Total Reflectance*) (FTIR-ATR) e de ressonância magnética nuclear de ^{13}C com polarização cruzada (CP, sigla inglesa de *Cross Polarization*) e rotação em torno do ângulo mágico (MAS, sigla inglesa de *Magic Angle Spinning*) (RMN CPMAS de ^{13}C) de estado sólido, mas também através da avaliação da respectiva composição elementar. A caracterização estrutural da MOSA dos aerossóis recolhidos na zona urbana confirmou o carácter heterogéneo deste tipo de matéria orgânica, traduzido por uma multiplicidade de grupos funcionais. De um modo geral, foi possível concluir que as estruturas alifáticas, as estruturas aromáticas, os grupos hidroxilo e os grupos carboxilo constituem funcionalidades comuns às amostras estudadas. A avaliação semi-quantitativa dos dados de RMN CPMAS de ^{13}C mostrou igualmente diferentes distribuições dos diversos grupos funcionais, entre as amostras de aerossóis colhidos em diferentes períodos sazonais. A presença de sinais típicos de estruturas derivadas de lignina nos espectros de RMN CPMAS de ^{13}C e FTIR-ATR das amostras de MOSA típicas de estações sazonais mais frias sugere

que as propriedades de MOSA de partículas atmosféricas são influenciadas pelos processos de queima da madeira para aquecimento doméstico.

Complementarmente às técnicas espectroscópicas anteriormente referidas, foi também utilizada a técnica de cromatografia líquida bidimensional abrangente (LC x LC) acoplada aos detectors de fotodíodos, fluorescência e evaporativo com dispersão de luz, com o objectivo de resolver a heterogeneidade das amostras de MOSA e, simultaneamente, mapear a hidrofobicidade *versus* distribuição de tamanhos moleculares das amostras. A utilização de uma coluna de cromatografia de interacção hidrofílica operada sob condições de fase reversa na primeira dimensão e de uma coluna de cromatografia de exclusão por tamanhos na segunda dimensão, revelou-se muito útil para a separação das amostras de MOSA em frações com hidrofobicidades e tamanhos moleculares distintos. A distribuição de massa molar média (Mw) obtida neste estudo variou entre 48 e 942 Da e 45 a 1241 Da, em termos de detecção por UV e fluorescência, respectivamente. Os resultados obtidos sugerem ainda que as fracções com menor valor de Mw tendem a ter um carácter relativamente mais hidrofóbico.

keywords

Atmospheric aerosols, urban area, carbonaceous materials, water-soluble organic matter, elemental composition, structural characterization, spectroscopy, comprehensive two-dimensional liquid chromatography.

abstract

Water-soluble organic matter (WSOM) from atmospheric particles comprises a complex array of molecular structures that play an important role on the physic-chemical properties of atmospheric particles and, therefore, are linked to several global-relevant atmospheric processes which impact the climate and public health. Due to the large variety of sources and formation processes, adequate knowledge on WSOM composition and its effects on the properties of atmospheric aerosol are still limited.

Therefore, this thesis aims at providing new insights on the molecular composition of WSOM from fine atmospheric aerosols typical of an urban area (Aveiro, Portugal). In a first step, adsorption phenomena of semi-volatile organic compounds on quartz fibre filters employed in the collection of atmospheric aerosols were assessed. Afterwards, atmospheric aerosol samples were collected during fifteen months, on a weekly basis. A mass balance of aerosol samples was performed in order to set the relative contribution of elemental carbon, WSOM and water-insoluble organic matter to the aerosol mass collected at the urban area of Aveiro, with a special focus on the assessment of the influence of different meteorological conditions.

In order to assess the chemical complexity of the WSOM from urban aerosols, their structural characteristics were studied by means of Fourier transform infrared infrared - Attenuated Total Reflectance (FTIR-ATR) and solid-state cross polarization with magic angle spinning ^{13}C nuclear magnetic resonance (CPMAS ^{13}C NMR) spectroscopies, as well as their elemental composition. The structural characterization of aerosol WSOM samples collected in the urban area highlighted a highly complex mixture of functional groups. It was concluded that aliphatic and aromatic structures, hydroxyl groups and carboxyl groups are characteristic to all samples. The semi-quantitative assessment of the CPMAS ^{13}C NMR data showed different distributions of the various functional groups between the aerosol samples collected at different seasons. Moreover, the presence of signals typical of lignin-derived structures in both CPMAS ^{13}C NMR and FTIR-ATR spectra of the WSOM samples from the colder seasons, highlights the major contribution of biomass burning processes in domestic fireplaces, during low temperature conditions, into the bulk chemical properties of WSOM from urban aerosols.

A comprehensive two-dimensional liquid chromatography (LC x LC) method, on-line coupled to a diode array, fluorescence, and evaporative light scattering detectors, was employed for resolving the chemical heterogeneity of the aerosol WSOM samples and, simultaneously, to map the hydrophobicity *versus* the molecular weight distribution of the samples. The LC x LC method employed a mixed-mode hydrophilic interaction

column operating under aqueous reversed phase mode in the first dimension, and a size-exclusion column in the second dimension, which was found to be useful for separating the aerosol WSOM samples into various fractions with distinct molecular weight and hydrophobic features. The estimative of the average molecular weight (Mw) distribution of the urban aerosol WSOM samples ranged from 48 to 942 Da and from 45 to 1241 Da in terms of UV absorption and fluorescence detection, respectively. Findings suggest that smaller Mw group fractions seem to be related to a more hydrophobic nature.

Table of contents

List of tables

List of figures

List of abbreviations

ACN	Acetonitrile
CCN	Cloud condensation nuclei
CPMAS ^{13}C NMR	Cross polarization with magic angle spinning ^{13}C nuclear magnetic resonance
DAD	Diode array detector
ELSD	Evaporative light scattering detector
EC	Elemental carbon
EEM	Excitation-emission matrix
FLD	Fluorescence detector
FTIR-ATR	Fourier transformed infrared - attenuated total reflectance
HILIC	Hydrophilic interaction liquid chromatography
IEC	Ion-exchange chromatography
LC	Liquid chromatography
LC x LC	Comprehensive two-dimensional liquid chromatography
MeOH	Methanol
Mn	Number average molecular weight
MW	Molecular weight
Mw	Weight average molecular weight
NP	Normal phase
NDIR	Non-dispersive infrared
NPOC	Non-purgeable organic carbon
NMR	Nuclear magnetic resonance
OA	Organic aerosol
OC	Organic carbon
OM	Organic matter
PALC	Per aqueous liquid chromatography

PC	Pyrolytic carbon
$PM_{2.5}$	Particulate matter with aerodynamic diameter less than 2.5 μm
$PM_{2.5-10}$	Particulate matter with aerodynamic diameter between 2.5 and 10 μm
RH	Relative humidity
RP	Reversed phase
SEC	Size-exclusion chromatography
SOA	Secondary organic aerosol
SVOC	Semi-volatile organic carbon
TC	Total carbon
UV-Vis	Ultraviolet-Visible
VOC	Volatile organic carbon
WINSOC	Water-insoluble organic carbon
WSOC	Water-soluble organic carbon
WINSOM	Water-insoluble organic matter
WSOM	Water-soluble organic matter
1^{st} dimension	First dimension
2^{nd} dimension	Second dimension
1D-LC	One-dimensional liquid chromatography

I

Objectives & thesis outline

1.1. Introduction

Atmospheric aerosols were defined by Seinfeld and Pandis (2006) as solid or liquid particles suspended in the air, comprising a myriad of sizes, ranging from a few nanometers to several tens of micrometers. Depending on the nature and location of their sources, these atmospheric particles vary in terms of chemical composition and physical properties, as well as in terms of spatial and temporal distribution (Poschl, 2005; Seinfeld and Pandis, 2006). Atmospheric aerosols are typically classified into three categories: ultrafine mode (aerodynamic diameter (d_{ae}) less than 0.1 micrometers, $d_{ae} < 0.1$ μm, designated as $PM_{0.1}$), fine mode ($d_{ae} < 2.5$ μm, designated as $PM_{2.5}$), and coarse mode ($2.5 < d_{ae} < 10$μm, designated as $PM_{2.5-10}$) (Seinfeld and Pandis, 2006). This division is very advantageous since fractions of different d_{ae} in general have distinct origins, chemical and physical properties (Jacobson et al., 2000). The nucleation of gas molecules produces ultrafine particles, which grow rapidly to the fine particle size range by condensation of precursor gases and by coagulation. These fine airborne particles can further undergo chemical and physical aging in the atmosphere (e.g., gas uptake or chemical reactions), thus changing their size, structure, and composition. These ultrafine and fine particles have both anthropogenic and natural origin and their atmospheric lifetime is days to weeks. $PM_{2.5-10}$, on the other hand, is derived mainly from wind-driven or traffic-related suspension of road, soil, and mineral dust, sea salt, and biological materials (e.g. plant fragments, microorganisms, pollen). As such, their atmospheric lifetime range from minutes to hours . The $PM_{2.5}$ fraction has been related to adverse effects on human health (namely, some respiratory and cardiovascular diseases) as well as on climate (Poschl, 2005) and, therefore, has been the focus of major scientific and policy concern during the last two decades.

Atmospheric aerosol particles are composed of a complex mixture of water-soluble inorganic salts, insoluble mineral dust, and a highly variable fraction of carbonaceous material having both primary and secondary origin (Seinfeld and Pandis, 2006). This carbonaceous component is predominantly found in the fine size mode and has been usually classified as: inorganic carbon (IC), elemental carbon (EC) and organic carbon (OC) (Seinfeld and Pandis, 2006). The IC fraction typically consists of mineral carbonates

and it is derived almost exclusively from soil dust (Seinfeld and Pankow, 2003). The EC fraction is directly emitted into the atmosphere as a result of incomplete combustion of fossil fuels and burning biomass, thus having a predominantly primary origin (Seinfeld and Pandis, 2006). From a chemical and morphological point of view, the EC fraction can be pictured as more or less disordered stacks of graphene layers or large polycyclic aromatics with a surface coverage by oxygen-containing functional groups and nitrogen species (Smith and Chughtai, 1995; Gelencser, 2004). The OC component contributes to 10% to 70% of the total mass of dry fine particles (Turpin et al., 2000) and it is composed of thousands of organic compounds, ranging from low molecular-weight compounds (e.g. malonic and oxalic acids) (Sempére and Kawamura, 1994) to *n*-alkanes, polycyclic aromatic hydrocarbons, terpens, carbonyls, and n-alkanols (Alves et al., 2002). Several studies (Facchini et al., 1999; Zappoli et al., 1999; Decesari et al., 2001; Sullivan et al., 2004; Duarte et al., 2007; Timonen et al., 2008) have further demonstrated that an important fraction of the OC component in atmospheric aerosols is water-soluble. Studies performed in both urban (Decesari et al., 2001; Kim et al., 2011) and rural (Duarte et al., 2007) locations have shown that the water-soluble organic carbon (WSOC) typically ranged from 35 to 55% of the OC fraction in fine atmospheric aerosols.

WSOC concentrations in fine atmospheric aerosols from urban areas or from places impacted with biomass burning can reach relatively high values (e.g., 10–15 μg C m^{-3} (Jaffrezo et al., 2005) or 46 μg C m^{-3} (Mayol-Bracero et al., 2002), respectively), whereas in rural areas they can be as low as 5 μg C m^{-3} (Duarte et al., 2007). In marine environments, WSOC concentrations can reach up to 0.2 μg C m^{-3} (Yoon et al., 2007). This wide range of atmospheric concentration values reflects the relative importance of primary emissions and/or secondary organic aerosol formation at the different locations. Duarte et al. (2007) have also shown that the concentrations of WSOC follow a seasonal trend, with maximum values during Autumn, Autumn/Winter and Winter (colder seasons), and minimum concentrations during warmer periods. The water-soluble organic matter (WSOM) comprises a complex mixture likely composed of aliphatic structures, oxygenated alkyls, carboxylic acids and aromatic structures (Decesari et al., 2000; Duarte et al., 2005, 2007; Sannigrahi et al., 2006), and contributes up to 10-42% of the total fine aerosol mass (Duarte, 2006; Sun et al., 2011).

Due to the large variety of sources and formation processes, adequate knowledge on WSOM composition and its effects on the properties of atmospheric aerosol are still limited. The traditional approach of compound speciation by gas and liquid chromatography coupled to mass spectrometry (GC-MS and LC-MS) provided a long list of individual organic compounds, which accounts for less than 11% (Graham et al., 2002; Mayol-Bracero et al., 2002; Decesari et al., 2006) and 14% (Yang et al., 2004) of total WSOC, respectively. These results suggest that further research is needed focusing on the detailed characterization of the chemical features (e.g. elemental composition, functional groups, and fingerprinting) of the bulk WSOM from atmospheric aerosols through a multidimensional approach based on the synergistic application of advanced analytical techniques.

1.2. Objectives of the thesis

Taking into account the current state of the art, this PhD project was designed with the purpose of acquiring new and in-depth knowledge on the carbon chemical environments of the WSOM from $PM_{2.5}$ in an urban area. To accomplish this main goal, aerosol samples collected at Aveiro (Portugal) during fifteen months, between November 2009 and March 2011, will be the basis for the investigation.

The specific objectives of this thesis are:

1. To achieve a global carbon balance (organic carbon (OC) vs. elemental carbon (EC) vs. water-soluble organic carbon (WSOC)) and a mass closure for the whole mass of fine aerosol collected, and infer on their seasonal variability;
2. To assess the structural features of WSOM in fine air particles at an urban location, focusing on their seasonality;
3. To identify fingerprints of possible aerosol emission sources in the integral structural features of the WSOM;
4. To infer on the contribution of primary and secondary sources to fine particulate OM through full functional group analysis, and relevant meteorological parameters.

It must also be emphasized that atmospheric aerosol sampling employing quartz fibre filters in high-volume samplers, as performed in this study, are prone to adsorption – positive bias and overestimation of OC content – or evaporation – negative bias and underestimation of OC content – of semi-volatile organic carbon (SVOC). As such, the first task of this research work encompassed the assessment of such phenomena and the identification of the main limitations of such widely employed methodology.

The structural characterization of the fine urban aerosol WSOM samples was accomplished by means of UV-Vis, Fourier transformed infrared - attenuated total reflectance (FTIR-ATR), excitation-emission matrix (EEM) fluorescence, and solid-state cross-polarization with magic angle spinning ^{13}C nuclear magnetic resonance (CPMAS ^{13}C NMR) spectroscopies. Moreover, a comprehensive two-dimensional liquid chromatography (LC x LC) technique, employing two independent separation mechanisms (per-aqueous liquid chromatography (PALC) and size exclusion chromatography (SEC)), was applied for mapping the hydrophobic character *versus* molecular weight (MW) distribution of aerosol WSOM and, simultaneously, offering a new perspective on the structural heterogeneity of this complex organic aerosol component.

1.3. Structure of the thesis

This thesis is organized into seven chapters, structured as follows:

- Chapter I includes a general description of the thesis and a contextualization of the scientific relevance and specific objectives of the research work.
- Chapter II reviews the atmospheric importance of WSOM, its sources and formation mechanisms, including also the likely trend to achieve a detailed chemical characterization of WSOM from atmospheric aerosols.
- Chapter III presents a description of the materials and experimental methods employed in this research work, from sample collection to the analytical procedures for structural characterization of the collected WSOM samples.
- Chapter IV describes the assessment of the annual ambient concentrations of $PM_{2.5}$ and $PM_{2.5-10}$, and their TC, OC, EC, and WSOC contents. A global mass balance for the fine

atmospheric aerosol samples is also presented. This chapter also addresses the procedure adopted to acquire a representative WSOM sample of the different seasonal periods, including also the isolation/fractionation procedure employed to obtain a WSOM fraction amenable to further spectroscopic analysis. This chapter also presents the results of the SVOC adsorption assessment during the aerosol sampling procedure.

- Chapter V presents and discusses the results of the structural characterization of WSOM from the fine atmospheric aerosols collected in the urban area, focusing on the influence of different meteorological conditions on their structural composition.
- Chapter VI describes the application of LC x LC technique (namely, PALC x SEC) for: (i) resolving the chemical heterogeneity of the WSOM samples; (ii) determining how size-distinguished fractions differ in hydrophobicity; and (3) assessing the MW properties of the studied WSOM samples in regard to number (Mn) and weight (Mw) average MW, and polydispersity (Mw/Mn).
- Chapter VII highlights the main contributions of this research work to the structural characterization of fine urban aerosol WSOM, and outlines a roadmap for future studies built upon the work developed in this thesis in order to achieve a detailed structural and molecular characterization of the complex aerosol WSOM.

II

Water-soluble organic matter from atmospheric aerosols: current state of the art

2.1. Importance of WSOM in atmospheric aerosols

WSOM is a ubiquitous constituent of atmospheric particles and its contribution to particulate organics in the atmosphere range from 10 to 80% (Duarte and Duarte, 2011a). Currently, it is recognized the important role played by WSOM on the hygroscopic properties of aerosols (Dinar et al., 2007), surface- tension behavior (Salma et al., 2006) and effective density (Dinar et al., 2006) of atmospheric particles and, thus, on the processes of droplets and cloud formation. As such, WSOM can be an important contributor to the indirect effects of aerosols over the Earth's radiative balance (Facchini et al., 1999; IPCC, 2001; Gysel et al., 2004; Mladenov et al., 2010). Supporting this assumption some studies can be cited: Gysel et al. (2004) have measured the hygroscopic properties of the less hydrophilic fraction of WSOM to model the hygroscopic growth and the authors observed that at 90% relative humidity, 20 to 38 % of particulate water in the samples is associated to WSOM. Chan et al. (2005) demonstrated that some amines (namely glycine, alanine, and asparagines) and other organic species (such as levoglucosan, mannosan, and galactosan) originated from biomass burning could participate in liquid droplet formation since they can retain water at low relative air humidity. Using two different aerosol chemical compositions (the classical inorganic case, and the inorganic plus organic case), Mircea et al. (2002) concluded that the cloud condensation nuclei (CCN) number concentration depends not only on the percentage of WSOC, but also on the type of inorganic constituents. Asa-Awuku et al. (2008) also characterized the CCN activity of water-soluble organics in biomass burning aerosol. The authors concluded that the presence of salts, primarily $(NH_4)_2SO_4$, improved substantially the surface tension decreasing of the most hydrophobic constituents of the WSOC, and their synergistic effects considerably enhance CNN activity, exceeding that of the pure inorganic salt. Therefore, increasing the CCN concentrations will result in increased cloud drop concentrations, smaller drop radii, and more reflective clouds, a phenomenon generally referred to as the "first indirect effect" (Kanakidou et al., 2005). On the other hand, a decrease in cloud drop effective radius may lead to lower coalescence rates and, therefore, reduced precipitation and a longer cloud lifetime, a phenomenon usually referred to as the "second indirect effect" of atmospheric aerosol (Kanakidou et al., 2005). In either

case, it is clear that clouds can significantly impact the amount of solar radiation absorbed by the planet, and thus affect climate.

Atmospheric aerosols, including their water-soluble and water-insoluble organic and inorganic fractions, can also influence Earth's radiative balance directly by scattering and absorbing the incoming solar radiation. By intercepting incoming solar radiation, aerosols reduce the energy flux arriving at the Earth's surface, thus producing a cooling effect (Charlson et al., 1992). On the other hand, aerosols containing black graphitic and tarry carbon strongly absorb incoming sunlight. The effect of this type of aerosol are twofold, both warming the atmosphere and cooling the surface, thus reducing the atmosphere's vertical temperature gradient and causing a decline in evaporation and cloud formation (Kaufman et al., 2002). In the particular case of the WSOM fraction, Hoffer et al. (2006) investigated the optical properties of WSOM from biomass burning aerosols and concluded that the relative contribution of WSOM to light absorption in the entire solar spectrum was of about 7 %. The results of Hoffer et al. (2006) suggest that aerosol WSOM could have an active, yet highly uncertain, role in the radiative transfer and in photochemical processes occurring in the atmosphere. To this uncertainty it highly contributes the lack of adequate knowledge on the chemical composition of aerosol WSOM, the individual effects of WSOM constituents into the radiative process (absorption and/or scattering of solar radiation), their emission sources (natural and anthropogenic), and the synergistic effects resulting from the interactions between the organic and inorganic fractions and their location (inside or at the surface) in the scattering aerosol particle.

2.2. Sources and formation mechanisms of WSOM in atmospheric aerosols

Although the detailed structural characterization of the WSOM in atmospheric particles is a focus of major scientific concern, its sources and mechanisms of formation is another emerging issue, for which the atmospheric research community has only qualitative but not sufficient understanding.

Some authors have postulated that WSOM components may be derived primarily from biomass combustion (Facchini et al., 1999; Zappoli et al., 1999; Mayol-Bracero et al., 2002; Duarte et al., 2007). Mayol-Bracero et al. (2002) have anticipated different mechanistic pathways for the formation of WSOM during biomass combustion, including: (a) soil-derived and/or decaying leaf litter humic matter lofted during combustion, (b) WSOM generation through chemical transformations of the biomass fuel and/or the initial volatile combustion products, as well as thermal breakdown of plant lignins and cellulose, and (c) recombination and condensation reactions of volatile, low molecular weight, primary products of combustion (Mayol-Bracero et al., 2002). Another potential origin of WSOM in aerosols includes primary marine sources. Bubble bursting at the ocean surface has been suggested as a possible mechanistic pathway for the presence of WSOM in marine aerosols ((Graber and Rudich, 2006) and references therein).

Secondary organic aerosol (SOA) formation may also be a major contributor to the presence of water-soluble organic species in air particles (Graham et al., 2002; Decesari et al., 2006; Miyazaki et al., 2006; Duarte et al., 2007; Kondo et al., 2007; Weber et al., 2007; Saarikoski et al., 2008; Snyder et al., 2009). For example, Saarikoski et al. (2008) reported for PM_1 samples, collected at an urban background site during Summer that, on average, 78% of the SOA is water-soluble. Indeed, SOA formation in the atmosphere has been the subject of several studies and, according to the critical review of Fuzzi et al. (2006), different mechanistic pathways for the SOA formation can be put forward: i) partitioning of semi-volatile organic compounds (SVOC) from the gas phase into/onto pre-existing particles; ii) participation of SVOC in the formation of new particles (nucleation); and iii) formation of low- or non-volatile organic compounds by heterogeneous or multiphase reactions of VOC or SVOC on the surface or in the bulk of aerosol and cloud particle (atmospheric evolution). The typical SOA formation mechanisms are illustrated in Fig. II-1.

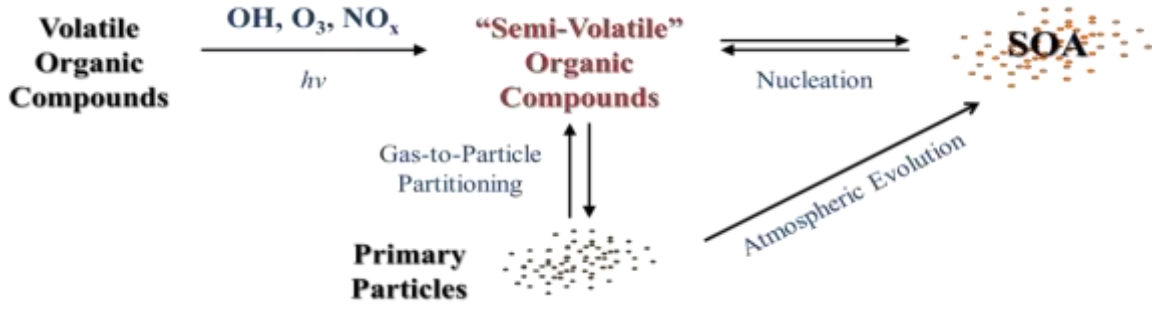

Fig. II-1. Pathways for SOA formation in the atmosphere (adapted from Seinfeld and Pankow (2003)).

The SOA formation by means of a nucleation pathway occurs when VOCs, with both an anthropogenic and natural origin, are oxidized in the atmosphere to form products (e.g. polar organic molecules) with lower volatility (SVOCs), which are distributed between the particulate and the gas phase (Seinfeld and Pankow, 2003). The SVOCs so formed can condense onto particles already existing in the atmosphere, or they can form new particles by nucleation. A number of laboratory studies have further suggested the formation of SOA through photochemical and oxidative processes. For example, SOA formation from biogenic hydrocarbons through oxidation with hydrogen peroxide under acidic conditions, and/or through photo-oxidation of biogenic isoprene has been suggested by Claeys et al. (2004a) and (2004b), respectively. Indeed, isoprene and monoterpenes emissions from biogenic sources are considered to be the mainly contributors to SOA formation due to their high emission rates from forest vegetations (annual global emission of about 500 Tg) (Claeys et al., 2004a). Limbeck et al. (2003) also presented evidences of SOA formation of atmospheric polymers by means of heterogeneous reaction of dienes (e.g. isoprene) in the presence of sulfuric acid. Competing oxidants such as ozone or the presence of humidity decreased the reaction yield, but the formation of polymeric organic matter was not disabled. Kleindienst et al. (2007) has also suggested that the photo-oxidation of isoprene, α-pinene, β-caryophyllene, and toluene are an important source in the formation of SOA in the atmosphere. Besides biogenic VOCs, the formation of SOA can also involve VOCs with an anthropogenic origin. On this regard and using WSOC as a measure of SOA, Weber et al. (2007) provided evidences that SOA was highly correlated with anthropogenic emissions (carbon monoxide) and anthropogenic secondary organic VOCs (isopropyl nitrate) in a region containing a mix of both anthropogenic and biogenic emissions. These findings are also in agreement with those found by Chen et al. (2010),

who studied the sources and percursors of SOA in a populated and highly polluted region during a wintertime episode. The major SOA sources were solvent use (28% of SOA), catalyst gasoline engines (25% of SOA), wood smoke (16% of SOA), non-catalyst gasoline engines (13% of SOA), and other unidentified anthropogenic sources (11% of SOA). In terms of SOA precursors, long-chain alkanes were predicted to be the largest SOA contributor, followed by aromatic compounds. The study of Duarte et al. (2008b) also showed evidences that aliphatic material with long-chain (carbons greater than 3 or 4) and branched mono- and dicarboxylic acids, carbonyl, and ester structural types present in WSOM samples are likely to be associated with SOA formation from photo-oxidation of VOCs emitted from either biogenic or local anthropogenic sources.

2.3. Progress and issues in the analysis of WSOM from atmospheric aerosols

During the past decade, different off-line methods have been developed to deal with the complexity of WSOM and to acquire knowledge on the structure and composition of this aerosol component. Commonly-used off-line methods include those focused on identification and quantification of individual molecular species, and those based on functional group analysis and characterization of molecular fragments. Analysis of WSOM based on the typical compound speciation approach usually elucidates less than 20% of the mass of aerosol WSOM (Facchini et al., 1999; Graham et al., 2002). These methods typically employ the extraction of the water-soluble organic species from the sampled fibre filters, followed by LC-MS (Pól et al., 2006; Stone et al., 2009; Zhang et al., 2010) or GC-MS (Graham et al., 2002; Carvalho et al., 2003; Yu et al., 2004), ion chromatography (IC) and high-performance liquid chromatography (HPLC) with diode-array detection (DAD) (HPLC-DAD) (Yang et al., 2004). Off-line techniques that identify functional group composition, molecular bonds, and molecular fragments, such as one- and two-dimensional NMR and FTIR spectroscopies and high-resolution MS (Decesari et al., 2000; Krivacsy et al., 2001a; Graham et al., 2002; Duarte et al., 2005, 2007, 2008b; Sannigrahi et al., 2006; Reemtsma, 2009; Schmitt-Kopplin et al., 2010), usually provide a more complete description of WSOM mass, but less detailed information on the individual species (Duarte

and Duarte, 2011a). However, before its structural characteristics can be comprehensively defined through these advanced spectroscopic techniques, the WSOM must be isolated from other compounds, especially from inorganic species, since they interfere with the application of such sophisticated analytical techniques. The isolation procedure to be employed should allow obtaining a representative sample of the original WSOM sample, without changing its chemical characteristics. In this sense, several methodologies have been proposed to isolate/fractionate the aerosol WSOM. An in-depth survey of the literature shows that solid-phase extraction (e.g. hydrophobic bonded-phase silica sorbents and polymer-based packing materials) (Varga et al., 2001; Andracchio et al., 2002; Kiss et al., 2002; Duarte and Duarte, 2005; Duarte et al., 2005, 2007, 2008b; Sullivan and Weber, 2006; Sannigrahi et al., 2006; Wozniak et al., 2008; Reemtsma, 2009; Mazzoleni et al., 2010; Schmitt-Kopplin et al., 2010), ion-exchange chromatography (IEC) (Havers et al., 1998; Decesari et al., 2000, 2001, 2005; Fuzzi et al., 2001; Graham et al., 2002; Cavalli et al., 2006), and size-exclusion chromatography (SEC) (Krivacsy et al., 2000; Andracchio et al., 2002) have been employed to isolate, and simultaneously fractionate, WSOM from the aerosol aqueous extracts. Of the available isolation procedures, IEC and solid-phase extraction are currently the most commonly used methods. Isolation procedures based on the use of IEC exploit the acidic character of the WSOM and allow fractionating the WSOM mixture into (a) neutral compounds; b) mono- and di-carboxylic acids; and c) polycarboxylic acids. This procedure does not require any adjustments of the original acidity of the aerosol aqueous extracts, it allows separating the original WSOM sample into three main classes of compounds in only one extraction step, and the recoveries are in the order of 90% of the total mass of WSOM (Decesari et al., 2001). The major drawbacks are that inorganic species are not removed from the obtained fractions, and the organic solutes only elute from the resin with high ionic strength solutions (Graber and Rudich, 2006). In what concerns the use of hydrophobic bonded-phase silica (e.g. C_{18} and Oasis-HLB) and polymer-based sorbents (e.g. XAD resins), the leading principal is that these methods fractionate the WSOM samples at pre-adjusted acidic conditions (pH≈2) into operationally defined hydrophobic and hydrophilic fractions (Kiss et al., 2002; Duarte and Duarte, 2005; Sannigrahi et al., 2006; Duarte et al., 2007; Schmitt-Kopplin et al., 2010). With these sorbents, approximately 23-78% of the most hydrophobic and highly conjugated compounds of the WSOM can be isolated in pure organic form, i.e., free from

inorganic species, which are removed through a desalting step (Kiss et al., 2002; Duarte et al., 2007). It must be emphasized, however, that the application of functionalized solid sorbents for WSOM extraction has some disadvantages, namely: (i) the back-elution of the adsorbed organic solutes is time-consuming; (ii) the solid sorbents must be thoroughly cleaned in order to prevent contamination of the WSOM sample due to resin bleeding; and (iii) the irreversible adsorption of organic compounds onto the sorbents surfaces (Duarte et al., 2007).

A special reference is given here to the use of polymer-based sorbents, which were employed in this work for the isolation/fractionation of aerosol WSOM (Chapter 3, section 3.8). Non-ionic macropourous XAD-8 and XAD-4 resins, in tandem, were first used by Duarte and Duarte (2005) to separate rural aerosol WSOC samples into hydrophobic acids and hydrophilic acids fractions. The XAD-8 eluate, which accounted for 47 to 60% of total WSOC, is represented by partially acidic compounds with significant hydrophobic moieties (Duarte and Duarte, 2005; Duarte et al., 2007). The XAD-4 eluate holds the most hydrophilic and of low molecular size compounds of the original WSOC sample, and accounts for 7 to 12% of the total WSOC (Duarte and Duarte, 2005; Duarte et al., 2007). Using a method similar to those developed to separate humic and fulvic acids in aqueous samples, Sullivan and Weber (2006) and Sannigrahi et al. (2006) also applied an XAD-8 resin to separate urban aerosol WSOC into hydrophilic and hydrophobic fractions. The research paper of Sannigrahi et al. (2006) reports recoveries of about 23% of total WSOC for the hydrophobic fraction (i.e., from the XAD-8 resin). The major difference between the methods of Duarte and Duarte (2005) and Sannigrahi et al. (2006) is the solution used to back elute the organic matter retained in the XAD-8 resin. Sannigrahi et al. (2006) employed a solution of 0.1 M NaOH, whereas Duarte and Duarte (2005) used a solution of methanol/ultra-pure water in the proportion 2:3 (40% MeOH). The use of a NaOH solution has been associated to irreversible hydrolytic reactions of the organic matter. Thus, the possibility of obtaining a fraction that is not truly representative of the original organic material is very high and cannot be neglected. In this sense, the use of a 40% MeOH solution to back elute the retained organic matter is an advantage over the alkaline solution since it offers the potential to isolate/fractionate the WSOC samples with minimal introduction of bias due to unwanted reactions (Duarte and Duarte, 2005).

The need to study the atmospheric behavior and physico-chemical characteristics of WSOC on a near real-time scale has also led to the development of methodologies for continuous on-line measurement of this aerosol component. An approach involving a particle-into-liquid sampler (PILS) coupled to ion chromatography (IC) was developed in 2001 by Weber and co-workers for a rapid and continuous measurement of the major inorganic components (e.g. nitrate, sulphate, and ammonium) of aerosol samples (Weber et al., 2001). This PILS on-line collector was further combined with a total organic carbon (TOC) analyzer for measurements of total WSOC content in ambient aerosol particles (Sullivan et al., 2004; Peltier et al., 2007). Aerosol mass spectrometry (AMS) is another widely used on-line technique that has been used for assessing the chemical submicrometer non-refractory inorganic and organic particles with high time resolution sensitivity (DeCarlo et al., 2006). However, AMS does not provide measures of WSOC in atmospheric aerosols. Furthermore, this technique does not characterize individual molecules in ambient air. Instead, this on-line technique, together with a custom principal component analysis, has been used to deconvolute and quantify the mass concentrations of two types of organic aerosols: oxygenated (OOA) and hydrocarbon-like (HOA) (Zhang et al., 2005a, 2005b). Kondo et al. (2007) has anticipated that the derived mass concentrations of OOAs can be used as an indirect measure of the WSOC content in aerosols, assuming that the organic compounds forming OOAs and WSOCs are similar due to the solubility of OOAs in water. These authors reported that approximately 88 ± 29% of OOAs is water-soluble on the basis of the comparison of the WSOC concentrations measured by PILS-TOC with those of OOA derived from AMS data. Timonen et al. (2010) also reported a strong correlation ($r = 0.88$) between aerosol WSOC (measured by PILS-TOC) and particulate organic matter (measured by AMS), with the WSOC accounting on average for 51% of the particulate organics. Using the AMS mass spectra, Zhang et al. (2005a, 2005b) also investigated the possible sources of both OOA and HOA. The authors concluded that OOA is likely SOA (from either anthropogenic or biogenic precursors) and, on a much lower scale, they have contributions from atmospheric oxidation of HOA and/or biomass burning. Their observations also suggest that HOA is likely primary aerosol from local, combustion-related emissions. Overall, it is clear that the on-line AMS is a powerful tool for routine and real-time measurements of the bulk-chemical nature of OA. However, this technique has very limited application for the structural characterization of airborne

WSOM, being able to provide only a qualitative assessment of the degree of oxidation of organic aerosols.

2.4. Main achievements on the structural characterization of WSOM in atmospheric aerosols

The elucidation of the origin and structure of aerosol WSOM have become one of the main research lines on particulate organics in the atmosphere. Numerous off-line methodologies have been developed to study the chemical composition of this organic fraction (Havers et al., 1998; Decesari et al., 2000, 2007; Kiss et al., 2000, 2002; Krivacsy et al., 2001a; Gelencser et al., 2002; Duarte et al., 2005, 2007, 2008a, 2008b; Sannigrahi et al., 2006; Reemtsma, 2009; Stone et al., 2009; Schmitt-Kopplin et al., 2010). These methods are based on a combination of total organic carbon analysis, isolation/fractionation procedures, and characterization by different analytical techniques (e.g. NMR, FTIR, UV-Vis and molecular fluorescence spectroscopies, elemental analysis, and pyrolysis GC-MS).

The elemental analysis has been widely used, in combination with other advanced analytical techniques, to study natural organic matter (NOM) from different environmental matrices (e.g. soil, waters, and atmospheric aerosols). Although little structural information can be drawn from the elemental composition data, the content of C, H, O, and N has been used to deduce on the origin (terrestrial or microbial) of NOM. Additionally, the atomic ratio H/C has been also used as an indicator of the amount of saturation of C atoms within a molecule, whereas the atomic O/C ratio has been assumed to indicate the degree of oxidation of the NOM samples (Abbt-Braun et al., 2004). The elemental analysis data reported thus far for aerosol WSOM are in the order of 51-58%, 5.6-6.7%, 2.0-3.8%, and 32-39% for the C, H, N, and O contents, respectively, and regardless of the area under study (rural areas (Kiss et al., 2002; Duarte et al., 2007) and a high-alpine area (Krivacsy et al., 2001a)). H/C and O/C values for the aerosol WSOM samples have also been assessed, being reported atomic ratios in the range of 1.21-1.35 and 0.41-0.55, respectively (Krivacsy et al., 2001a; Duarte et al., 2007). These data allowed the authors to suggest that the aerosol WSOM encompass highly oxygenated aliphatic structures. Data on the content

of S in aerosol WSOM samples has not been reported yet due to its low concentration, typically below the detection limit of the analytical instrumentation (Krivacsy et al., 2001a; Kiss et al., 2002).

The UV-Vis spectroscopy has been quite often applied as a rapid screening method for the bulk characterization of NOM from different environmental matrices. A typical UV-Vis spectra of NOM samples, including those of WSOM from aerosols (Krivacsy et al., 2001a, 2008; Duarte et al., 2003, 2005, 2008a; Baduel et al., 2010) exhibits a monotonically decrease of the absorbance with increasing wavelength. Although providing little structural information, the examination of both the quotient E_{250}/E_{365} (absorbance values at 250 nm and 365 nm) and specific absorptivity at 280 nm (ε_{280}) allow some qualitative information to be withdrawn. According to Peuravuori and Pihlaja (1997), there is a relationship between the E_{250}/E_{365} ratio and the percentage of aromaticity and the molecular size of aquatic humic substances. Higher E_{250}/E_{365} ratios are usually associated with lower molecular sizes and lower percentages of aromaticity. On the other hand, higher ε_{280} values have been associated with higher percentages of aromaticity of the NOM samples (Duarte et al., 2003). Using estimates of these two parameters for assessing the bulk properties of aerosol WSOC samples collected during Summer and Autumn seasons at a rural location, Duarte et al. (2005) reported a seasonal trend in the values of the quotient E_{250}/E_{365}, with higher values being found for the samples collected during Summer season. Such a pattern allowed the authors to suggest that the WSOM of the summer samples exhibit a lower molecular size and a lower degree of aromaticity than those collected in the Autumn season. Duarte et al. (2005) also reported higher ε_{280} values for the samples collected during the Autumn season, suggesting that these samples include compounds with complex unsaturated bond systems, where more than two π-bond orbital overlap leading to an increase in the absorptivities values. Krivacsy et al. (2008) also presented estimates of the quotient E_{250}/E_{365} for WSOM samples collected in different locations with different levels of pollution. The authors reported an increase of the E_{250}/E_{365} ratio when moving from a polluted urban site to a clean marine environment. The authors suggested that such a pattern could likely be associated to a decrease in the aromatic content of the WSOM samples collected at more pristine environments. Krivacsy et al. (2008) also reported estimates of the specific absorptivity at different wavelengths (250, 285, 330, 350, and 400 nm). A close examination of the reported values, particularly

at 285 nm, shows higher values for samples collected under polluted conditions. This indicates, as it might be expected, that such samples are likely to be enriched in complex unsaturated bond systems.

Over the past decades, fluorescence spectroscopy (either emission, excitation, synchronous, or EEM fluorescence spectroscopy) has been applied extensively as a relatively simple analytical tool for the characterization, differentiation and classification of NOM in both terrestrial and aquatic environments (Senesi et al., 1991; Coble, 1996; Parlanti et al., 2000; McKnight et al., 2001; Santos et al., 2001; Chen et al., 2002; Peuravuori et al., 2002a). The most efficient fluorophores in NOM are known to be substituted, condensed aromatic rings, and/or highly unsaturated aliphatic chains (McDonald et al., 2004). In an opposite way to UV-Vis absorbance, the fluorescence intensity usually decreases with increasing molecular weight and aromatic content of the NOM samples (Duarte et al., 2003). The application of molecular fluorescence spectroscopy, based on the fluorescence emission spectra, in the study of aqueous extracts of OM aerosols, revealed a single broad band given that the information obtained from this type of fluorescence spectra is limited. Krivacsy et al. (2001a) and Kiss et al. (2002), have used the fluorescence spectroscopy to characterize the WSOC fraction in aerosol collected at high-alpine and at a rural site, as a preliminary evaluation of solid-phase extraction procedure. The authors obtained a broad band of fluorescence emission with maximum wavelength at about 405-410 nm when excited with UV wavelength of 235 nm, which is usually related to polyconjugated molecular structures (e.g., aromatic rings). Duarte et al. (2004) showed that the EEM fluorescence spectra of WSOC of atmospheric aerosols has the advantage of obtaining a comprehensive view of the fluorescence characteristics and allow to identify the major differences in the fluorescent properties of fractions obtained from the isolation/fractionation procedure of the WSOC of aerosol. In such study, the authors demonstrated that the fluorescing constituents of WSOM of aerosol from coastal zone present three fluorescent peaks located at the following excitation/emission ($\lambda_{Exc}/\lambda_{Em}$) wavelengths: 240/405nm; 310/405nm; and 280/340 nm. The authors also verified that the first two peaks ($\lambda_{Exc}/\lambda_{Em}\approx$240/405 nm and $\lambda_{Exc}/\lambda_{Em}\approx$310/405 nm) are located at wavelengths shorter than those reported for aquatic humic substances, indicating a smaller content of both aromatic structures and condensed unsaturated bond systems in the WSOC fraction (Duarte et al., 2004). Duarte et al (2004), also analysed the EEM data to obtain the

data of the synchronous spectra at three different Δλ values (20 nm, 40 nm and 60 nm; $\lambda_{em}=\lambda_{exc}+\Delta\lambda$) in order to find the best Δλ and to found the quickest and most suitable Δλ for distinguish samples of WSOC from aerosols with different chemical properties. The authors concluded that the best peak resolution was achieved by applying a Δλ of 20 nm, where two well-defined bands were distinguished at λ_{Exc} of ≈280 nm and ≈340 nm. Synchronous spectra profiles of WSOC fractions obtained by the XAD-8/XAD-4 isolation procedure revealed that the fractions original WSOC and XAD-8 eluate had a shoulder at λ_{Exc} ≈ 300 nm, and this shoulder was not present in the synchronous spectra of the other fractions (XAD-8 effluent, XAD-4 eluate and XAD-4 effluent). The synchronous spectra of XAD-8 effluent, XAD-4 eluate and XAD-4 effluent presented a peak at lower wavelength (λ_{Exc} ≈ 320 nm) than the original WSOC fraction (λ_{Exc} ≈ 340 nm), suggesting that such fractions had simpler structural units, with fewer aromatic functional groups and conjugated systems than the original WSOC sample (Duarte et al., 2004). The synchronous fluorescence spectra with Δλ=20 nm was also used by Duarte et al. (2005) for studying the spectroscopic characteristics of the WSOM isolated from atmospheric aerosols collected at the rural site under different atmospheric conditions (Summer and Autumn). The authors observed that all WSOC spectra from atmospheric aerosols exhibited maximum fluorescence intensities at 285 and 342 nm, and the fluorescence peak at λ_{Exc} ≈ 285 nm is usually attributed to aromatic amino acids, phenol-like components and proteinaceous material, while fluorescence peak at 342 nm is assigned to humic-like compounds (Parlanti et al., 2000; Yamashita and Tanoue, 2003). Various subsequent studies have also found protein and humic compounds in WSOC of atmospheric aerosols by fluorescence spectroscopy (Duarte et al., 2005; Krivacsy et al., 2008; Nakajima et al., 2008; Mladenov et al., 2010, 2011). For example, Nakajima et al. (2008) studied the fluorescent characteristics of water-soluble fraction from bulk aerosols collected in urban area of Okinawa, Japan, based on EEM fluorescence spectra and observed that many water-soluble samples displayed two peaks at $\lambda_{Exc}/\lambda_{Em}$ of 250–275/375–455 and 300–320/400–440 nm, which can be signatures for fulvic acid-like compounds. The authors also observed that the several samples collected in Winter periods showed another fluorescence peak at $\lambda_{Exc}/\lambda_{Em}$ of 260–290/305–345 nm, which could be attributed to the presence of aromatic amines (such as tyrosine and tryptophan).

FTIR spectroscopy provides a preliminary assessment of the functional group composition of WSOM from atmospheric aerosols. The advantages in applying FTIR spectroscopy to investigate the global structural features of WSOM is that a relatively small amount of sample is required {c.a. 1 mg of WSOM) (Duarte et al., 2007)}, and the easiness of obtaining the spectrum. However, the acquired structural information is mainly qualitative and, in general, complete, unambiguous interpretation of a FTIR spectrum is rather difficult. A typical FTIR spectrum of WSOM isolated from atmospheric aerosols exhibits overlapping bands, which clearly indicate multiple functionality as a result of the complex mixture of organic compounds (Kiss et al., 2002; Duarte et al., 2005, 2007). Overall, the main functional groups reported in the published studies include aliphatics, carboxylic acids, hydroxyls, primary amines, carbonyl groups from aldehydes and ketones, and aromatic structures. The functional groups identified in aerosol WSOM shows seasonal patterns in their relative importance. For example, Duarte et al. (2005, 2007) reported the prevalence of aromatic carbons in samples collected in a rural area during Winter comparatively the Summer samples. The authors attributed this finding to the presence of lignin breakdown components associated to intensive wood burning in Winter. Since only some specific bands can be clearly assigned in the FTIR spectrum of such complex samples, it becomes crucial to corroborate the assignments of the vibrational frequencies to structural groups using additional spectroscopic methods, such as NMR spectroscopy.

For appropriate FTIR analysis, some potential interferents such as water soluble inorganic ions, namely Cl^-, K^+, NO_3^- and CO_3^{2-} must be previously separated of the organic fraction. Furthermore, prior to FTIR analysis, the WSOM should be freeze-drieded. Despite the utility of these procedures, some studies based on FTIR spectroscopy (Maria et al., 2002; Coury and Dillner, 2009; Hawkins and Russell, 2010; Takahama et al., 2011) have been applied, by using the direct analysis of the filters substrate onto the equipment. The results obtained by these two FTIR approaches differ one to the other, the FTIR spectra obtained by direct filter analysis being less defined because of increasing of complexity and overlapping. To bypass the problem of complexity and overlapping peaks by other means without prior removal of interfering species, the FTIR system must be calibrated using multi-component calibration standards and a multivariate algorithm (Coury and Dillner, 2008). Although the composition profile is obtained, i.e., several

characteristic absorption bands are often seen in the sample, the heterogeneity of aerosol WSOM produces broad overlapping bands, and the comparison of spectra will only give an indication of whether the functional groups of each sample are similar or not.

NMR spectroscopy, either one-dimensional liquid-state ^{1}H NMR and solid-state CPMAS ^{13}C NMR or two-dimensional liquid-state NMR, has become the most important spectroscopic method for the structural characterization of complex organic mixtures, such as those of WSOM from atmospheric aerosols. This spectroscopic technique allows a more complete description of the whole mass of atmospheric WSOM while providing resolution on functional groups and sub-structural components. Liquid-state ^{1}H NMR spectroscopy is the most widely used NMR technique and it has been applied for functional group analysis (Decesari et al., 2001; Graham et al., 2002; Cavalli et al., 2006), molecular modeling (Fuzzi et al., 2001), and source apportionment (Decesari et al., 2007) of WSOM from atmospheric particles. Due to the small chemical shift dispersion of protons (0~10 ppm) and the chemical complexity of the aerosol WSOM samples, the typical ^{1}H NMR spectrum consists of a complex overlapping profile, with broad bands superimposed by a relatively small number of sharp peaks. Usually, only four main categories of functional groups carrying C-H bonds are identified in the aerosol WSOM samples: 1) Ar-H: aromatic protons (6.5-8.3 ppm); 2) H-C-O: protons bound to oxygenated aliphatic carbons atoms, such as aliphatic alcohols, ethers, and esters (3.3-4.1 ppm); 3) H-C-C=: protons bound to aliphatic carbon atoms adjacent to unsaturated groups, such as alkenes, carbonyl, imino or aromatic groups (1.9-3.2 ppm); and 4) H-C: aliphatic protons in extended alkyl chains (0.5-1.9 ppm). Using quantitative integration of each spectral region, it has been concluded that protons in aliphatic structures are the dominant moieties in atmospheric WSOM, followed by oxygenated aliphatic compounds and unsaturated aliphatic groups (including H-C-C=O and H-C-C=C), and only a minor contribution from aromatic groups (Decesari et al., 2001; Graham et al., 2002; Cavalli et al., 2006). It should be emphasized, however, that ^{1}H NMR spectroscopy has low sensitivity for detecting functional groups which do not carry protons (e.g. substituted aromatic compounds), or contain acidic functions with rapidly exchangeable protons (e.g. carboxylic acids) (Fuzzi et al., 2001; Cook, 2004). In this sense, solid-state CPMAS ^{13}C NMR spectroscopy can be viewed as a much more attractive technique for aerosol WSOM characterization since it gives information about the carbon backbone of the complex organic structures. However, high quality solid-state CPMAS ^{13}C

NMR spectra are very difficult to obtain due to the low carbon contents of these aerosol components. In fact, it requires about 20 to 100 mg of sample (depending on the size of the NMR probe), and the WSOM must also be isolated from the inorganic matrix (including the naturally occurring paramagnetic trace elements) and prepared as a solid prior to analysis (Duarte et al., 2005, 2007). Indeed, the only applications to date of CPMAS ^{13}C NMR spectroscopy to the study of aerosol WSOM were conducted by Subbalakshmi et al. (2000), Duarte et al. (2005, 2007) and Sannigrahi et al. (2006). In their studies, the authors combined the aerosol samples in accordance to similar ambient conditions in order to obtain sufficient sample mass for the NMR analysis. Despite the above-mentioned challenges, the CPMAS ^{13}C NMR technique exhibits important advantages, especially when compared to one-dimensional liquid-state ^{1}H NMR spectroscopy in the analysis of aerosol WSOM: a) it is non-destructive and, after analysis, the WSOM samples can be used for other complementary structural investigations (Duarte et al., 2005, 2007); b) it is not prone to solvent effects that may alter chemical shifts of the functional groups, mask some of the chemical resonances due to solvent signals, or even cause the loss of some peaks (especially those of the carboxylic acids due to the presence of rapidly exchangeable protons) (Cook, 2004; Sannigrahi et al., 2006); and c) the limited solubility of the organic material in the selected solvent may result in lower resolution and sensitivity in the liquid-state ^{1}H NMR spectra (Cook, 2004). Additionally, the CPMAS ^{13}C NMR data can be employed for obtaining a semi-quantitative measure of the relative contribution of the different functional groups to the organic carbon present in the aerosol WSOM. These data can be further used for assessing the structural variations of WSOM with changes in parameters such as aerosol sources and meteorological conditions (Sannigrahi et al., 2006; Duarte et al., 2007).

The ^{13}C chemical shift ranges used to identify WSOM constituents in aerosols are thoroughly described in the literature (Sannigrahi et al., 2006; Duarte et al., 2007; Duarte and Duarte, 2009, 2011a), and structural assignment is based on those found for terrestrial and aquatic natural organic matter (Abbt-Braun et al., 2004; Simpson and Simpson, 2009). The works reported thus far demonstrate that almost all CPMAS ^{13}C NMR spectra are very broad with overlapping peaks, just allowing the identification of typically 5 to 8 types of functional groups, namely: 0–45 ppm (unsubstituted saturated aliphatic carbons, including straight-chain methylene (21 ppm) and methane (29 ppm) carbons, and methylene carbons

of branched alkyl chains (35 ppm)); 45–60 ppm (substituted aliphatic carbons (e.g., those found in amines (45 ppm) and methoxyl groups (55 ppm)); 60–95 ppm (oxygenated aliphatic carbons (e.g., those found in polysaccharides, alcohols, or anhydrosugars)); 95–110 ppm (aliphatic carbons bonded to two oxygen atoms (e.g., anomeric carbons of polysaccharides)); 110–140 ppm (alkyl-substituted aromatic carbons and unsaturated carbons); 140–160 ppm (aromatic carbons bonded to one oxygen atom); 160–190 ppm (carboxylic, ester and amide carbons); and 190–230 ppm (carbonyl carbons of aldehydes and ketones) (Duarte and Duarte, 2011a). The published CPMAS ^{13}C NMR data also shows evidence that the WSOM from aerosols collected at different locations (rural, urban and biomass burning) exhibit the same main carbon functional groups, but their relative abundances are quite different (Sannigrahi et al., 2006; Duarte et al., 2007). Overall, the results reported thus far show that the WSOM is mostly aliphatic (41–62% of total NMR peak area), followed by oxygenated aliphatics (15–21%) and carboxylic acid (5.4–13.4%) functional groups. Duarte et al. (2007) also provided evidences of differences between aerosol WSOM sources in the warmer and colder periods at a rural location. The aromatic content of samples collected in Autumn and Winter seasons is higher (15%) than that of samples collected during the warmer period (6–10%). Furthermore, the Autumn and Winter samples showed resonances attributable to methoxyl groups (55 ppm) and oxygen-substituted aromatic ring carbons (147 ppm). These structures were associated with lignin and its degradation products, which highlights the major contribution of wood-burning processes in domestic fireplaces to the bulk properties of WSOM from aerosols. The ^{13}C NMR results of Sannigrahi et al. (2006) at an urban area also suggested the presence of aromatic carboxylic acids in the WSOM sample, which were associated with motor-vehicle emissions or SOA-producing reactions.

Recently, two studies demonstrated the success of two-dimensional liquid-state NMR techniques in revealing valuable information on the substructures present in WSOM from atmospheric aerosols (Duarte et al., 2008b; Schmitt-Kopplin et al., 2010). The combined used of the information provided by ^{1}H-^{1}H homonuclear (in Correlation Spectroscopy (COSY) or Total Correlation Spectroscopy (TOCSY)) and ^{1}H-^{13}C heteronuclear (in Heteronuclear Single Quantum Coherence (HSQC) or Heteronuclear Multiple Bond Correlation (HMBC)) connectivities, allows a higher spectral resolution and therefore greater detail on the C-H backbone of the substructures present in the complex

aerosol organic matter mixtures. The HSQC is considered as the most important two-dimensional NMR method since it provides information on the C-H couplings over one bond, i.e., it identifies the C-H units in a molecular substructure (Simpson, 2001). After HSQC, COSY and TOCSY are likely the most useful two-dimensional NMR experiments for the analysis of organic structures. The COSY method distinguishes protons that are interacting through one bond, whereas TOCSY identifies protons that are interacting over two to three bonds (Simpson, 2001). Finally, the HMBC experiment only detects ^{1}H-^{13}C couplings over two and three bonds (i.e. H-C-C or H-C-C-C) while single C-H bonds are absent from the spectrum (Simpson, 2001). This experiment has also an important advantage over HSQC in that quaternary carbons can be detected with HMBC (Simpson, 2001), thus complementing the chemical shift assignments of the HSQC method. In a similar fashion of one-dimensional liquid-state ^{1}H NMR spectroscopy, in two-dimensional NMR experiments it is also important to consider: 1) the amount of sample used (high sample concentrations could promote molecular aggregation), 2) the sample solubility (the amount of dissolved organic carbon could be too low for the application of liquid-state ^{13}C NMR techniques), and 3) the interference from the solvent signals (Duarte and Duarte, 2013).

In what concerns the structural information provided by these two-dimensional NMR methods, Duarte et al. (2008b) combined COSY, HSQC, and HMBC experiments techniques to study WSOM from fine atmospheric aerosols collected during Winter and Spring/Summer seasons at a rural location with high agricultural activity. The authors concluded that the aliphatic material of both samples consisted mostly of long-chain (carbons greater than 3 or 4) and branched mono- and dicarboxylic acids, carbonyl and ester structural types. The presence of such structural fragments was associated with SOA formation. Spectral signatures typical of anhydrosugars from cellulose and methoxyphenols from lignin were also clearly identified among the carbohydrate and aromatic moieties of the Winter sample. Their presence was linked to the occurrence of wood burning processes in domestic fireplaces during the colder period. Schmitt-Kopplin et al. (2010) combined liquid-state 2D NMR techniques (COSY, TOCSY, HSQC, HMBC, and Distortionless Enhancement by Polarization Transfer (DEPT)-HSQC) with high-resolution MS to investigate the molecular signatures of the water-soluble fraction of secondary organic aerosols. The typical aliphatic chemical environment within the studied

samples was heteroatom-substituted functional groups adjacent to highly branched aliphatics (e.g., terpenoid-like molecules). Aromatics were found to be highly substituted, and electron withdrawing groups and (O)NO_x substitution was considerably more common than the presence of electron donating oxygen-containing functional groups and neutral substitution (aliphatic carbon). The obtained results allowed the authors to improve the current knowledge on SOA formation by suggesting possible chemical reaction pathways involving CHO precursor molecules and sulfuric acid in gas-phase photoreactions.

Despite the serious efforts to unravel the predominant structures in aerosol WSOM, a comprehensive molecular characterization of this fraction is far from being complete. Furthermore, linking the composition of WSOM to their sources and formation mechanisms still remains an issue. Improving the current knowledge of the molecular structures of aerosol WSOM is therefore highly required to better describe the climate-relevant properties of atmospheric aerosols.

2.5. Molecular weight assessment of WSOM in atmospheric aerosols

Concerning the assessment of the MW distribution of aerosol WSOM a few studies have already been reported. Using LC coupled with electrospray ionization mass spectrometry, Kiss et al. (2003) showed that the number average molecular weight (Mn) of WSOM collected at rural site is in the range of 215-345 Da. Samburova et al. (2005) applied laser desorption/ionization mass spectrometry (LDI-MS) to aerosol WSOM samples collected in an urban ambient. The authors reported a broad range of peaks between m/z 150 and m/z 500 for the studied samples. Using SEC coupled with diode array detection, Duarte and Duarte (2011b) reported MW values in the range of 365-1957 Da for a WSOM sample collected during Spring/Summer season, and of 249-1957 Da for a WSOM sample collected during the Winter season, both at a rural location. Recently, Wang et al. (2013) characterized the water-soluble organic fraction of carbonaceous particles, clouds, and fog samples through SEC coupled with inline OC detection. The authors reported a distribution of WSOM across a wide range of nominal MW (120-10 kDa). The authors also showed that the selected samples presented a substantial fraction of

organic matter in a very high MW region (>10 kDa), which the authors associated with biogenic nanoscale or macromolecular materials.

A recent study conducted by Barros (2011) using LC x LC (specifically, PALC x SEC) coupled with diode array, fluorescence and evaporative light-scattering (ELSD) detectors, provided evidences that WSOM from atmospheric particles collected during Winter season at a rural location has an average MW distribution within the range of 157-891 Da. This apparent MW distribution of the WSOM sample was found to be lower than that reported previously by Duarte and Duarte (2011b) using the traditional one-dimensional SEC approach (i.e., 249-1957 Da). This feature was associated to the application of a pre-separation procedure (i.e. PALC) in the LC x LC method, which produces small-size WSOM aggregates. In the conventional SEC procedure reported in the literature, the WSOM aggregates are analyzed as a whole, thus suggesting that they may not be so easily dissociated during diffusion through the SEC column, yielding therefore higher MW values (Duarte et al., 2012). Overall, these results highlight the huge potential of LC x LC as a promising tool for resolving the chemical heterogeneity of the complex WSOM in fine atmospheric aerosols. Furthermore, when combined with subsequent offline structural characterization (e.g., by NMR spectroscopy), LC x LC can be of particular value for targeting unique molecular structures within the complex aerosol WSOM.

III

Experimental procedures

3.1. Introduction

This third chapter presents a description of the reagents and experimental methods employed in this research work, including the sampling procedure for the collection of $PM_{2.5-10}$ and $PM_{2.5}$ samples, the extraction of the water-soluble organic fraction from the $PM_{2.5}$ samples, and the procedure for the isolation/fractionation of WSOM from the aqueous extracts of the collected $PM_{2.5}$ samples. A description of the analytical procedures employed in the determination of OC, EC, and WSOC contents in both $PM_{2.5-10}$ and $PM_{2.5}$ samples, and in the spectroscopic characterization (UV-Vis, EEM fluorescence, FTIR-ATR, and CPMAS ^{13}C NMR spectroscopies) and LC x LC separation of the WSOM from the $PM_{2.5}$ samples is also presented.

3.2. Reagents

All the chemicals used in this work were of analytical reagent grade and obtained from commercial suppliers without further purification. All the solutions were prepared with high purity water (18 M Ω cm).

The measurement of the dissolved organic carbon (DOC) content in the aerosol aqueous extracts required the use of hydrochloric acid (HCl) and phosphoric acid (H_3PO_4) of ultrapure grade in a glass bottle (purchased from Sigma-Aldrich). A stock DOC standard solution of 1000 mg C L^{-1} was monthly prepared from reagent grade potassium hydrogen phthalate ($HO_2CC_6H_4CO_2K$) (obtained from Merck). This solution was used to prepare, every week, DOC stock solutions of 100 mg C L^{-1}. A stock standard solution of 1000 mg C L^{-1} of inorganic carbon (IC) was prepared from a mixture of anhydrous sodium carbonate (Na_2CO_3) and sodium hydrogen carbonate ($NaHCO_3$) (obtained from Merk). All standard solutions were stored in dark glass bottles.

Mobile phases for the LC x LC experiments were prepared with HPLC grade acetonitrile (ACN) obtained from Fisher Scientific (Leicestershire, UK), ammonium acetate (CH_3COONH_4), acetic acid (CH_3COOH), and ammonium hydrogenocarbonate (NH_4HCO_3), all three purchased from Fluka (Buchs, Switzerland). Prior to use, the mobile

phases were filtered through hydrophilic polyvinylidene fluoride (PVDF) membrane (Durapore®, Millipore) of 0.22 μm pore size.

3.3. Aerosol sampling campaigns

Atmospheric aerosol samples were collected in the campus of University of Aveiro (40°38'N, 8°39'W), which is located at about 7 km from the coast on the outskirts of the small town of Aveiro with approximately 78.400 inhabitants and an urban area of 13.5 km² (Fig. III-1). The sampling site is placed at 2 m above the ground level (Fig. III-1), about 1 km away from the A25 motorway, and adjacent to a residential area and a salt pans area of the Lagoon of Ria de Aveiro. An industrial complex, which includes the production of nitric acid, aniline and nitrobenzene, is located at about 10 km to the north of Aveiro. The sampling site is impacted by both marine air masses travelling from the Atlantic Ocean and anthropogenic emissions from vehicular transport, residential, and industrial sources.

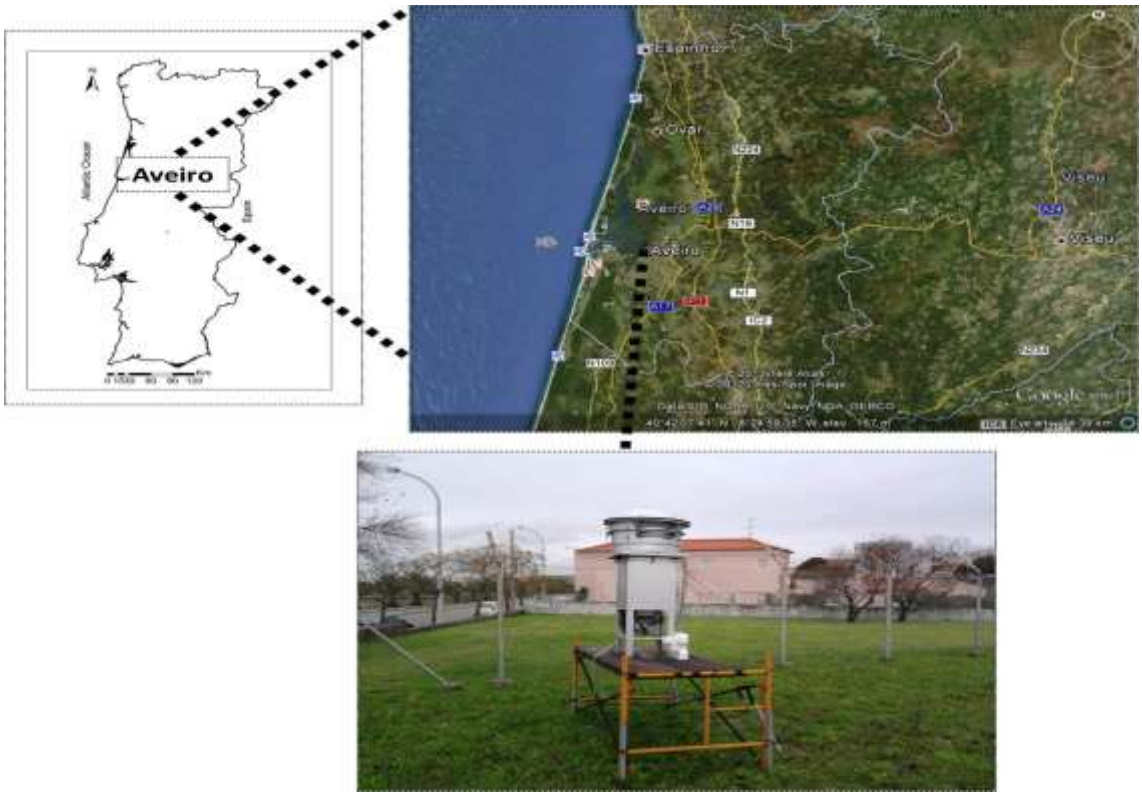

Fig. III-1. Location of the sampling site and picture of the high-volume sampler used in the aerosol sampling campaigns.

The particulate matter was sampled with a high-volume air sampler, Model TE-6070V, from Tisch Environmental, Inc. Aiming at separate particles into two size fractions ($d_{ae} < 2.5$ μm and $2.5 < d_{ae} < 10$ μm), the high-volume sampler was equipped with a size selective PM_{10} inlet (Model TE-6001, Tisch Environmental, Inc.) and a $PM_{2.5}$ single-stage impactor (Model TE-231, Tisch Environmental, Inc.). Sampling was carried out on pre-fired (at 500 °C for 12h) quartz fibre filters (20.3×25.4 cm; Whatman QM-A) with an air flow rate of 1.13 m^3 min^{-1}. The aerosols samples were collected on a weekly basis (7 days) in order to accumulate enough material for the analysis.

In a first stage, and in order to assess positive sampling artifacts in particulate OC measurements in an urban environment, both $PM_{2.5}$ and $PM_{2.5-10}$ samples were collected using a tandem filter method, i.e., on sets of two (front and back) quartz fibre filters directly on top of each other. In this field campaign, hereafter designated as *sampling campaign I*, a total of 12 filter pairs (Table IV-1, section 4.2.1) were collected from 23 June to 29 July 2008 (Summer 2008), 27 April to 01 June 2009 (Spring 2009), and 01 June to 09 August 2009 (Summer 2009). In a second stage, and in order to assess the seasonal trend of the chemical composition of WSOM in fine urban aerosol samples, a second intensive field campaign, hereafter designated as *sampling campaign II*, was carried out from 23 November 2009 to 29 March 2011. The sampling details of the intensive field *campaign II* is summarized in Table A. 1, Annex A. In this second field campaign, a total of 47 aerosol samples ($PM_{2.5}$ and $PM_{2.5-10}$) and 11 field blank samples were collected using the conventional sampling approach, i.e., one filter placed at each size range. The field blank samples were prepared, stored, transported and analysed in the same way as the exposed filter samples, with the exception that no air was forced across the filters, in order to control possible sample contamination, including field operations. During this second sampling campaign, several aerosol samples could not be collected properly as result of equipment breakdown associated with bad weather conditions and electricity supply failures, mainly in January 2010 and 2011, and March 2010, and damaged internal motor parts (mostly, brushes). The 47 aerosol samples were grouped together (groups of three, four, and five samples), according to similar ambient conditions, on a total of 10 groups representative of different seasonal periods (additional information is provided in section 4.5, Chapter 4). The meteorological data, including air temperature, relative humidity (RH), precipitation, and wind velocity, are summarized in section 4.2 of Chapter 4. These

data were provided by the Portuguese Sea and Atmosphere Institute and by the Department of Physics from the University of Aveiro.

In both sampling campaigns, the concentrations of both $PM_{2.5}$ and $PM_{2.5-10}$ (in μg m^{-3}) were determined by weighting the filters under controlled moisture conditions before and after exposure. Before sampling, the pre-fired quartz fibre filters were placed inside a box for 24h at room temperature and approximately 50% relative humidity. The filters were then weighted in an analytical balance (OHAUS, Model Pioneer™ Analítica-PA64C), and the weighing precision was ±0.0001 g. After sampling, filter samples were folded in two, with the exposed side face to face, wrapped in pre-fired aluminium foil and immediately transported to the laboratory, where they were again placed inside the above-mentioned box for 24h and weighted. Finally, the field blank and loaded filter samples were stored frozen until further analysis.

3.4. Determination of organic and elemental carbon content in $PM_{2.5}$ and $PM_{2.5-10}$ samples

The determination of OC and EC content in the aerosol samples was performed at the Portuguese Agency of Environment, using a Lab OC-EC Aerosol Analyzer (Sunset Laboratory Inc.) and following a thermo-optical method (Birch and Cary, 1996). As with other procedures (thermal and thermo-optical) applied into the analysis of OC and EC in aerosol samples, the contents of OC and EC are operationally defined. A brief description of the procedure follows:

- *Part A*: in a completely oxygen (O_2)-free helium (He) atmosphere, a small portion (1.5 cm^2) of the quartz fibre filter is heated in four increasing temperature steps (60 sec at 315 ºC, 60 sec at 475 ºC, 60 sec at 615 ºC, and 90 sec at 870ºC) to remove all OC from the filter. The transition from the third to the fourth temperature (i.e., from 615 ºC to 870 ºC) quickly decomposes inorganic carbonates, producing a sharp, characteristic peak. During this first stage of analysis, a fraction of OC is usually pyrolitically converted to EC, called pyrolytic carbon (PC). This pyrolitic conversion is continuously monitored by measuring the transmission of a laser through the filter. As the organic

compounds are vaporized, they are immediately oxidized to carbon dioxide (CO_2) in an oxidizer oven which follows the sample oven. The flow of He, containing the CO_2, then goes to a methanator oven where the CO_2 is reduced to methane (CH_4). The CH_4 is then detected by a flame ionization detector (FID).

- *Part B*: at the end of the fourth temperature (*Part A*), the sample oven is cooled to 550 ºC (50 sec). After this step, the pure He is switched to a 2% O_2/He mixture in the sample oven and the temperature is stepped up to 940 °C. During this second stage of analysis, both the original EC and the PC (*Part A*) are oxidized to CO_2 due to the presence of O_2 in the carrier gas. As previously, the CO_2 is then reduced to CH_4 and detected by the FID. The darkness of the filter is continuously monitored throughout all stages of the analysis.
- *Part C*: after all carbon has been oxidized from the sample, a known volume and concentration of CH_4 is injected into the sample oven in order to calibrate each measurement to a known quantity of carbon. This also provides a means of checking the operation of the instrument. Based on the FID response and laser transmission data, the quantities of OC and EC are calculated for each sample. The TC content of the aerosol sample is determined as OC + EC.

3.5. Extraction of WSOM from the $PM_{2.5}$ and $PM_{2.5-10}$ samples

The extraction of WSOC from the $PM_{2.5}$ and $PM_{2.5-10}$ samples was based on the procedure developed by Duarte and Duarte (2005). In this procedure, 280 cm^2 and 25 cm^2 of each $PM_{2.5}$ and $PM_{2.5-10}$ filter sample, respectively, was extracted with 150 and 30 mL of ultrapure water, respectively, by mechanical stirring during 5 min plus ultrasonic bath during 15 min. The final slurry so obtained was filtered through a membrane filter (PVDF, Durapore®, Millipore) of 0.22 μm pore size.

3.6. Determination of dissolved organic carbon content in the aqueous extracts from the $PM_{2.5}$ and $PM_{2.5-10}$ samples

The dissolved organic carbon (DOC) content of each aqueous extract of the aerosol samples was measured by means of a Shimadzu TOC-5000A analyser with a regular sensitive catalyst, which offers two independent methods for measuring DOC: i) an indirect method, where the DOC content is calculated as the difference between the total carbon (TC) and inorganic carbon (IC) contents; and ii) a direct method, named Non-Purgeable Organic Carbon (NPOC), where the sample is acidified and sparged with high purity air for eliminating the IC component prior to DOC measurement. The principle of DOC analysis is based on the injection of the sample into an oven where it is catalytically oxidized to CO_2 at 680 °C, being then purified by filters, dried, and flushed into the non-dispersive infrared (NDIR) detector by means of a carrier gas flow. Fig. III-2 schematically illustrates the indirect and direct methods for DOC analysis.

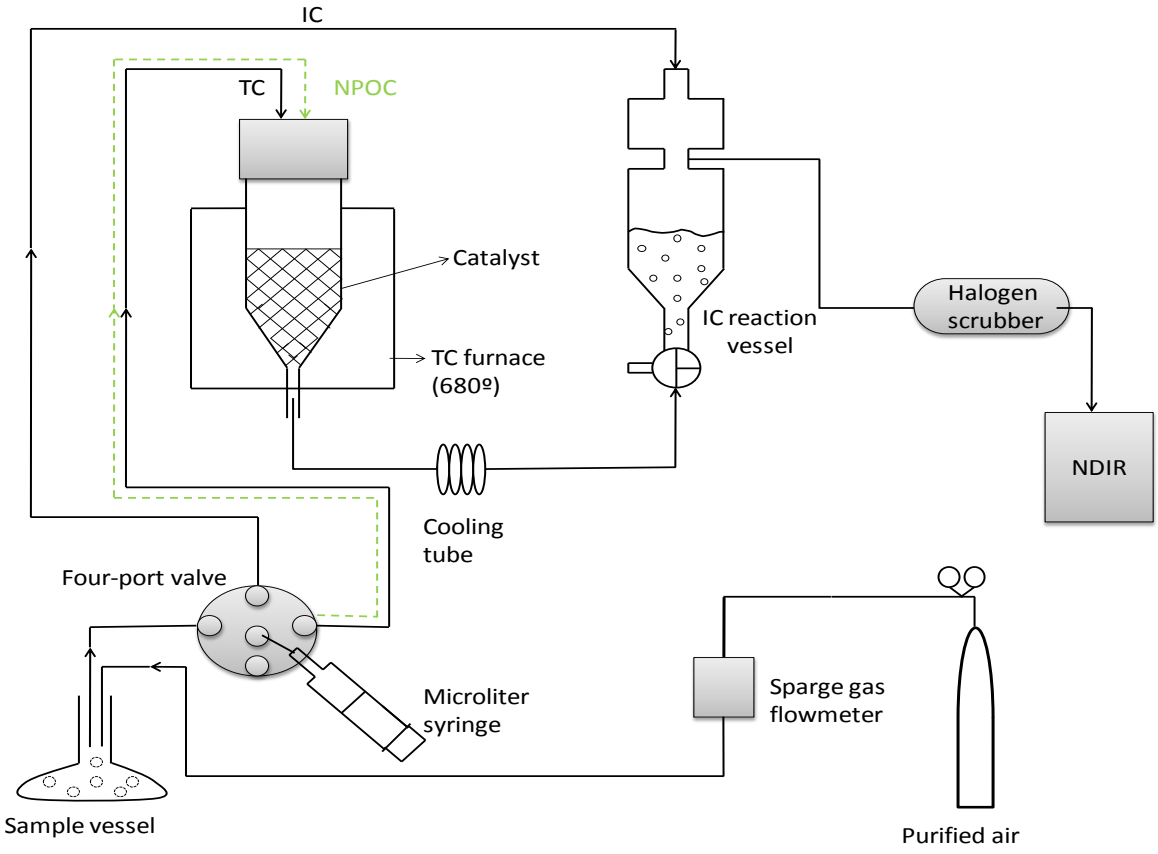

Fig. III-2. Flow diagram for DOC analysis using the indirect (black solid line, TC and IC measurement) and direct (green dashed line, NPOC measurement) methods.

Although the methods used here are standard protocols, the analytical nature of this work requires their description. A key point about analysing aqueous samples with low DOC concentrations, such as those of atmospheric aerosol samples, is the need to ensure the precision of the analytical method (indirect and direct) and, simultaneously, avoid any possible disturbance/contamination during DOC analysis. A few examples of possible sources of disturbance/contamination during DOC analysis include the HCl stock bottle (in direct method), time of sparging in the direct method, and the intensity of the analytical signal of the blanks (ultra-pure water). Thus, in this work, the results obtained by means of the indirect and direct methods were compared and the effect of the procedure adopted in each method was assessed: a) in the indirect method, the analysis of TC followed by the analysis of IC or the analysis of IC followed by the analysis of TC, and the volume of the sample injected into the analyser; b) in the direct method, the adequate time of sparging, the volume of the sample injected into the analyser, and the type of container (glass or plastic) used to preserve the HCl reagent.

As shown in Table III-1, in the indirect method, the measurement of IC content previously to that of TC yielded a lower average intensity for the analytical signal acquired in the analysis of ultrapure water than when performing the opposite sequence.

Table III-1. Results obtained from the procedure adopted in the indirect method in terms of the analytical signal for TC and IC.

Procedure	**TC** *(Peak area count)*		**IC** *(Peak area count)*		**Volume of sample (ultrapure water)**
	Avg [a]	**sd** [b]	**Avg** [a]	**sd** [b]	
TC followed by IC	608	52	550	107	100 µl
IC followed by TC	372	41	370	72	

[a] Avg: average of 5 measurements;
[b] sd: standard deviation.

When assessing the most appropriate volume of sample (ultrapure water) to be injected into the analyser, it was found that an injection volume of 25 µL yielded the lowest variability for the analytical signal in both indirect (analysis of IC followed by TC) and direct methods, as shown in Table III-2.

Table III-2. Peak area counts acquired through the indirect (analysis of IC followed by TC) and direct methods using different volumes of sample (ultrapure water).

Volume of sample (µL)	**Indirect Method** [a]		**Direct Method**	
	difference of Avg [b] *(Peak area count)*	**sd** [c] *(Peak area count)*	**Avg** [b] *(Peak area count)*	**sd** [c] *(Peak area count)*
10	-221	186	198	28
25	144	116	324	41
50	683	317	571	176

[a] Value of the analytical signal = Peak area count of TC – Peak area count of IC;
[b] Avg: average of 10 measurements;
[c] sd: standard deviation.

As such, it was decided to adopt an injection volume of 25 µL for the subsequent analyses. Using the values of the peak area counts obtained for ultrapure water with this injection volume, the following step was focused on testing whether the direct method is more precise than the indirect method through an *F*-test. As shown in Table III-3, the calculated value of *F* exceeds that of the critical value, thus indicating that the variance of the indirect method is significantly greater than that of the direct method at the 5% probability level, i.e. the direct method is more precise.

Table III-3. Results obtained from the *F* test applied to the values of the peak area counts acquired through the indirect (analysis of IC followed by TC) and direct methods using ultrapure water.

Volume of sample	**Analytical method**	**Peak area count**		**Degrees of freedom**	$\mathbf{F_{calculated}}$	$\mathbf{F_{critical}}$ *(P = 0.05)*
		Avg [a]	**sd** [b]			
25 µL	Indirect	144	116	9	8.005	3.179
	Direct	324	41			

[a] Avg: average of 10 measurements;
[b] sd: standard deviation.

Therefore, it was decided to apply the NPOC method for determining the DOC content (as a measure of the WSOC content) of each aqueous extract of the aerosol samples. Within the NPOC method, several sparging periods with high purity air were also tested in order to assess the most appropriate time to remove the IC (as CO_2) from the acidified sample. As shown in Fig. III-3, 2 minutes are proved to be sufficient to remove

any IC present in the sample. Furthermore, the average peak area count remains almost constant for times of sparging longer than 2 minutes.

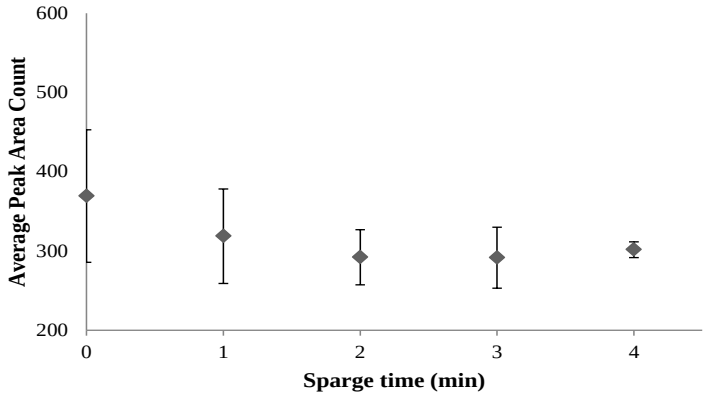

Fig. III-3. Effect of the sparging time in the average peak area counts (grey diamonds, 5 replicas) obtained in NPOC method using ultrapure water as a sample. The errors bars correspond to the standard deviation.

Another important aspect when using the NPOC method is the type of container (glass or plastic) employed to store the HCl reagent, which will be used to acidify the samples. As shown in Table III-4, when using the HCl stored in plastic containers, the average peak area count is higher than when using the HCl stored in glass containers. As such, only HCl stored in glass containers will be used in the subsequent analyses.

Table III-4. Effect of the type of HCl container on the average peak area counts (5 replicas, standard deviation in brackets) obtained in NPOC method using ultrapure water as a sample.

	Type of container	
	Plastic	**Glass**
Before acidification	257 (63)	254 (24)
After acidification	397 (67)	186 (9)

In this work, the determination of DOC by the NPOC method was performed using a six point calibration graph, established every week and obtained from standards of $HO_2CC_6H_4CO_2K$ prepared in ultrapure water ranging between 0 mg C L^{-1} and 1 mg C L^{-1}. Fig. III-4 represents an example of a calibration graph used for determining the DOC content of the aerosol aqueous extracts. Because the confidence interval of intercept does

not include the zero, each calibration equation was calculated by the algebraic form y = *b*x + *a*. The standard deviation of the slope S_b and the intercepted S_a ranged between, 6.747-13.02 and 4.085-7.883, respectively, and the standard error ranged between 12.63 and 24.36. The correlation coefficients range between 0.9986 and 0.9996. The detection limit of the method (0.016 mg C L^{-1}) was calculated according to Miller and Miller (2005), based on the blank (ultrapure water) signal plus three standard deviations of the blank.

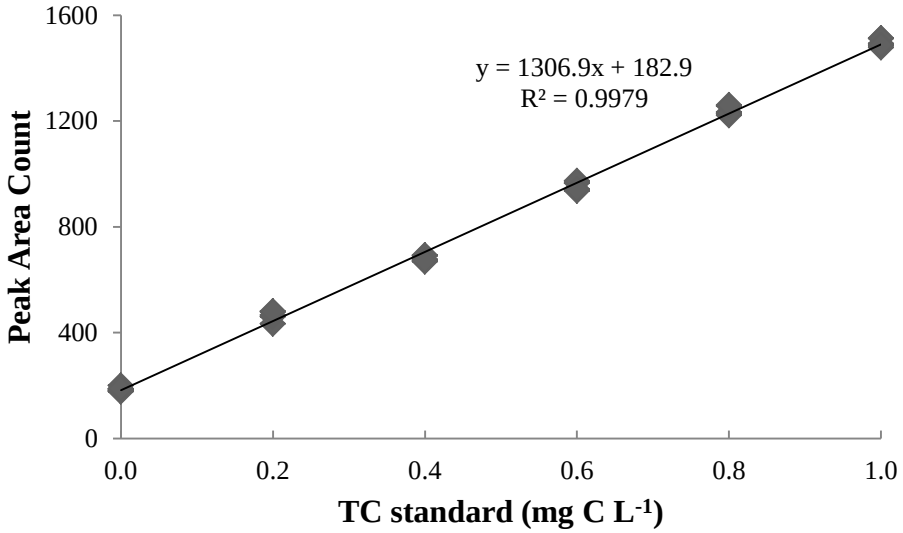

Fig. III-4. Example of a calibration graph used for determining the DOC content of the aerosol aqueous extracts using the NPOC method.

Briefly, the procedure adopted to determine the DOC content started by acidifying 10 mL of each standard/sample with 6 µL of 6M HCl (pH < 3) immediately before sparging with high purity gas for 2 minutes. Then, the standard/sample was injected into the TC furnace of the analyzer, where it was catalytically oxidized to CO_2 according to the principle of the NPOC method. For each standard and sample, five measurements of DOC were performed using an injection volume of 25 µL.

3.7. Isolation and fractionation of WSOM from the $PM_{2.5}$ samples

Prior to the isolation and fractionation of aerosol WSOC, and to obtain sufficient mass for the subsequent elemental analysis and structural characterization of the WSOM

samples, the aqueous extracts were batched together according to similar features in terms of ambient conditions and DOC content. These groups are described in section 4.5.

The aerosols WSOC samples were isolated and fractionated using a procedure similar to that developed by Duarte and Duarte (2005), which is illustrated in Fig. III-5. In the procedure developed by those authors, an Amberlite^{TM} XAD-8 resin was used to isolate the most hydrophobic WSOC components of the aerosol aqueous extracts. However, the XAD-8 resin is no longer commercially available and it was replaced by the comparable Supelite^{TM} DAX-8 resin, which has been employed to concentrate and isolate DOM from diverse environments, including the WSOM in this study. The aqueous extracts were acidified at pH 2.2 with 6M HCl and then pumped onto the DAX-8 resin at a flow rate of 0.8 mL min^{-1}. After this concentration stage, the organic matter adsorbed onto the resin was washed with one column volume (35 mL) of ultrapure water, also at a flow rate of 0.8 mL min^{-1}, to remove the inorganic species. The desalting effluent from the DAX-8 resin was also collected separately. At a first stage, specifically for aerosols WSOC samples collected in *sampling campaign I*, the organic matter retained in the resin was back eluted with a solution of MeOH:H_2O in the proportion 1:1, following the procedure of Duarte and Duarte (2005). The eluates were evaporated almost to dryness (final volume < 1 mL) in a rotary evaporator at 30ºC and then re-dissolved in ultra-pure water. Before and after each step, the UV-Vis absorbance at 250 nm and the DOC content (by the NPOC method) of the influents and effluents from the DAX-8 column and also of the desalting effluents and reconstituted eluates were measured for assessing losses of organic matter during the isolation procedure. Finally, the eluates were freeze-dried and kept on a dessicator over silica gel for further analysis.

At the end of this first stage, it was verified that the percentage of DOC recovery from the DAX-8 resin was lower than those reported by Duarte and Duarte (2005) for the Amberlite^{TM} XAD-8 resin (additional information in section 4.7.1). In order to improve the DOC recovery from the DAX-8 resin, two different solutions with different proportions of MeOH:H_2O were tested using a fulvic acid reference sample (Pony Lake, 1R109F) obtained from the International Humic Substances Society (IHSS). In this study, aqueous solutions (0.9 -1.25 mg C L^{-1}) of the Pony Lake fulvic acids were pumped onto the DAX-8 resin. A desalting procedure similar to that previously described was also applied, followed

by the back elution of the retained organic matter with solutions of MeOH:H_2O in the following proportions: 1:1 and 3:2. In a similar fashion, the eluates were evaporated almost to dryness in a rotary evaporator at 30 ºC and then re-dissolved in ultra-pure water. The results of this study are described in the section 4.7.1, and they indicate that the percentage of DOC recovery from the DAX-8 resin is higher when employing a higher content of organic solvent (i.e. MeOH). Therefore, at a second stage, specifically for aerosols WSOC samples collected in *sampling campaign II*, the back elution of the retained organic matter was performed using a solution of MeOH:H_2O in the proportion 3:2.

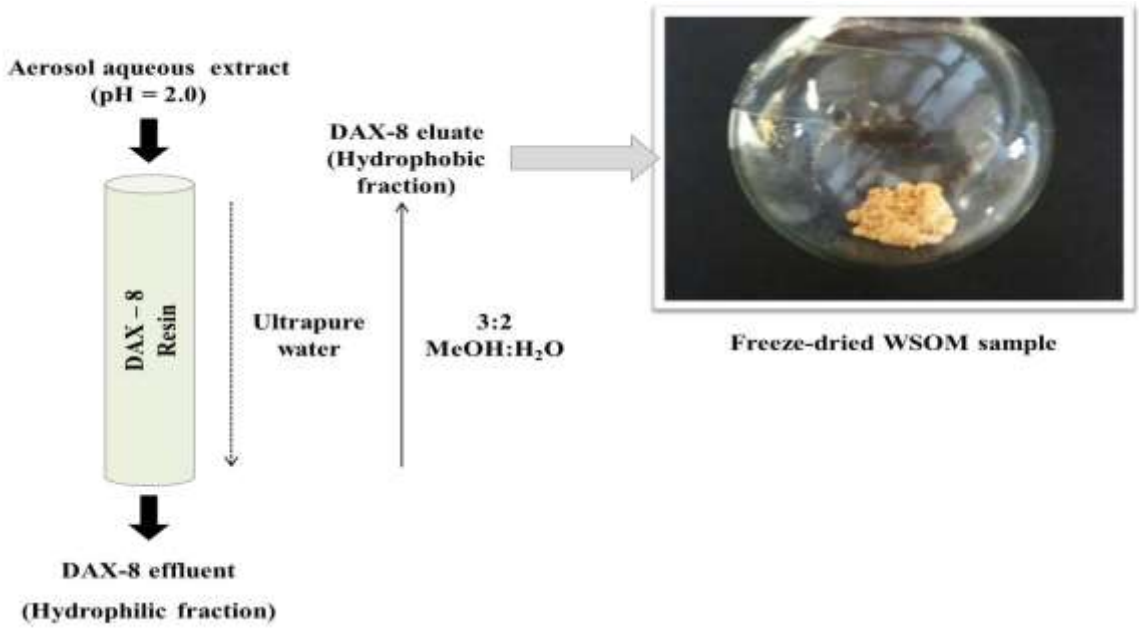

Fig. III-5. Scheme of the isolation/fractionation procedure of the aerosol WSOM samples.

3.8. Elemental analysis of the WSOM from the $PM_{2.5}$ samples

Elemental analysis of the isolated WSOM was performed with a Truspec 630-200-200 analyzer. Three replica of the contents of carbon (C), hydrogen (H), and nitrogen (N) were performed and corrected for the moisture and ash content of the samples, using the information obtained by thermogravimetric analysis (Duarte, 2006).Usually, the samples are heated until 750 ºC under an air stream. The temperature program used includes three steps of heating at 10 ºC min^{-1}, with a hold time at the final temperature of each step: 60

min at 60 ºC, 60 min at 100 ºC, and 30 min at 750 ºC. The moisture content refers to the weight lost after 1h at 60 ºC and the ash content to the final weight at 750 ºC. Taking into account that at the end of the isolation procedure, very small quantities of the WSOM fractions were obtained (additional information in section 4.5), in this study it was decided to use the thermogravimetric data (median values of the percentages of weight loss (at 60 ºC) and ash content) obtained by Duarte (2006) for the aerosol WSOM collected in Moitinhos, Portugal in order to correct the content of C, H, and N. The oxygen (O) content of each WSOM sample was calculated by subtraction from 100% (%O = 100-(%C + %H + %N)) after the previous correction. The atomic ratios H/C, O/C and N/C were also calculated.

3.9. Spectroscopic characterization of the WSOM from the $PM_{2.5}$ samples

3.9.1. Ultraviolet- Visible (UV-Vis) spectroscopy

The UV-Vis spectra (in the range of 210–500 nm) were recorded on a UV–Vis spectrophotometer Shimadzu (Dusseldorf, Kent, Germany) Model UV 2101PC in 1cm path length quartz cells. Ultrapure water was used as a blank.

3.9.2. Excitation-Emission matrix (EEM) fluorescence spectroscopy

The Emission-Excitation Matrix (EEM) fluorescence spectra were recorded on a spectrophotometer JASCO (Tokyo, Japan), Model FP-6500. The EEM fluorescence spectroscopy involved scanning and recording of 20 individual emission spectra (230-510 nm) at sequential increments of 10 nm of excitation wavelength between 220 and 400 nm. The spectra were recorded at a scan speed of 100 nm min^{-1} using excitation and emission slit bandwidths of 10 nm. The peaks due to water Raman scatter were removed from all spectra by subtracting the ultrapure water blank spectra. In order to avoid concentration effects, the spectra were also normalized to DOC content of the sample and are shown as

specific fluorescence intensity (g^{-1} C L) versus excitation and emission wavelengths (nm). Additional corrections for fluctuation of instrumental factors and scattering effects (inner filter effects) were not applied to the acquired spectra. Nevertheless, all spectra were recorded using the same instrument and the same experimental conditions, allowing comparison between them and a qualitative discussion of the fluorescence features.

The synchronous fluorescence spectra presented in this work contain fluorescence intensity data withdrawn from the EEM fluorescence profiles. The synchronous spectra with $\Delta\lambda$ of 60 nm were obtained by fitting the mathematical equation $\lambda_{Emission} = \lambda_{Excitation} + \Delta\lambda$ to the EEM profiles and are also shown as specific fluorescence intensity (g^{-1} C L) versus excitation wavelength (nm).

3.9.3. Fourier transform infrared - attenuated total reflectance (FTIR-ATR) spectroscopy

The FTIR-ATR spectra of the isolated aerosol WSOM samples (section 5.5) were recorded for frequencies between 550 and 4000 cm^{-1} in a PerkinElmer FTIR spectrophotometer (FTIR System Spectrum BX). The spectral resolution was 4 cm^{-1} and 64 scans were averaged in each spectrum acquisition.

3.9.4. Solid-state cross polarization with magic angle spinning ^{13}C nuclear magnetic resonance (CPMAS ^{13}C NMR) spectroscopy

All CPMAS ^{13}C NMR spectra were acquired at 125.77 MHz on a Bruker Avance-500 NMR spectrometer using a standard 4 mm double-bearing probe head. Transients were recorded with a contact time of 1.5 ms and a spinning rate of 9 kHz. The recycle delay was 5s and the length of the proton 90º pulse was 3.5 μs. Chemical shifts are quoted in ppm from the external calibrant tetramethylsilane.

The solid-state CPMAS ^{13}C NMR spectra were split into seven spectral regions on the ppm scale (0–50, 50-60, 60-95, 95-110, 110-160, 160-190, 190-230), each

corresponding to different carbon functional groups, which are assigned in section 5.6. The integrated areas of each spectral region were determined off-line using the ACDLabs software free package. Percentage peak areas of individual peaks were calculated by dividing their areas by the total spectral peak area of the sample.

3.10. Comprehensive two-dimensional liquid chromatography of WSOM from $PM_{2.5}$ samples

The procedure adopted for the analysis of aerosol WSOM samples by means of LC x LC was based on the method developed by Duarte et al. (2012). The aerosol WSOM samples were prepared by diluting each sample (before freeze-drying, section 3.7) in 10% of the mobile phase (v/v) of the 1st dimension. The DOC concentrations of the analysed WSOM samples (were in the range of 0.1 and 0.4 mg C mL^{-1}).

The 1st dimension consisted of a JASCO semi-micro HPLC pump (model PU-2085 Plus), a Rheodyne injection valve (model 7725i) equipped with a 20 μL loop, and an Acclaim Mixed-Mode HILIC-1 column (Dionex; diameter 4.6 mm; length 150 mm; comprised of 5 μm high-purity, porous, spherical silica particles with 120 ˚A diameter pores bonded with alkyl diol functional groups). The 1st dimension was operated in isocratic mode using a mobile phase composition consisting of 20 mM CH_3COONH_4 (pH adjusted to 6.0 with 1.1 mM CH_3COOH) and 10% (v/v) ACN. The flow rate was 0.020 mL min^{-1} and the temperature of the analytical column was maintained at 30 ºC in a JASCO column oven (model CO-2065 Plus).

In the 2nd dimension, a JASCO quaternary low pressure gradient pump (model PU-2089 Plus) and a PSS Suprema 30 ˚A analytical column (Polymer Standards Service GmbH; diameter 8 mm; length 150 mm; particle size 10 μm; separation range 100–30,000 Da; stationary phase polyhydroxymethacrylate copolymer) were applied. The 2nd dimension was also operated in isocratic mode with a mobile phase composition consisting of 20 mM NH_4HCO_3 (pH 8.0) and 11% (v/v) ACN. The flow rate was 2.5 ml min^{-1} and the temperature of the analytical column was also maintained at 30 ºC in a JASCO column oven. The outlet of the 2nd dimension column was also connected to three detectors in

series: a diode array detector (JASCO, model MD-2010) operating at 254 nm, a fluorescence detector (JASCO, model FP-2020 Plus) operating at emission/excitation wavelengths of 240/410 nm and 320/415 nm, and an evaporative light-scattering detector (SEDEX, model 80-LT-ELSD) operating at 60 °C and 3.5 bar.

The 1st and 2nd dimensions were interfaced with an eight port high pressure two-position interfacing valve (VICI® AG International) equipped with two identical 50 μL sampling loops. Modulation time was 150 s. The valve was controlled by the PSS WinGPC Unity software (Polymer Standards Service GmbH) by receiving a start-up signal from a PSS Universal Data Center (model UDC 810). This software was also used for the acquisition and handling of all data set. The SEC column in the 2nd dimension was calibrated using sodium polystyrenesulfonate standards (MW at peak maximum, (Mp): 208, 891, 4210, 6430, and 15800 Da, obtained from Sigma Aldrich), and HPLC grade acetone (58 Da) 5% (v/v), which also served as a permeation volume probe. These standards were prepared by dissolving approximately 1 mg of each compound in 1mL of the mobile phase of the 2nd dimension.

IV

Global carbon balance and isolation of water-soluble organic matter from atmospheric aerosols

4.1. Introduction

This chapter begins with an assessment of the meteorological parameters recorded during the *sampling campaigns I* and *II* in order to group together the atmospheric aerosol samples according to similar ambient conditions, which will be representative of different seasonal periods. Then, the average ambient concentrations of the $PM_{2.5}$, $PM_{2.5-10}$, TC, OC, EC, and WSOC for each collected aerosol sample will be evaluated. Based on the average ambient concentrations of the carbonaceous aerosol fractions, an aerosol mass balance was also performed in order to infer on its seasonal variability and further assist on the evaluation of the contribution of primary and secondary sources to fine particulate WSOM. This chapter also describes the isolation/fractionation procedure employed to obtain a representative aerosol WSOM fraction of the different seasonal periods.

4.2. Assessment of the meteorological parameters recorded during the sampling campaigns

The meteorological data, including air temperature, RH, precipitation, and wind velocity, were provided by the Portuguese Sea and Atmosphere Institute and by the Department of Physics of the University of Aveiro. The air mass back trajectories were also computed and evaluated for each sampling campaign. The air mass back trajectories were obtained by means of the HYbrid Single Particle Lagrangian Integrated Trajectory (HYSPLIT4) model (24 h interval, 7 day), using the Reanalyses (Global, until October 2010) and the Global Data Assimilation System (GDAS, from November 2010) meteorological databases, accessed via National Oceanic and Atmospheric Administration (NOAA) Air Resources Laboratory READY website (Draxler and Rolph, 2013; http://www.arl.noaa.gov/HYSPLIT.php, last access on March 2013).

4.2.1. Meteorological parameters recorded during *sampling campaign I*

Table IV-1 summarizes the meteorological data acquired during *sampling campaign I* in Summer 2008 and 2009 and in Spring 2009. The median of the air temperature values were very similar among the different sampling periods, varying from ca. 15 to 23ºC. The lowest values for the air temperature were recorded during the Spring 2009 season, during the night periods. Also, the total precipitation accumulated was higher during this somewhat colder season (36.9 mmH_2O) than in the warmer periods (3.9 and 0.4 mmH_2O for Summer 2008 and 2009, respectively). The widest ranges of variation of the RH values were also verified for the Spring season, thus yielding the lowest median values for this meteorological parameter during this period. The median of the wind speed values were also very similar among the different sampling periods, varying from 1.7 to 2.9 m s^{-1}. The air mass back trajectories during the *sampling campaign I* (Annex A), indicates that the sampling location is mostly under the influence of wind derived from both maritime and continental surroundings. The calculated air mass back trajectories also showed that only two sampling periods in Summer 2008 had air masses travelling most of the time above the continent. In the sampling periods of 22– 29 July 2008, 01– 08 June 2009, and 27 July – 03 August 2009, the air masses came from the maritime surroundings and travelled mainly above the Atlantic Ocean.

Table IV-1. Meteorological data obtained during *sampling campaign I* (additional information in section 3.3).

Season	Sample Code	Sampling date	Air temperature (°C)		Precipitation [b] (mmH_2O)	RH (%)		Wind velocity (ms^{-1})		Air mass back trajectory
			Range [a]	Median		Range [a]	Median	Range [a]	Median	
Summer 2008	**SU08-1**	23 -30 Jun 2008	14.4 – 23.0	17.7	0.0	67 - 98	88	0.5 - 7.7	2.6	Continental
	SU08-2	08-15 Jul 2008	13.6 – 26.6	18.1	1.0	45 - 94	80	0.3 – 8.4	2.6	Maritime/continental
	SU08-3	15-22 Jul 2008	15.7 - 26.6	23.4	0.0	45 - 98	85	0.3 – 5.2	1.7	Continental
	SU08-4	22-29 Jul 2008	14.4 - 20.7	20.7	2.9	62 - 98	84	0.6 – 5.4	2.0	Maritime
Spring 2009	**SP09-1**	27 April – 4 May 2009	8.2 - 26.1	15.2	9.7	31 - 95	76	0.0 – 7.1	2.9	Maritime/continental
	SP09-2	04-11 May 2009	12.7 – 25.4	16.4	21.1	33 - 92	76	0.2 – 5.7	2.0	Maritime/continental
	SP09-3	18-25 May 2009	9.8 – 20.6	15.7	6.1	52 - 95	79	0.2 – 7.1	2.4	Maritime/continental
	SP09-4	25 May – 01 Jun 2009	12.0 – 31.8	19.2	0.0	20 - 95	72	0.1 – 7.4	2.4	Maritime/continental
Summer 2009	**SU09-1**	01-08 Jun 2009	15.0 – 21.4	17.9	0.2	63 - 95	79	0.3 – 6.7	1.8	Maritime
	SU09-2	06-13 Jul 2009	14.6 – 24.5	18.6	0.0	57 - 93	79	0.2 – 7.4	2.7	Maritime/continental
	SU09-3	27 Jul – 03 Aug 2009	13.2 – 22.9	19.0	0.1	56 - 94	80	0.1 – 6.6	2.3	Maritime
	SU09-4	03-09 Aug 2009	14.7 – 23.0	19.1	0.1	62 - 94	83	0.5 – 5.7	2.4	Maritime/continental

[a] Maximum and minimum values recorded during each sampling period.
[b] Total precipitation accumulated in each sampling period.

4.2.2. Meteorological parameters recorded during *sampling campaign II*

The weekly and seasonal variability, in terms of median, minimum, and maximum values, of the air temperature, RH, wind velocity, and total precipitation accumulated is shown in Fig. IV-1. As expected, the highest median values for the temperature (Fig. IV-1a) were verified during the Summer season (the highest value, 39ºC, was recorded in week AVE 33), although higher median values were also verified in weeks AVE 23, 25, and 27 during Spring 2010 and weeks AVE 40 to 43 in Autumn 2010. By the end of week AVE 46, in Autumn 2010, the temperature gradually started to decrease, reaching a minimum of 0 ºC in week AVE 4 in mid December 2009 and of 2 ºC in weeks AVE 50 and 58, in early December 2010 and late January 2011, respectively. In what concerns the annual distribution of the RH (Fig. IV-1c), the range of variation was between 20% and 99%. Typically, and regardless of the seasonal period, the values of the RH follow a daily pattern, with higher values during the night, coincident with lower air temperatures, as can be observed in Fig. IV-2. Regarding the median values of the wind velocity (Fig. IV-1d), values lower than 3 ms^{-1} were observed across most of the sampling period, although during weeks AVE 20 and 22 in Spring and week AVE 61 in Winter 2011 it reached 4 ms^{-1}.

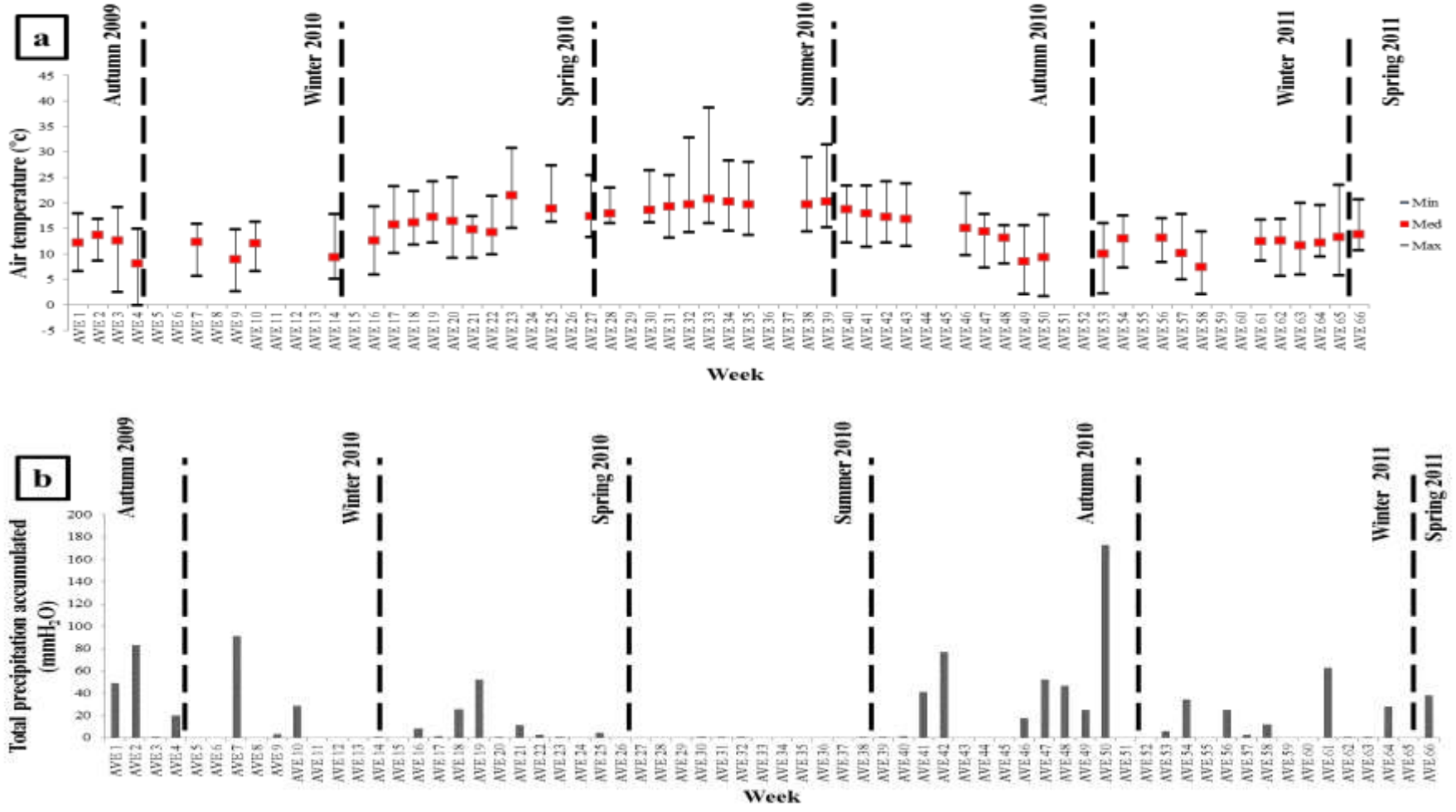

Fig. IV-1. Weekly and seasonal variability (in terms of median, minimum, and maximum values) of the (a) air temperature (in ºC), (b) total precipitation accumulated (in mmH_2O), (c) RH (in %), and (d) wind velocity (in ms^{-1}) recorded during the *sampling campaign II*.

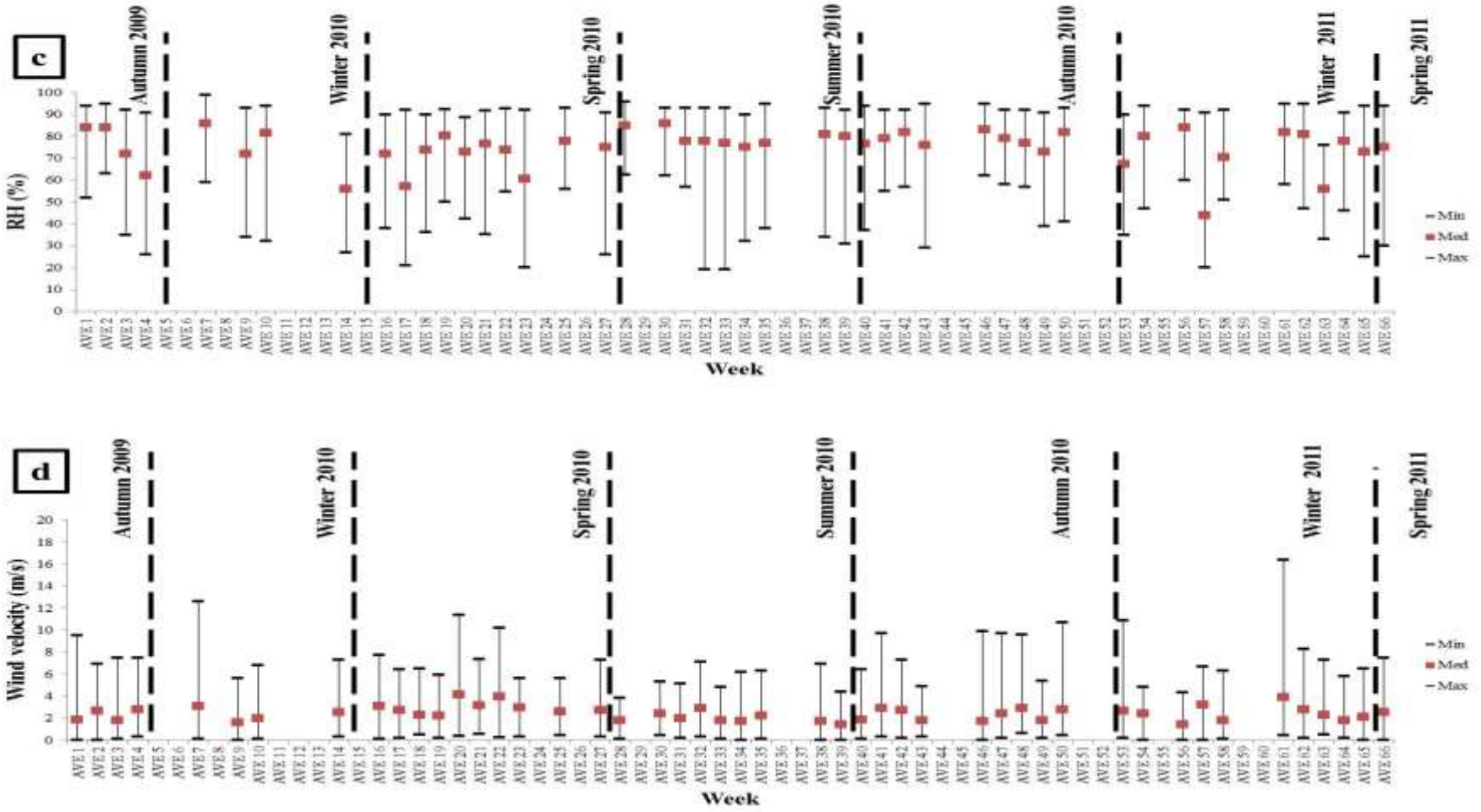

Fig. IV-1. *Continued*.

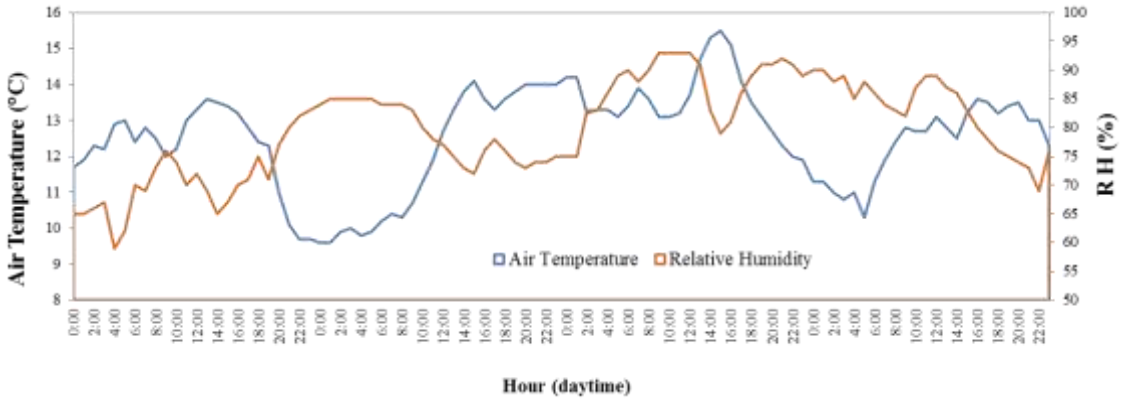

Fig. IV-2. Daily variability of the air temperature (in ºC) and HR (in %) recorded between 1 and 4 January 2010.

Fig. IV-1b illustrates the weekly variation of the total accumulated precipitation recorded during the *sampling campaign II*. As shown, the occurrence of precipitation was much lower in the Summer season (total of 2 mmH_2O between weeks AVE 28 and AVE 39) than in the colder seasons (ranging from 0 to 173 mmH_2O), with the highest value being recorded in week AVE 50 (in Autumn 2010).

The air mass backward trajectories were also calculated for each week of the *sampling campaign II*. The entire record of air mass backward trajectories during this sampling campaign can be found in Annex C. Fig. IV-3 presents the predominant air mass back trajectories in each season (Autumn 2009, Winter 2010, Spring 2010, Summer 2010, Winter 2011, and Spring 2011). As shown in Fig. IV-3, during Autumn 2009 and Autumn 2010, the sampling location is mostly under the influence of wind derived from maritime surroundings, whereas in Winter 2010, Spring 2010, Winter 2011 and Spring 2011 the air masses come from both maritime and continental surroundings. The calculated air mass back trajectories also show that in Summer 2010, the air masses were travelling most of the time above the continent. Additionally, during this season, the occurrence of massive forest fires episodes was registered, with the largest incidence being verified between weeks 33 and 35, coincident with the period of highest air temperature (maximum of 39 °C). According to the report of the Agriculture, Rural Development and Fisheries Ministry (MADRP-Direcção de Unidade de Defesa da Floresta, 2011), the total burnt area of forest land was about 133 090 ha in 2010 at Portugal Continental, with 388 "Hot flashes" and 41 fires occurring between weeks 28 and 32, and 972 "Hot flashes" and 79 fires occurring

between weeks 33 and 35 at District of Aveiro (total burnt area of forest land was about 8 299 ha). In Winter 2010, Winter 2011 and Spring 2011, the air masses trajectories came from both maritime and continental surroundings, although sporadically they also travelled above North Africa.

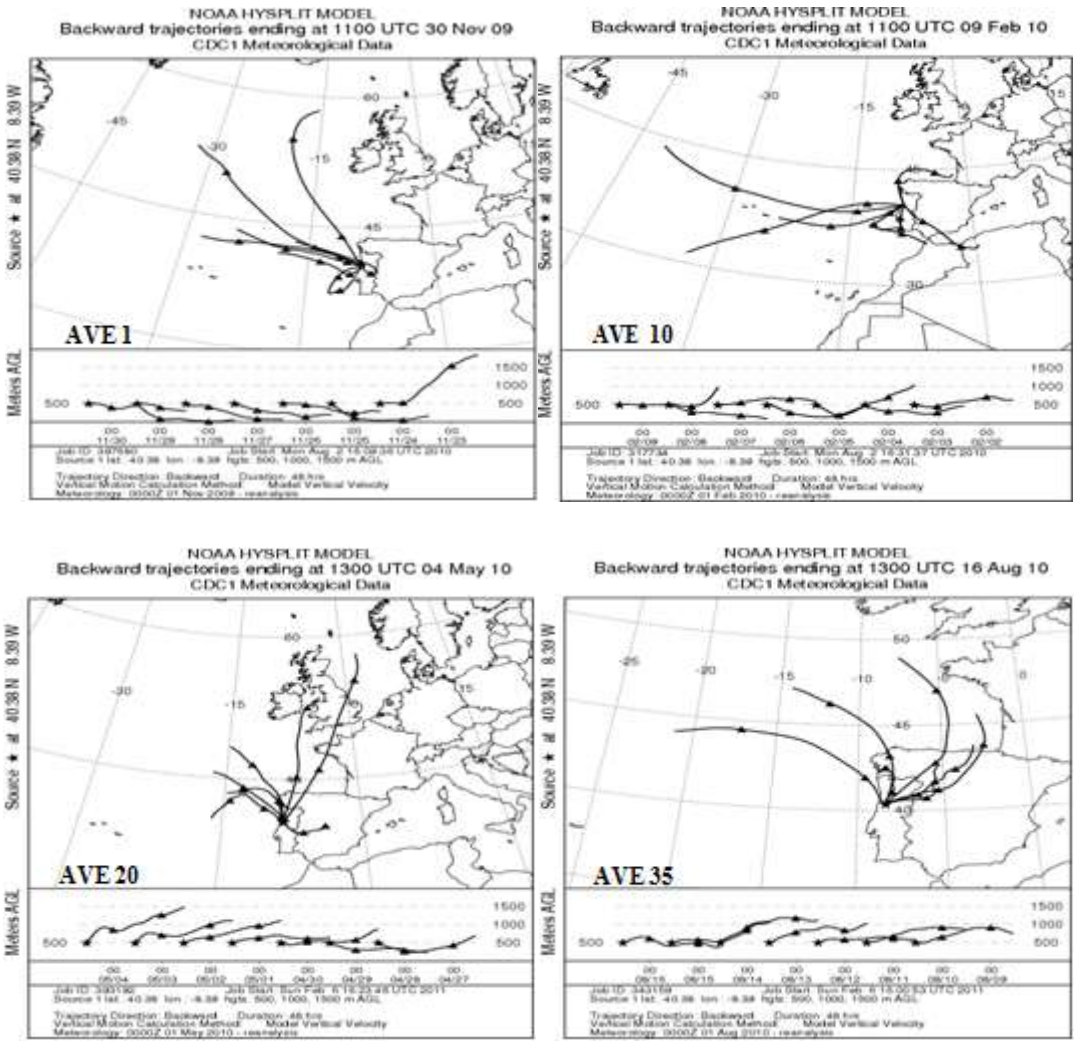

Fig. IV-3. Air mass backward trajectories ending at Aveiro at distinct altitudes (>500 m a.g.l.) during: Autumn 2009 (AVE 1, 23–30 November 2009); Winter 2010 (AVE 10, 2-9 February 2010); Spring 2010 (AVE 20, 27 April to 4 May 2010); Summer 2010 (AVE 35, 09–16 August 2010); Autumn 2010 (AVE 46, 2-9 November 2011), Winter 2011 (AVE 64, 8-15 March 2011), and Spring 2011 (AVE 66, 22-29 March 2011).

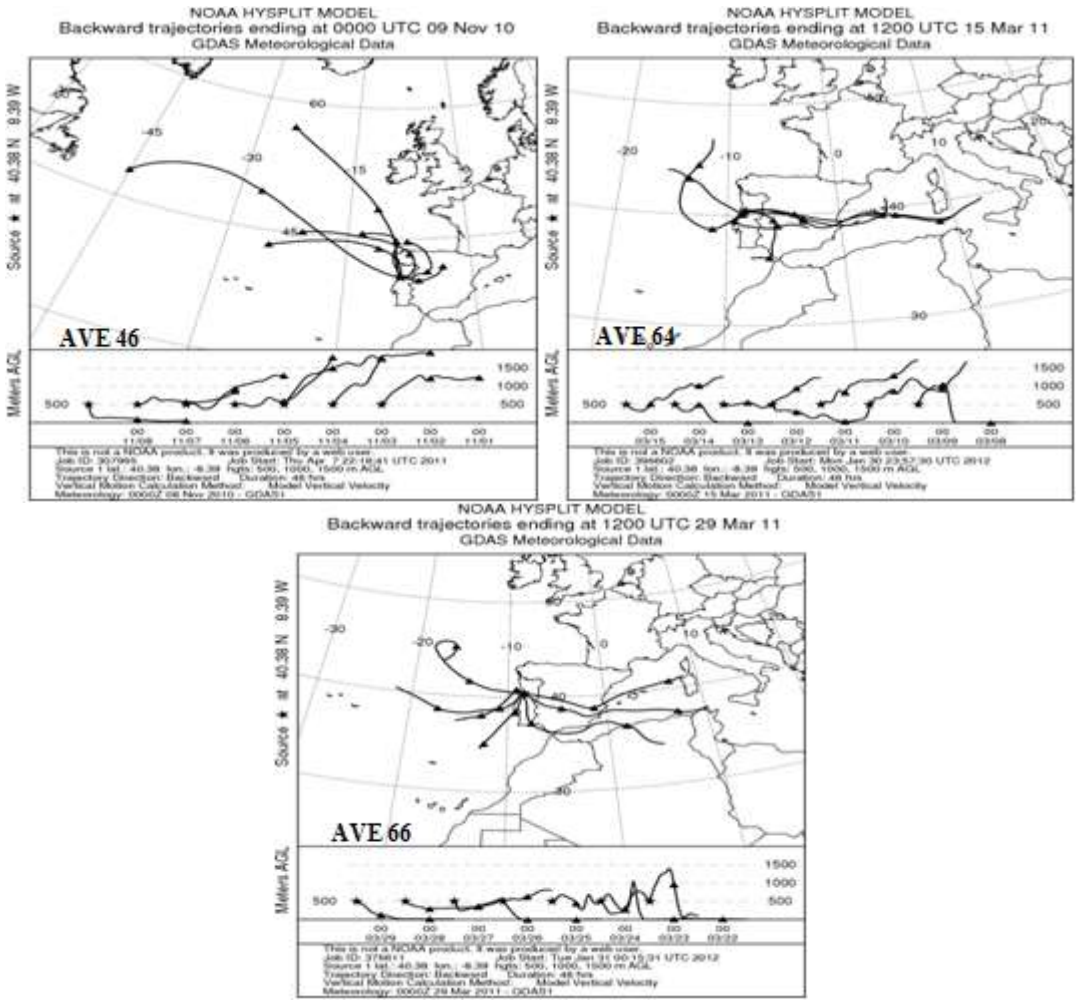

Fig. IV-3. *Continued.*

4.3. Assessment of OC adsorption phenomena onto quartz filters during aerosol sampling

The most common approach for determining the composition of atmospheric aerosols involves the collection of the particulate matter onto filter substrates. The sampling time depends on the analytical sensitivity of the different methodologies, and it can vary typically from several hours in urban areas to a day or more under clean background conditions or in areas with very low particle concentrations (Jacobson et al., 2000; McMurry, 2000). The collection of aerosol particles by means of a high-volume sampler using quartz fibre filters is known to be subjected to potential sampling bias. From

one side, the volatilization of SVOC has been referred as a significant source of negative bias, whereas the adsorption of gas-phase compounds onto filters during and/or after sample collection is considered as a source of positive bias (Turpin et al., 1994). The occurrence of such phenomena has been reported in several studies (Mayol-Bracero et al., 2002; Viana et al., 2006a; Salma et al., 2007; Mkoma et al., 2010) and it can affect the composition of the collected aerosols particles in relation to the real atmosphere composition when filter-based devices are used. Negative bias during aerosol particles sampling can be estimated using carbon-impregnated in backup glass filter approach (Subramanian et al., 2004), whereas positive bias can be assessed using a tandem filter method (Turpin et al., 1994). This latter method consists of (1) a Teflon filter followed by a quartz filter or (2) a set of two (front and back) quartz fibre filters (Turpin et al., 1994). According to comprehensive review conducted by Turpin et al. (2000), sampling bias contributions to OC mass measurements range from –80% for volatilization-induced bias up to +50% for adsorption-induced bias.

Several papers have also reported that the occurrence of volatilization and/or adsorption phenomena during aerosol sampling are of importance for the WSOC component (Mayol-Bracero et al., 2002; Salma et al., 2007). Using quartz fibre filters tandem method for aerosol sampling in Amazonia (forest environment), Mayol-Bracero et al. (2002) reported back-to-front filters ratios for the WSOC concentration of about 5%. Salma et al. (2007) have also studied sampling bias on an urban environment using the tandem quartz fibre filter method. The authors reported an average back-to-front ratio of 28% for the WSOC, which was even higher than that estimated for the OC component (17%). These results allowed the authors to suggest that the organic compounds that are mainly responsible for the positive (adsorptive) sampling bias are likely to be more water soluble, thus they possibly contain more polar functional groups or they may be more oxidized than the organic matter in general (Salma et al., 2007).

Taking into account the results reported in the literature for the occurrence of sampling artefacts when using filters-based devices, this work also entailed an assessment of the positive sampling artefacts (using the tandem quartz fibre filter method) eventually existing during aerosol collection at Aveiro (*sampling campaign I*). The $PM_{2.5}$ and $PM_{2.5-10}$ mass concentrations ($\mu g\ m^{-3}$) from both the front and back filters are shown in Fig. IV-4.

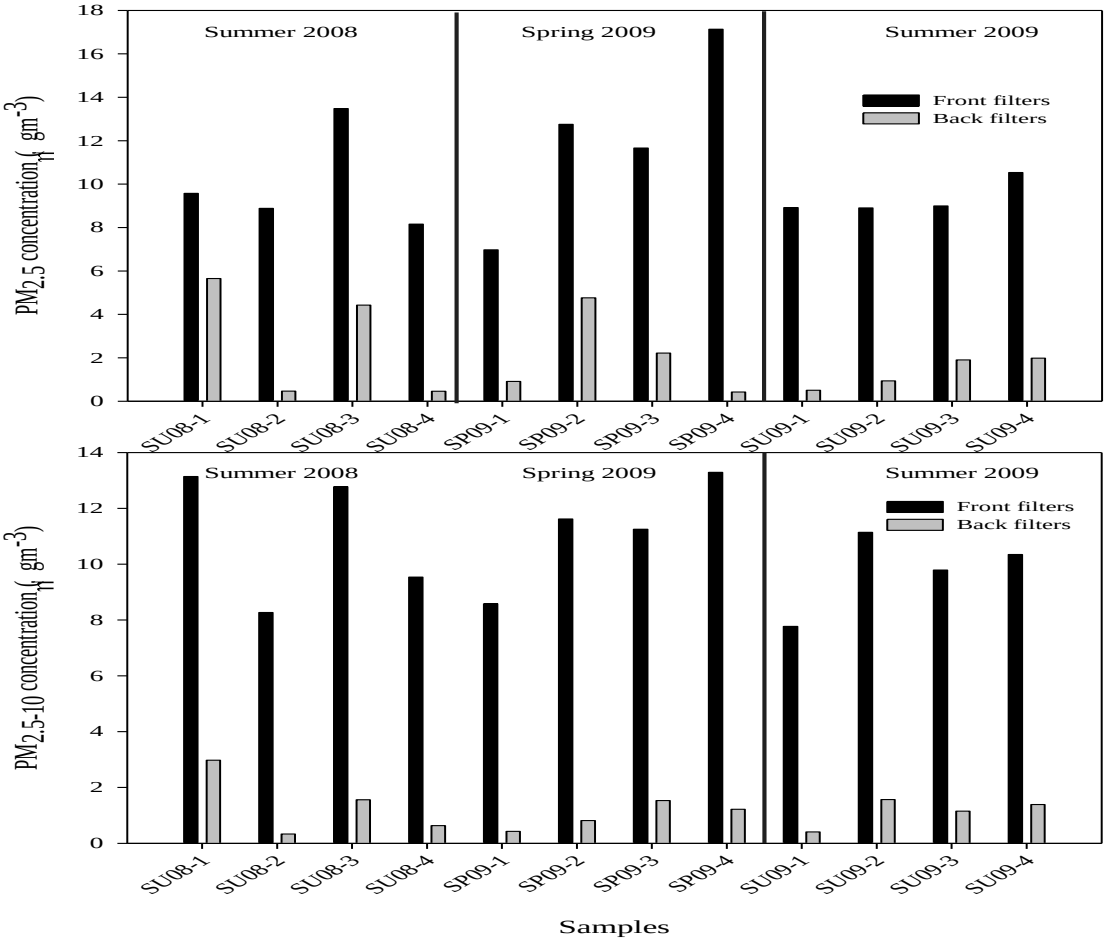

Fig. IV-4. Distribution of $PM_{2.5}$ and $PM_{2.5-10}$ mass concentrations (μg m^{-3}) on the front and back filters during *sampling campaign I*.

The weekly $PM_{2.5}$ concentrations in the top filter varied from 8.2 to 13.5, 7.0 to 17.1 and 8.9 to 10.5 μg m^{-3} for Summer 2008, Spring 2009 and Summer 2009 seasons, respectively. Regarding the $PM_{2.5-10}$ fraction, the mass concentrations in the front filters ranged from 8.2 to 13.5, 8.6 to 13.3 and 7.8 to 11.1 μg m^{-3} for Summer 2008, Spring 2009 and Summer 2009, respectively. The back-to-front ratios for the $PM_{2.5}$ concentration ranged from 5.3 to 59.1, 2.5 to 37.4, and 5.6 to 21.2 % for the Summer 2008, Spring 2009 and Summer 2009 seasons, respectively, whereas the back-to-front ratio for the $PM_{2.5-10}$ fraction and for the same seasons ranged from 4.0 to 22.7, 5.0 to 13.6 and 5.2 to 14.1 %, respectively.

The average concentrations (μg C m^{-3}) and standard deviations for the OC, EC, and WSOC fractions in the front and back filters from both $PM_{2.5}$ and $PM_{2.5-10}$ samples are

summarized in Table IV-2. The OC concentrations in the front filters varied from an average of 0.94 (0.09) to 1.98 (0.17) μg C m^{-3} for the $PM_{2.5}$ samples and 0.28 (0.03) to 0.51 (0.04) μg C m^{-3} for the $PM_{2.5-10}$ samples, with the samples collected in the Spring season presenting higher average values than those collected during the warmer periods.

Table IV-2. Average concentration (in μg C m^{-3}) and standard deviation (in brackets) of the main carbonaceous components from both $PM_{2.5}$ and $PM_{2.5-10}$ in the top and back filters during *sampling campaign I*. The number of aerosol samples in each season was 4.

Season / PM	OC (μg C m^{-3})		EC (μg C m^{-3})		WSOC (μg C m^{-3})	
	Front	**Back**	**Front**	**Back**	**Front**	**Back**
$PM_{2.5}$						
Summer 2008	1.21 (0.13)	0.41 (0.06)	0.31 (0.14)	n.d.	0.64 (0.10)	0.17 (0.03)
Spring 2009	1.98 (0.17)	0.35 (0.03)	0.08 (0.02)	n.d.	0.85 (0.06)	0.28 (0.04)
Summer 2009	0.94 (0.09)	0.19 (0.03)	0.13 (0.01)	n.d.	0.43 (0.03)	0.14 (0.01)
$PM_{2.5-10}$						
Summer 2008	0.48 (0.06)	0.02 (0.02)	0.02 (0.03)	n.d.	0.12 (0.01)	n.a.
Spring 2009	0.51 (0.04)	0.03 (0.01)	0.02 (0.02)	n.d.	0.12 (0.04)	n.a.
Summer 2009	0.28 (0.03)	0.02 (0.00)	0.01 (0.00)	n.d.	0.08 (0.01)	n.a.

n.d.: not detected; n.a.: not assessed

These results suggest that during Summer, the higher temperatures favor the gaseous phase in the gas-particle partitioning of the SVOC. Moreover, the highest OC concentrations were found in the fine size range particles, as should be expected from the typical conceptual segmentation models of chemical species *versus* the aerosol mass size distribution (Seinfeld, 1986; Krivácsy and Molnár, 1998; Seinfeld and Pandis, 1998; Samara and Voutsa, 2005).

Overall, the back-to-front ratios for the OC in the $PM_{2.5}$ samples ranged from 15 to 47%, 11 to 38%, and 17 to 21% in Summer 2008, Spring 2009, and Summer 2009 seasons, respectively. For the same seasons, but in the coarse particles, the back-to-front ratios for the OC are much lower, ranging from 2.6 to 8.4%, 4.4 to 9.4%, and 6.7 to 9.6%, respectively. The EC concentration in front filters varied from an average of 0.08 (0.02) to

0.31 (0.14) μg C m^{-3} for the $PM_{2.5}$ samples and 0.01 (0.00) to 0.02 (0.03) μg C m^{-3} for the $PM_{2.5-10}$ samples. Since EC has predominantly primary origin (Seinfeld and Pandis, 2006), no EC was detected in the back filters. This finding is in accordance with those of reported by Viana et al (2006a), Salma et al. (2007), Mkoma et al. (2010). With regard to the WSOC in the front filters of the $PM_{2.5}$ samples, this water-soluble fraction accounts, on average, to (53±9)%, (42±3)%, and (46±11)% of the OC for the Summer 2008, Spring 2009, and Summer 2009 seasons, respectively. In the $PM_{2.5-10}$ samples, also in the front filters, the contribution of WSOC to the OC is somewhat lower, accounting on average to (24±9)%, (23±4)%, and (28±7)% for the Summer 2008, Spring 2009, and Summer 2009 seasons, respectively. When looking at the back-to-front ratios for the WSOC in the $PM_{2.5}$ samples, the obtained values ranged from 16 to 39%, 19 to 68%, and 24 to 53% in Summer 2008, Spring 2009, and Summer 2009, respectively. With the exception for the Summer 2008 season, the back-to-front ratios for the WSOC in the $PM_{2.5}$ samples are higher than those for OC. These results suggest that the organic compounds that are responsible for the positive sampling bias (adsorptive phenomenon) seem to be more water-soluble in nature. These findings are in agreement with those of Salma et al. (2007), who reported back-to-front ratios of 28% for the WSOC fraction and of 17% for the OC in $PM_{2.5}$ samples collected in an urban area, during a non-heating Spring season. These results also suggest that during sampling the water-soluble organic compounds in the back filters were formed via adsorption on the filter surface of volatile gaseous precursors from both anthropogenic and biogenic emission sources, and by heterogeneous reactions with oxidants (Salma et al., 2007).

Several methods have been proposed to correct the sampling bias phenomena when collecting atmospheric aerosols, including the backup filter subtraction to estimate the positive bias (e.g. Viana et al., (2006a) and Salma et al., (2007)), and the use of denuder-based methods to correct positive and negative (volatilization) bias (Turpin et al., 2000). Recently, Maimone et al. (2011) have discussed bias correction options in large routine sampling networks, and the authors presented a regression method based on the assumption of a linear relationship between the measured OC and the mass of particulate matter, whose linearity are not always valid. The authors concluded that, taking into account that the adsorption of organic gases increases with increasing atmospheric concentrations of organics products, the subtraction of an average bias from all samples

will underestimate OC for lower-concentration samples and will overestimate OC for higher-concentration samples (Maimone et al., 2011).

Apparently, one of the easiest ways for obtaining sampling-positive bias-corrected atmospheric concentrations of OC and WSOC is by subtraction of their respective amounts determined on the back quartz filters. Nevertheless, for applying this method one must assume that the back-to-front ratios for both OC and WSOC are independent of the seasonal period in order to apply the same correction factor for the all set of atmospheric aerosol samples. This assumption seems difficult to accomplish since both OC and WSOC concentrations in the back quartz fibre filters vary in accordance to the meteorological parameters (i.e., season). Therefore, in this work, and for the *sampling campaign II*, the collection of atmospheric aerosol samples was performed without any attempt for controlling adsorption/desorption phenomena on the filter, because of practical difficulties in applying methodologies such as backup filter subtraction, denuder for pre-removal of gaseous oxidants and SVOCs, and foam plugs for post-filter collection of volatilized particulate components from filter surfaces, with extended high-volume sampling. Consequently, volatilisation/condensation processes of SVOCs are likely to occur on the filter or on particles surface. Also, oxidation of filter deposited organics by strong oxidants, such as ozone, may happen during filtration. Therefore, the measured concentrations for oxygenated organic species, WSOC in particular, represent an upper limit of the true atmospheric levels (Pio et al., 2001).

4.4. Seasonal trend of fine and coarse aerosol in Aveiro

Fig. IV-5 shows the weekly ambient concentrations of both $PM_{2.5}$ and $PM_{2.5-10}$ samples collected in *sampling campaign II*. Due to technical reasons and collection of field blank (as already referred in section 3.3), only four samples were collected during the Winter season in 2010. It is possible to verify that the highest concentrations of particulate matter predominate in the fine size fraction of the aerosol.

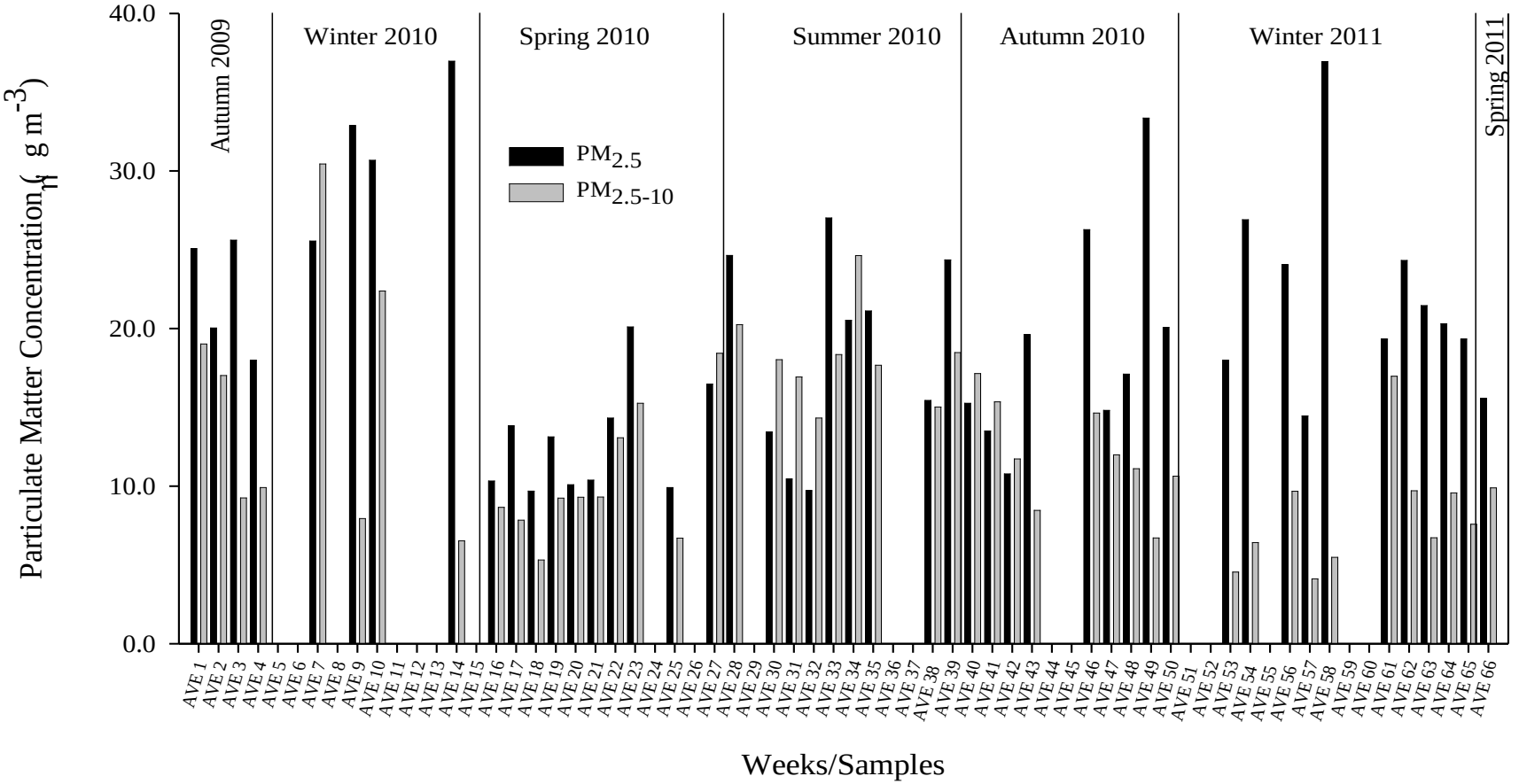

Fig. IV-5. $PM_{2.5}$ and $PM_{2.5-10}$ concentrations (in μg m^{-3}) during the annual *sampling campaign II* in Aveiro.

Overall, the total aerosol mass ranged from 8 to 37 μg m^{-3} and from 4 to 30 μg m^{-3} for $PM_{2.5}$ and $PM_{2.5-10}$ fractions, respectively, with the highest concentrations being observed during the colder periods (Winter 2010, Autumn 2010, and Winter 2011). The annual trend of total aerosol mass also shows an increase in the levels of both $PM_{2.5}$ and $PM_{2.5-10}$ fractions in Summer 2010, particularly when compared with the levels obtained during Spring 2010. As it will be explained in the following paragraphs, this increase in the total aerosol mass could be associated with forest fire events occurring in Summer 2010, which are an important source of atmospheric particles in the region.

Similar annual trends for the $PM_{2.5}$ mass concentrations (except for Summer season) have also been reported in the literature for other urban locations: based on daily sampling in the urban area of Xiamen, China, the average $PM_{2.5}$ concentrations varied in the order of Summer < Spring < Autumn < Winter (Zhang et al., 2011); in three European cities (Amsterdam, Barcelona, and Ghent), the $PM_{2.5}$ mass was higher in the Winter and lower in the Summer seasons (Viana et al., 2007). The results for $PM_{2.5}$ mass concentrations obtained in this study also show a similar trend to those observed by Duarte et al., (2007) in a rural area, with high agricultural activity, located near the city of Aveiro. Although a rural site typically refers to a site distanced from population centers, roads and industrial areas, thus having low particulate matter concentrations, the results of this study suggests that there is no clear difference on the levels of $PM_{2.5}$ between urban and rural areas in the region of Aveiro.

The $PM_{2.5-10}$ mass concentrations do not seem to follow a seasonal trend similar to that of $PM_{2.5}$. Indeed, the $PM_{2.5-10}$ mass concentrations are lower in the colder periods (namely, in Spring 2010, Autumn 2010, and Winter 2011) than in the warmer period (Summer 2010). The coarse particles have a short residence time in the atmosphere and are rapidly removed from the air by sedimentation. This feature alongside the high levels of precipitation accumulated during the colder periods, as shown in Fig. IV 1b, may have promoted the removal of the coarse particles from the atmosphere, thus reducing its concentration in the atmosphere. The higher levels of $PM_{2.5-10}$ found in the warmer period could be related to local emission sources, such as industrial activities, intense traffic load, and wind driven re-suspension of road dust, that could considerably contribute to enhance the levels of coarse particles in the atmosphere. During the Summer season, particularly

between weeks AVE 33 and AVE 35, the unusual high total aerosol masses ($PM_{2.5-10}$ + $PM_{2.5}$) could also be explained by the emissions from the forest fires that took place in those periods (referred in section 4.2.2). For the weeks AVE 33, AVE 34, and AVE 35, the air mass backward trajectories (in Annex A) indicate the continental transport of the smoke from different inland regions of the Iberian Peninsula to the western coastal sampling site of Aveiro, thus promoting an increase of the total aerosol mass collected in these periods. These findings are corroborated by those of Pio et al (2008), also for the region of Aveiro, during Summer 2003, when unusually large forested areas (>300,000 ha) were destroyed by fire. The authors reported that during these wildfire episodes, the particulate matter levels were elevated 2- to 3-fold above the prior and post smoke baseline periods.

During the Spring and Summer seasons in *sampling campaign II*, Portugal, as well the rest of Europe, was under the influence of the transport and input of dust derived from natural sources, including the dust from the Sahara desert (5 to 19 July 2010) and the ashes from the Eyjafjallajökull volcano eruption in Iceland (between April and May 2010). As an example, Fig. IV-6 shows a map of the dispersion of the volcano ashes in the European airspace at May 9th 2010, which correspond to week AVE 21 (Spring 2010).

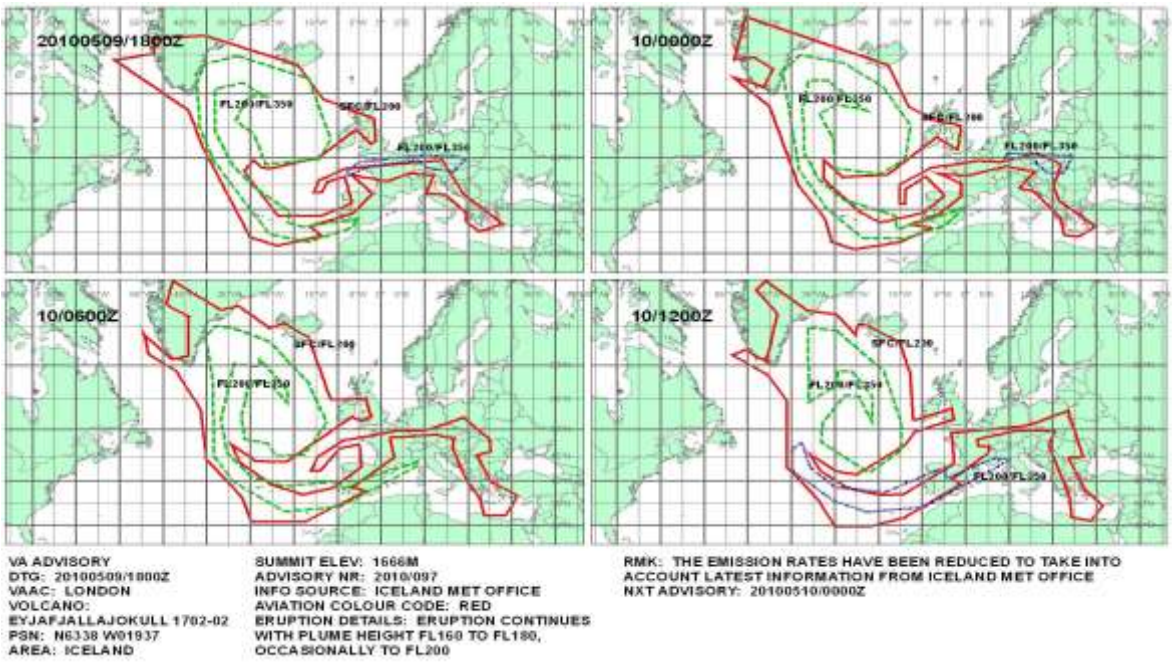

Fig. IV-6. Map of plume of ash trajectories emitted from the Iceland Eyjafjallajökull volcano eruption in 9th May 2010, obtained from VAAC at the Meteorological Office London website (http://www.metoffice.gov.uk/aviation/vaac/vaacuk_vag.html).

The map was obtained from the Volcanic Ash Advisory Centre (VAAC) at the Meteorological Office London website. The Eyjafjallajökull volcano firstly erupted on April 14th 2010 and a second eruption was verified in May 2010, emitting great amounts of particulate matter into the atmosphere. Due to atmospheric conditions over Iceland, the plume of ashes was transported towards western European, leading to the close of most of the European airspace. It is expected that the emissions from these natural sources could contribute to an increase in the levels of particulate matter in the atmosphere. For example, according to Remoundaki et al. (2012), an intense Sahara dust storm was responsible for the highest $PM_{2.5}$ concentration (100 μg m^{-3}) recorded in the urban environment of Athens, where the Sahara dust accounted for 96% of the collected $PM_{2.5}$ mass. Navrátil et al. (2012) have demonstrated that the deposition of particulate matter in Prague-Suchdol due to dust deposition in the period affected by volcanic ash, increased gradually from 0.001 g m^{-2} day^{-1} on 14 (14–15) April 2010 to 0.150 g m^{-2} day^{-1} on 19 (19–20) April, with an excessive maximum of 0.600 g m^{-2} day^{-1} on 21 (21–22) April. It should be mentioned, however, that the assessment of the impact of the aforementioned natural events (volcano eruption and Sahara dust) on the total amount of atmospheric particles in Aveiro was not verified in this study and, therefore, no conclusions can be withdrawn regarding this issue.

Fig. IV-7 shows the weekly variation of the $PM_{2.5}$-to-PM_{10} ratio ($PM_{2.5}/PM_{10}$, where PM_{10} is calculated as $PM_{2.5}$ + $PM_{2.5-10}$) for the samples collected during *sampling campaign II*. As shown, the majority of the $PM_{2.5}/PM_{10}$ ratios are higher than 50%. A few exceptions are seen for week AVE 7 in Winter 2010, as well as for week AVE 27 in Spring 2010, weeks AVE 30 to AVE 32 and AVE 34 in Summer 2010, and weeks AVE 40 to AVE 42 in Autumn 2010, where the $PM_{2.5}/PM_{10}$ ratios are between 30 and 50%, thus implying that the $PM_{2.5-10}$ fraction prevailed over the $PM_{2.5}$ fraction at this sampling site.

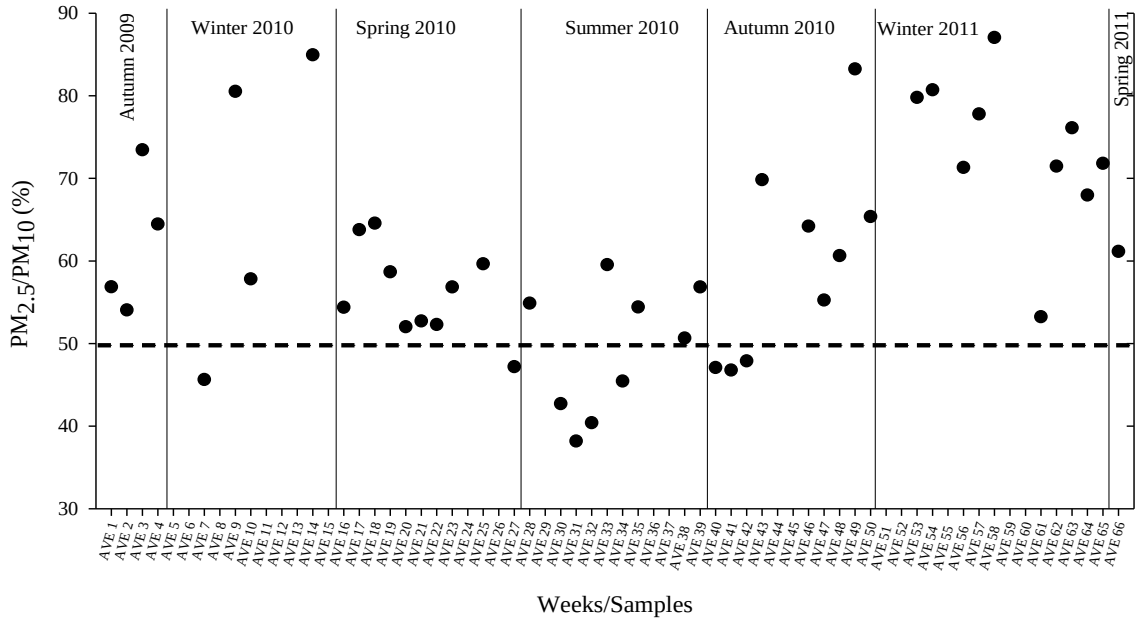

Fig. IV-7. Weekly variation of the $PM_{2.5}/PM_{10}$ ratio *during sampling campaign II*.

According to Harrison et al. (2012), high $PM_{2.5}/PM_{10}$ ratios (0.4-0.9) are likely due to a higher contribution of particulate matter with a markedly secondary origin, in urban background sites across UK. $PM_{2.5}/PM_{10}$ ratios values higher than 50% were also found by Lin et al. (2009) for an urban sites in central Taiwan (Taichun City: average of 0.56 ± 0.09 and Changhwa: average of 0.57 ± 0.11, respectively) during the Winter and Spring sampling periods. At a coastal site, Wuchi, the authors observed a $PM_{2.5}/PM_{10}$ ratio value of 0.48 ± 0.12. The authors attributed this ratio to both high contribution of sea salt aerosol and suspended dust under the strong wind speed conditions during sampling. $PM_{2.5}/PM_{10}$ ratios ranging from 0.44 to 0.90 were found across Europe and no general relationship can be established to the location (site type –urban or rural) or to its geographical location in the continent (Putaud et al., 2010). In the present study, $PM_{2.5}/PM_{10}$ ratios lower than 50% in Summer 2010 are probably due to the occurrence of forest fire events. Another explanation may be related to the proximity of the sampling site to the sea and, consequently, the greater influence of sea spray particles, which are likely to predominate in the coarse fraction of the total particulate matter in the atmosphere.

Fig. IV-8 shows the weekly variation of the total $PM_{2.5\text{-}10}$ mass concentrations as well as the average concentrations (and the standard deviation) of TC, EC, OC, and WSOC in the $PM_{2.5\text{-}10}$ samples collected during *sampling campaign II*. The concentrations of TC

and OC follow a similar seasonal trend, with maximum values during Autumn and Winter seasons and minimum concentrations during the warmer periods (Summer and Spring seasons). The OC is the predominant component of the carbonaceous material in the $PM_{2.5-10}$ samples, accounting for more than 69% of the TC, while the EC and WSOC contribution to the TC content of the $PM_{2.5-10}$ samples was in the range of 0 to 33% and 4 to 20%, respectively. The EC concentration for $PM_{2.5-10}$ fraction varied from 0 to 0.175 μg C m^{-3} during the *sampling campaign II* (Fig. IV-8). The concentrations of WSOC in the $PM_{2.5-10}$ samples were an average of in the range of 0.024 (0.001) – 0.161 (0.008) μg C m^{-3}, with the higher concentrations being found in the Autumn periods (0.042 (0.003) – 0.135 (0.005) μg C m^{-3}), except the highest one which was found in Summer (AVE 38- 0.161 (0.008) μg C m^{-3}), and the lowest values in the Spring 2010 season (0.024 (0.001) – 0.087 (0.006) μg C m^{-3}).

The average concentrations of WSOC in the coarse particles collected in Summer 2010 (0.069 (0.018) μg C m^{-3}) and Winter 2011 (0.047 (0.012) μg C m^{-3}) seasons were found to be lower than those reported for a coastal urban site in China (1.1 μg C m^{-3} in Summer and 1.9 μg C m^{-3} in Winter) (Huang et al., 2006). Also, the average concentrations of WSOC obtained in the present study during the Summer season are lower than those found in the city of Oporto (0.20 (0.70) μg C m^{-3}) for particles within the 3.0–10 μm size range collected in the period between August and September 2004 (Duarte et al., 2008a). These differences are likely be related to the contribution of the different dominant sources to the concentration levels of the WSOC aerosol component.

The contribution of WSOC to OC (WSOC/OC) in the $PM_{2.5-10}$ fraction varied between 4 and 20%, with higher average values being found during Summer 2010 (13 (4)%). For weeks AVE 33 to AVE 35, corresponding to the high forest fire pollution event, the WSOC concentration ranged between 0.06 and 0.08 μg C m^{-3}, which could be suggested to a contribution from wood combustion and the average WSOC/OC ratio during these week was low (11%). The average of WSOC/OC ratio of the aerosol samples observed during Summer 2010 (13 (4) %) was in the range of the data reported for coastal-rural site (13.2 (±4.6)%) and lower than those found for urban area (17.6 (±2.7)%) during Summer 2004 for particles within the coarse size range (3.0–10 μm) (Duarte et al., 2008a).

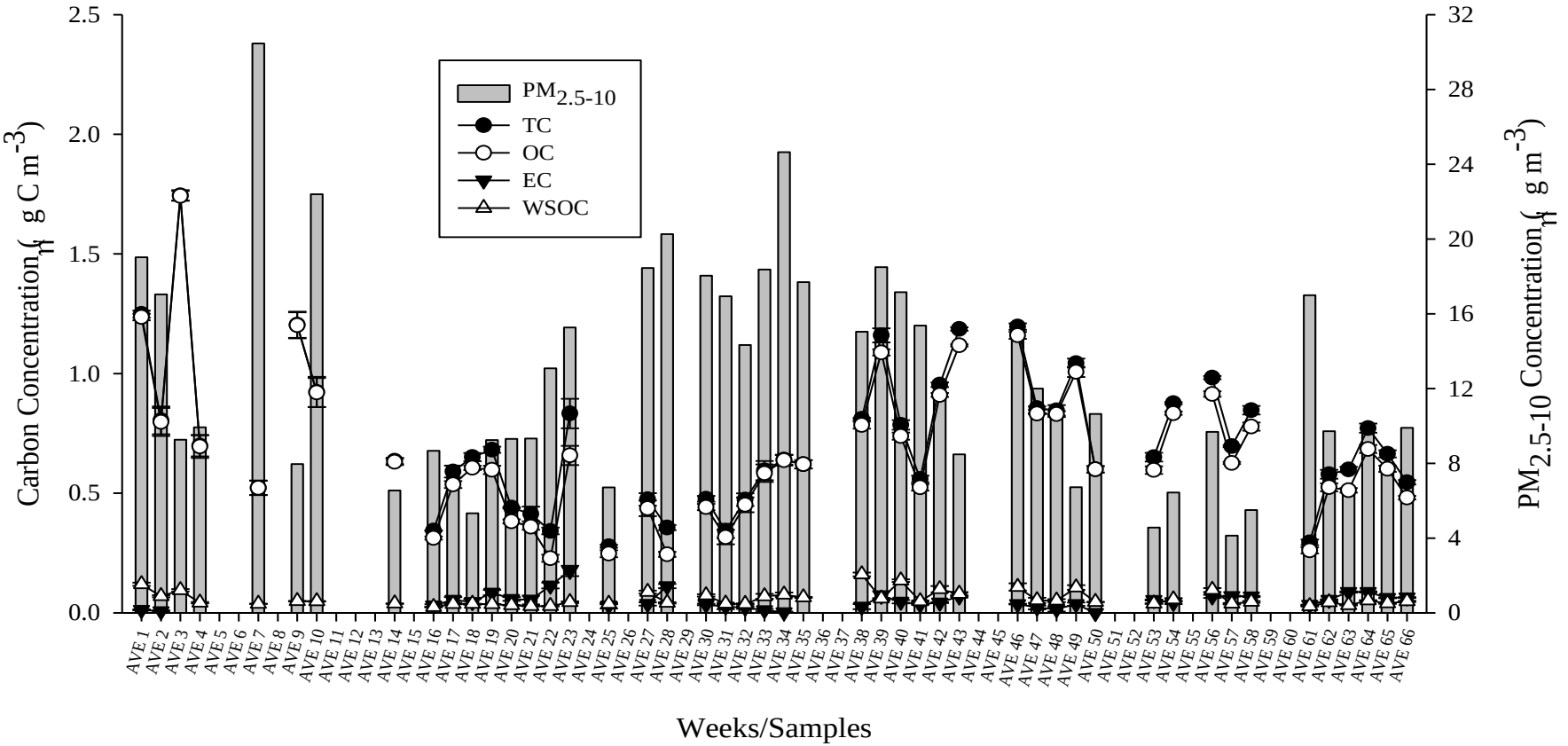

Fig. IV-8. Weekly variation of the $PM_{2.5-10}$ mass concentration (in µg m^{-3}) and average concentrations of the carbonaceous fractions (in µg C m^{-3}) of the $PM_{2.5-10}$ samples collected during *sampling campaign II*. Error bars refers to standard deviation.

In general, the seasonal distribution of the average ambient concentrations of $PM_{2.5}$, TC, OC, EC, WSOC, and WINSOC (water-insoluble organic carbon, (WINSOC=OC−WSOC)) are shown in Fig. IV-9. The concentrations of TC, OC, and WSOC showed a similar trend, with minimum values in Spring and in the first weeks of Summer (AVE 28 to AVE 31) and maximum concentrations in Autumn and Winter. During *sampling campaign II*, the OC was the predominant fraction of the carbonaceous material in the $PM_{2.5}$ samples, accounting for more than 57% of the TC, while EC was found to have only a minor contribution to the TC content during Autumn 2009 (0.29-0.49%), and Winter 2011 (1.28-3.85%). For Spring and Summer periods, the contribution of EC to TC ranged from 16.06 to 42.48% and 11.60 to 42.73%, respectively. OC concentrations in $PM_{2.5}$ ranged from 0.57 to 13 μg C m^{-3}, and they were systematically higher than those found in $PM_{2.5-10}$. Regarding the EC levels in $PM_{2.5}$, the concentrations ranged from 0.02 to 1.44 μg C m^{-3}, being also higher than those found in $PM_{2.5-10}$. During the whole sampling period of campaign II, the EC concentration in $PM_{2.5}$ reached higher values in Autumn 2010 (ranging from 0.506 (0.021) to 1.441 (0.031) μg C m^{-3}), and lower values in Autumn 2009 (ranging from 0.0245 (0.0068) to 0.028 (0.010) μg C m^{-3}).

The average EC concentration measured in this work for the summer season (0.69 (0.07) μg C m^{-3}) was found to be higher than that reported by Duarte et al. (2007) for a coastal- rural area near the city of Aveiro (0.45 (0.02) μg C m^{-3}). However, for the Autumn and Winter seasons, the authors reported higher average EC concentrations (1.27 (0.22) μg C m^{-3} and 1.30 (0.44) μg C m^{-3}, respectively) than those obtained in this study for Autumn 2010 (0.881 (0.113) μg C m^{-3}) and for Winter 2011 (0.144 (0.045) μg C m^{-3}). It was also verified that the levels of EC increased for samples collected in weeks AVE 33 to AVE 35 ((0.977 (0.042) – 1.10 (0.027) μg C m^{-3}) (during the forest fire events in the Summer season, although the highest values were obtained for samples collected during Autumn 2010 season (0.507 (0.021) - 1.441 (0.031) μg C m^{-3}). Surprisingly, the lowest levels of EC were found for samples collected during the Autumn 2009 (0.0245 (0.0068) – 0.028 (0.010) μg C m^{-3}).

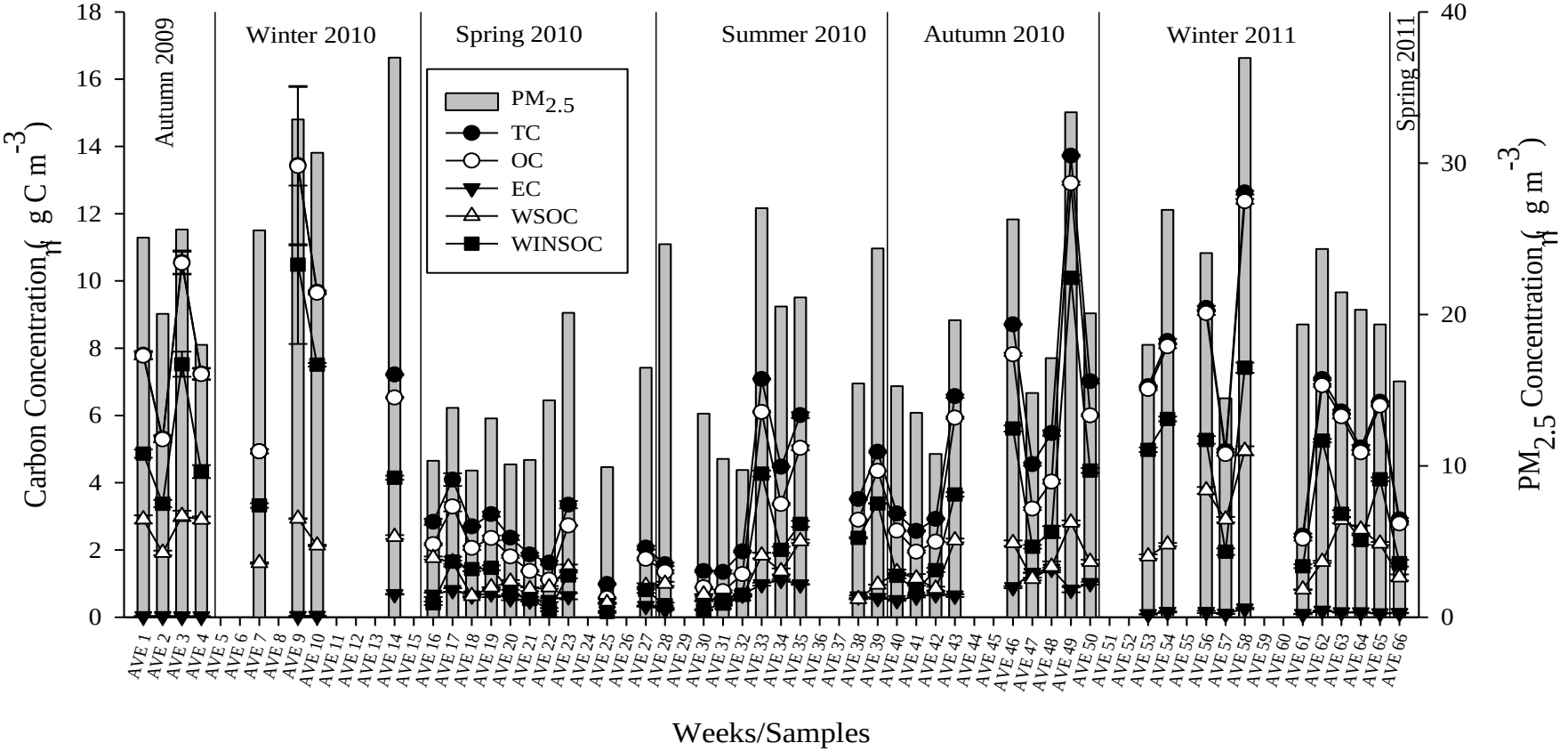

Fig. IV-9. Weekly variation of the $PM_{2.5}$ mass concentration (in μg m^{-3}) and average concentrations of the carbonaceous fractions (in μg C m^{-3}) of the $PM_{2.5}$ samples collected during *sampling campaign II*. Error bars refers to standard deviation.

A number of other studies had measured the EC levels of $PM_{2.5}$ at urban area. For example: Viidanoja et al (2002) observed an average EC concentration of 0.6 (0.2), 1.3 (0.7) and 2.1 (1.3) for warmer months (July 2000, August 2000 and September 2000, respectively) and 1.1 (0.4), 1.1 (0.3), and 1.0 (0.4) for colder months (December 2000, January 2001, and February 2001, respectively) in an urban area in Helsinki, Finland; Kim et al (2011) found an average EC concentration of 2.32 (0.44), 3.69 (0.38), 3.88 (0.79), and 2.14 (0.69) (μg m^{-3}) for summer 2009, fall 2009, Winter 2010 and Spring 2010, respectively in an urban area of Japan (Saitama City); Zhang et al (2011) also observed that the average EC concentration were 2.34 (0.52), 3.71 (0.42), 4.99 (0.58), and 2.16 (0.47) Summer, Autumn, Winter and Spring at urban area in Xiamen, China. The average EC concentrations in this study are relatively lower when compared with above studies for distinct seasons.

The average WINSOC concentrations and associated standard deviation were 5.02 (0.45), 6.37 (2.36), 0.87 (0.24), 1.83 (0.18), 3.53 (0.30), and 4.18 (0.31) μg C m^{-3} for the Autumn 2009, Winter 2010, Spring 2010, Summer 2010, Autumn 2010, and Winter 2011 seasons, respectively. During the 1st week of Spring 2011 (AVE 66) the average WINSOC concentration and standard deviation was 1.61 (0.10) μg C m^{-3}. As it can be observed, from Fig. IV-9, the levels of WINSOC tend to be higher in the colder seasons and lower in the warmer periods. A similar seasonal trend in the average mass concentrations of WINSOC was found by Kim et al. (2011) for the fine aerosol samples at an urban area. During *sampling campaign II*, the WINSOC accounts for a significant fraction of OC, ranging from 60 to 71, 63 to 78, 19 to 69, 24 to 82, 41 to 78, and 40 to 76% of the OC content in Autumn 2009, Winter 2010, Spring 2010, Summer 2010, Autumn 2010 and Winter 2010 seasons, respectively. Comparing the average WINSOC/OC ratio obtained in this study for Summer season (55%) and Winter (61%), with those reported in the literature, it is possible to verify that the average ratio obtained in Aveiro is higher than those obtained in Atlanta (35%) during the summer season and lower than those obtained in St. Louis (64%) during the Winter season (Sullivan and Weber, 2006). It has been suggested that in urban areas, the WINSOC fraction is associated with anthropogenic emissions (Miyazaki et al., 2006; Park and Cho, 2011), which comprises great amounts of incompletely combusted products and biogenic detritus, such as wax esters, aliphatic hydrocarbons, triglycerides, long-chain ketones, alkanols, and polycyclic aromatic

hydrocarbons (Mayol-Bracero et al., 2002). Similar indication was reported by Sun et al. (2011), who found that WINSOC was associated with primary combustion emissions, showing strong correlation with EC (r = 0.82), CO (r = 0.75), and NOx (r = 0.68). In fine marine aerosol, Facchini et al. (2008) found that the WINSOC fraction was the most important constituent of the TC component (average ratio and associated standard deviation of 94 ± 4% of TC).

In what concerns the WSOC concentration, it accounts on average to 35, 27, 43, 33, 30, and 38 % of TC content in Autumn 2009, Winter 2010, Spring 2010, Summer 2010, Autumn 2010, and Winter 2011 seasons, respectively. For the single aerosol sample collected in Spring 2011, the WSOC/TC was about 41 %. The WSOC concentrations during the *sampling campaign II* ranged between 0.368 (0.028) - 4.95 (0.13) μg C m^{-3}. A large variability of WSOC concentration (0.821 (0.012)) - 4.95 (0.13) μg C m^{-3}) among samples of Winter 2011, suggested much dependence or great influence of local conditions. The concentrations of WSOC were found to be lower in Spring 2010 and Summer 2010 seasons (average and standard deviation values of 1.05 (0.16) and 1.07 (0.15) μg C m^{-3}, respectively) and higher in Autumn 2009 and Winter 2011 seasons (average and standard deviation values of 2.68 (0.23) and 2.57 (0.24) μg C m^{-3}, respectively), as can be observed in Fig. IV-9. This seasonal variability in WSOC concentrations in $PM_{2.5}$ samples has been also reported in other studies performed at a urban area (Jaffrezo et al., 2005; Viana et al., 2006b), a suburban location of India (Khare et al., 2011), at a rural area of Portugal (Duarte et al., 2007). However, in a marine location, the WSOC concentrations in aerosol samples collected during the Summer season were found to be higher than those determined in samples collected during the Winter season (Yoon et al., 2007). The authors suggested that this seasonal pattern is likely to be associated to differences in biological activity between such seasons. The increase in the domestic heating and the lower ambient temperatures which promote the particulate phase in the gas-particle equilibrium (the SVOCs tend to be in the particulate phase at lower temperatures (Kiss et al., 2002)). Overall, the results reported in the literature alongside those described in the present study suggest that the WSOC component has different primary sources (either anthropogenic and natural) and is dependent on the sampling area and season. It was also observed an increase in the ambient concentrations of WSOC in

weeks AVE 33 to 35 during the Summer 2010 season, coincident with the intense forest fires events in the region of Aveiro.

Fig. IV-10 depict the annual variation of the WSOC/OC and OC/EC ratios for the collected $PM_{2.5}$ samples. These ratios have been used to deduce about SOA formation in urban and rural sites (Ho et al., 2002; Viana et al., 2007; Ram and Sarin, 2010).

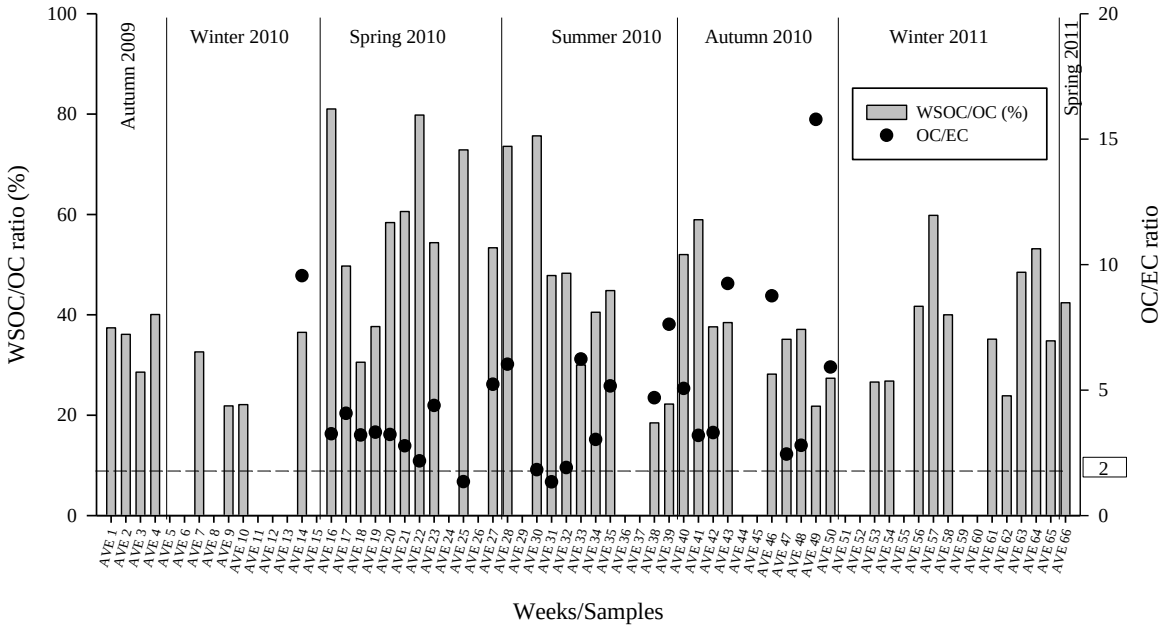

Fig. IV-10. Seasonal distribution of WSOC/OC and OC/EC concentration ratio in $PM_{2.5}$ fraction during the *sampling campaign II*.

Overall, the WSOC/OC ratios ranged from 22 to 81%, while the OC/EC ratios varied between 1.3 and 16. Despite the wide variability, these ratios tend to be higher in Spring and Summer seasons than in the other periods. The median WSOC/OC ratios were 36.8, 27.4, 56.4, 44.8, 37.1, and 37.6% for the Autumn 2009, Winter 2010, Spring 2010, Summer 2010, Autumn 2010, and Winter 2011 seasons, respectively. The $PM_{2.5}$ sample collected in Spring 2011 exhibited a WSOC/OC ratio of 42.4%. The high median WSOC/OC ratios observed during Spring and Summer seasons at the urban location focused in this study suggest that the warmer ambient temperature, higher solar radiation, and the likely presence of oxidants (e.g. O_3 and OH) in the atmosphere may enhance the oxidation of the particulate organic matter, leading to a higher water-solubility of the organic fraction. Viana et al. (2007) have related the WSOC/OC ratios between 33 and

43% in summer to the photochemical oxidation of primary organic aerosols, which increased the WSOC fraction due to the formation of more oxygenated functional groups. Average WSOC/OC ratios ranging from 34 to 61 during the warmer period (i.e., summer) at different urban areas were reported by Sullivan and Weber (2006), Miyazaki et al. (2006), and by Viana et al. (2007). Kondo et al. (2007) found that 35% (in median) of OC was water-soluble at an urban location Tokyo, Japan, during summer. Furthermore, the WSOC/OC ratios obtained in a previous study at a rural site near the city of Aveiro (Duarte et al., 2007) were in the range of those found in this study. On the other hand, the WSOC/OC ratios for samples collected between weeks AVE 33 and AVE 35 are higher than those found in the final weeks of summer 2010 (namely week AVE 38 and AVE 39), and comparable to the previous weeks, may suggest the influence of the forest fire events occurred in the region of Aveiro during these sampling periods. Similarly, low median WSOC/OC ratios (0.35-0.37) were found for $PM_{2.5}$ samples collected during biomass burning events in northern India (Ram and Sarin, 2010).

The OC/EC ratios (Fig. IV-10) ranged between 1.3 and 16 from week AVE 14 to week AVE 50. For the aerosol samples collected in Autumn 2009, Winter 2010 (namely, weeks AVE 7 to AVE 10), Winter 2011, and Spring 2011, the values of OC/EC (data not shown) were in the range of 202.5- 430.3, 259.6- 405.3, 25.0-77.4, and 22.8, respectively. These unusual high OC/EC ratios are a consequence of the very low EC concentrations found in the aerosol samples, although the sampling site is under the influence of well identified anthropogenic sources of EC (e.g., emissions from vehicle traffic, industrial, and other human activities). Generally, OC/EC ratios above 2, except for samples AVE 25 and AVE 31, can be indicative of the presence of secondary OC in atmospheric aerosols (Castro et al., 1999). The lowest values of the OC/EC ratios were obtained for samples collected in weeks AVE 25 and AVE 31 (1.4 and 1.3, respectively), suggesting that the OC measured in these samples may have a primary origin. During these two sampling periods, the sampling site was under the influence of air masses travelling from the continent (Annex C) and, therefore, more enriched in anthropogenic EC emissions from the surrounding urban areas. The low OC/EC ratios obtained for samples AVE 25 and AVE 31 (in Spring 2010 and summer 2010 seasons, respectively) may also be due to a low OC concentration since during those periods the air temperature is higher, thus favoring the gaseous phase in the gas-particle partitioning of the SVOCs. Furthermore, the OC/EC

ratios obtained in this study, for the period in question (AVE 25 and AVE 31), are higher than those obtained in other urban European locations (Castro et al., 1999). As shown in Fig. IV-10, samples AVE 14 and AVE 49 exhibit the highest OC/EC ratios (~10 and ~16, respectively). Note that for sample AVE 49, the concentration of OC was one of the highest (Fig. IV-10), contributing to about 94% of the TC in fine atmospheric particles. During the high period of forest fires (Summer B 2010) the OC/EC ratios ranged between 3.0 and 6.2. Saarikoski et al. (2008) have reported distinct OC/EC ratios values on measurements at urban environment: 0.71 for traffic emissions; 3.3 for secondary organic carbon; 6.6 for biomass combustion; and 12 for long-range transport. A large variability of OC/EC ratios (range: 2.4–14.5, Av=7.87±2.4, n=77) were obtained at urban sites, which can be related to a predominance of contributions from biomass burning sources (wood-fuel and agriculture waste) (Ram and Sarin, 2010).

4.5. Seasonal sample division and natural event identification

The $PM_{2.5}$ samples collected in *sampling campaign II* were grouped together according to similar meteorological conditions (section 4.2, Fig. IV-1), air masses trajectories (section 4.2, Fig. IV-3), and WSOC concentrations, on a total of 10 groups, corresponding to different seasonal events, as shown in Table IV-3. Thus, in Autumn 2009, samples collected in weeks AVE 1 to AVE 4 were grouped together. In Winter 2010, because of the mentioned drawback during the sampling campaign (section 3.3, Chapter 3), sample collected in week AVE 14 was grouped with samples collected during weeks AVE 16 and AVE 17 in Spring 2010; for this reason, this group was termed Winter/Spring 2010. In Spring 2010, it was possible to set two additional groups of samples, named Spring A 2010 and Spring B 2010, where the samples of the former group were collected during the volcanic eruption events occurred in Iceland. In Summer 2010, two different natural events were recorded during the sampling campaign, thus originating two groups of samples: Summer A 2010, where it was observed the intrusion of Sahara Desert dust over the Iberian Peninsula, and Summer B 2010, where it was observed the occurrence of forest fires episodes.

Table IV-3. Summarized information regarding the assembled $PM_{2.5}$ samples collected in *sampling campaign II*.

Sample / Season	Week	Origin of air masses	Natural events	Median Temperature (°C)	Maximum RH (%)	Maximum Wind velocity (m/s)	Accumulated Rainfall (mmH2O)	WSOC (µg C m^{-3})	
								Avg	sd
Autumn 2009	AVE 1	Maritime		12.1	94	9.5	49.1	2.91	0.12
	AVE 2			13.7	95	6.9	83.4	1.91	0.07
	AVE 3	Maritime/Continental		12.6	92	7.5	0.1	3.01	0.16
	AVE 4			8.1	91	7.5	20	2.90	0.10
Winter/Spring 2010	AVE 14	Continental		9.3	81	7.3	0.6	2.38	0.06
	AVE 16	Maritime/Continental		12.5	90	7.7	8.6	1.76	0.05
	AVE 17			15.8	92	6.4	1.8	1.63	0.05
Spring A 2010	AVE 19	Maritime/Continental	Volcanic eruptions in Iceland	17.1	92	5.9	52.5	0.89	0.00
	AVE 20			16.4	89	11.3	0.5	1.05	0.05
	AVE 21			14.7	92	7.4	11.4	0.83	0.06
	AVE 22			14.2	93	10.2	2.9	0.89	0.04
Spring B 2010	AVE 23	Maritime/Continental		21.5	92	5.6	0.5	1.48	0.08
	AVE 25			18.8	93	5.6	4.8	0.69	0.03
	AVE 27			17.3	91	7.3	0	0.93	0.08
Summer A 2010	AVE 28	Continental	Sahara Desert dust	17.9	96	3.8	0	0.99	0.06
	AVE 30	Maritime/Continental		18.6	93	5.3	0.1	0.67	0.01
	AVE 31	Maritime		19.3	93	5.1	1.1	0.37	0.03
	AVE 32	Maritime/Continental		19.6	93	7.1	0.2	0.62	0.02
Summer B 2010	AVE 33	Maritime/Continental	Forest fires	20.8	93	4.8	0	1.83	0.08
	AVE 34			20.2	90	6.2	0	1.36	0.09
	AVE 35			19.6	95	6.3	0	2.26	0.05
Autumn A 2010	AVE 40	Maritime/Continental		18.7	94	6.4	1.6	1.34	0.08
	AVE 41	Maritime		17.9	92	9.7	41.1	1.15	0.13
	AVE 42			17.2	92	7.3	76.8	2.28	0.06
Autumn B 2010	AVE 46	Maritime/Continental		15	95	9.9	17.5	2.20	0.08
	AVE 47			14.3	92	9.7	52	1.13	0.04
	AVE 48			13.05	92	9.6	46.9	1.50	0.16
	AVE 49			8.4	91	5.4	25	2.81	0.07
	AVE 50			9.3	93	10.7	172.9	1.64	0.07
Winter 2011	AVE 54	Maritime/Continental		12.9	94	4.8	34	2.16	0.05
	AVE 56			13.1	92	4.3	25.2	3.77	0.10
	AVE 57	Continental		10.05	91	6.7	2.6	2.90	0.08
	AVE 58			7.4	92	6.3	11.8	4.95	0.13
Winter/Spring 2011	AVE 63	Continental		11.65	76	7.3	0.1	2.89	0.09
	AVE 64	Maritime/Continental		12.2	91	5.8	28	2.60	0.12
	AVE 65		Pollen particles in filters	13.3	94	6.5	0	2.19	0.05
	AVE 66			13.8	94	7.5	38.1	1.18	0.09

In Autumn 2010, two groups of samples were assembled, with the first group (Autumn A 2010) being collected under ambient conditions more closely related to those recorded in Summer 2010, and the second group (Autumn B 2010) being collected under more colder temperatures and wet conditions than the previous group. In Winter 2011, which was period with very unstable meteorological conditions, only one group of samples was set. Finally, the group of samples named Winter/Spring 2011, include three samples collected in the late Winter 2011 and one sample collected in early Spring 2011, corresponding to a period of four consecutive weeks with similar ambient conditions.

Before the isolation and fractionation of the WSOM from the atmospheric particles, the aqueous extracts from each quartz filter were grouped together according to the groups of samples previously established. The reason for combining the aqueous extracts is to ensure enough material for the subsequent structural characterization by the various analytical techniques (Chapters 5 and 6), which means that the focus will be set on the seasonal variability of the chemical characteristics of both $PM_{2.5}$ and carbonaceous material.

4.6. Impact of forest fire emissions on $PM_{2.5}$ and carbonaceous material

Since forest fires are a major source of carbonaceous aerosol in many European regions, it was decided to include in this study the evaluation of the impact on the concentrations of both $PM_{2.5}$ and carbonaceous material of the forest fire events that occurred in the region of Aveiro. In order to accomplish this objective, four groups of samples were selected: two samples collected in *sampling campaign I* (Summer 2008 and Summer 2009) and two samples collected in *sampling campaign II* (Summer A 2010 and Summer B 2010).

Over the past decade, forest fires have been recurrent and identified as a problematic phenomenon mainly in the northern and center of Portugal. Fig. IV-11 shows the number of forest fires events ("hot flashes" and fires) recorded during the selected seasons. The higher temperatures during these summer periods (namely, in Summer A and B 2010) alongside a RH around 20% (in minimum) helped to extend the duration and

spread of the forest fires. From Fig. IV-11, it can be noticed that the highest number of forest fires events occurred in Summer B 2010 and the lowest number occurred in Summer 2009. The forest fires are responsible for the loss of many of the Portuguese forested areas, and the report of Agriculture, Rural Development and Fisheries Ministry *(MADRP-Direcção de Unidade de Defesa da Floresta, 2011)* reveals that the total burnt area of forest land was about 17564 ha, 87420 ha, and 133090 ha in the years 2008, 2009, and 2010, respectively.

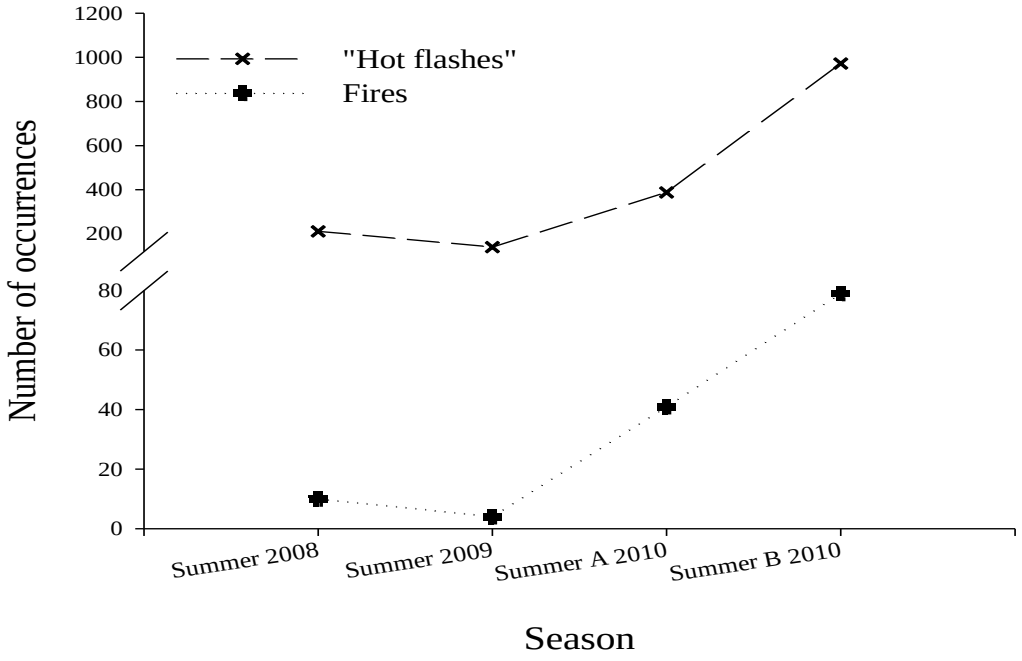

Fig. IV-11. Number of forest fires events recorded during the selected sampling seasons.

The concentrations of the total fine aerosol ($PM_{2.5}$) and of the carbonaceous materials (TC, OC, EC, and WSOC) for these periods are shown in Fig. IV-12. The $PM_{2.5}$ mass concentrations varied from 8.2 to 13.5 μgm^{-3} in Summer 2008 (SU08-1 – SU08-4), from 8.9 to 10.5 μgm^{-3} in Summer 2009 (SU09-1 – SU09-4), from 9.7 to 24.6 μgm^{-3} in Summer A 2010 (AVE 28, AVE 30–AVE 32), and from 20.5 to 27.0 μgm^{-3} in Summer B 2010 (AVE 33–AVE 35). The highest values of $PM_{2.5}$ were registered in Summer B 2010 season, matching the period with the highest number of forest fire emissions and the influence of air masses travelling from the continent surroundings. These results suggest that the forest fire emissions may have an important contribution to the increase of the

concentration of fine particles in the atmosphere. The lowest concentrations of fine air particles were found during Summer 2008 and Summer 2009, when the sampling site was under the influence of clean air masses travelling from the maritime surroundings.

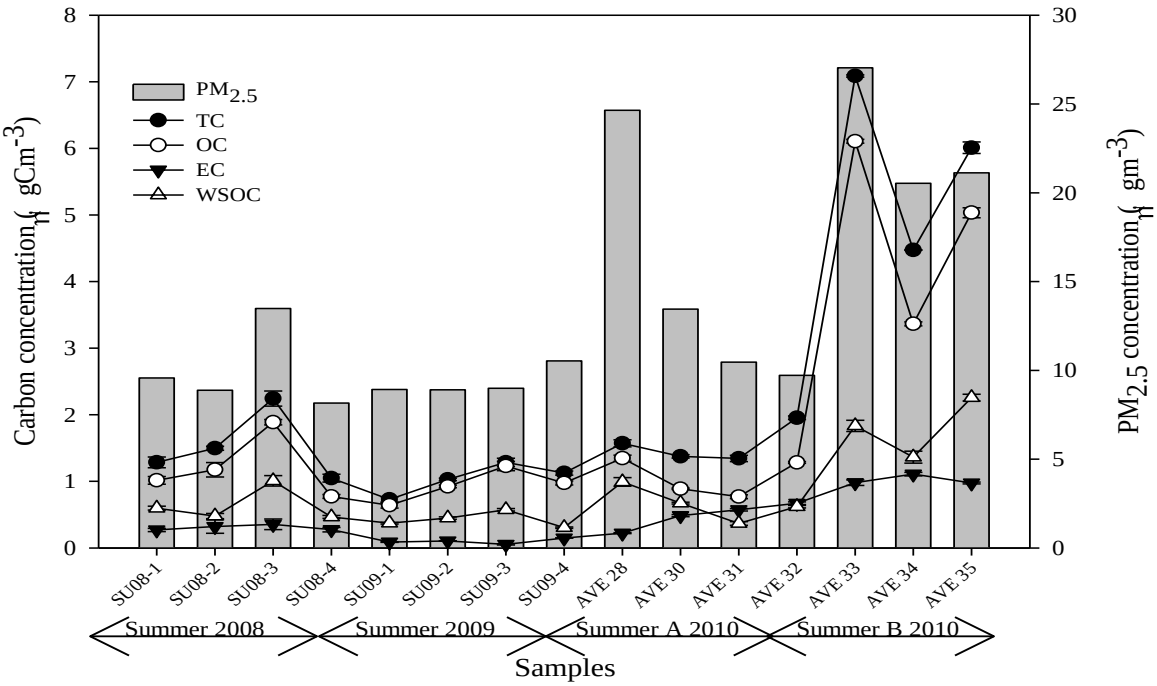

Fig. IV-12. Ambient concentrations of $PM_{2.5}$ (in μg m^{-3}) and TC, OC, EC, and WSOC (in μg C m^{-3}) for the samples collected during Summer 2008, Summer 2009, Summer A 2010, and Summer B 2010.

Fig. IV-12 shows that the highest concentration values for OC and EC were recorded during the Summer B 2010 season: 3.36 – 6.11 μg C m^{-3} and 0.98 – 1.10 μg C m^{-3}, respectively. During Summer 2008, Summer 2009, and Summer A 2010, the OC concentrations varied between a minimum of 0.64 μg C m^{-3} and a maximum of 1.35 μg C m^{-3}, whereas the EC concentrations ranged between 0.05 μg C m^{-3} and 0.67 μg C m^{-3}. These levels of OC and EC are much lower than those reported for an urban site under forest fires ambient (from 17 to 71 μg C m^{-3} and between 8 and 31 μg C m^{-3}, respectively) (Mayol-Bracero et al., 2002), and also lower than those observed in Shanghai (from 1.1 to 2.7 μg C m^{-3}) (Feng et al., 2006). For Summer 2008, Summer 2009, and Summer A 2010, the concentrations of WSOC were found to be lower than 1 μg C m^{-3}, whereas the highest values were verified during summer B 2010 season (above 1.3 μg C m^{-3}), as shown in Fig. IV-12. The concentrations of WSOC during these latest seasonal period are comparable to

those reported by Feng et al. (2006) (0.7-1.9 μg C m^{-3}) for a urban area during the summer season; however, such values are much lower than those reported by Mayol-Bracero et al. (2002) (11–46 μg C m^{-3}), where the measurements of WSOC were made under highly active forest fires events. In the present study, the lowest WSOC concentrations were measured for the samples collected during Summer 2009 period, which is characterized by air masses originating primarily from the maritime surroundings and by a low number of forest fire events.

Fig. IV-13 depicts the WSOC/OC ratios for the aerosol samples collected during the selected periods. The WSOC/OC ratios ranged from 40.8% to 60.3% in Summer 2008, 31.4% to 58.2% in Summer 2009, 47.8 % to 75.6 % in Summer A 2010, and 30.0% to 44.8 % in Summer B 2010. WSOC/OC ratios higher than 40% have been reported for aerosol samples from biomass burning episodes (Mayol-Bracero et al., 2002; Saarikoski et al., 2007). The ratios did not vary considerably throughout the summer seasons, but Summer 2010 A shows two weeks (AVE 28 and AVE 30) with higher WSOC/OC ratios. The low WSOC/OC ratio for the SU09-4 and AVE 33 samples (31.4% and 30.0%, respectively) is likely due to the low WSOC concentration in comparison to the levels of OC. This finding suggests that OC collected during these weeks is less oxidized, and thus less water-soluble. The low WSOC/OC ratios in the samples previously mentioned (SU09-4 and AVE 33) may also reflect a larger contribution of local sources to the carbonaceous material, which is also suggested by Miyazaki et al. (2006), who found a WSOC/OC ratio of 35% for fine particles collected during summer 2004 in Tokyo.

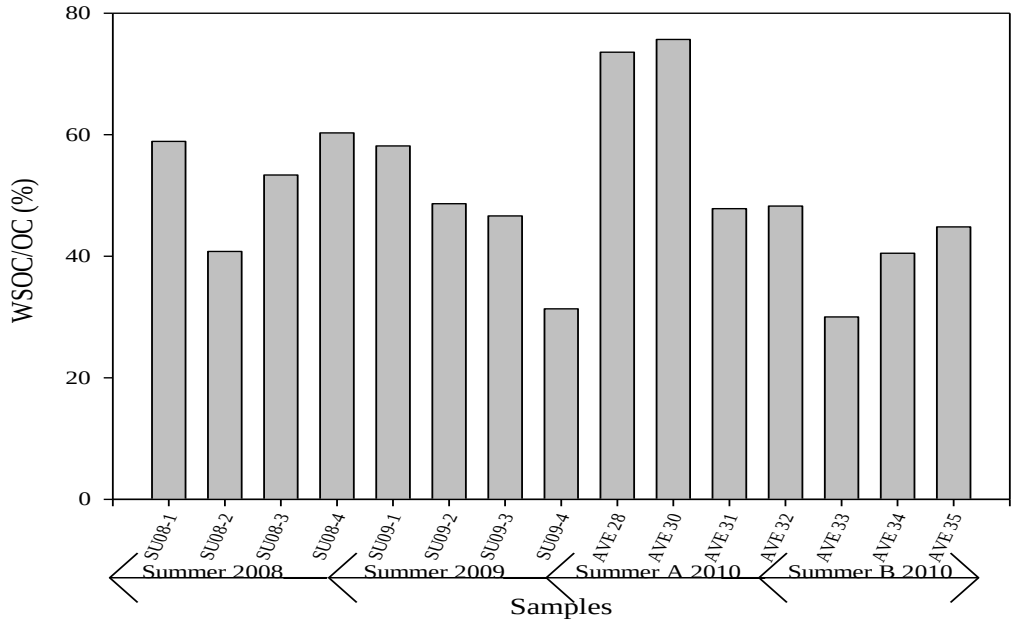

Fig. IV-13. WSOC/OC ratio for each $PM_{2.5}$ sample collected during the warmer periods.

The OC/EC ratios ranged from 2.8 to 5.3, 7.2 to 21.0, 1.4 to 6.0 and 3.0 to 6.2 for Summer 2008, Summer 2009, Summer A 2010, and Summer B 2010 seasons, respectively. OC/EC ratios higher than 2.0 has been associated to the presence of secondary OC in atmospheric particles (Chow et al., 1996; Castro et al., 1999; Krivacsy et al., 2001b; Ho et al., 2003). The results previously reported suggest that in the small town of Aveiro during the warmer periods, the OC and EC components have different emission sources, where the increase in OC concentrations is not accompanied by significant increases also in EC. Those results may also suggest the existence of a regional contribution of aged aerosol with higher secondary OC content, thus increasing the OC/EC ratios. The OC/EC ratios measured in the small town of Aveiro during the warmer periods were also found higher than those reported for the more polluted area of Shanghai (average OC/EC ratio = 2.2) (Feng et al., 2006), of Beijing (average OC/EC ratio = 2.4), and also during the Summer season and without forest fire episodes ((Pio et al., 2008); OC/EC ratio < 3). For Summer B 2010, corresponding to the period with the highest number of forest fire events, the obtained OC/EC ratios (3.0-6.2) are of the same order of magnitude of those reported for biomass burning aerosols (OC/EC ratios from 3 to 7) (Pio et al., 2008). These results suggest that both biomass burning primary and secondary sources can jointly contribute to the presence of OC in atmospheric particles in warmer periods.

4.7. Isolation and fractionation of water-soluble organic matter from atmospheric particles

As previously mentioned, the isolation and fractionation of WSOM was performed following the procedure of Duarte and Duarte (2005) and two fractions were obtained: WSOC hydrophobic acids (recovered from the DAX-8 resin) and WSOC hydrophilic acids (not retained in the resin).

4.7.1. Preliminary tests to improve the recovery of organic matter from the DAX-8 resin

During the isolation and fractionation procedure of each sample, the UV absorbance at 250nm (UV_{250}) and the DOC content of the each obtained fraction was measured in order to account for the total amount of recovery and losses of chromophoric organic compounds and DOC, respectively.

As mentioned in section 3.7, Duarte and Duarte (2005) employed a solution of MeOH:H_2O in the proportion 1:1 for recovering the organic matter adsorbed onto a XAD-8 resin. In the present study, a DAX-8 resin was used instead and it was concluded that a solution with a higher content of organic solvent (i.e. MeOH) is required for improving the amount of organic matter (in terms of UV_{250} and DOC) that is actually recovered from the DAX-8 resin. As such, two different solutions with different proportions of MeOH:H_2O (1:1 and 3:2) were tested using a Pony Lake fulvic acids reference sample (1R109F) obtained from the IHSS. The distribution and average percentages of retention, recovery, and loss of UV_{250} and DOC from three replicas of the isolation/fractionation procedure of aqueous solutions of Pony Lake fulvic acids using different proportions of MeOH:H_2O (1:1 and 3:2) for recovering the adsorbed organic matter are shown in Table IV-4.

Table IV-4. Distribution and average percentages (± standard deviation) of retention, recovery, and loss of UV_{250} and DOC from three replicas of the isolation/fractionation procedure of aqueous solutions of Pony Lake fulvic acids. Three replicas were performed.

	Eluent			
	MeOH:H_2O 1:1		**MeOH:H_2O 3:2**	
	UV_{250}	DOC	UV_{250}	DOC
Retained onto DAX-8 resin	83.0 (±2.9)	73.4 (±6.8)	83.0 (±2.7)	77.2 (±1.8)
Recovered from DAX-8 resin	41.6 (±2.6)	31.5 (±7.4)	62.8 (±5.5)	54.7 (±7.1)
Losses due to the desalination procedure	6.5 (±0.7)	3.0 (±1.8)	7.7 (±5.4)	3.8 (±1.3)
Losses due to irreversible adsorption onto DAX-8 resin	34.9 (±3.6)	38.8 (±5.3)	12.5 (±5.9)	18.8 (±8.1)
Not retained in DAX-8 resin	17.0 (±2.9)	26.6 (±6.8)	17.0 (±2.7)	22.8 (±1.8)

As shown in Table IV-4, approximately 32% of DOC was recovered from the DAX-8 resin using a 1:1 MeOH:H_2O solution, whereas this percentage increases to almost 55% using a 3:2 MeOH:H_2O solution. It can also be observed that approximately 39% and 19 % of DOC was irreversibly adsorbed onto the resin's polymers when using solutions of MeOH:H_2O in proportions 1:1 and 3:2, respectively. Overall, an increase of approximately 23% in the amount of DOC recovered from the DAX-8 resin was achieved using a 3:2 MeOH:H_2O solution. This solution also allowed an increase in the amount of UV_{250} that is recovered from the resin of approximately 21%. The EEM fluorescence spectra of the recovered fractions (data not shown) suggested that no significant effects on the fluorescence features of the sample was verified using a 3:2 MeOH:H_2O solution for the elution step. Thus, in the isolation/fractionation procedure of the WSOM samples obtained in *sampling campaign II*, it was decided to apply as eluent a 3:2 MeOH:H_2O solution.

Table IV-5 summarizes the percentages of losses and recovery of DOC and UV_{250} during the isolation procedure. The percentages of UV_{250} and DOC retained in the DAX-8 resin were in the range of 65 to 90% and 51 to 70%, respectively. In terms of percentage of UV_{250} recovered from the DAX-8 resin (here operationally designated as "WSOC hydrophobic acids" fraction), it ranged from 51 to 68 %, while in terms of DOC it was possible to recover between 42 and 53 %, with the lowest values being found for the Summer A 2010 sample. Additionally, between 12 and 35 % of UV_{250} and between 30 and 49 % of DOC was not retained onto the DAX-8 resin.

Table IV-5. Distribution and percentage (average (± sd)) of recovery and loss of UV-Vis absorbance at 250 nm (UV_{250}) and DOC from the isolation/fractionation procedure of WSOM from atmospheric samples collected in *sampling campaign II*. ([1]number of replicate=2; [2]number of replicate=3)

Sample/Season	**Retained onto DAX-8 resin**		**Recovered from DAX-8 resin**		**Not retained in DAX-8 resin**		**Losses due to irreversible adsorption onto DAX-8 resin**		**Losses due to the desalination**	
	UV_{250}	DOC	UV_{250}	DOC	UV_{250}	DOC	UV_{250}	DOC	UV_{250}	DOC
Autumn 2009[1]	88.4 (± 0.7)	65.7 (± 0.5)	64.3 (± 5.2)	50.9 (± 4.8)	11.6 (± 0.7)	34.3 (± 0.5)	21.6 (± 4.4)	10.8 (± 4.2)	2.5 (± 0.0)	3.9 (± 0.1)
Winter/Spring 2010[1]	87.1 (± 2.6)	70. 0(± 2.4)	68.2 (± 2.2)	53.1 (± 2.7)	12.9 (± 2.6)	30.0 (± 2.4)	15.2 (± 0.5)	12.5 (± 1.6)	3.7 (± 0.9)	4.4 (± 1.3)
Spring A 2010[1]	80.0 (± 1.0)	66.4 (± 3.9)	61.7 (± 4.9)	53.0 (± 0.9)	20.0 (± 1.0)	33.6 (± 3.9)	14.9 (± 3.7)	8.2 (± 3.2)	3.4 (± 0.2)	5.2 (± 0.1)
Spring B 2010[1]	75.4 (± 2.5)	65.6 (± 2.9)	59.4 (± 1.3)	50.5 (± 2.1)	24.6 (± 2.5)	34.4 (± 2.9)	11.7 (± 0.2)	9.9 (± 0.8)	4.2 (± 0.9)	5.2 (± 0.1)
Summer A 2010[1]	64.7 (± 1.5)	51.3 (± 4.3)	51.0 (± 2.0)	41.6 (± 2.1)	35.3 (± 1.5)	48.7 (± 4.3)	9.2 (± 0.4)	4.2 (± 2.8)	4.4 (± 0.1)	5.5 (± 0.7)
Summer B 2010[1]	84.5 (± 1.7)	68.2 (± 0.2)	63.6 (± 6.3)	49.7 (± 6.2)	15.5 (± 1.7)	31.8 (± 0.2)	14.9 (± 3.0)	11.8 (± 5.3)	5.9 (± 1.7)	6.7 (± 0-6)
Autumn A 2010[1]	82.8 (± 1.9)	70.5 (± 1.0)	66.0 (± 0.3)	51.0 (± 1.1)	17.2 (± 1.9)	29.5 (± 1.0)	13.1 (± 1.7)	14.0 (± 1.1)	3.7 (± 0.4)	5.5 (± 1.1)
Autumn B 2010[2]	89.0 (± 0.7)	62.6 (± 2.2)	67.3 (± 4.3)	50.8 (± 2.3)	11.0 (± 0.7)	37.4 (± 2.2)	19.1 (± 4.7)	6.4 (± 0.6)	2.7 (± 0.1)	5.4 (± 0.2)
Winter 2011[2]	90.5 (± 2.1)	60.1 (± 4.5)	60.0 (± 4.2)	44.9 (± 1.3)	9.5 (± 2.1)	39.9 (± 4.5)	27.6 (± 2.7)	8.0 (± 3.4)	2.9 (± 0.6)	7.2 (± 2.3)
Winter/Spring 2011[2]	88.8 (± 2.0)	57.5 (± 2.2)	60.3 (± 2.2)	45.3 (± 1.7)	11.2 (± 2.0)	42.5 (± 2.2)	25.1 (± 1.6)	4.7 (± 1.6)	3.4 (± 0.7)	7.5 (0.9)

It also can be observed in Table IV-5 that the values of the percentage of recovery in terms of UV_{250} are higher than those in terms of DOC content. This difference was explained by Duarte and Duarte (2005) as being due to the enrichment of the DAX-8 fraction in organic compounds with highly conjugated π bond systems. As already stated, during the isolation and fractionation procedure, two kinds of losses must be accounted: (1) losses due to the irreversible adsorption of organic compounds onto the resin polymers, ranging from 4.2 to 14% in terms of DOC and 9.2 to 27.6% in terms of UV_{250}; and (2) losses due to the washout from the resin of the very weakly retained compounds that are desorbed together with the inorganics during the desalting procedure, accounting for 3.9–7.5% of DOC and 2.5–5.9% of UV_{250}.

Table IV-6 shows a comparison of the percentages of retention and recovery of DOC and UV_{250} obtained from the application of the isolation/fractionation procedure to two aerosol WSOM samples collected at different locations: the Autumn 2009, Autumn A 2010, and Autumn B 2010 samples collected in this study at the urban location and an Autumn sample collected by Duarte and Duarte (2005) at a rural location.

Table IV-6. Distribution and percentage (average (± sd)) retention and recovery of UV absorbance at 250 nm (UV_{250}) and DOC from the isolation/fractionation procedure of WSOM from atmospheric samples collected in the Autumn season at two different locations.

Fraction	**WSOM from urban atmospheric aerosols - Autumn (2009)** (this study)		**WSOM from urban atmospheric aerosols - Autumn A 2010** (this study)		**WSOM from urban atmospheric aerosols - Autumn B 2010** (this study)		**WSOM from rural atmospheric aerosols – Autumn** (Duarte and Duarte, 2005)	
	DOC	UV_{250}	DOC	UV_{250}	DOC	UV_{250}	DOC	UV_{250}
Retained onto the resin	65.7 (± 0.5)	88.4 (± 0.7)	70.5 (± 1.0)	82.8 (± 1.9)	62.6 (± 2.2)	89.0 (± 0.7)	75.9 (±3.8)	93.6 (±2.2)
Recovery from resin	50.9 (± 4.8)	64.3 (± 5.2)	51.0 (± 1.1)	66.0 (± 0.3)	50.8 (± 2.3)	67.3 (± 4.3)	54.1 (±7.1)	79.3 (±6.7)

As shown in Table IV-6 the DAX-8 resin allows the recovery of a slightly smaller amount of WSOC hydrophobic acids (~ 51% of DOC for all Autumns samples –this study) as compared to that of the XAD-8 resin (~ 54% of DOC) reported by Duarte and Duarte (2005). Given that the percentages of UV_{250} and DOC retention and recovery for the XAD-

8 resin were higher than those for the DAX-8 resin, one can suggest that these differences are likely to be related to the different physical characteristics (e.g. pore size) of the resins. Using aquatic humic solutes, Peuravuori et al. (2002b) has reported that the sorptive power of the DAX-8 resin was systematically somewhat greater compared to that of the XAD-8 resin. Nevertheless, the authors also concluded that the DAX-8 and XAD-8 resins seem to isolate humic solute bulks almost equally, although the content of aliphatics is slightly greater for the former, producing mixtures with similar structural compositions for general purposes. In the present study, another relevant reason for the different sorptive power exhibited by the two resins for the aerosol WSOM samples may be related with the different nature of the WSOM samples since they were collected at two completely different areas (urban and rural).

The average ambient concentrations (and standard deviations) of WSOC hydrophilic and WSOC hydrophobic acids fractions (measured as DOC) obtained from the isolation procedure of each group of aerosol samples representative of different seasonal periods was also calculated and are summarized in Table IV-7. This table also presents the amount (in mg) of solid residue of each WSOC hydrophobic acids fraction obtained at the end of the freeze-drying procedure. As can be observed from Table IV-7, the Summer A 2010 sample contains the lowest amounts of WSOC hydrophobic acids. Lower levels of WSOC hydrophobic acid were also reported by Sannigrahi et al. (2006), and Sullivan and Weber (2006), for fine aerosols collected at an Atlanta urban site during stagnation events during the summer season, when the air quality was poorest. Since there was little biomass burning influence, Sullivan and Weber (2006) also concluded that SOA results from the production of low molecular weight hydrophilic compounds.

As it can be seen from Table IV-7, the total amount of WSOC hydrophilic acids fractions obtained for the various samples are typically lower than those of the WSOC hydrophobic acids fractions, thus hindering the structural characterization of the hydrophilic fractions. Therefore, the structural characterization that will be presented and discussed in the next section is focused only on the WSOC hydrophobic acids fractions of each group of aerosol samples.

Table IV-7. Average (Avg.) ambient concentrations (in µg C m^{-3}) and associated standard deviation (sd) of total WSOC, and isolated WSOC hydrophobic acids and WSOC hydrophilic acids fractions. The amount (in mg) of solid residue of each WSOC hydrophobic acids fraction after freeze-drying is also presented.

Season	**Filter/sample**	**WSOC** (µg C m^{-3})		**WSOC Hydrophobic Acid** (µg C m^{-3})		**WSOC Hydrophilic Acid** (µg C m^{-3})		**Amount of solid residue of each WSOC hydrophobic acids fraction** (mg)
		Avg.	sd	Avg.	sd	Avg.	sd	
Autumn 2009	AVE 1 AVE 2 AVE 3 AVE 4	2.68	0.23	1.36	0.13	0.92	0.01	50.6
Winter/Spring 2010	AVE 14 AVE 16 AVE 17	1.93	0.09	1.02	0.05	0.58	0.05	25.8
Spring A 2010	AVE 19 AVE 20 AVE 21 AVE 22	0.91	0.09	0.48	0.01	0.31	0.04	13.9
Spring B 2010	AVE 23 AVE 25 AVE 27	0.94	0.12	0.48	0.02	0.32	0.03	19.6
Summer A 2010	AVE 28 AVE 30 AVE 31 AVE 32	0.66	0.07	0.28	0.01	0.32	0.03	15.0
Summer B 2010	AVE 33 AVE 34 AVE 35	1.82	0.13	0.90	0.11	0.58	0.00	35.7
Autumn A 2010	AVE 40 AVE 41 AVE 42	1.11	0.16	0.57	0.01	0.33	0.01	12.8
Autumn B 2010	AVE 46 AVE 47 AVE 48 AVE 49 AVE 50	1.86	0.21	0.96	0.03	0.67	0.01	52.9
Winter 2011	AVE 54 AVE 56 AVE 57 AVE 58	3.44	0.19	1.57	0.02	1.46	0.02	60.7
Winter/Spring 2011	AVE 63 AVE 64 AVE 65 AVE 66	2.22	0.18	0.99	0.03	0.96	0.05	43.8

4.8. Aerosol mass balance of fine atmospheric aerosols

An aerosol mass balance was performed for assessing the contribution of each carbonaceous fraction (namely, WSOC, WINSOC, and EC) for the total $PM_{2.5}$ aerosol mass. The relative contribution of each carbonaceous fraction to the total $PM_{2.5}$ mass during *sampling campaign II* at the city of Aveiro is shown in Fig. IV-14.

The mass of WSOM, water-insoluble organic matter (WINSOM), and EC fractions were estimated by applying a conversion factor to the concentrations of WSOC, WINSOC and EC concentration, respectively. In this work, the conversion factor employed for estimating the amount of WSOM was 1.6, which was determined based on the results of elemental analysis (see section 5.3) of the WSOM samples. A similar value has been suggested in the literature for estimating the amount of WSOM in atmospheric aerosols collected in urban areas (Turpin and Lim, 2001; Timonen et al., 2010). For the estimative of the amount of WINSOM and EC, it was decided to use a conversion factor of 1.2 and 1, respectively, in a similar fashion to what has been applied in previous studies (Zappoli et al., 1999; Krivacsy et al., 2001b; Duarte, 2006).

As shown in Fig. IV-14, the total fine aerosol mass contains a highly variable fraction (between 16 and 47%) of carbonaceous organic matter, while 53 to 84% remains to be identified (NID). This component probably comprises inorganic species and trace metals as suggested by Duarte (2006). For marine aerosols, Claeys et al. (2010) suggested that the crustal matter (mineral dust) could be a major aerosol component of the NID fraction. The carbonaceous fraction in $PM_{2.5}$ tends to be higher during Autumn 2009 and Winter 2011 (~47%) periods, whereas the lowest levels were found for Spring B 2010 and Summer A 2010 seasons (~16%). The EC fraction accounted for less than 6% of the total $PM_{2.5}$ mass during the annual *sampling campaign II*. The amount of WSOM was higher than that of WINSOM for samples collected in Winter/Spring 2010, Spring A 2010, Spring B 2010, Summer A 2010, Autumn A 2010, and Winter/Spring 2011 seasons and the opposite in the other samples.

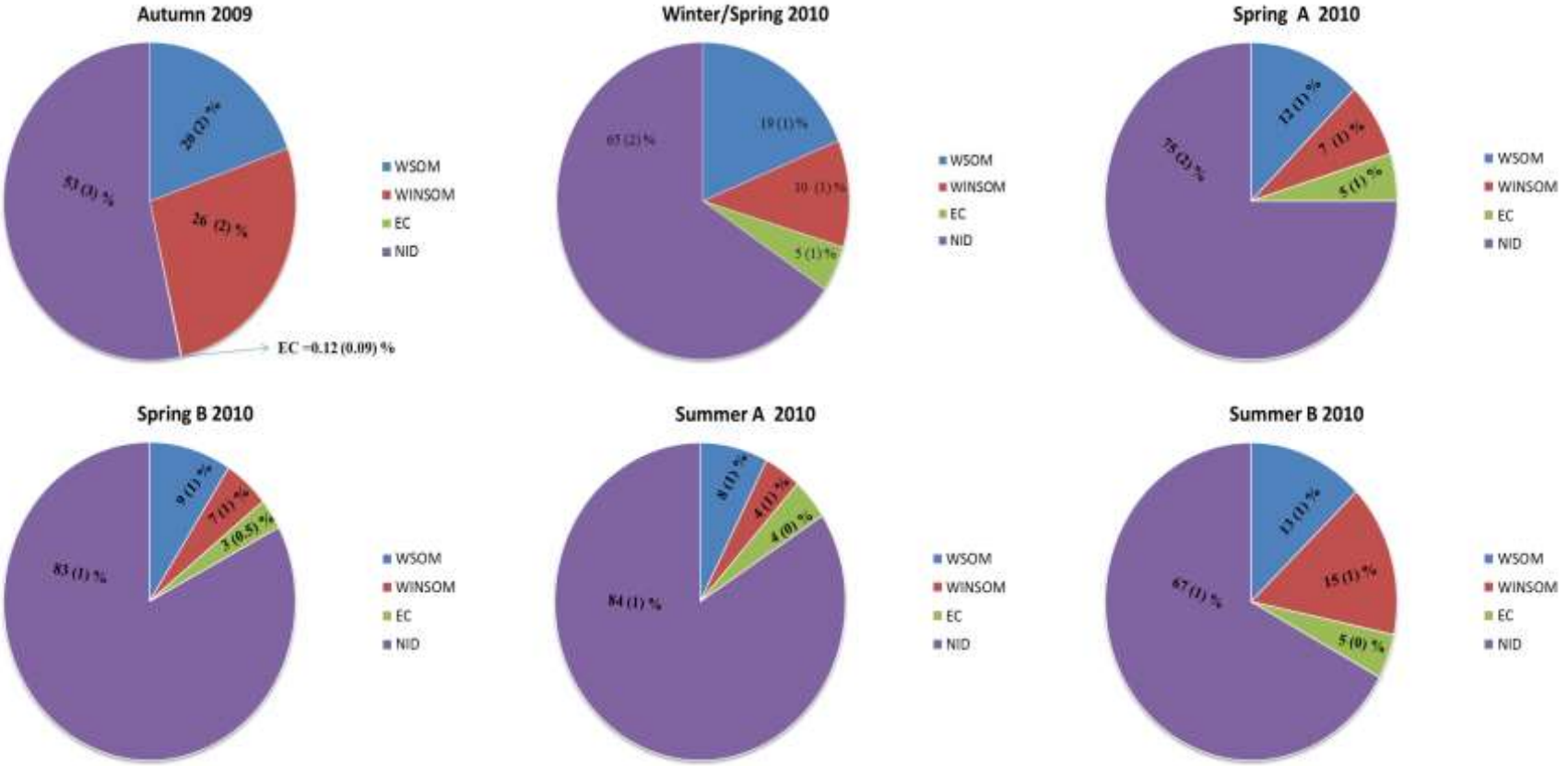

Fig. IV-14. Aerosol mass balance for the fine atmospheric particles collected in Aveiro during Autumn 2009, Winter/Spring 2010, Spring A 2010, Spring B 2010, Summer A 2010 and Summer B 2010, Autumn A 2010, Autumn B 2010, Winter 2011, and Winter/Spring 2011 seasons. "NID" refers to the mass of aerosol that was not identified.

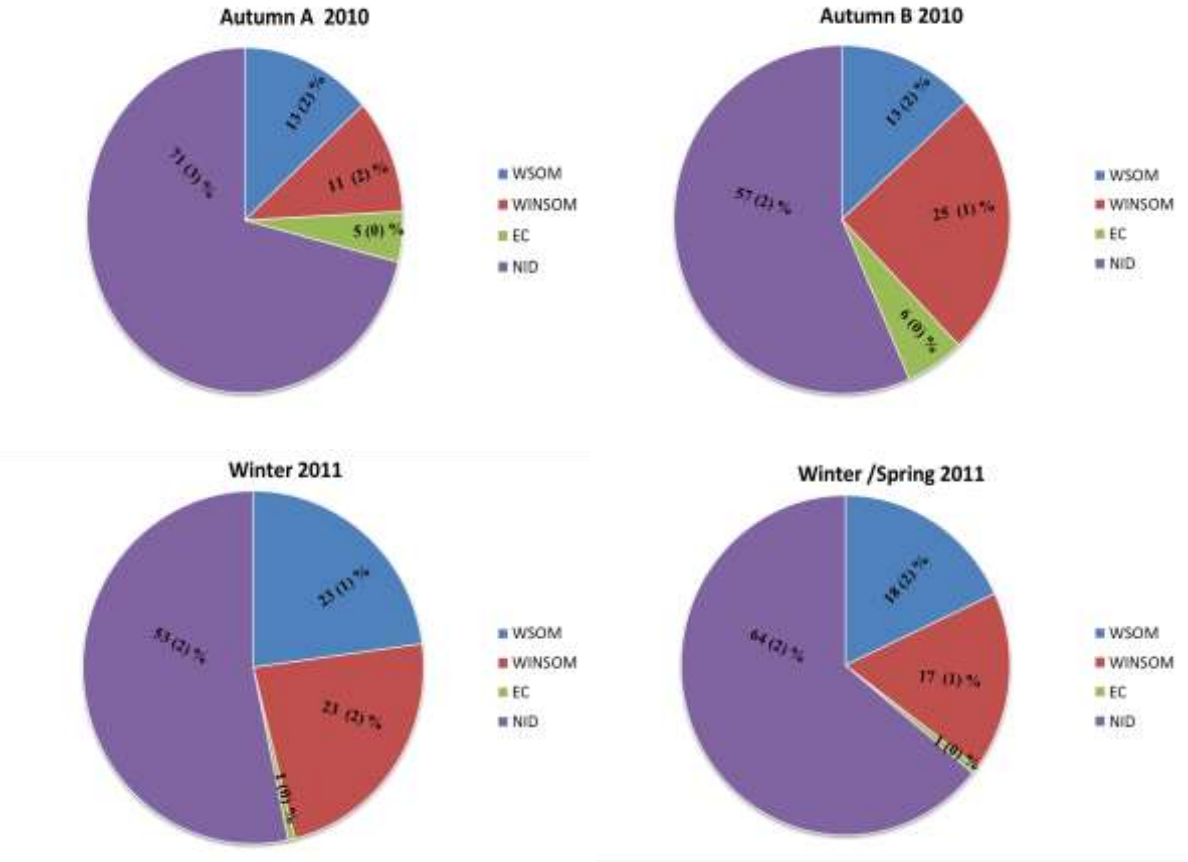

Fig. IV-14. *Continued*.

On the other hand, the Summer B 2010 sample exhibit a higher percentage of WINSOM as compared to that of the WSOM, suggesting a higher contribution of less water-soluble primary organic aerosols, which seems to be in agreement with the occurrence of local forest fires emissions. In a previous study conducted by Duarte (2006), it was reported that the WSOM accounted for 30%, WINSOM for 13%, and EC for 2% of the total fine aerosol mass collected during the Winter season at the city of Aveiro. The unidentified fraction accounted for 55% of the total fine aerosol mass. In the present study, for the Winter 2011 season, it was found that both WSOM and WINSOM fractions account for 23%, EC for 1%, and NID for 53% of the total fine aerosol mass. The difference between the values reported by Duarte (2006) and those obtained in this study for the amount of WSOM and WINSOM may be related to the fact that the sampling time applied by Duarte (2006) was only one week while in this study the values shown in Fig. IV-14 correspond to a 4-week composite sample.

4.9. Conclusions

The assessment of the adsorption phenomena of SVOC and VOC during the sampling procedure of atmospheric aerosols using quartz fibre filters revealed that these phenomena accounts for less than 27% and 13% of the total $PM_{2.5}$ and $PM_{2.5\text{-}10}$ mass, respectively. On the other hand, these phenomena can contribute to 22-33% and 4-7% of OC present in $PM_{2.5}$ and $PM_{2.5\text{-}10}$ samples, respectively.

Overall, the seasonal trend found for the total $PM_{2.5}$ mass concentrations was as follows: Winter 2010>Winter 2011>Autumn2009>Autumn 2010>Summer 2010>Spring 2010. For the total $PM_{2.5–10}$ mass concentrations, no clear seasonal trend can be foreseen; however, the seasonal variability was as follows: Summer 2010>Winter 2010>Spring 2010>Autumn2009>Autumn 2010> Winter 2011. Episodes of high $PM_{2.5}$ and $PM_{2.5–10}$ mass concentrations in Summer B 2010 season are clearly associated with emissions from local forest fires events. Carbonaceous materials (WSOM + WINSOM + EC) have an important contribution to the total $PM_{2.5}$ mass, accounting for 16-47% of the total fine particulate matter. A considerable fraction (53-84%) of the total $PM_{2.5}$ mass remains to be identified, although it is likely that this component comprises inorganic species and trace

metals, as previously suggested by Duarte (2006). The WSOC is also preferentially distributed in the fine aerosol samples, accounting for a highly variable fraction (27% to 41%) of the TC in $PM_{2.5}$. The highest ambient WSOC concentrations were found in the fall and Winter seasons, and the lowest values in the Spring and Summer seasons. The WSOC/OC ratios are generally high (22-81%), which suggests that the contribution of SOA is important for the total amount of WSOC in fine particulate matter.

The DAX-8 resin allowed the pre-concentration, isolation, and fractionation of the organic matter dissolved in the aqueous extracts of the atmospheric aerosol samples. Two fractions were obtained with this procedure: WSOC hydrophilic acids and WSOC hydrophobic acids. The WSOC hydrophobic acids fractions, which were recovered from the resin with a solution of MeOH:H_2O in the proportion 3:2, represents 42 to 53% of the total WSOC present in the aqueous extracts. Being the most important fraction, the structural characterization that will be presented and discussed in the next chapter is focused only on the WSOC hydrophobic acids fractions.

V

Structural characterization of water-soluble organic matter from fine urban atmospheric aerosols

5.1. Introduction

In this chapter, the results obtained from the application of Ultraviolet-Visible (UV-Vis) and excitation-emission matrix (EEM) fluorescence spectroscopies to the WSOC fractions of the various fine atmospheric aerosol samples are presented and discussed. It is also presented and discussed the results of the structural characterization of the WSOC hydrophobic acids fractions from the atmospheric aerosols collected in the different seasons using the following techniques: Fourier transform infrared - attenuated total reflectance (FTIR-ATR) and solid-state cross-polarization with magic angle spinning ^{13}C nuclear magnetic resonance (CPMAS ^{13}C NMR) spectroscopies, and elemental analysis. The study of the WSOM from atmospheric aerosols complemented with meteorological data analysis will lead to a better understanding of the mechanisms of WSOM formation as well as its sources for the city of Aveiro.

5.2. UV-Vis and EEM fluorescence spectroscopy of the aerosol water-soluble organic carbon

5.2.1. UV-Vis spectroscopy

Before the isolation/fractionation procedure of the aerosol WSOM samples, the UV-Vis spectra of all aqueous extracts were acquired. The typical UV-Vis spectra of aerosol WSOC fractions are shown in Fig. V-1. In order to avoid concentration effects and facilitate the comparison between the different fractions, the spectra are shown as specific absorptivity (ε, g^{-1} C L cm^{-1}) versus wavelength (nm). These spectra are featureless and characterized by a monotonically decrease of the specific absorptivity with increasing wavelength.

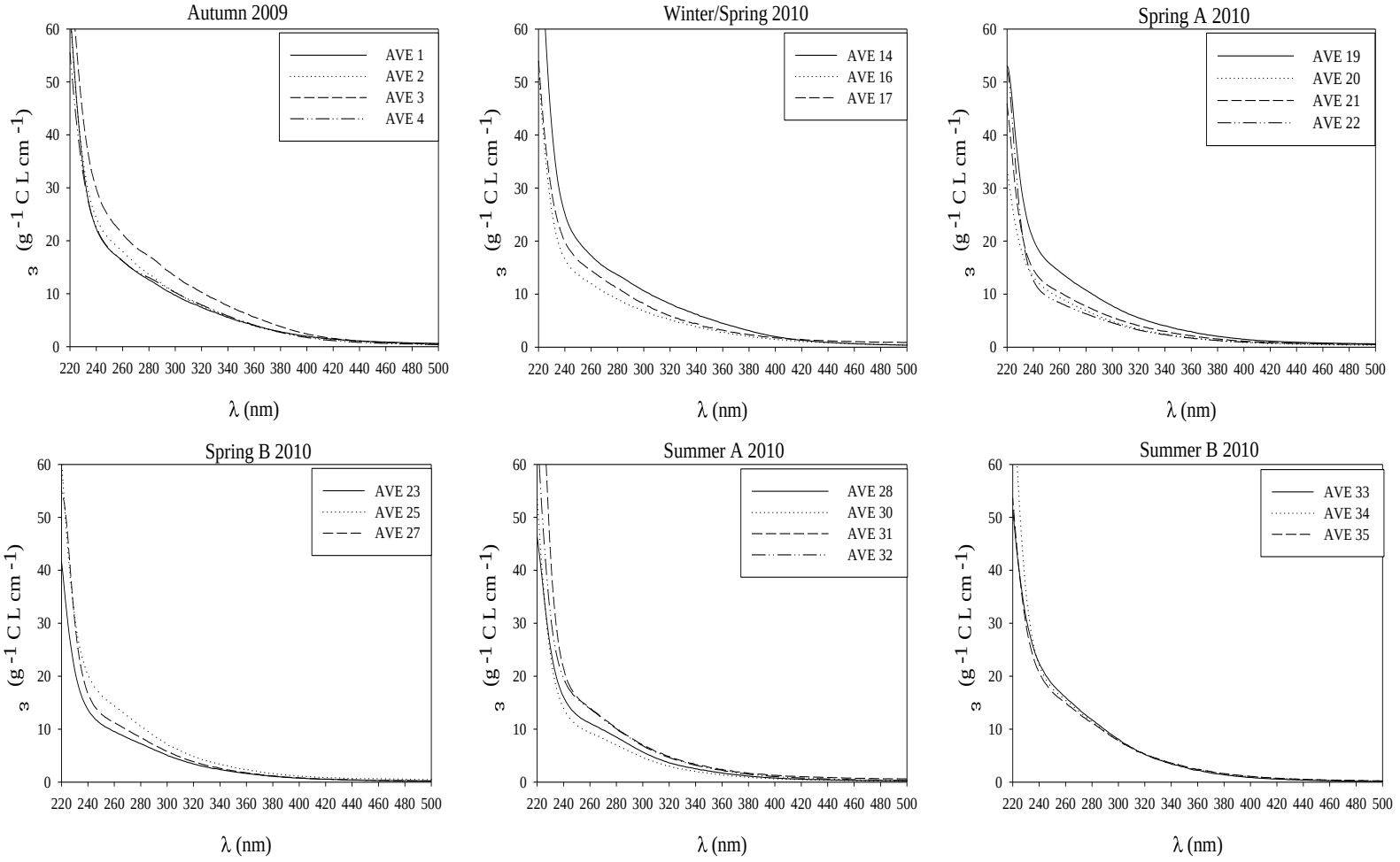

Fig. V-1. UV–Vis spectra (specific absorptivity ε (g^{-1} C L cm^{-1}) vs. wavelength (nm)) of the WSOC fractions extracted from the aerosol samples collected in the different seasons.

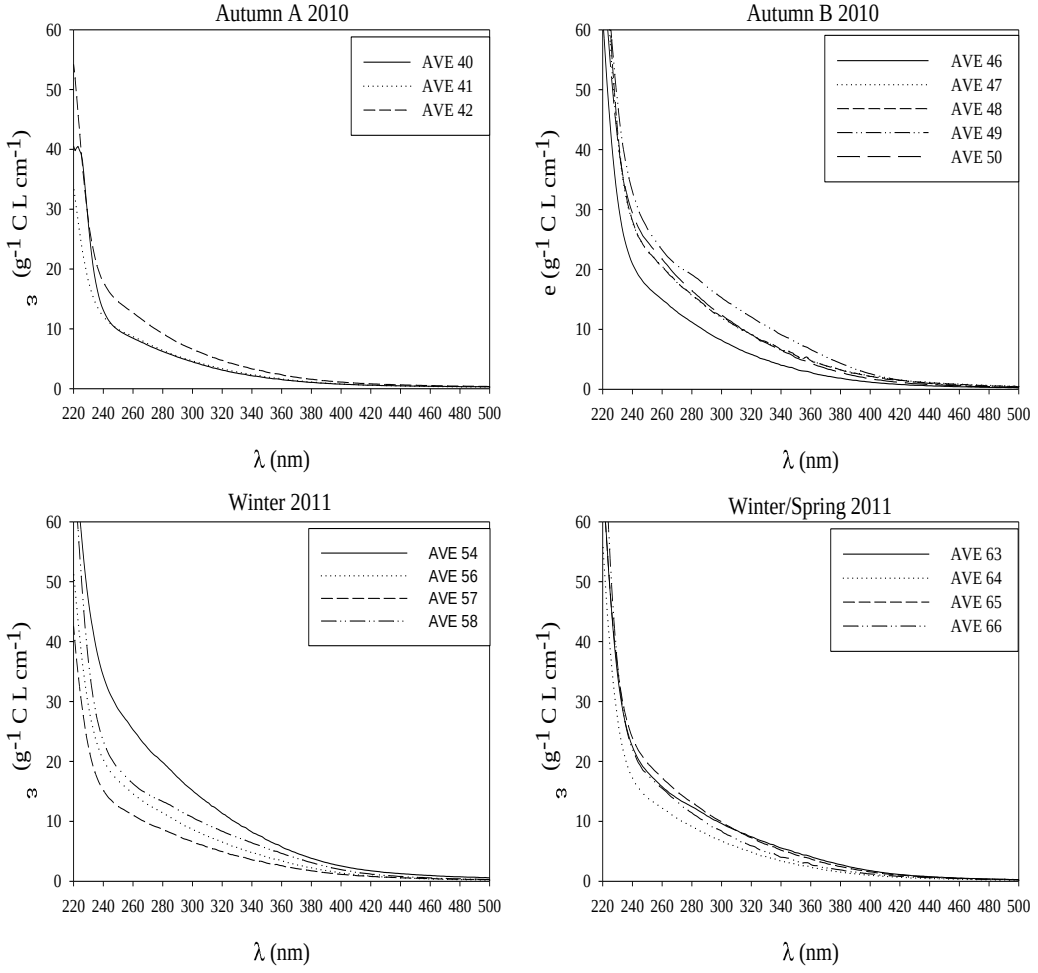

Fig. V-1. *Continued*.

A similar behaviour has been reported in previous studies focusing on the spectroscopic characterization of the WSOC fraction from atmospheric aerosols (Krivacsy et al., 2001a, 2008; Duarte and Duarte, 2005; Duarte et al., 2005). Nevertheless, some UV-Vis spectra exhibit an ill-defined shoulder between 250 and 300 nm, which has been attributed to the presence of conjugated π-bond systems (Duarte et al., 2003).

Little structural information can be drawn from the UV-Vis spectra of the aerosol WSOC, but the examination of the values of the two different parameters, the quotient E_2/E_3 (absorbances at 250 and 365 nm) and the specific absorptivity at 280 nm (ε_{280}, g^{-1} C L cm^{-1}), some qualitative information can be made. Fig. V-2 shows the obtained results for both the ratio E_2/E_3 and ε_{280}. Apparently, there is a seasonal trend in the values of both parameters despite the similarity of the UV-Vis spectra. A clear seasonal variation of the E_2/E_3 ratio can be observed, with the highest values being found for samples collected during the warmer periods. This seasonal pattern of the E_2/E_3 ratios can be associated with differences in the chemical structure of the aerosol WSOM typical of the different seasons; usually, larger E_2/E_3 is representative of a shifting in UV–Vis absorbance towards low wavelengths associated with a lower degree of humification of the WSOM (Duarte et al., 2005). A similar seasonal trend was also verified by Duarte et al. (2005) at rural location, and by Krivacsy et al. (2008) and Baduel et al., (2010) at an urban site. The variation in the E_2/E_3 ratios observed between samples within the same season may be due to the different nature of the WSOM in the $PM_{2.5}$ sampled under different atmospheric conditions.

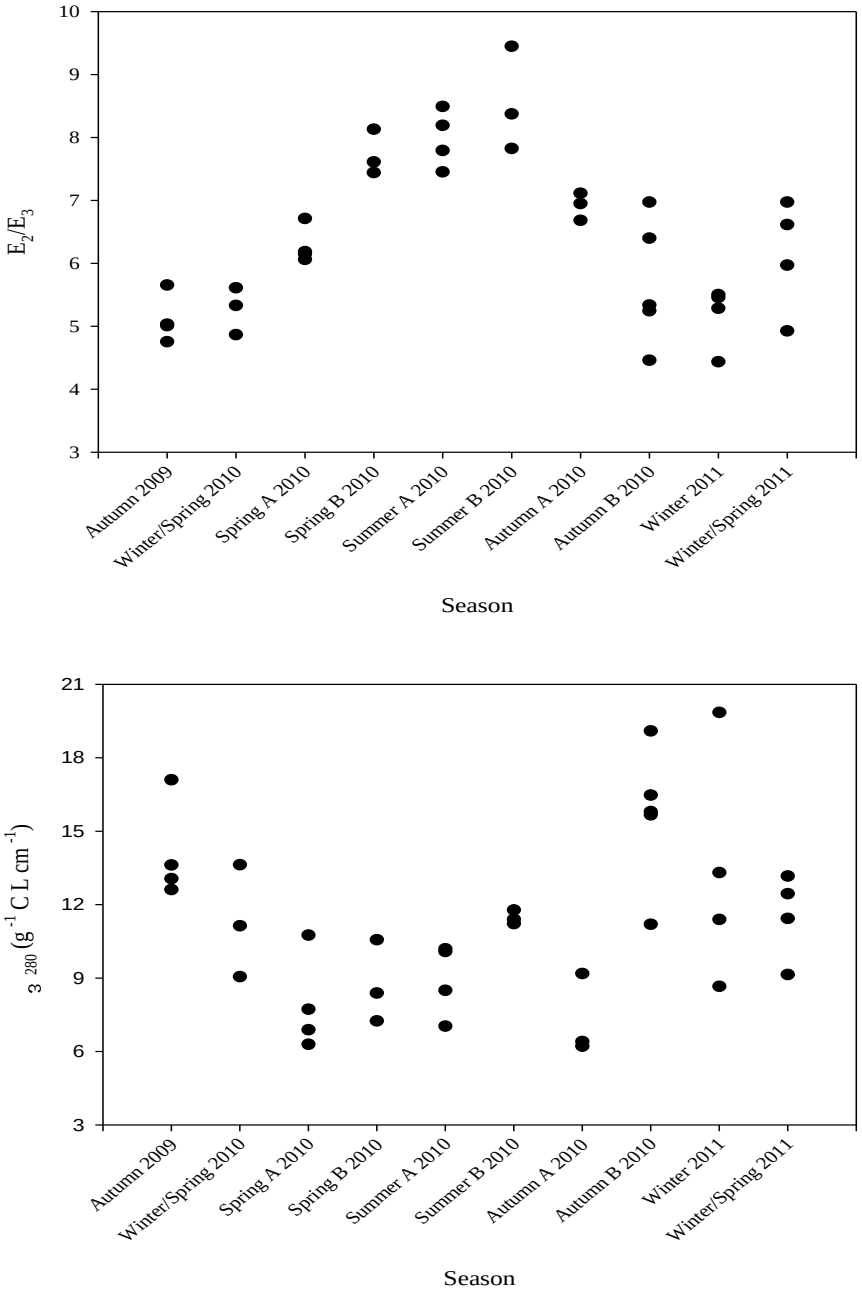

Fig. V-2. E_2/E_3 ratio and ε_{280} (g^{-1} C L cm^{-1}) of the aerosol WSOC extracts collected at the different seasons.

According to Peuravuori and Pihlaja (1997), there is also a relationship between the ratio E_2/E_3 and the percentage of aromaticity and the molecular size of aquatic dissolved organic matter. Higher E_2/E_3 ratios are generally associated with lower molecular sizes and lower degree of aromaticity. Thus, a pattern such of that reported in Fig. V-2 suggests that

the organic matter of the water-soluble fraction of the aerosol samples collected in the Summer A 2010 and Summer B 2010 seasons exhibit a lower molecular size and a lower degree of aromaticity than those collected in the Autumn 2009, Winter/Spring 2010, Autumn B 2010, Winter 2011, and Winter/Spring 2011 seasons.

The values of ε_{280} for the aerosol WSOC fractions (see Fig. V-2) also show that the specific absorptivity increases for samples collected during the colder periods. Such behavior suggests that these samples hold compounds with complex unsaturated bond systems, where more than two π-bond orbitals overlap leading to an increase in the absorptivities values (Duarte et al., 2005). These results are in good agreement with those derived from the E_2/E_3 ratio. The analysis of the specific absorptivity values in Fig. V-2 also reveals that the WSOC samples collected within the Summer B 2010 period, exhibit higher ε_{280} values than those for Spring, Summer A 2010, and Autumn A 2010 seasons. These results suggest the Summer B 2010 samples may be more enriched in unsaturated bond systems, which could likely be a consequence of the impact of local forest fires occurring in this period on the chemical characteristics of the WSOC.

5.2.2. EEM fluorescence spectroscopy

Although the EEM spectra of all aerosol WSOC fractions collected at the different seasons have been recorded, it was decided to show in this section only some selected examples of the acquired spectra, namely the EEM spectra of the WSOC fraction from the first aerosol sample collected at each main season. The complete set of EMM spectra is presented in Annex B. To avoid concentration effects and in order to facilitate the qualitative comparison between the samples, the spectra were normalised for the DOC content of the sample (in g L^{-1}) and to maximum fluorescence intensity and are shown as specific fluorescence intensity (g^{-1} C L) versus excitation and emission wavelengths (nm). The typical EEM spectra of the aerosol WSOC samples from the selected seasons (AVE 1 – Autumn 2009) are illustrated in Fig. V-3. These spectra depict four distinct fluorophores, identified here by letters A, B, C, and D on the EEM spectrum of the AVE 1 – Autumn

2009 sample: peak A at approximately $\lambda_{Excitation}/\lambda_{Emission}$ ($\lambda_{Ex}/\lambda_{Em}$) = 240/400-410, peak B at $\lambda_{Ex}/\lambda_{Em}$ = 310-320/415-418, peak C at $\lambda_{Ex}/\lambda_{Em}$ = 280/340, and peak D at $\lambda_{Ex}/\lambda_{Em}$ = 230/340. A similar fluorescence signature was observed for all the aerosol WSOC samples collected in *sampling campaign II*. In general, fluorophores of type A and B are associated with the presence of fulvic- and humic-like fluorophores (Coble, 1996), and the results obtained is this study may indicate presence of constituents with similar fluorescence features in the aerosol WSOM fractions. Bands in the same $\lambda_{Ex}/\lambda_{Em}$ range as those of A and B have also been identified in EEM fluorescence spectra of both microbial and terrestrial derived aquatic fulvic acids (McKnight et al., 2001). Peak C in marine samples has been assigned to protein-like fluorophores (Coble, 1996; Yamashita and Tanoue, 2003), and to aromatic amino acids (e.g. tryptophan) in freshwaters samples (Peuravuori et al., 2002a). In atmospheric aerosols, peak C could also be due to aromatic nitrogen organic species present in the collected atmospheric particles (Facchini et al., 1999). Further, other species such as phenol-like moieties, e.g., catechol (Simoneit et al., 1999), 5-isopropyl-2-methyl-phenol and 3-tert-butyl-phenol (Alves et al., 2001), may contribute to fluorescence of WSOC at $\lambda_{Ex}/\lambda_{Em}$ = 280/340. A similar EEM fluorescence profile exhibiting bands at the same $\lambda_{Ex}/\lambda_{Em}$ of peaks A, B, and C have already been identified in WSOC fractions from atmospheric aerosols collected at a rural site (Duarte et al., 2004) and in DOM from rainwater samples (Santos et al., 2009). Peak D at $\lambda_{Ex}/\lambda_{Em}$ = 230/340 has also been assigned to aromatic amino acids, such as tyrosine, in marine samples (Coble, 1996; Yamashita and Tanoue, 2003).

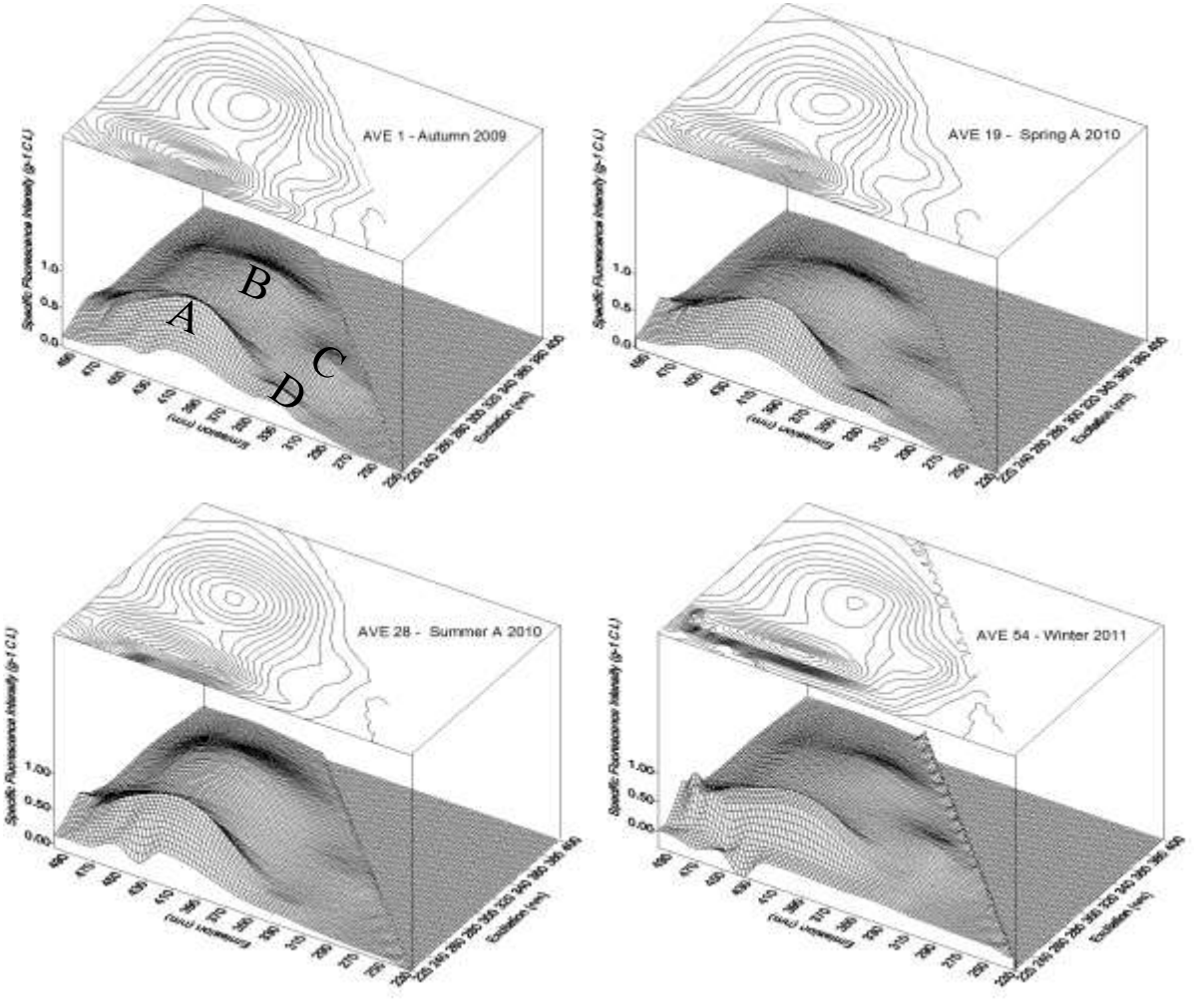

Fig. V-3. EEM spectra (specific fluorescence intensity (g^{-1} C L) versus excitation and emission wavelengths (nm)) of the WSOC fractions extracted from the aerosol samples collected in Autumn 2009, Spring A 2010, Summer A 2010 and Winter 2011 seasons.

According to Chen et al. (2002), synchronous fluorescence provides a better sensitivity and peak resolution in comparison to the conventional emission fluorescence scan mode, thus enabling the differentiation between the fluorescence spectra of samples from different sources. The synchronous fluorescence spectra with a $\Delta\lambda$ of 60 nm were obtained from the EEM profiles of each WSOC fraction by fitting the mathematical equation $\lambda_{Em} = \lambda_{Ex} + \Delta\lambda$ to the EEM profiles. The obtained spectra are shown in Fig. V-4 data were normalized to the DOC content (in g L^{-1}) of the sample. All synchronous fluorescence spectra of the aerosol WSOC samples show a well-defined peak at a λ_{Ex} of approximately 330 nm, but with different specific fluorescence intensity values. The peak at $\lambda_{Ex} \approx 330$ nm in sea water samples has been assigned to marine humic-like material (Yamashita and Tanoue, 2003). The synchronous fluorescence spectra of the aerosol WSOC samples from Autumn 2009, Autumn B 2010, and Winter 2011 seasons also exhibit second well-defined band at approximately 280 nm, whose relative specific fluorescence intensity is lower than that of peak at $\lambda_{Exc} \approx 330$ nm. Duarte et al. (2004) suggested that the peak at $\lambda_{Exc} \approx 280$ nm could be due to aromatic nitrogen organic species and phenol-like moieties present in the collected atmospheric particles. A similar fluorescence pattern, but considerable more intense, has also been identified in humic and fulvic acid fractions isolated from Kraft pulp mill effluents, being attributed to lignin-derived structural moieties (Duarte et al., 2003). The fluorescence at $\lambda_{Exc} \approx 280$ nm in the aerosol WSOC samples collected in the colder periods could also be due to the presence of lignin-derived structures resulting from wood burning processes in domestic fireplaces for house heating during those periods (Duarte, 2006). This band also appears in the synchronous spectra of aerosol WSOC samples collected in warmer periods (Spring and Summer), but as an ill-defined shoulder, being almost absent in the spectra of Summer A 2010 samples. Surprisingly, this band is more pronounced in the synchronous spectra of the aerosol WSOC samples collected in Summer B 2010 period under intense forest fire emissions, which supports the assumption that the direct emission into the atmosphere of organic compounds from biomass burning processes play an important role in the bulk chemical properties of WSOC fractions.

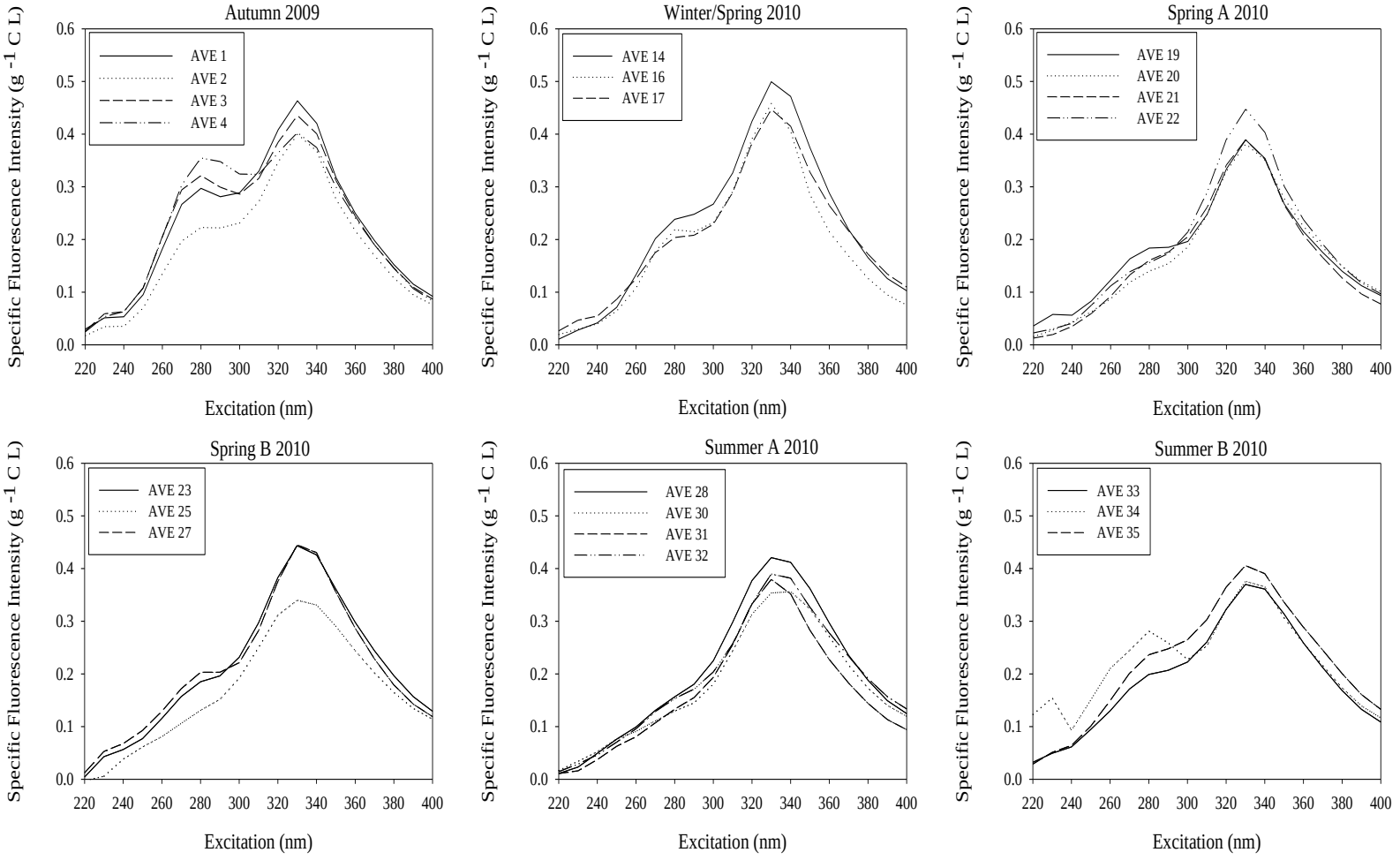

Fig. V-4. Synchronous fluorescence spectra with Δλ of 60 nm of the WSOC extracts from aerosol samples collected in Autumn 2009, Winter/Spring 2010, Spring A 2010, Spring B 2010, Summer A 2010, Summer B 2010, Autumn A 2010, Autumn B 2010, Winter 2011, and Winter/Spring 2011 seasons.

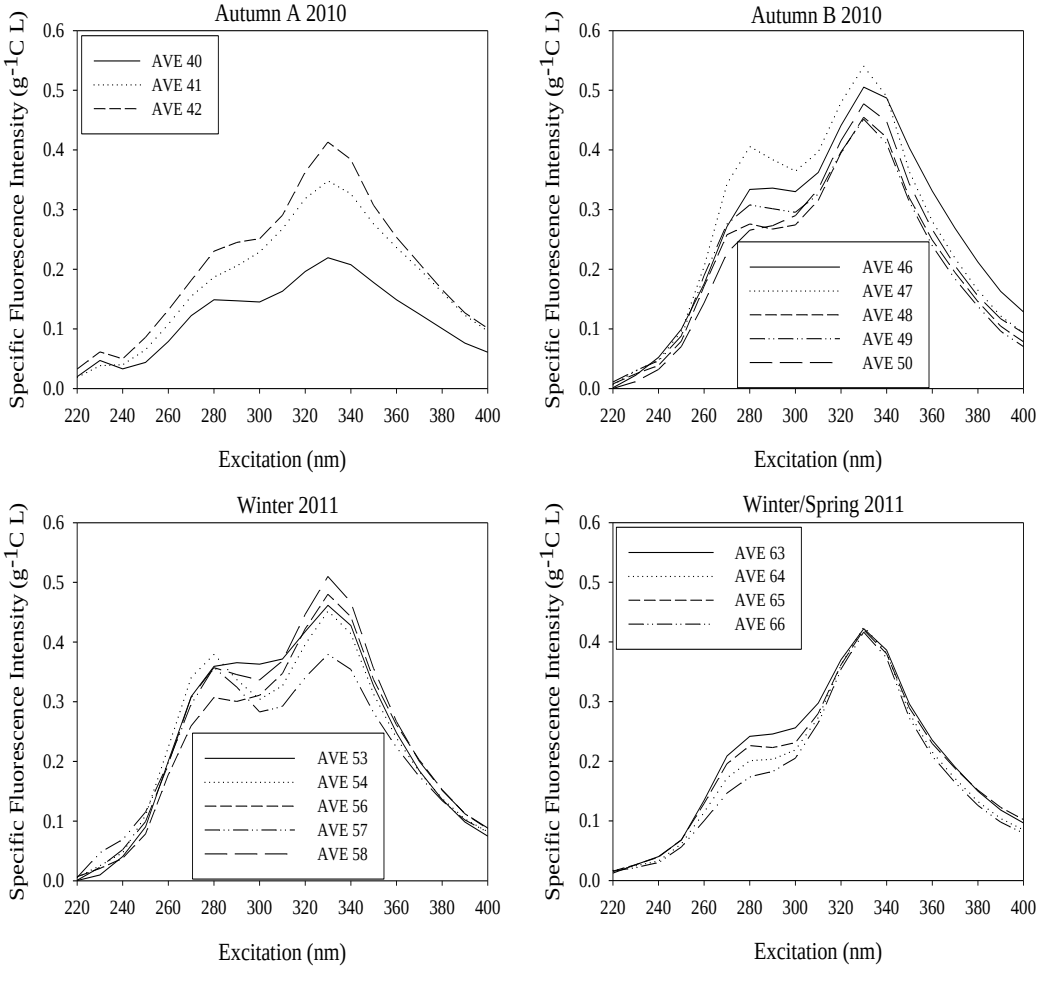

Fig. V-4. *Continued.*

5.3. Elemental analysis of aerosol water-soluble organic carbon hydrophobic acids

The elemental analysis data (average values and associated standard deviation, on an ash- and moisture free basis) and atomic ratios of the isolated WSOC hydrophobic acids from the atmospheric aerosol samples collected at different seasons are reported in Table V-1. The values obtained for the various WSOC hydrophobic acids fractions are of the same order of magnitude and no distinct seasonal variation can be discern, although a slight decrease in the relative quantity of carbon (%C) with concomitant increase in the relative quantities of hydrogen (%H), nitrogen (%N), and oxygen (%O) can be observed for the Spring and Summer samples.

Table V-1. Elemental composition (average (avg) and associated standard deviation (sd)) and atomic ratios of aerosol WSOC hydrophobic acids collected at different seasons in *sampling campaign II*. Three replicas were performed.

Sample	% C		% N		% H		% O		Atomic ratios		
	avg	sd	avg	sd	avg	sd	avg	sd	H/C	O/C	N/C
Autumn 2009	65.7	0.06	2.64	0.06	5.83	0.05	25.9	0.16	1.07	0.31	0.034
Winter/Spring 2010	61.9	0.48	3.23	0.01	5.86	0.03	29.0	0.52	1.14	0.36	0.045
Spring A 2010	59.3	0.49	3.93	0.07	6.21	0.05	30.6	0.45	1.22	0.39	0.063
Spring B 2010	57.9	1.56	4.52	0.17	6.25	0.20	31.4	1.92	1.27	0.40	0.067
Summer A 2010	58.2	0.27	4.19	0.10	6.32	0.09	31.3	0.46	1.31	0.44	0.063
Summer B 2010	60.4	0.18	2.34	0.05	6.08	0.02	31.2	0.21	1.20	0.40	0.033
Autumn A 2010	61.6	0.71	3.66	0.06	6.27	0.09	28.5	0.82	1.20	0.35	0.050
Autumn B 2010	62.9	0.37	2.35	0.01	5.68	0.03	29.1	0.40	1.10	0.35	0.032
Winter 2011	63.7	0.19	2.37	0.03	5.61	0.05	28.4	0.18	1.06	0.35	0.032
Winter/Spring 2011	61.6	0.25	2.62	0.02	5.64	0.04	30.1	0.29	1.11	0.37	0.037

Overall, the values of C, H, N, and O were in the range of 57.9 (±1.56)% (Spring B 2010) to 65.7 (±0.06)% (Autumn 2009), 5.61 (±0.05)% (Winter 2011) to 6.32 (±0.09)% (Summer A 2010), 2.34 (±0.05)% (Summer B 2010) to 4.52 (±0.17)% (Spring B 2010), and 25.9 (±0.16)% (Autumn 2009) to 31.4 (±1.92)% (Spring B 2010), respectively. For WSOC samples from fine atmospheric aerosols collected during the Summer period at the

high-alpine site of Jungfraujoch, Switzerland, Krivacsy et al. (2001a) reported the following elemental analysis data (average values and standard deviation in brackets) 52.3 (0.2)% for C, 6.7 (0.4)% for H, 2.5 (0.9)% for N, and 38.5 (1.1)% for O. Similar elemental composition data were reported for a rural site in Hungary (K-puszta): 52% for C, 6.2% for H, 2.5% for N, and 39% for O (Kiss et al., 2002). Duarte et al. (2007) also reported elemental analysis data for WSOC samples from fine atmospheric aerosols collected during one year period at a rural site near the city of Aveiro. The obtained values for C, H, N, and O were in the range of 51.5-58.3%, 5.7-6.2%, 2.1-3.8%, and 31.8-36.6% , respectively, with no distinct seasonal variation. In comparison to the values reported in the literature, the WSOC hydrophobic acids fractions at the city of Aveiro exhibit a higher relative quantity of C and a lower relative quantity of O. Apparently, the WSOC samples collected in this study are less oxidized, thus reflecting the important role played by local anthropogenic sources on the structural features of urban aerosol WSOC as compared to those collected at more clean environments (Krivacsy et al., 2001a; Kiss et al., 2002; Duarte et al., 2007).

The examination of the atomic ratios (H/C, O/C, and N/C) also allow for some qualitative estimation to be made. For sedimentary fulvic and humic acids from aquatic and terrestrial environments, a high H/C atomic ratio has been related to a lower content of unsaturated structures (Giovanela et al., 2004). On this regard, the WSOC hydrophobic acids from Spring B 2010 and Summer A 2010 seasons show the highest H/C atomic ratios, thus suggesting a higher aliphatic character of these samples compared to those of the less warmer seasons. In comparison to the H/C atomic ratios reported by Duarte et al. (2007) for fine aerosol WSOC samples collected at a rural site near the city of Aveiro, the values obtained in present study are lower, thus suggesting a lower aliphatic character of the urban aerosol WSOC samples (this feature is consistent with the results obtained in the CPMAS ^{13}C NMR spectroscopy, in section 5.5).

The highest value for the O/C atomic ratio, which is used as an indicator of the oxidation level of organic matter from terrestrial and aquatic environment (Abbt-Braun et al., 2004), was obtained for the aerosol WSOC hydrophobic acids collected in Summer A 2010 season (as shown in Table V-1). Indeed, the O/C ratios also seem to follow a seasonal trend, with the lowest values being determined for samples collected during the colder

periods. These findings suggest that the aerosol WSOC hydrophobic acids samples collected during these periods exhibit a lower degree of oxidation than those collected during Spring and Summer seasons. This is also in agreement with the assumption that atmospheric WSOM has different origins depending of the season, with Summer values probably having a higher contribution from photochemical oxidation processes (SOA formation) and Winter values resulting from direct emissions of oxygenated particulate organics from various anthropogenic sources, including biomass burning. According to Krivacsy et al. (2001a), an O/C atomic ratio of 0.55 indicates that the organic structures have a high degree of oxidation. In this study, the aerosol WSOC hydrophobic acids show O/C atomic ratios lower than the value reported by Krivacsy et al. (2001a). Moreover, the values obtained in the present study are lower than those reported by Duarte et al. (2007) for a rural location near the city of Aveiro (0.41-0.55), thus suggesting that the urban aerosol WSOC hydrophobic acids exhibit a lower degree of oxidation than the rural aerosol WSOM.

Table V-1 also shows the atomic N/C ratios for the WSOC hydrophobic acids fractions from the urban aerosol samples. The N/C ratios exhibit a seasonal variation, with the higher values being observed for aerosol samples collected during Spring and Summer A 2010 seasons. Duarte et al. (2007) also reported a similar annual trend for the atomic N/C ratios of WSOC hydrophobic acids fractions from rural aerosol samples. The authors suggested that the higher N/C ratio of samples collected during the warmer periods, i.e. higher content in organic nitrogen compounds, could be associated with the enhancement of photochemical reactions of individual vapor phase organic compounds with reactive inorganic forms of nitrogen during these periods of high solar intensity. Surprisingly, the N/C ratio for samples collected during the Summer B 2010 season is of the same order of magnitude of those collected during Autumn and Winter seasons. The decrease in the value of N/C for the Summer B 2010 samples could be the end result of the direct emission of organic compounds from biomass burning processes during this period of intense forest fires. This finding supports the assumption that in this particular warmer period, the aerosol WSOC hydrophobic acids fractions have an important primary origin.

The elemental analysis data were also used for calculating a mass conversion factor that will be used for converting the amount of aerosol WSOC into mass of aerosol WSOM.

Using this approach an aerosol mass closure was achieved on the basis of carbonaceous fractions alone (please see section 4.8 for additional details). The conversion factors calculated for the aerosol WSOM samples collected at the city of Aveiro ranged between 1.5 and 1.8, with an average (and standard deviation) value of 1.6 (0.1). This parameter was slightly higher for samples collected during the Spring and Summer seasons (1.7-1.8) than for those collected during the colder seasons (1.5-1.6). The conversion factors obtained in the present study are slightly lower than those reported by Duarte (2006) for aerosol WSOM samples collected at a rural location (between 1.7 and 1.9, with an average value of 1.8), somehow reflecting the influence of the different levels of pollution at both sampling sites. Apparently, the conversion factor parameter varies over time and from site to site; nevertheless, in the present study, a constant value of 1.6 was used to calculate the mass of aerosol WSOM (additional information is provided in section 4.8).

5.4. FTIR-ATR spectroscopy of aerosol water-soluble organic carbon hydrophobic acids

The FTIR-ATR spectra of the aerosol WSOC hydrophobic acids samples are shown in Fig. V-5. Overall, the spectra exhibit predominantly the presence of oxygen containing functional groups and aliphatic C-H groups, with the majority of the valence vibrations being characteristics to all samples. These spectra are also very similar to those of aerosol WSOC hydrophobic acids collected at a rural site near the city of Aveiro (Duarte et al., 2007).

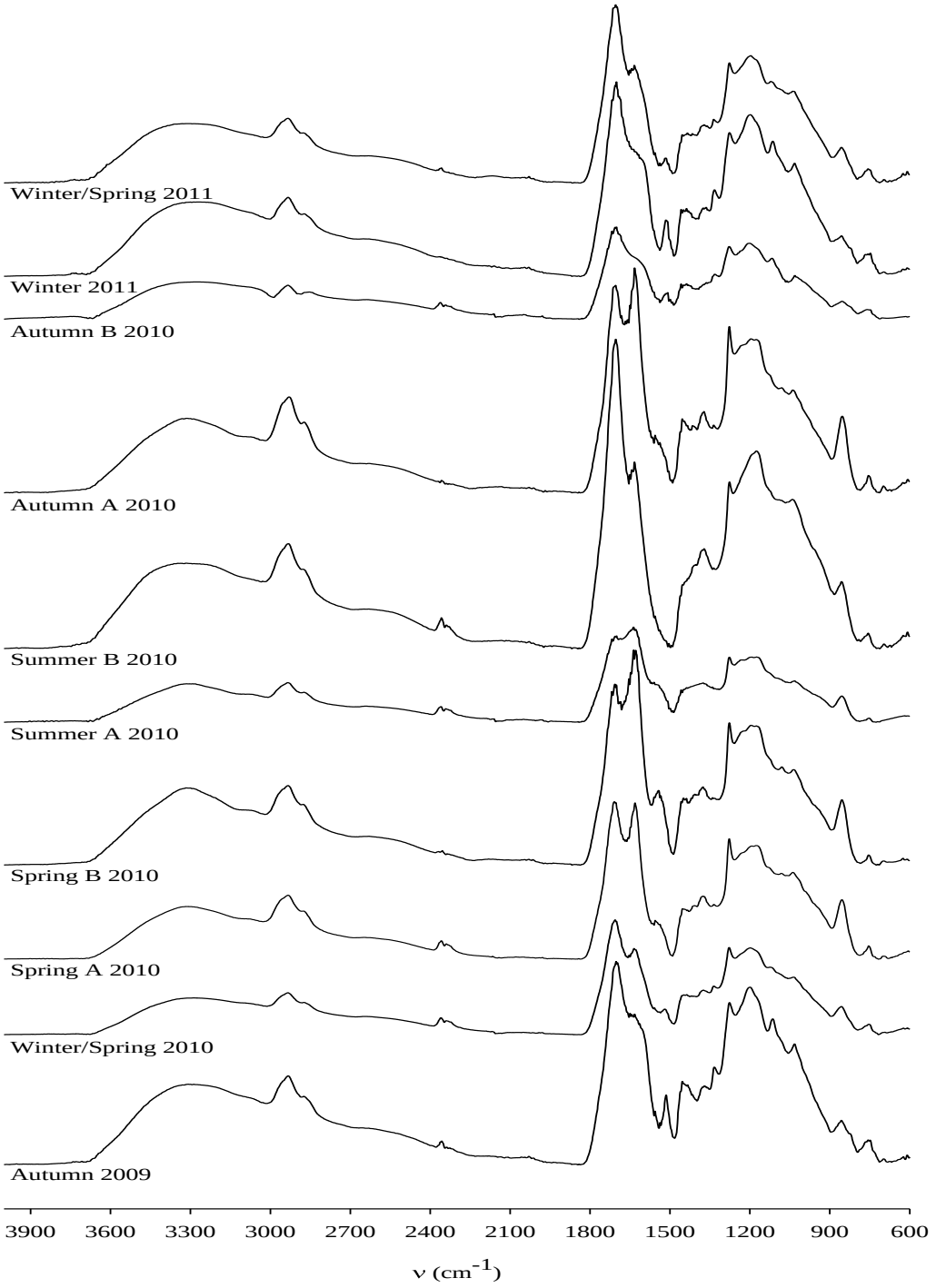

Fig. V-5. FTIR-ATR spectra (4000–600 cm^{-1}) of aerosol WSOC hydrophobic acids samples from the different seasons.

The interpretation of the FTIR-ATR spectra was based on the assignments given in the literature for natural organic matter from different environmental matrices. As such, the following infrared absorption bands are common to all spectra: 1) a broad band centred at around 3340 cm^{-1}, which is usually assigned to O-H stretching of hydroxyl, carboxyl and phenol groups (Bellamy, 1975; Santos and Duarte, 1998; Kiss et al., 2002; Duarte et al., 2007): 2) the bands in the 2970-2840 cm^{-1} region, which are usually attributed to C-H stretching of methyl (centred at around 2959 cm^{-1}) and methylene (centred at around 2893 cm^{-1}) groups of aliphatic chains (Santos and Duarte, 1998; Duarte et al., 2007); 3) the strong band at near 1710 cm^{-1} (ranging from 1705 cm^{-1} to 1718 cm^{-1}), which is generally assigned to unconjugated carbonyl (C=O) stretching mainly of carboxyl groups and, in a lesser extent, of aldehydic and/or ketonic C=O groups (Santos and Duarte, 1998; Duarte et al., 2007); 4) the band centred at near 1630 cm^{-1}, which is usually attributed to the C–C stretching of aromatic rings and to the C=O stretching of conjugated carbonyl groups (Santos and Duarte, 1998). It is noteworthy that bending vibration of water is centered at 1640 cm^{-1} and may also contribute to infrared absorption in this region if the sample is not thoroughly dried (Duarte et al., 2007); 5) the band centred at approximately 1200 cm^{-1}, which is assigned to O-H bending and C-O stretching vibrations mainly of carboxyl groups (Santos and Duarte, 1998), and finally, 6) the band at approximately 853 cm^{-1}, which is usually assigned to out-of-plane deformation vibrations of C=C bonds of alkanes (Bellamy, 1975).

One of the major differences between the spectra of the aerosol WSOC hydrophobic acids lays in the band at around 1630 cm^{-1}, whose relative intensity is higher in the spectra of the Spring B 2010, Summer A 2010, and Autumn A 2010 samples. In the spectrum of the Spring A 2010 sample, the intensity of such band appears to be of the same order of magnitude of that centred at 1710 cm^{-1}. Another difference is the presence of a weak absorption band centred at around 1512-1517 cm^{-1} in the FTIR-ATR spectra of the WSOC hydrophobic acids from Autumn 2009, Winter/Spring 2010, Autumn B 2010, Winter 2011, and Winter/Spring 2011 samples. A band at this same wavenumber is typical and quite strong in spectra of lignins (Santos et al., 2000; Duarte et al., 2003) and is due to the C-C stretching vibrations of aromatic rings of siringyl and guaiacyl units (Fengel and Wegner, 1984; Faix, 1992). These spectra also show a very weak band at approximately 1333-1340 cm^{-1}, which is usually attributed to ring breaking vibrations of siringyl units in

lignin spectra (Fengel and Wegner, 1984). The presence of these aromatic signals due to lignin derived structures corroborates those found in the CPMAS ^{13}C NMR spectroscopy (section 5.5), highlighting the contribution of wood burning processes into the chemical properties of the WSOC fractions during the colder periods. A similar FTIR-ATR signature was also found in the FTIR spectra of WSOC hydrophobic acids collected at a rural site during Autumn, Autumn/Winter and Winter seasons (Duarte et al., 2007). Another feature observed in the FTIR-ATR of the WSOC fractions from the Spring A 2010, Spring B 2010, and Summer A 2010 seasons is a week band at near 1575 cm^{-1}. This band is not shown in spectra of other WSOC samples and, to the best of our knowledge, this band is unusual in infrared spectra of aerosol WSOM from other sites. According to Coates (2006), N-H bending vibrations of secondary amines could contribute to absorption at this frequency. An additional feature observed in the FTIR-ATR spectra of the WSOC hydrophobic acids samples collected during the colder periods (Autumn, Winter, and Winter/Spring) is the presence of a weak absorption band between1449 and 1456 cm^{-1}, usually attributed to asymmetric bending vibrations of C–H bonds of methyl and methylene groups of aliphatic chains (Bellamy, 1975).

5.5. CPMAS ^{13}C NMR spectroscopy of aerosol water-soluble organic carbon hydrophobic acids

This section is devoted to the investigation of the main structural features of aerosol WSOC hydrophobic acids samples collected during *sampling campaign II* in the city of Aveiro by means of solid-state cross polarization with magic angle spinning ^{13}C NMR (CPMAS ^{13}C NMR) spectroscopy. Due to the low amount of solid residue of WSOC hydrophobic acids fractions at the end of the freeze-drying procedure, only five aerosol WSOM samples were characterized by this technique, namely those collected in Autumn 2009, Summer B 2010, Autumn B 2010, Winter 2011, and Winter/Spring 2011 seasons. Fig. V-6 shows the solid-state CPMAS ^{13}C NMR spectra of these five aerosol WSOC hydrophobic acids samples.

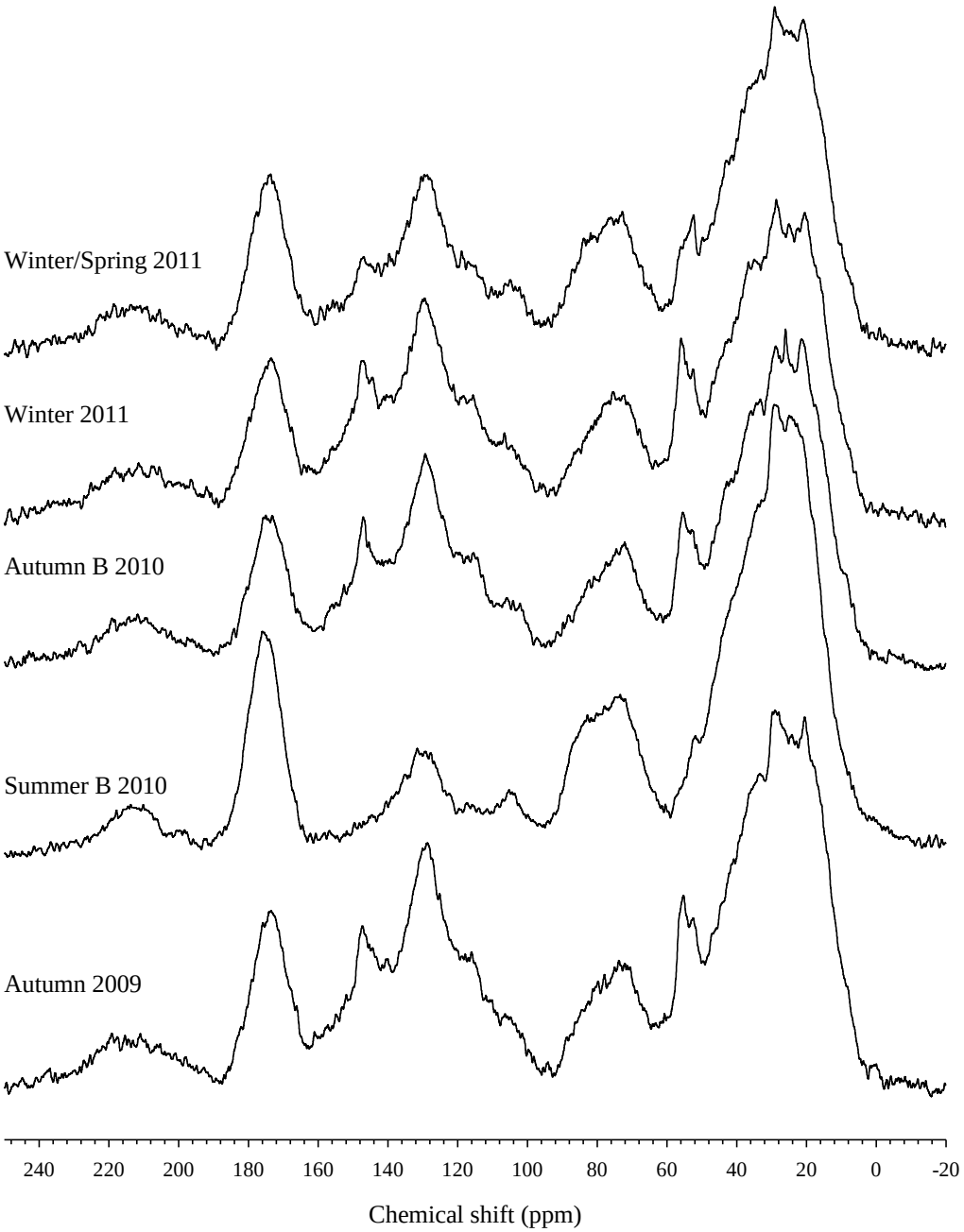

Fig. V-6. Solid-state CPMAS ^{13}C NMR spectra of WSOC hydrophobic acids fractions of five aerosol samples representative of different seasonal periods.

In accordance with the assignments described in the literature for natural organic matter from various sources, including aerosol WSOM from other locations (Malcolm,

1989; Santos et al., 2000; Lambert and Lankes, 2002; Duarte et al., 2005, 2007, 2013), four major regions were considered in these CPMAS ^{13}C NMR spectra: 0-50 ppm (unsubstituted saturated aliphatic carbons), 60-95 ppm (aliphatic carbons singly bonded to one oxygen or nitrogen atom), 110-160 ppm (aromatic and unsaturated carbons), and 160-190 ppm (carboxyl, ester and amide carbons). Minor peaks are also seen at 50-60 ppm (carbons of methyl groups of methyl ethers), 95-110 ppm (aliphatic carbons bonded to two oxygen atoms, such as anomeric carbons of polysaccharides), and 190-230 ppm (carbonyl carbons of aldehydes and ketones). Table V-2 gives the ^{13}C NMR estimates (as percentage peak areas) of carbon distribution in WSOC hydrophobic acids.

Table V-2. Percentage distribution of carbon in aerosol WSOC hydrophobic acids based on solid-state CPMAS ^{13}C-NMR analysis. "N.D." refers to NMR signal not detected.

Sample	**Percentage peak area in each spectral region on the ppm scale**						
	190-230	**160-190**	**110-160**	**95-110**	**60-95**	**50-60**	**0-50**
Autumn 2009	5.3	9.4	25.3	2.7	10.1	5.4	41.8
Summer B 2010	5.4	12.0	11.4	3.2	14.9	N.D.	53.2
Autumn B 2010	6.8	10.0	24.5	3.5	11.0	5.2	38.9
Winter 2011	6.9	10.3	25.6	3.7	11.6	5.5	36.4
Winter/Spring 2011	6.5	10.9	20.7	3.5	13.2	4.2	41.0

The CPMAS ^{13}C NMR spectra in Fig. V-6 reveal that the various aerosol WSOC hydrophobic acids samples hold similar carbon functional groups; however, they differ in terms of the relative carbon distribution (as seen in Table V-2). The most noticeable feature in these spectra is the strong and broad aliphatic carbon signal (36.4-53.2% of the total NMR peak area). Furthermore, signal intensities for aliphatic carbons in WSOC hydrophobic acids vary with the sampling period, being slightly lower in samples collected in Autumn and Winter seasons compared to those collected during the Summer period. The presence of three peaks centred at 21 ppm, 25 ppm, and 29 ppm, with the first peak attributed to methylene groups in alkyl chains and the other two peaks to methine groups in

alkyl chains (Malcolm, 1989), are also seen in the spectra of WSOC hydrophobic acids collected in the colder seasons. The spectrum of the sample collected in Winter 2011 also exhibit an unresolved peak at 35 ppm, usually assigned to methylene carbons of branched alkyl chains (Malcolm, 1989). This resonance appears to be shifted towards lower chemical shift region, i.e., ≈ 33 ppm, in the spectra of the samples collected in Autumn and Winter/Spring seasons. A possible assignment for this resonance is the presence of methylene carbons α, β, δ, and ε from terminal methyl group (Hayes et al., 1989). The peaks centred at 21 ppm, 29 ppm, and 35 ppm were also identified in WSOC hydrophobic acids collected by Duarte et al. (2007) in Autumn and Winter seasons at a rural site.

The CPMAS ^{13}C NMR spectra of aerosol WSOC hydrophobic acids samples from the colder seasons also exhibit resonance at approximately 55 ppm and 147 ppm. These two peaks are absent from the spectrum of the WSOC hydrophobic acids collected in the Summer season. A spectroscopic signature similar to those of peaks at 55 ppm and 147 ppm is typical in spectra of lignin structural units (Haw et al., 1984; Hatfield et al., 1987), and they are also present, but considerably more intense, in the spectra of humic and fulvic acids from Kraft pulp mill effluents (Duarte et al., 2003). While peak at 55 ppm is due to methoxyl groups such as those of syringyl and guaiacyl units, the signal at 147 ppm is attributed to oxygen-substituted aromatic ring carbons (Haw et al., 1984; Hatfield et al., 1987). Biomass combustion processes appears to be a definite and significant source for the presence of lignin derived structures in aerosol WSOC hydrophobic acids samples of colder seasons. During these periods the air temperature reached low values leading to an increase in domestic heating, mainly by means of wood combustion processes in domestic fireplaces. Besides levoglucosan and related anhydrosaccharides (e. g. mannosan and galactosan), which are often used as tracers for smoke particulate matter from burning of biomass, fine aerosol fractions of smoke samples can also contain thermally unaltered and partially altered lignin-derived compounds, such as aromatic phenols (e.g. siringyl and guaiacyl derivatives), aldehydes, ketones, acids and alcohols (Simoneit et al., 1993; Rogge et al., 1998). Lignin pyrolysis products have generally the same substituent pattern (OH, OCH_3) on the aromatic rings as the precursor aromatic alcohols from which they were derived (Simoneit et al., 1993). Wood burning can also explain the higher aromatic content (total percentage peak areas in the 160-110 ppm range) of the WSOC hydrophobic acids samples collected in colder seasons (20.7-25.6%) compared to that collected in the

Summer period (11.4%). These results are in good agreement with the studies of Duarte et al. (2007, 2008b), where it has been clearly identified a biomass-burning fingerprint in aerosol WSOC samples collected during Fall/Winter seasons at a rural location. In the Spring/Summer seasons, on the other hand, the same authors suggested that the WSOC might be due to secondary atmospheric oxidation processes, thus indicating a change in the sources which are active in the various seasons. Samburova et al. (2005) likewise suggested the primary emissions from wood combustion during Winter months, and photochemical production during the Summer months, as possible sources for atmospheric WSOC in an urban area. Sannigrahi et al. (2006) also reported a measurable amount of aromatic carbon in WSOC hydrophobic acids fraction from urban atmospheric aerosols collected during the Summer season. The authors suggested that the aromatic structures present in their samples are likely to be mainly a product of motor vehicle emissions or SOA-producing reactions. Taking into account these reports, one may also suggest that motor vehicle exhaust and SOA formation could be possible sources of aromatic carbon to the aerosol WSOC hydrophobic acids collected during Summer 2010 season at the city of Aveiro.

All spectra also exhibit a week resonance at approximately 52 ppm. Using two-dimensional liquid NMR spectroscopy for characterizing an aerosol WSOC sample collected during the Winter season, Duarte et al. (2008b) found evidence of the presence of a ^{13}C signal at 52 ppm, which the authors associated to amino sugar residue containing a single ketoamide group within the hexose unit. Baldock et al. (1992) also reported that amino carbon of protein structures resonate in the 45-65 ppm chemical shift region. The resonance in the 60–95 ppm region is also common to all spectra (10.1-14.9% of the NMR peak area) and it is likely to originate from the various HC‑OH fragments of cellulose or other carbohydrates structures (Hayes et al., 1989; Keeler et al., 2006; Duarte et al., 2008b, 2013; Simpson and Simpson, 2009). The presence of a downfield resonance at approximately 104 ppm, which is representative of anomeric C, further corroborates the presence of carbohydrate-like moieties in the aerosol WSOC hydrophobic fractions. Unsubstituted aromatic C also show resonance within this spectral region (Duarte et al., 2008), thus suggesting that ^{13}C NMR intensity in the 95‑110 ppm region could also have a small contribution from such structural moieties.

Integration of the 160-190 ppm spectral region reveals that 9.4% to 12% of the carbon in WSOC hydrophobic acids is associated with carboxylic acid functional groups (Fig. V-6; Table V-2), with the highest value being obtained for samples collected during the Summer 2010 season. As early mentioned, ester and amide carbons are also likely to contribute to resonance in this spectral region. All spectra of the WSOC hydrophobic acids also show evidences for the presence of carbonyl carbons of aldehydes and ketones (190-230 ppm range), which accounts to 5.3-6.9% of the total NMR peak area.

5.6. Conclusions

This chapter presents the structural characterization of the aerosol WSOC hydrophobic acids by means of UV-Vis, EEM fluorescence, FTIR-ATR, and CPMAS ^{13}C NMR spectroscopies, and elemental analysis. In general, the results obtained by the different techniques showed differences among the WSOM samples from the different seasons.

The results obtained with UV-Vis spectroscopy, namely the E_2/E_3 ratio and ε_{280}, suggest the existence of a seasonal trend in the values of both parameters despite the similarity of the UV-Vis spectra. The E_2/E_3 ratios also suggested that the WSOC hydrophobic acids of the aerosol samples collected in the Summer A 2010 and Summer B 2010 seasons exhibit a lower molecular size and a lower degree of aromaticity than those collected in Autumn 2009, Winter/Spring 2010, Autumn B 2010, Winter 2011, and Winter/Spring 2011. The ε_{280} values also revealed that the WSOC samples collected during Summer B 2010 period are likely to be more enriched in unsaturated bond systems, which could be a consequence of the impact of local forest fires registered during this period.

The EEM spectra of the aerosol WSOC samples exhibit four distinct fluorophores, being this fluorescence signature observed in all spectra of the samples collected in sampling campaign II. Additionally, the synchronous fluorescence spectra with a $\Delta\lambda$ of 60 nm collected in the colder periods (Autumn 2009, Autumn B 2010, and Winter 2011 seasons) exhibit fluorescence at $\lambda_{Exc} \approx 280$ nm, suggesting the presence of lignin-derived structures resulting from wood burning processes in domestic fireplaces for house heating

during those periods. The synchronous fluorescence spectra of the aerosol WSOC samples collected in Summer B 2010 period, also shows such fluorescence band which may be associated with the occurrence of forest fires. These features support the assumption that the direct emission into the atmosphere of organic compounds from biomass burning processes plays an important role in the bulk chemical properties of WSOC fractions.

In regard to the elemental analysis, results suggest that the values of C, H, N, and O for the WSOC hydrophobic acids fractions were in the range of 57.9-65.7%, 5.61-6.32 %, 2.34-4.52%, and 25.9-31.4%, respectively, with no distinct seasonal variation. Nevertheless, WSOC hydrophobic acids from Spring and Summer apparently have a slight decrease in the relative quantity of C with simultaneous increase in the relative quantities of H, N, and O. Results also suggest that the aerosol WSOC hydrophobic acids samples collected during the colder seasons exhibit a lower degree of oxidation than those collected during Spring and Summer seasons.

In general, the FTIR-ATR spectra exhibit predominantly the presence of oxygen containing functional groups and aliphatic C-H groups, with the majority of the valence vibrations being characteristics to all samples. CPMAS ^{13}C NMR data showed that the WSOC hydrophobic acids from atmospheric aerosols are mostly aliphatic in nature, followed by aromatics, oxygenated alkyls, and carboxylic acid functional groups. Moreover, the aerosol WSOC hydrophobic acids collected during colder periods have a higher aromatic content than those collected during the Summer season. The presence of signals typical of lignin-derived structures (e.g., syringyl and guaiacyl units) in both CPMAS ^{13}C NMR and FTIR-ATR spectra of aerosol WSOC hydrophobic acids samples collected during colder seasons highlights the major contribution of wood burning processes during these periods of low temperatures conditions into the bulk chemical properties of WSOM from atmospheric particles.

VI

Comprehensive two-dimensional liquid chromatography of water-soluble organic matter from fine urban atmospheric aerosols

6.1. Introduction

The comprehensive two-dimensional liquid chromatography (LC × LC) technique combines two liquid chromatographic modes with different separation mechanisms, where all components in a sample mixture are subjected to the two separation modes. The 1st dimension and 2nd dimension columns are connected in series by means of a transfer system (i.e., a switching valve equipped with two identical loops) located between them. The function of this interface is to cut and then re-inject continuous fractions of the 1st dimension column effluent onto the fast separation 2nd dimension column. In order to achieve comprehensive analysis and to preserve the separation in the 1st dimension, the fractions injected onto the 2nd dimension column must undergo elution before the following re-injection. The retention times in the 2nd dimension separation mode must be equal or less than the duration of the modulation period (i.e., time during which a fraction of the 1st dimension column effluent is being accumulated in one of the loops of the switching valve). The 2nd dimension column is usually connected to a detection system (a single detector or detectors connected in series, depending on the purpose of the analysis), such as a DAD, fluorescence detector (FLD), evaporative light scattering detector (ELSD), or MS detector.

An important practical principle of LC × LC concerns the orthogonality of the LC modes, i.e. the selectivity of the two separation modes must be completely independent form each other and separate two properties of a given sample in a single run without influencing themselves. As recently reviewed by Duarte et al. (2012), several approaches to comprehensive LC × LC have been described in the literature, including IEX × reversed phase (RP), IC × RP, RP × SEC, PALC × SEC, or normal phase (NP) × RP. Although orthogonal (independent), the combination of NP with RP is probably the most difficult to accomplish due to the immiscibility of the mobile phases at the interface of both separation modes, which can cause broad and distorted peaks (Stoll et al., 2007; Dugo et al., 2008). According to Dugo et al. (2008), the great advantage of LC × LC relatively to the one-dimensional LC (1D-LC) is the maximum number of compounds that can be separated in a single chromatographic run. Besides an increased peak capacity, LC × LC also generates increased selectivity and resolution. As recently reviewed by Matos et al. (2012), data

processing of LC × LC is also a rapid evolving subject since there is a general lack of commercial software associated to analytical instrumentation. According to Matos et al. (2012), the first algorithms developed for data processing in LC × LC were generalizations of concepts from 1D chromatography; nowadays, there are already methods for non-targeted and targeted analyses fully developed to deal with multidimensional chromatographic data (Matos et al., 2012).

LC × LC, coupled to different detectors, has proven to be useful for the separation of a large number of components in several complex matrices, such as the separation and identification of compounds in Chinese medicines (Chen et al., 2004), analyses of triacylglycerols in natural lipidic matrixes (Dugo et al., 2006), and analyses of antioxidant phenolic acids in herb extracts (Kivilompolo and Hyötyläinen, 2007) and in wines (Dugo et al., 2009; Matos et al., 2013). For the analysis of complex environmental samples, only three studies have been produced thus far concerning the application of LC × LC, namely the analysis of acidic compounds in atmospheric aerosols (Pól et al., 2006) and the separation of NOM from aquatic (Duarte et al., 2012) and atmospheric particles (Barros, 2011). Pól et al., (2006) used a LC x LC method, consisting of a strong cation-exclusion column in the 1st dimension and a RP column in the 2nd dimension, coupled to a TOF-MS detection system for the quantitative determination of carboxylic acids in methanolic extracts of rural and urban atmospheric aerosols. Duarte et al. (2012) used a mixed-mode hydrophilic interaction liquid chromatography (HILIC) column operated under aqueous RP conditions in the 1st dimension and a SEC column in the 2nd dimension, for mapping the hydrophobicity versus molecular weight (MW) distribution of two well-known complex organic mixtures: Suwannee River Fulvic Acids and Pony Lake Fulvic Acids. The LC × LC fractions were screened on-line by three detectors connected in series: DAD, FLD, and ELSD. According to Duarte et al. (2012), the packing material of the mixed-mode HILIC column used in their work features an alkyl long chain with hydrophilic diol functional groups at the end, thus allowing this packing material to be used in either HILIC mode (with organic-rich mobile phase) or RP mode (with water-rich mobile phase). In order to distinguish the features of this chromatographic mode from traditional HILIC and RP, a new term was employed by the authors: *per* aqueous liquid chromatography (PALC). This designation was proposed by Pereira et al. (2009) in their study on the reversing of HILIC mechanism into PALC retention mechanism for the separation of highly polar ionizable

solutes. Thus, using a PALC × SEC method, Duarte et al. (2012) concluded that the combination of two independent separation mechanisms is promising in extend the range of NOM separation. For the cases where NOM separation was accomplished, smaller MW group fractions seem to be related to a more hydrophobic nature. Regardless of the detection method, the authors also concluded that the complete range of MW distribution provided by their LC x LC method was lower than those reported in the literature for Suwannee River Fulvic Acids and Pony Lake Fulvic Acids. It should also be mentioned that Góra et al. (2012) have introduced an off-line method combining a RP column with a SEC column for the fractionation of soil humic acids. This study totally differ from that of Duarte et al. (2012) mostly because the second employed an on-line method, thus meaning that the whole sample is subjected to separation in both chromatographic modes. Conversely, Góra et al. (2012) collected only a small volume around the peaks maximum obtained in the RP separation procedure before off-line re-injection into the SEC column. It must also be emphasized that Góra et al. (2012) did not provided any information about the size distribution of the soil humic acids, neither demonstrated how the different size fractions relate with their hydrophobic nature.

As already mentioned in section 2.5 (Chapter 2 of this thesis), Barros (2011) also employed the PALC × SEC method for fractionating WSOM from atmospheric particles collected during Winter season at a rural location (Duarte et al., 2007). Besides resolving the chemical heterogeneity of the aerosol WSOM sample, the PALC × SEC method also allowed the estimative of the average MW distribution of the sample (157-891 Da). Overall, the results of Barros (2011) highlighted the huge potential of LC x LC as a promising tool for resolving the chemical heterogeneity of the complex WSOM in fine atmospheric aerosols. Therefore, in this chapter, the PALC x SEC technique developed by Barros (2011) and Duarte et al. (2012) was employed for: (i) resolving the chemical heterogeneity of the urban aerosol WSOC hydrophobic acids samples characterized in Chapter 5; (ii) determining how size-distinguished fractions differ in hydrophobicity; and (iii) assessing the MW properties of the studied WSOM samples in regard to number (Mn) and weight (Mw) average MW, and polydispersity (Mw/Mn).

6.2. Development of PALC × SEC method for the analysis of urban aerosol WSOC hydrophobic acids

As described by Duarte et al. (2012), when performing LC x LC analysis of complex mixtures, the first procedure must entail the setup of the experimental conditions of both chromatographic dimensions in regard to mobile phase composition, flow rate, modulation period, and total analysis time. Besides mobile phase compatibility, important for avoiding adsorption phenomena of the analytes into the 2^{nd} dimension column under the injection plug (i.e. transfer volume) conditions, the speed of analysis in the 2^{nd} dimension will determine the sampling rate of the effluent from the 1^{st} dimension column (i.e. the modulation period) and, ultimately, the time needed for accomplishing a high resolved LC x LC map of the sample (Duarte et al., 2012).

Although the PALC× SEC method employed in this study was based on the works of Barros (2011) and Duarte et al. (2012), the separation of the urban aerosol WSOC hydrophobic acids samples was first screened in the 1^{st} and 2^{nd} dimension columns, independently. This important step was necessary to set the flow rate at the 1^{st} dimension, the modulation period, the number of fractions of the effluent from the 1^{st} dimension column that were transferred into the 2^{nd} dimension column, and the total time of analysis, thus aiming at ensure a good performance of the PALC x SEC method for resolving the chemical heterogeneity of the urban aerosol WSOM samples.

Fig. VI-1 and Fig. VI-2 show the 1D chromatograms obtained under PALC and SEC conditions, respectively, for the urban aerosol WSOC hydrophobic acids samples collected in Autumn 2009, Summer B 2010, Autumn B 2010, Winter 2011, and Winter/Spring 2011 seasons. For method development purposes in the 1^{st} dimension, and to avoid long elution times (almost three hours) in this first procedure, the flow rate used in PALC separation was set at 0.5 mL min^{-1}, which is 25 times higher than the flow rate actually applied in the PALC × SEC separations. It was assumed that the flow rate had negligible effects on the chromatographic profile of the WSOC hydrophobic acids samples in the 1^{st} dimension. Three and two replicates of PALC and SEC separation of each sample were performed, respectively; however, for better visualization, only the chromatograms corresponding to the first replica obtained in each separation technique are shown.

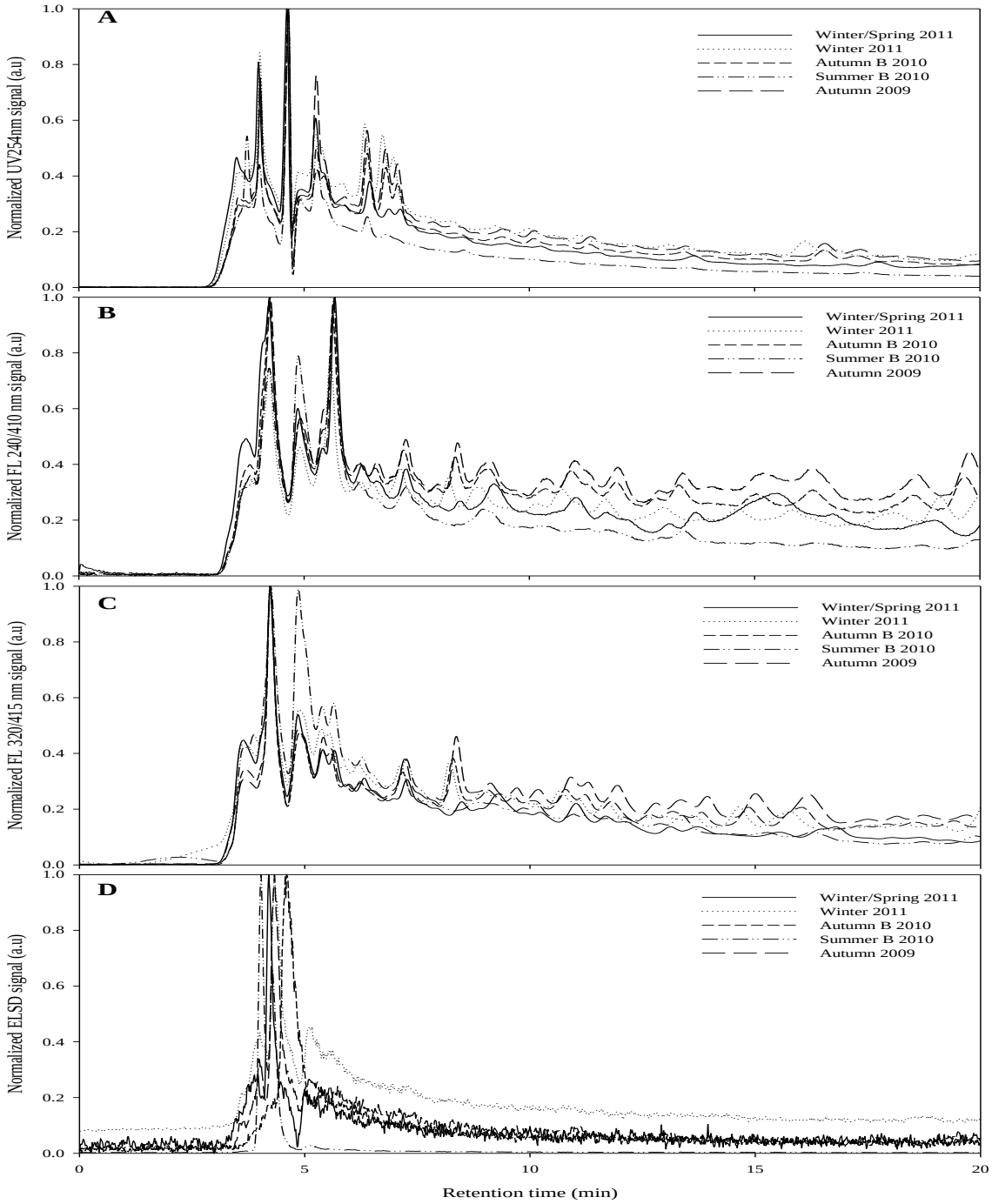

Fig. VI-1. One-dimensional (1D) chromatograms of the urban aerosol WSOC hydrophobic acids obtained with the PALC technique, and recorded by different detection methods: (A) DAD operating at 254 nm, FLD at (B) $\lambda_{Exc}/\lambda_{Em}$ = 240/410 nm and (C) $\lambda_{Exc}/\lambda_{Em}$ = 320/415 nm, and (D) ELSD. Additional details about the chromatographic conditions in terms of mobile phase composition can be found in section 3.10 (Chapter 3). The flow rate in PALC was 0.5 ml min^{-1}.

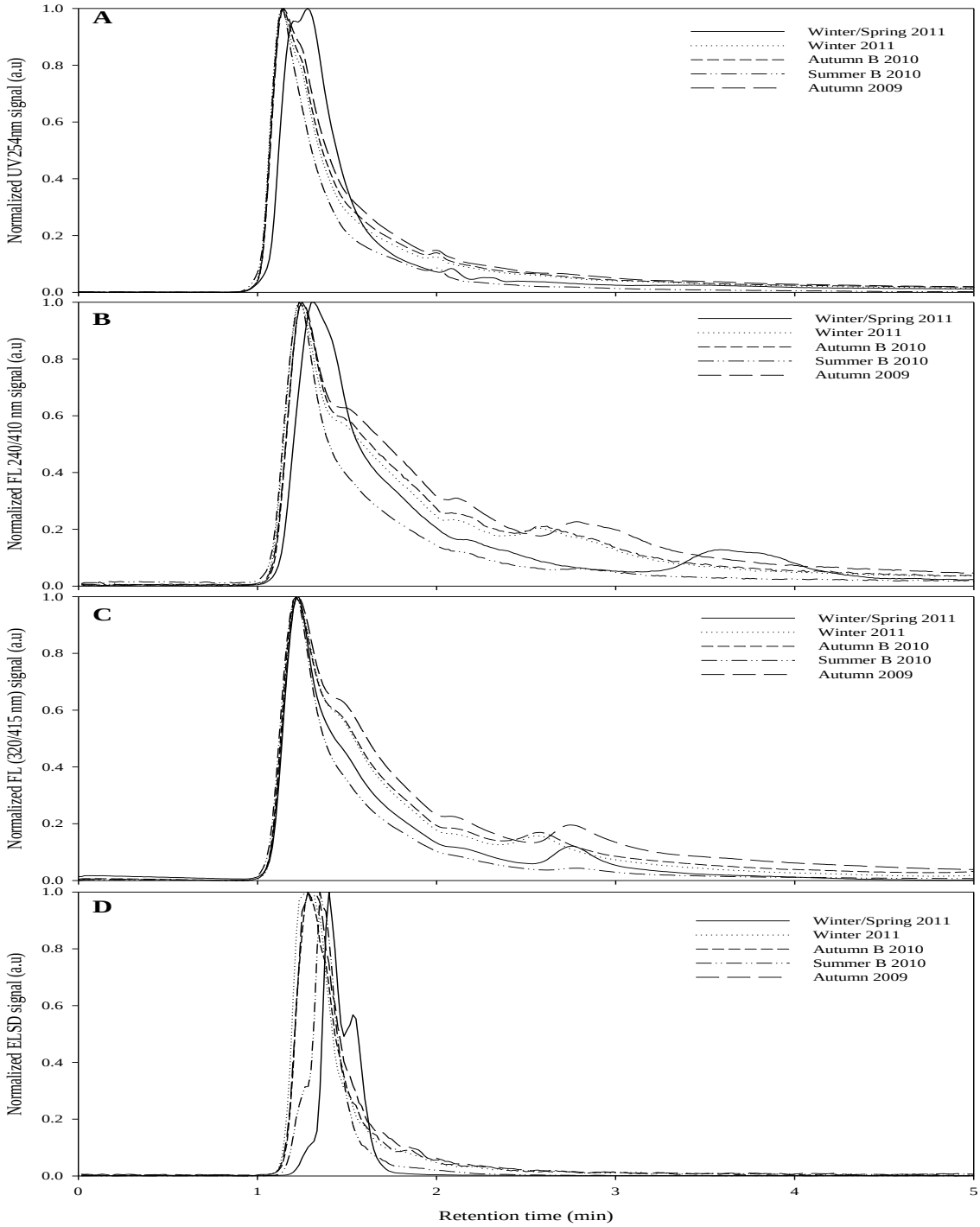

Fig. VI-2. One-dimensional (1D) chromatograms of the urban aerosol WSOC hydrophobic acids obtained with the SEC technique, and recorded by different detection methods: (A) DAD operating at 254 nm, FLD at (B) $\lambda_{Exc}/\lambda_{Em}$ = 240/410 nm and (C) $\lambda_{Exc}/\lambda_{Em}$ = 320/415 nm, and (D) ELSD. Additional details about the chromatographic conditions in terms of mobile phase composition can be found in section 3.10 (Chapter 3). The flow rate in SEC was 2.5 ml min^{-1}.

Overall, a fractionation of the urban aerosol WSOC hydrophobic acids has occurred on the 1st dimension mixed-mode HILIC column, operated under PALC conditions, as suggested by the presence of unresolved peaks between approximately 3.5 and 7.0 min in the chromatographic profiles acquired by both UV and fluorescence detection. In terms of ELSD detection, the obtained chromatograms are more featureless when compared to those of the other two detectors. Unlike UV and molecular fluorescence, ELSD detection is independent of the optical properties (i.e. type of chromophores) of the organic components contained in the WSOM samples, being only dependent on their concentration (Duarte et al., 2012). Therefore, the results obtained under PALC conditions reported in Fig. VI-1 suggest that the relative contribution to absorbance and quantum yield of fluorescence of the organic compounds with highly conjugated π bond systems is higher than that of ELSD, thus giving to some extent more feature-rich chromatograms.

In what concerns the SEC chromatograms shown in Fig. VI-2, most of the aerosol WSOC hydrophobic acids samples elute from the SEC column in about 150 s (2.5 min), which was set as the modulation period. Nevertheless, the fluorescence chromatograms obtained at $\lambda_{Exc}/\lambda_{Em}$ of 240/410 nm and 320/415 nm, also show that some minor fluorophores are still eluting from the SEC column at retention times higher than 2.5 min. Despite this observation, it was decided to establish the retention time of 2.5 min as the modulation period for two main reasons: 1) the SEC profiles of Fig. VI-2 were obtained for the whole sample, whereas in the LC× LC method, we are dealing with fractions from the 1st dimension column effluent, which experience some mixing and dilution with the mobile phase of the 2nd dimension, thus arriving with a somewhat lower concentration at the SEC column and subsequent detection systems; and 2) setting the modulation period for values higher than 4 min (suggested by fluorescence detection at $\lambda_{Exc}/\lambda_{Em}$ = 240/410 nm) will yield a total time of analysis in the LC× LC method of 600 min (10 hours), which is totally unfeasible in practical terms. With a modulation period of 150 s, the total time of analysis in the LC× LC method was set as 375 min. As depicted in Fig. VI-2, the SEC profiles of the aerosol WSOC hydrophobic acids show a unimodal distribution under the selected chromatographic conditions, although the ELSD chromatogram of the sample collected during the Winter/Spring 2011 season exhibit an additional unresolved peak at 1.5 min. Furthermore, the UV, fluorescence at $\lambda_{Exc}/\lambda_{Em}$ = 240/410 nm, and ESLD chromatograms of

this sample are slightly shifted towards higher retention times as compared to those of the other samples. This feature suggests that the WSOC hydrophobic acids from the Winter/Spring 2011 season may encompass organic structures with somewhat lower molecular weight than those of the other aerosol WSOM samples.

6.3. Analysis of urban aerosol WSOC hydrophobic acids through PALC × SEC methodology

The contour plots obtained for the WSOC hydrophobic acids separations using the PALC × SEC method are shown in Fig. VI-3 to Fig. VI-7. The fractions identified in each contour plot (labeled by numbers), their respective retention times in the 1st dimension, and the MW characteristics (Mn, Mw and Mw/Mn) generated from the PALC x SEC analyses of the WSOM samples are listed in Table VI-1 to Table VI-3. In this work, the Mn and Mw values were estimated using the PSS WinGPC Unity software package, after the calibration of the SEC column with sodium polystyrenesulfonate standards and HPLC grade acetone 5% (v/v) (section 3.10, Chapter 3).

As it can be seen in Fig. VI-3 to Fig. VI-7, the PALC × SEC method allowed the separation of the WSOC hydrophobic acids samples into several fractions, where the contour plots of UV absorption, fluorescence, and ELSD data display a different elution pattern not only for the same sample but also between the different samples. For example, the UV absorption contour plots of WSOM samples collected in Summer B 2010, Winter/Spring 2011, and Autumn 2009, exhibit 4, 6, 7 chromatographic peaks, respectively, while samples collected in Autumn B 2010 and Winter 2011 both have 8 chromatographic peaks. The only exception was verified for the ELSD data, where apparently no fractionation has been achieved and just a single broad chromatographic peak can be observed. As already stated (section 6.2), the ELSD detection is independent of the optical properties of the organic components contained in the WSOM samples. In this sense, the obtained ELSD data are less prone to be influenced by the unequal molar absorptivities and fluorescence properties of the organic moieties.

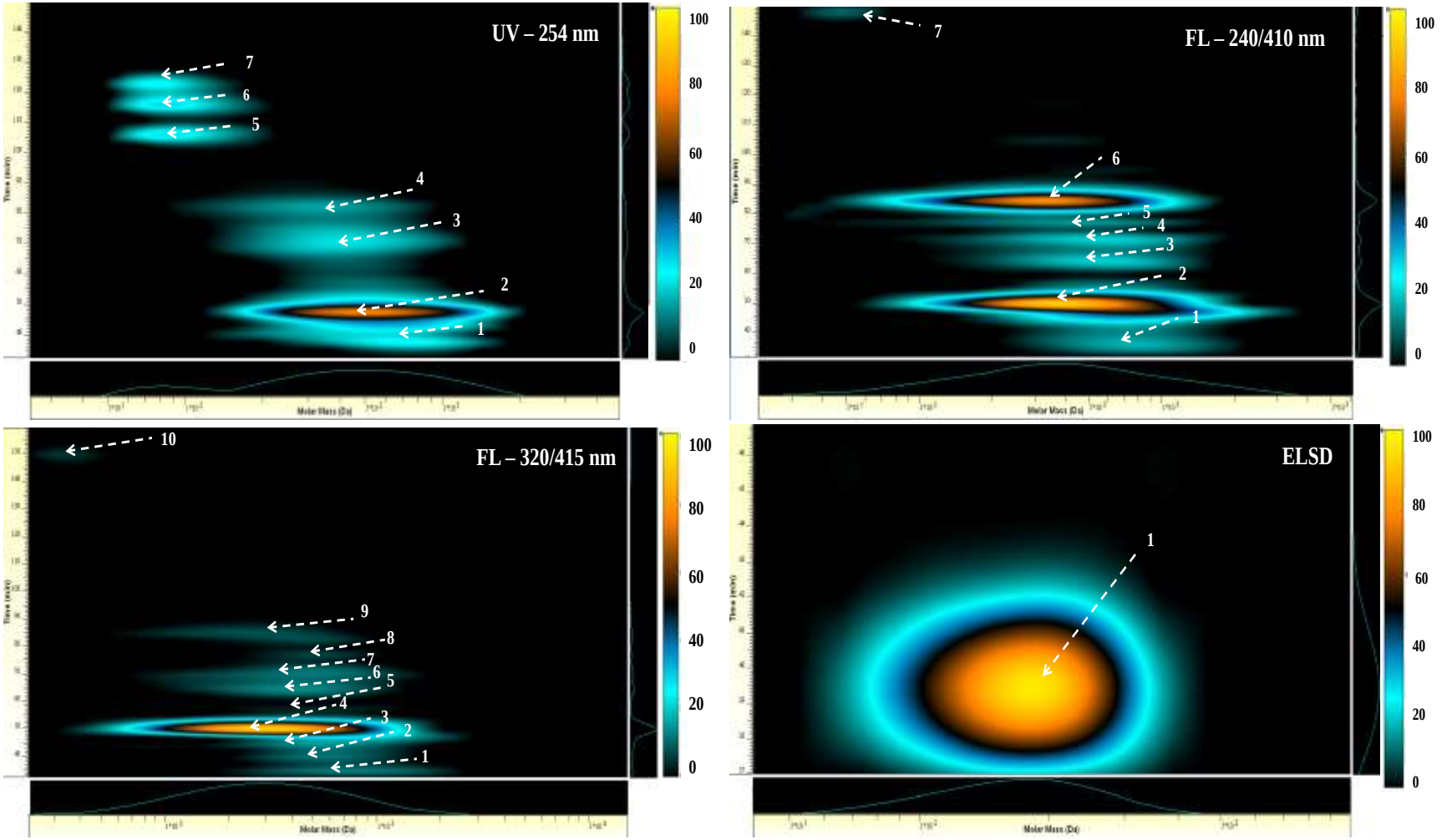

Fig. VI-3. PALC × SEC contour plots of aerosol WSOC hydrophobic acids from Autumn 2009 recorded by different detection methods (UV absorption at 254 nm, fluorescence (FL) at $\lambda_{Exc}/\lambda_{Em}$ of 240/410 nm and 320/415 nm, and evaporative light-scattering (ELSD)). Colours represent the intensity of the analytical signal.

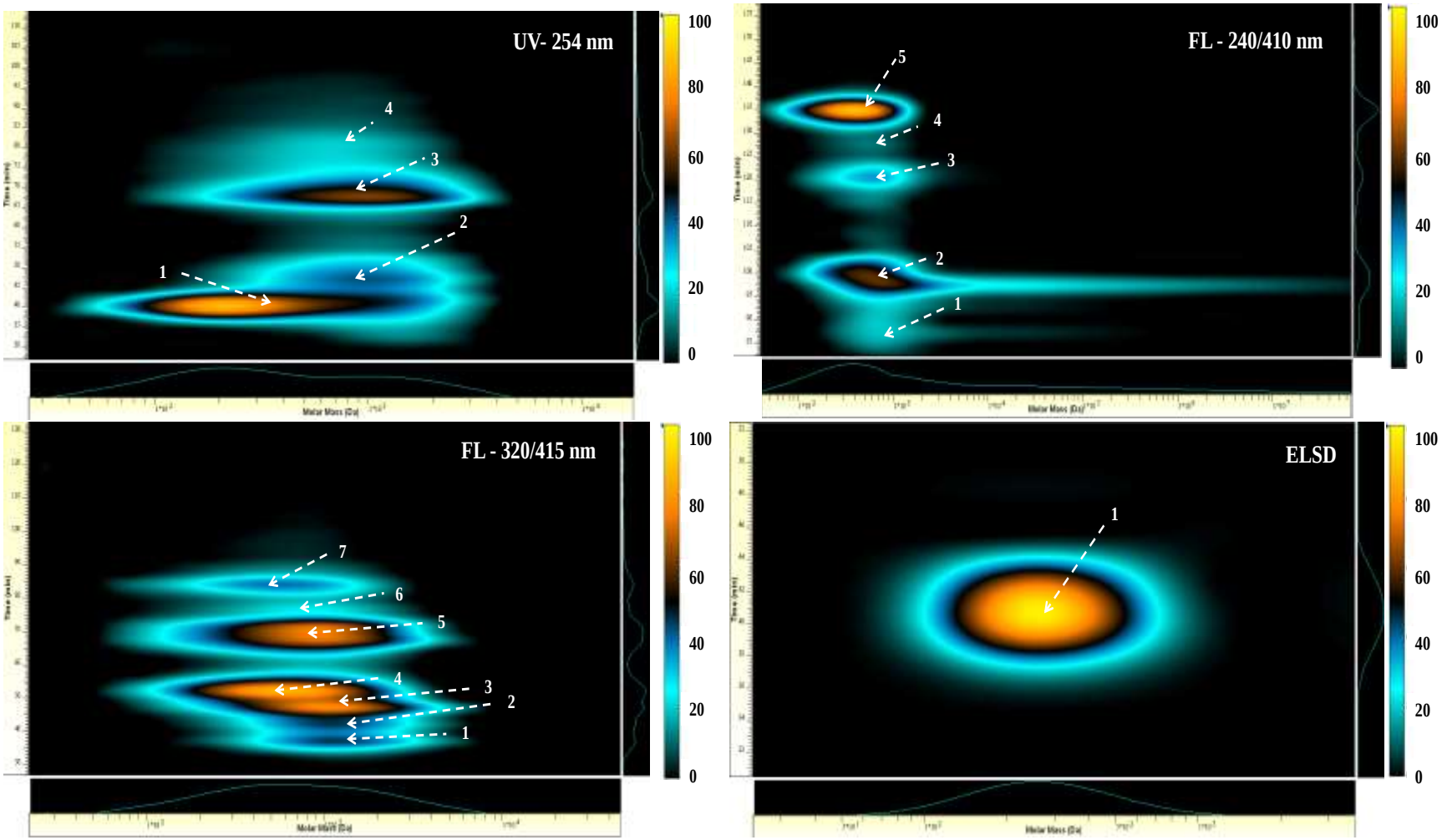

Fig. VI-4. PALC × SEC contour plots of aerosol WSOC hydrophobic acids from Summer B 2010 recorded by different detection methods (UV absorption at 254 nm, fluorescence (FL) at $\lambda_{Exc}/\lambda_{Em}$ of 240/410 nm and 320/415 nm, and evaporative light-scattering (ELSD)). Colours represent the intensity of the analytical signal.

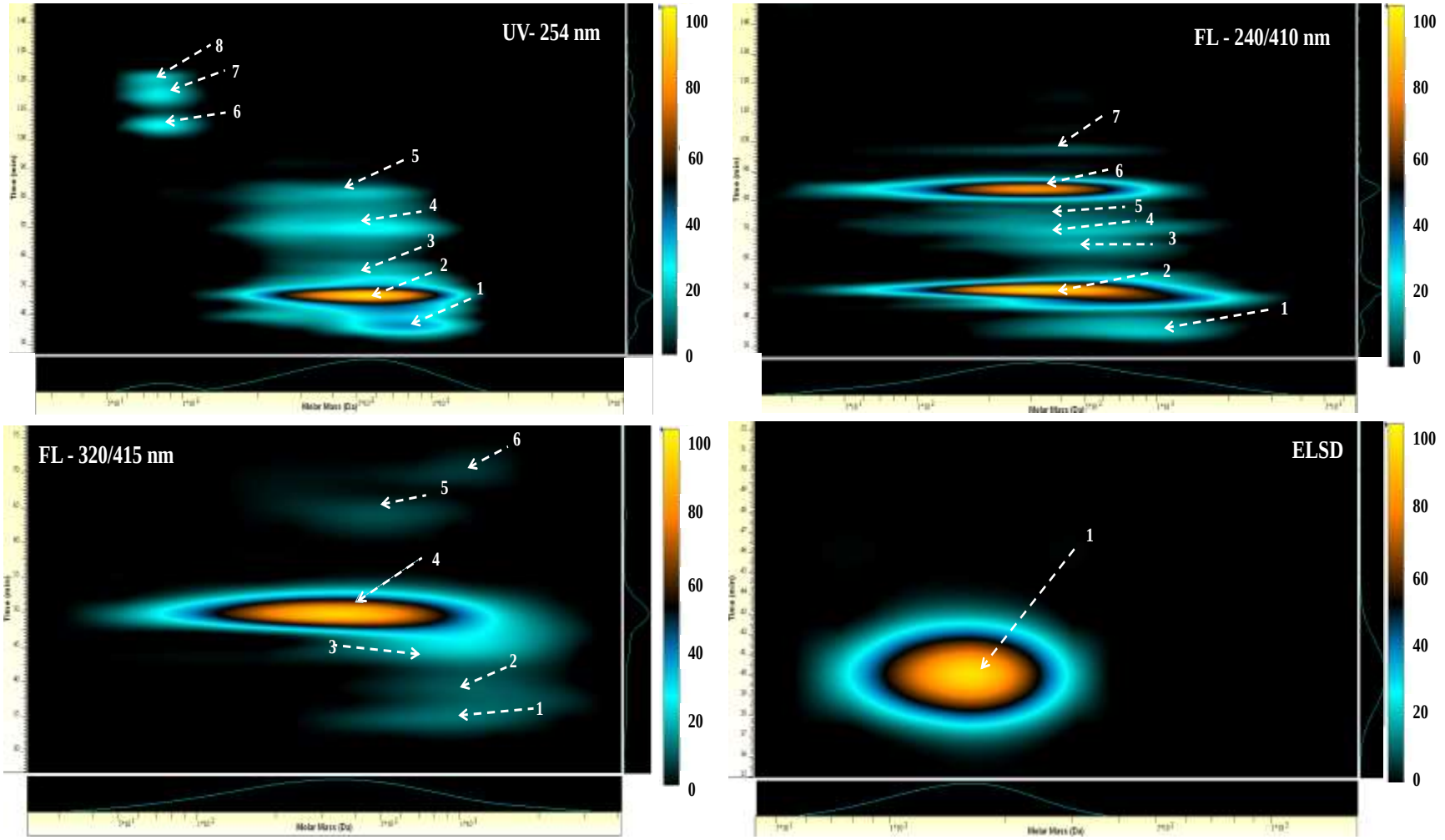

Fig. VI-5. PALC × SEC contour plots of aerosol WSOC hydrophobic acids from Autumn B 2010 recorded by different detection methods (UV absorption at 254 nm, fluorescence (FL) at $\lambda_{Exc}/\lambda_{Em}$ of 240/410 nm and 320/415 nm, and evaporative light-scattering (ELSD)). Colours represent the intensity of the analytical signal.

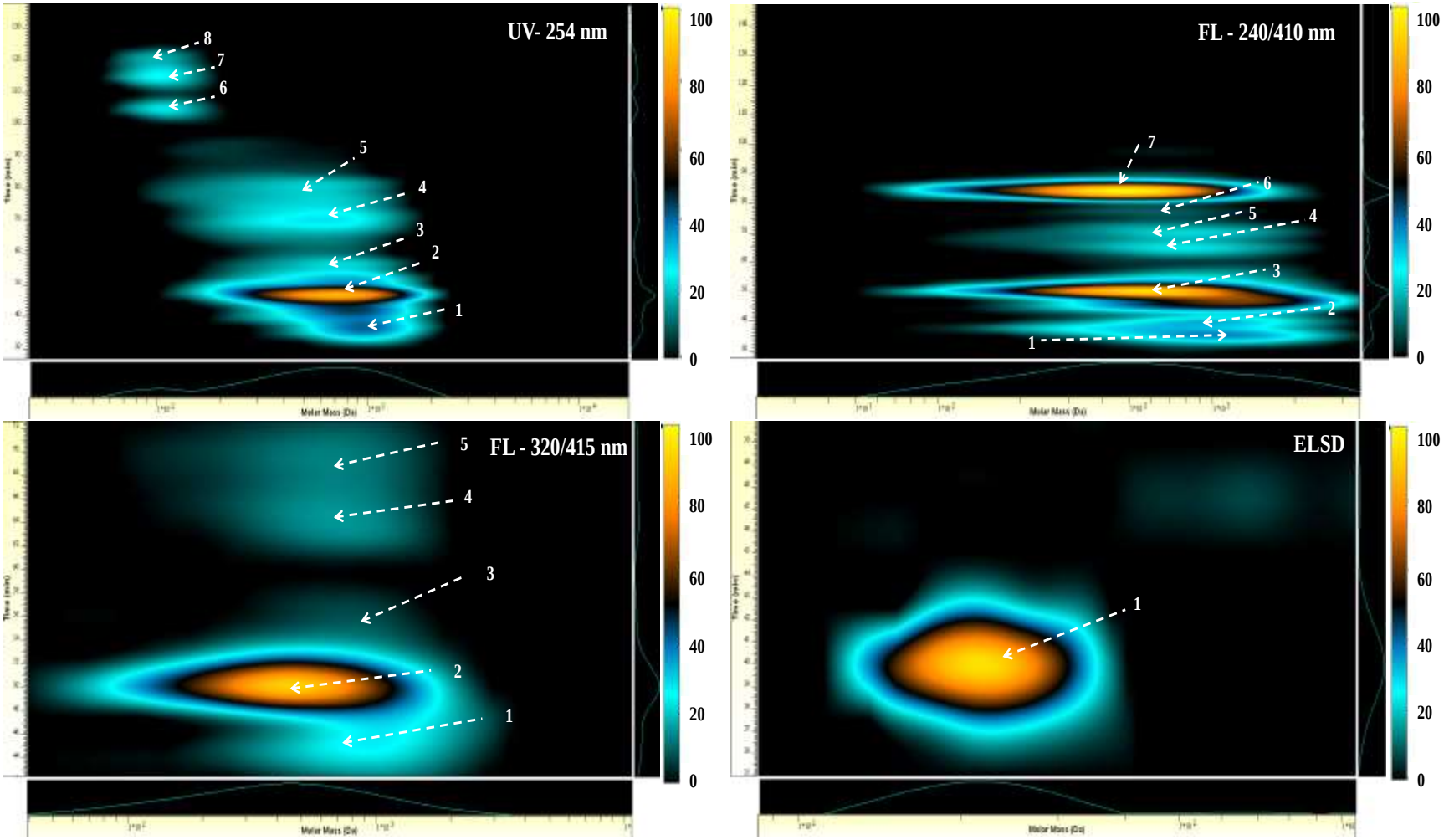

Fig. VI-6. PALC × SEC contour plots of aerosol WSOC hydrophobic acids from Winter 2011 recorded by different detection methods (UV absorption at 254 nm, fluorescence (FL) at $\lambda_{Exc}/\lambda_{Em}$ of 240/410 nm and 320/415 nm, and evaporative light-scattering (ELSD)). Colours represent the intensity of the analytical signal.

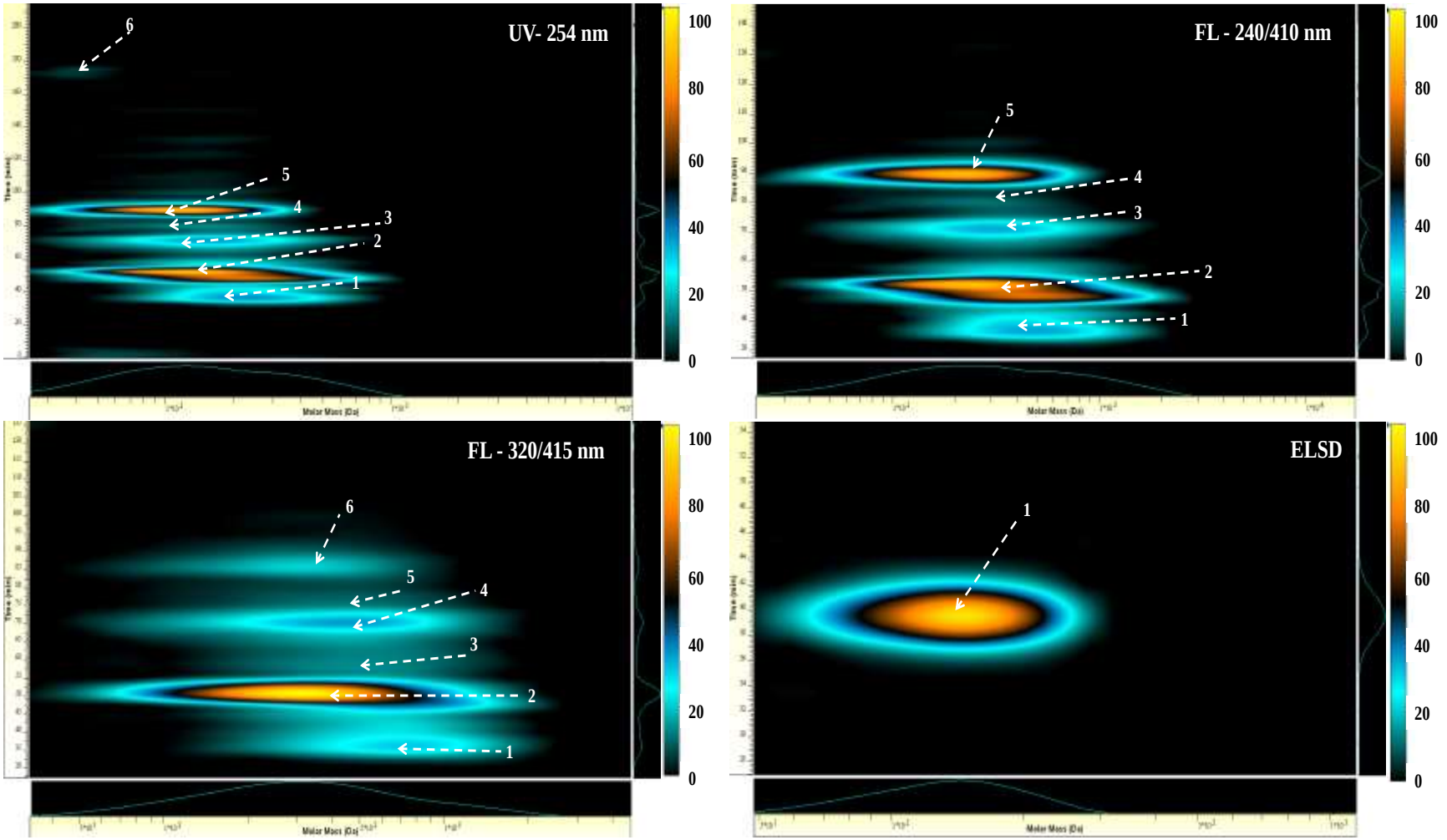

Fig. VI-7. PALC × SEC contour plots of aerosol WSOC hydrophobic acids from Winter/Spring 2011 recorded by different detection methods (UV absorption at 254 nm, fluorescence (FL) at $\lambda_{Exc}/\lambda_{Em}$ of 240/410 nm and 320/415 nm, and evaporative light-scattering (ELSD)). Colours represent the intensity of the analytical signal.

Table VI-1. Molecular weight characteristics of the aerosol WSOC hydrophobic acids from Autumn 2009 and Autumn B 2010, using the PALC × SEC methodology.

Detector	*Peak number*	Autumn 2009				Autumn B 2010			
		Elution Time 1st Dimension (min)	*Mn (Da)*	*Mw (Da)*	*Mw/Mn*	*Elution Time 1st Dimension (min)*	*Mn (Da)*	*Mw (Da)*	*Mw/Mn*
UV - 254 nm	1	38	525	614	1.17	37	687	711	1.04
	2	47	422	539	1.28	47	477	570	1.19
	3	71	323	391	1.21	52	457	505	1.10
	4	82	261	309	1.18	70	480	516	1.08
	5	106	89	94	1.06	82	438	467	1.07
	6	116	85	91	1.07	105	78	79	1.01
	7	123	75	78	1.04	116	78	79	1.01
	8					121	74	75	1.01
FL - 240/410 nm	1	43	614	710	1.16	43	689	827	1.20
	2	50	376	565	1.50	50	347	549	1.58
	3	64	438	547	1.25	65	472	529	1.12
	4	71	425	548	1.29	70	368	506	1.37
	5	80	308	394	1.28	80	304	354	1.16
	6	84	264	384	1.45	84	251	343	1.37
	7	148	45	46	1.01	97	333	357	1.07
FL - 320/415 nm	1	35	702	854	1.22	35	953	1100	1.15
	2	40	543	604	1.11	37	1137	1241	1.09
	3	46	557	641	1.15	46	978	1124	1.15
	4	50	250	405	1.62	50	330	496	1.50
	5	57	563	597	1.06	64	532	565	1.06
	6	64	369	474	1.29	70	1111	1125	1.01
	7	70	397	523	1.32				
	8	77	531	558	1.05				
	9	85	314	361	1.15				
	10	149	45	45	1.00				
ELSD	1	39	158	177	1.12	40	146	158	1.09

Table VI-2. Molecular weight characteristics of the aerosol WSOC hydrophobic acids from Summer B 2010, using the PALC × SEC methodology.

Detector	***Peak number***	**Summer B 2010**			
		Elution Time 1st Dimension (min)	***Mn (Da)***	***Mw (Da)***	***Mw/Mn***
UV - 254 nm	1	40	253	500	1.98
	2	47	774	942	1.22
	3	68	661	929	1.41
	4	75	597	702	1.18
FL - 240/410 nm	1	89	464	547	1.18
	2	99	437	738	1.69
	3	121	483	557	1.16
	4	129	449	492	1.09
	5	135	256	393	1.54
FL - 320/415 nm	1	37	866	1064	1.23
	2	45	818	986	1.20
	3	47	799	1021	1.28
	4	52	387	610	1.58
	5	70	505	885	1.75
	6	75	491	619	1.26
	7	84	391	509	1.30
ELSD	1	41	232	283	1.22

Table VI-3. Molecular weight characteristics of the aerosol WSOC hydrophobic acids from Winter 2011 and Winter/Spring 2011, using the PALC × SEC methodology.

Detector	Peak number	Winter 2011				Winter/Spring 2011			
		Elution Time 1st Dimension (min)	*Mn (Da)*	*Mw (Da)*	*Mw/Mn*	*Elution Time 1st Dimension (min)*	*Mn (Da)*	*Mw (Da)*	*Mw/Mn*
UV - 254 nm	1	43	832	889	1.07	37	257	296	1.15
	2	47	553	692	1.25	52	151	222	1.48
	3	54	535	622	1.16	71	188	212	1.13
	4	70	458	580	1.27	80	153	169	1.11
	5	76	370	437	1.18	90	109	140	1.29
	6	105	106	110	1.03	174	48	48	1.01
	7	115	102	106	1.04				
	8	119	94	96	1.02				
FL - 240/410 nm	1	35	886	1047	1.18	37	428	524	1.22
	2	39	743	895	1.20	52	277	452	1.63
	3	50	564	867	1.54	71	290	358	1.23
	4	65	654	815	1.25	80	282	317	1.12
	5	70	584	771	1.32	90	182	258	1.41
	6	80	535	587	1.10				
	7	84	361	517	1.43				
FL - 320/415 nm	1	47	652	772	1.18	36	625	708	1.13
	2	50	337	517	1.54	51	272	410	1.51
	3	54	591	634	1.07	67	385	463	1.20
	4	64	520	619	1.19	70	383	455	1.19
	5	67	496	585	1.18	75	343	400	1.17
	6					86	269	322	1.20
ELSD	1	40	209	220	1.05	40	127	138	1.09

Regarding the MW distribution of the samples, and in terms of UV absorption detection, the WSOC hydrophobic acids from Summer B 2010 have apparently higher Mw than the other WSOM samples, ranging from 500 to 942 Da. The Autumn 2009 and Autumn B 2010 show similar MW distribution, with the Mw values ranging approximately from 75 to 711 Da, whereas the Mw values of the Winter 2011 and Winter/Spring 2011 samples ranged between 96 and 889 Da, and 48 and 296 Da, respectively. In the UV contour plot of the Autumn 2009, Autumn B 2010, and Winter 2011 samples, there are cluster of fractions that have low Mw values (78-110 Da), but different hydrophobicity (indicated by the retention time in 1st dimension PALC separation). According to the work of Duarte and Duarte (2011b), the occurrence of organic compounds with such a low Mw range in these atmospheric aerosol samples may be indicative of the presence of freshly emitted SVOCs with low Mw. Nonetheless, the presence of fractions exhibiting somewhat higher Mw values (ranging from 300 to 890 Da) in these same samples could also be associated with the emission to the atmosphere of organic particles from other sources than those of SVOCs (e.g. wood burning). On the other hand, the presence of two fractions with apparently high Mw in the Summer B 2010 sample (namely peaks 2 and 3, with Mw values of 942 and 929 Da, respectively) may be explained by the long residence time in the atmosphere of low Mw organic compounds that undergo oligomerization and/or polymerization reactions mediated by solar radiation, thereby resulting in molecular structures with higher Mw (Gelencser et al., 2002).

The contour plots of the WSOC hydrophobic acids samples obtained with fluorescence detection exhibit between 5 and 10 chromatographic peaks (Fig. VI-3 to Fig. VI-7, and Table VI-1 to Table VI-3). Apparently, all WSOC hydrophobic acids samples contain a group of less hydrophobic fluorescent components (retention time in the 1st dimension between 35 and 99 min at both $\lambda_{Exc}/\lambda_{Em}$ pairs) whose average Mw values range between 738 and 1047 Da. The Autumn 2009 sample shows one additional more hydrophobic fluorescent fraction at the retention time of 148-149 min in the 1st dimension, whose average Mw is of approximately 45-46 Da. Using fluorescence detection at $\lambda_{Exc}/\lambda_{Em}$ = 240/410 nm, it is also possible to observe three additional more hydrophobic fluorescent fractions for the Summer B 2010 sample at the retention times in the 1st dimension between 121 and 135 min, with average Mw values ranging from 393 to 557 Da. The

ELSD detection method, on the other hand, generated only one chromatographic peak at the retention time of approximately 40 min in the 1st dimension and with average Mw values ranging from 138 to 283 Da. Findings suggest that the less hydrophobic acid components appear to have larger Mw than the highly hydrophobic acid components. Duarte et al (2012) also concluded that the fractions with low Mw have a more hydrophobic nature; however, depending on the detector, this trend was not observed in all samples analysed in this study. Results obtained in this study demonstrate that the PALC x SEC method offers a new perspective on the structural heterogeneity of WSOM, allowing to visualize differences between chromatographic fractions in terms of MW distribution and hydrophobicity.

As it can be seen in Tables VI-1 to VI-3, and regardless of the detection system, the Summer B 2010 sample has the highest values of the polydispersity index (Mw/Mn), reaching a value of 1.98 for the fraction labeled as 1 in the UV contour plot. These results suggest that the MW distribution of this Summer sample has higher heterogeneity than those of the other samples. On the other hand, polydispersity values close to 1.0 highlight the low heterogeneity of the MW distributions, thus suggesting that the PALC × SEC method was successful in resolving the chemical heterogeneity of the aerosol WSOM samples.

When comparing with the results reported in the literature, and only focusing on the results obtained by UV absorption detection, the results obtained in this study for the urban aerosol WSOC hydrophobic acids collected in Winter (Mw = 96-889 Da) are within the range of those reported by Barros (2011) for rural aerosol WSOC hydrophobic acids (Mw = 157-649 Da). Overall, the MW distribution of aerosol WSOM samples obtained in this study by means of PALC × SEC method is in agreement with a previous study conducted by Kiss et al. (2003), who reported Mw values of 200-300 Da for their aerosol WSOM samples. In the same way, the obtained MW distribution is within the range of those reported by Samburova et al. (2005), which used SEC/LDI-MS to confirm that the upper mass limit of their aerosol WSOM sample reached 700 Da.

6.4. Conclusions

An LC x LC method, combining a mixed-mode HILIC column operating under PALC conditions in the 1st dimension and a SEC column in the 2nd dimension, was applied with purpose of resolving the chemical heterogeneity of WSOC hydrophobic acids from atmospheric aerosols collected in different seasons. The following conclusions can be drawn:

a) the MW distribution of the all WSOC hydrophobic acids ranged from 48 to 942 Da and from 45 to 1241 Da in terms of UV absorption and fluorescence detection, respectively. The ELSD detection generated a MW distribution ranging between 128 and 283 Da;
b) fractions with high Mw values encompass organic structures with less hydrophobicity;
c) the occurrence of organic compounds with low Mw range (78-110 Da) in the aerosol WSOC hydrophobic acids collected in Autumn 2009, Autumn B 2010, and Winter 2011 periods may be indicative of the presence of freshly emitted SVOCs with low Mw;
d) the PALC × SEC method was successful in resolving the chemical heterogeneity of the aerosol WSOM samples. Both UV absorption and fluorescence detection seem to be appropriate as detection systems for these complex organic mixtures, whereas ELSD detection provides featureless chromatographic information.

VII

General conclusions

This thesis aimed at investigating the structural composition of the WSOM from fine aerosol particles typical of an urban location. In a first stage, the adsorption of SVOCs onto quartz fibre filters during the collection of aerosol particles was assessed. A global carbon balance was also performed, as well as a mass closure study for the whole mass of fine aerosol collected at the city of Aveiro. The UV-Vis and EEM fluorescence spectra of each WSOC sample were recorded, and the WSOC samples were assembled in different groups according to similar meteorological parameters before the isolation/fractionation of the assembled samples into WSOC hydrophobic and hydrophilic acids fractions. Afterwards, the WSOC hydrophobic acids fractions were characterized by means of elemental analysis, and FTIR-ATR and solid-state CPMAS ^{13}C NMR spectroscopies. Additionally, the WSOC hydrophobic acids fractions were further analyzed by a PALC x SEC methodology in order to resolve their chemical heterogeneity and to determine how size-distinguished fractions differ in terms of their hydrophobicity. The obtained results allowed the following conclusions:

a) Apparently, volatilisation/condensation processes of SVOCs may occur on the quartz fibre filters, or on particles surface, during aerosol sampling;

b) In the city of Aveiro, inhalable particulate matter is largely composed of fine particles, globally above 50 % by weight, except for Summer season. During the cold seasons, the atmospheric concentration of suspended particles exhibit a significant increase, specially the fine size range, which could be a consequence of local anthropogenic activities (e.g., wood burning). For fine particles, the carbonaceous fraction represents approximately 16 and 47 % of the aerosol mass in the warm (Summer A 2010) and cold (Autumn 2009 and Winter 2011) seasons, respectively, and less than 6 % of the carbonaceous matter consist of EC;

c) The elemental analysis of WSOC hydrophobic acids showed that the aerosol WSOC hydrophobic acids samples collected during the colder seasons exhibit a lower degree of oxidation than those collected during Spring and Summer seasons;

d) The analysis of the aerosol WSOC hydrophobic acids by CPMAS ^{13}C NMR suggests a more aromatic content of the samples collected during low-temperature conditions. The presence of signals typical of lignin-derived structures in the CPMAS ^{13}C NMR and FTIR-ATR spectra of WSOC hydrophobic acids samples from Autumn 2009, Autumn B 2010, Winter 2011, and Winter/Spring 2011 seasons highlights the importance of wood burning processes for domestic heating in the bulk chemical properties of WSOM from atmospheric aerosols.

e) Using a PALC x SEC method, it was found that the Mw distribution of aerosol WSOM ranged from 48 to 942 Da and from 45 to 1241 Da in terms of UV absorption and fluorescence detection, respectively. The WSOC hydrophobic acids fractions from Autumn 2009, Autumn B 2010, and Winter 2011 samples showed the presence of very low Mw components, which could be a consequence of fresh emitted organic particles. It was also observed that the components with smaller average Mw tend to have a more hydrophobic character. The PALC x SEC method coupled to multiple detectors (DAD, FLD, and ELSD) was successful in resolving the chemical heterogeneity of the aerosol WSOM samples;

f) Finally, the results obtained in this study are of great importance for a better characterization and understanding of the chemical composition of the WSOM from fine urban atmospheric aerosols.

For future work, it is suggested: i) the application of sophisticated high-resolution analytical techniques (namely, 2D-NMR spectroscopy and MALDI-TOF spectrometry) for a more in-depth insight into the molecular composition of the whole WSOM from fine urban aerosols; ii) the assessment of how the structural information of the aerosol WSOM vary with hydrophobicity and MW profile by the synergistic application of LC x LC and high-resolution spectroscopic and spectrometric techniques; and iii) unfolding the molecular complexity of aerosol WSOM from other urban environments.

References

Abbt-Braun, G., Lankes, U., Frimmel, F.H., 2004. Structural characterization of aquatic humic substances - The need for a multiple method approach. Aquat. Sci. 66, 151–170.

Alves, C., Carvalho, A., Pio, C., 2002. Mass balance of organic carbon fractions in atmospheric aerosols. J. Geophys. Res. Atmos. 107, 8345.

Alves, C., Pio, C., Duarte, A., 2001. Composition of extractable organic matter of air particles from rural and urban Portuguese areas. Atmos. Environ. 35, 5485–5496.

Andracchio, A., Cavicchi, C., Tonelli, D., Zappoli, S., 2002. A new approach for the fractionation of water-soluble organic carbon in atmospheric aerosols and cloud drops. Atmos. Environ. 36, 5097–5107.

Asa-Awuku, A., Sullivan, A.P., Hennigan, C.J., Weber, R.J., Nenes, A., 2008. Investigation of molar volume and surfactant characteristics of water-soluble organic compounds in biomass burning aerosol. Atmos. Chem. Phys. 8, 799–812.

Baduel, C., Voisin, D., Jaffrezo, J.L., 2010. Seasonal variations of concentrations and optical properties of water soluble HULIS collected in urban environments. Atmos. Chem. Phys. 10, 4085–4095.

Baldock, J.A., Oades, J.M., Waters, A.G., Peng, X., Vassallo, A.M., Wilson, M.A., 1992. Aspects of the chemical structure of soil organic materials as revealed by solid-state13C NMR spectroscopy. Biogeochemistry 16, 1–42.

Barros, A.C.C.A. de, 2011. Natural organic matter: study by two-dimensional liquid chromatography. Universidade de Aveiro.

Bellamy, L.I., 1975. The Infrared Spectra of Complex Molecules. Chapman and Hall, London.

Birch, M.E., Cary, R.A., 1996. Elemental carbon-based method for monitoring occupational exposures to particulate diesel exhaust. Aerosol Sci. Technol. 25, 221–241.

Carvalho, A., Pio, C., Santos, C., 2003. Water-soluble hydroxylated organic compounds in German and Finnish aerosols. Atmos. Environ. 37, 1775–1783.

Castro, L.M., Pio, C.A., Harrison, R.M., Smith, D.J.T., 1999. Carbonaceous aerosol in urban and rural European atmospheres: estimation of secondary organic carbon concentrations. Atmos. Environ. 33, 2771–2781.

Cavalli, F., Facchini, M.C., Decesari, S., Emblico, L., Mircea, M., Jensen, N.R., Fuzzi, S., 2006. Size-segregated aerosol chemical composition at a boreal site in southern Finland, during the QUEST project. Atmos. Chem. Phys. 6, 993–1002.

Chan, M.N., Choi, M.Y., Ng, N.L., Chan, C.K., 2005. Hygroscopicity of water-soluble organic compounds in atmospheric aerosols: Amino acids and biomass burning derived organic species. Environ. Sci. Technol. 39, 1555–1562.

Charlson, R.J., Schwartz, S.E., Hales, J.M., Cess, R.D., Coakley, J.A., Hansen, J.E., Hofmann, D.J., 1992. Climate Forcing by Anthropogenic Aerosols. Science (80-.). 255, 423–430.

Chen, J., Gu, B.H., LeBoeuf, E.J., Pan, H.J., Dai, S., 2002. Spectroscopic characterization of the structural and functional properties of natural organic matter fractions. Chemosphere 48, 59–68.

Chen, J., Ying, Q., Kleeman, M.J., 2010. Source apportionment of wintertime secondary organic aerosol during the California regional PM10/PM2.5 air quality study. Atmos. Environ. 44, 1331–1340.

Chen, X., Kong, L., Su, X., Fu, H., Ni, J., Zhao, R., Zou, H., 2004. Separation and identification of compounds in Rhizoma chuanxiong by comprehensive two-dimensional liquid chromatography coupled to mass spectrometry. J. Chromatogr. A 1040, 169–178.

Chow, J.C., Watson, J.G., Lu, Z., Lowenthal, D.H., Frazier, C.A., Solomon, P.A., Thuillier, R.H., Magliano, K., 1996. Descriptive analysis of PM25 and PM10 at regionally representative locations during SJVAQS/AUSPEX Atmos. Environ. .

Claeys, M., Graham, B., Vas, G., Wang, W., Vermeylen, R., Pashynska, V., Cafmeyer, J., Guyon, P., Andreae, M.O., Artaxo, P., Maenhaut, W., 2004a. Formation of secondary organic aerosols through photooxidation of isoprene. Science (80-.). 303, 1173–1176.

Claeys, M., Wang, W., Ion, A.C., Kourtchev, I., Gelencser, A., Maenhaut, W., 2004b. Formation of secondary organic aerosols from isoprene and its gas-phase oxidation products through reaction with hydrogen peroxide. Atmos. Environ. 38, 4093–4098.

Claeys, M., Wang, W., Vermeylen, R., Kourtchev, I., Chi, X.G., Farhat, Y., Surratt, J.D., Gomez-Gonzalez, Y., Sciare, J., Maenhaut, W., 2010. Chemical characterisation of marine aerosol at Amsterdam Island during the austral summer of 2006-2007. J. Aerosol Sci. 41, 13–22.

Coates, J., 2006. Interpretation of Infrared Spectra, A Practical Approach. In: Encyclopedia of Analytical Chemistry. John Wiley & Sons, Ltd.

Coble, P.G., 1996. Characterization of marine and terrestrial DOM in seawater using excitation emission matrix spectroscopy. Mar. Chem. 51, 325–346.

Cook, R., 2004. Coupling NMR to NOM. Anal. Bioanal. Chem. 378, 1484–1503.

Coury, C., Dillner, A.M., 2008. A method to quantify organic functional groups and inorganic compounds in ambient aerosols using attenuated total reflectance FTIR spectroscopy and multivariate chemometric techniques. Atmos. Environ. 42, 5923–5932.

Coury, C., Dillner, A.M., 2009. ATR-FTIR characterization of organic functional groups and inorganic ions in ambient aerosols at a rural site. Atmos. Environ. 43, 940–948.

DeCarlo, P.F., Kimmel, J.R., Trimborn, A., Northway, M.J., Jayne, J.T., Aiken, A. l, Gonin, M., Fuhrer, K., Horvath, T., Docherty, K.S., Worsnop, D.R., Jimenez, J.L., 2006. Field-Deployable, High-Resolution, Time-of-Flight Aerosol Mass Spectrometer. Anal. Chem. 78, 8281–8289.

Decesari, S., Facchini, M.C., Fuzzi, S., McFiggans, G.B., Coe, H., Bower, K.N., 2005. The water-soluble organic component of size-segregated aerosol, cloud water and wet depositions from Jeju Island during ACE-Asia. Atmos. Environ. 39, 211–222.

Decesari, S., Facchini, M.C., Fuzzi, S., Tagliavini, E., 2000. Characterization of water-soluble organic compounds in atmospheric aerosol: A new approach. J. Geophys. Res. 105, 1481–1489.

Decesari, S., Facchini, M.C., Matta, E., Lettini, F., Mircea, M., Fuzzi, S., Tagliavini, E., Putaud, J.P., 2001. Chemical features and seasonal variation of fine aerosol water-soluble organic compounds in the Po Valley, Italy. Atmos. Environ. 35, 3691–3699.

Decesari, S., Fuzzi, S., Facchini, M.C., Mircea, M., Emblico, L., Cavalli, F., Maenhaut, W., Chi, X., Schkolnik, G., Falkovich, A., Rudich, Y., Claeys, M., Pashynska, V., Vas, G., Kourtchev, I., Vermeylen, R., Hoffer, A., Andreae, M.O., Tagliavini, E., Moretti, F., Artaxo, P., 2006. Characterization of the organic composition of aerosols from Rondonia, Brazil, during the LBA-SMOCC 2002 experiment and its representation through model compounds. Atmos. Chem. Phys. 6, 375–402.

Decesari, S., Mircea, M., Cavalli, F., Fuzzi, S., Moretti, F., Tagliavini, E., Facchini, M.C., 2007. Source attribution of water-soluble organic aerosol by nuclear magnetic resonance spectroscopy. Environ. Sci. Technol. 41, 2479–2484.

Dinar, E., Mentel, T.F., Rudich, Y., 2006. The density of humic acids and humic like substances (HULIS) from fresh and aged wood burning and pollution aerosol particles. Atmos. Chem. Phys. 6, 5213–5224.

Dinar, E., Taraniuk, I., Graber, E.R., Anttila, T., Mentel, T.F., Rudich, Y., 2007. Hygroscopic growth of atmospheric and model humic-like substances. J. Geophys. Res. Atmos. 112, D05211.

Draxler, R.R., Rolph, G.D., 2013. HYSPLIT (HYbrid Single-Particle Lagrangian Integrated Trajectory) Model access via NOAA ARL READY Website. NOAA Air Resour. Lab.

Duarte, A.C., Duarte, R.M.B.O., 2009. Natural Organic Matter in Atmospheric Particles. In: Senesi, N., Xing, B., Huang, P.M. (Eds.), Biophysico-Chemical Processes Involving Natural Nonliving Organic Matter in Environmental Systems. John Wiley & Sons, Inc., New Jersey, pp. 451–485.

Duarte, R.M.B.O., 2006. Balanço mássico e caracterização da matéria orgânica de aerossóis atmosféricos. Tese de Doutoramento. Dep. Química. Universidade de Aveiro.

Duarte, R.M.B.O., Barros, A.C., Duarte, A.C., 2012. Resolving the chemical heterogeneity of natural organic matter: New insights from comprehensive two-dimensional liquid chromatography. J. Chromatogr. A 1249, 138–146.

Duarte, R.M.B.O., Duarte, A.C., 2005. Application of non-ionic solid sorbents (XAD resins) for the isolation and fractionation of water-soluble organic compounds from atmospheric aerosols. J. Atmos. Chem. 51, 79–93.

Duarte, R.M.B.O., Duarte, A.C., 2011a. A critical review of advanced analytical techniques for water-soluble organic matter from atmospheric aerosols. TrAC Trends Anal. Chem. 30, 1659–1671.

Duarte, R.M.B.O., Duarte, A.C., 2011b. Optimizing size-exclusion chromatographic conditions using a composite objective function and chemometric tools: Application to natural organic matter profiling. Anal. Chim. Acta 688, 90–98.

Duarte, R.M.B.O., Duarte, A.C., 2013. Atmospheric Organic Matter. In: eMagRes. John Wiley & Sons, Ltd.

Duarte, R.M.B.O., Fernández-Getino, A.P., Duarte, A.C., 2013. Humic acids as proxies for assessing different Mediterranean forest soils signatures using solid-state CPMAS 13C NMR spectroscopy. Chemosphere 91, 1556–1565.

Duarte, R.M.B.O., Mieiro, C.L., Penetra, A., Pio, C.A., Duarte, A.C., 2008a. Carbonaceous materials in size-segregated atmospheric aerosols from urban and coastal-rural areas at the Western European Coast. Atmos. Res. 90, 253–263.

Duarte, R.M.B.O., Pio, C.A., Duarte, A.C., 2004. Synchronous scan and excitation-emission matrix fluorescence spectroscopy of water-soluble organic compounds in atmospheric aerosols. J. Atmos. Chem. 48, 157–171.

Duarte, R.M.B.O., Pio, C.A., Duarte, A.C., 2005. Spectroscopic study of the water-soluble organic matter isolated from atmospheric aerosols collected under different atmospheric conditions. Anal. Chim. Acta 530, 7–14.

Duarte, R.M.B.O., Santos, E.B.H., Duarte, A.C., 2003. Spectroscopic characteristics of ultrafiltration fractions of fulvic and humic acids isolated from an eucalyptus bleached Kraft pulp mill effluent. Water Res. 37, 4073–4080.

Duarte, R.M.B.O., Santos, E.B.H., Pio, C.A., Duarte, A.C., 2007. Comparison of structural features of water-soluble organic matter from atmospheric aerosols with those of aquatic humic substances. Atmos. Environ. 41, 8100–8113.

Duarte, R.M.B.O., Silva, A.M.S., Duarte, A.C., 2008b. Two-Dimensional NMR Studies of Water-Soluble Organic Matter in Atmospheric Aerosols. Environ. Sci. Technol. 42, 8224–8230.

Dugo, P., Cacciola, F., Donato, P., Airado-Rodríguez, D., Herrero, M., Mondello, L., 2009. Comprehensive two-dimensional liquid chromatography to quantify polyphenols in red wines. J. Chromatogr. A 1216, 7483–7487.

Dugo, P., Cacciola, F., Kumm, T., Dugo, G., Mondello, L., 2008. Comprehensive multidimensional liquid chromatography: Theory and applications. J. Chromatogr. A 1184, 353–368.

Dugo, P., Kumm, T., Crupi, M.L., Cotroneo, A., Mondello, L., 2006. Comprehensive two-dimensional liquid chromatography combined with mass spectrometric detection in the analyses of triacylglycerols in natural lipidic matrixes. J. Chromatogr. A 1112, 269–275.

Facchini, M.C., Fuzzi, S., Zappoli, S., Andracchio, A., Gelencser, A., Kiss, G., Krivacsy, Z., Meszaros, E., Hansson, H.C., Alsberg, T., Zebuhr, Y., 1999. Partitioning of the

organic aerosol component between fog droplets and interstitial air. J. Geophys. Res. 104, 26821–26832.

Facchini, M.C., Rinaldi, M., Decesari, S., Carbone, C., Finessi, E., Mircea, M., Fuzzi, S., Ceburnis, D., Flanagan, R., Nilsson, E.D., Leeuw, G., Martino, M., Woeltjen, J., O'Dowd, C.D., 2008. Primary submicron marine aerosol dominated by insoluble organic colloids and aggregates. Geophys. Res. Lett. 35, L17814.

Faix, O., 1992. No Title. In: Lin, S.Y., Dence, C.W. (Eds.), Methods in Lignin Chemistry. Springer, Berlin, pp. 92–93.

Feng, J.L., Chan, C.K., Fang, M., Hu, M., He, L.Y., Tang, X.Y., 2006. Characteristics of organic matter in PM2.5 in Shanghai. Chemosphere 64, 1393–1400.

Fengel, D., Wegner, G., 1984. Wood: chemistry, ultrastructure, reactions. W. de Gruyter, Berlin.

Fuzzi, S., Andreae, M.O., Huebert, B.J., Kulmala, M., Bond, T.C., Boy, M., Doherty, S.J., Guenther, A., Kanakidou, M., Kawamura, K., Kerminen, V.-M., Lohmann, U., Russell, L.M., Pöschl, U., 2006. Critical assessment of the current state of scientific knowledge, terminology, and research needs concerning the role of organic aerosols in the atmosphere, climate, and global change. Atmos. Chem. Phys. 6, 2017–2038.

Fuzzi, S., Decesari, S., Facchini, M.C., Matta, E., Mircea, M., Tagliavini, E., 2001. A simplified model of the water soluble organic component of atmospheric aerosols. Geophys. Res. Lett. 28, 4079–4082.

Gelencser, A., 2004. Carbonaceous Aerosol. In: Atmospheric and Oceanographic Sciences Library. Springer, Dordrecht.

Gelencser, A., Hoffer, A., Krivacsy, Z., Kiss, G., Molnar, A., Meszaros, E., 2002. On the possible origin of humic matter in fine continental aerosol. J. Geophys. Res. 107.

Giovanela, M., Parlanti, E., Soriano-Sierra, E.J., Soldi, M.S., Sierra, M.M.D., 2004. Elemental compositions, FT-IR spectra and thermal behavior of sedimentary fulvic and humic acids from aquatic and terrestrial environments. Geochem. J. 38, 255–264.

Góra, R., Hutta, M., Rohárik, P., 2012. Characterization and analysis of soil humic acids by off-line combination of wide-pore octadecylsilica column reverse phase high performance liquid chromatography with narrow bore column size-exclusion chromatography and fluorescence detection. J. Chromatogr. A 1220, 44–49.

Graber, E.R., Rudich, Y., 2006. Atmospheric HULIS: How humic-like are they? A comprehensive and critical review. Atmos. Chem. Phys. 6, 729–753.

Graham, B., Mayol-Bracero, O.L., Guyon, P., Roberts, G.C., Decesari, S., Facchini, M.C., Artaxo, P., Maenhaut, W., Koll, P., Andreae, M.O., 2002. Water-soluble organic compounds in biomass burning aerosols over Amazonia - 1. Characterization by NMR and GC-MS. J. Geophys. Res. 107.

Gysel, M., Weingartner, E., Nyeki, S., Paulsen, D., Baltensperger, U., Galambos, I., Kiss, G., 2004. Hygroscopic properties of water-soluble matter and humic-like organics in atmospheric fine aerosol. Atmos. Chem. Phys. 4, 35–50.

Hatfield, G.R., Maciel, G.E., Erbatur, O., Erbatur, G., 1987. Qualitative and quantitative analysis of solid lignin samples by carbon-13 nuclear magnetic resonance spectrometry. Anal. Chem. 59, 172–179.

Havers, N., Burba, P., Lambert, J., Klockow, D., 1998. Spectroscopic characterization of humic-like substances in airborne particulate matter. J. Atmos. Chem. 29, 45–54.

Haw, J.F., Maciel, G.E., Schroeder, H.A., 1984. Carbon-13 nuclear magnetic resonance spectrometric study of wood and wood pulping with cross polarization and magic-angle spinning. Anal. Chem. 56, 1323–1329.

Hawkins, L.N., Russell, L.M., 2010. Oxidation of ketone groups in transported biomass burning aerosol from the 2008 Northern California Lightning Series fires. Atmos. Environ. 44, 4142–4154.

Hayes, M.H.B., MacCarthy, P., Malcolm, R.L., Swift, R.S., 1989. Humic substances II. In search of structure. John Wiley & Sons Ltd.

Ho, K.F., Lee, S.C., Chan, C.K., Yu, J.C., Chow, J.C., Yao, X.H., 2003. Characterization of chemical species in PM2.5 and PM10 aerosols in Hong Kong. Atmos. Environ. 37, 31–39.

Ho, K.F., Lee, S.C., Yu, J.C., Zou, S.C., Fung, K., 2002. Carbonaceous characteristics of atmospheric particulate matter in Hong Kong. Sci. Total Environ. 300, 59–67.

Hoffer, A., Gelencser, A., Guyon, P., Kiss, G., Schmid, O., Frank, G.P., Artaxo, P., Andreae, M.O., 2006. Optical properties of humic-like substances (HULIS) in biomass-burning aerosols. Atmos. Chem. Phys. 6, 3563–3570.

Huang, X., Yu, J.Z., He, L., Zibing, Z., 2006. Water-soluble organic carbon and oxalate in aerosols at a coastal urban site in China: Size distribution characteristics, sources, and formation mechanisms. J. Geophys. Res. Atmos. 111, D22212.

IPCC, 2001. Aerosols, their direct and indirect effects. Climate Change 2001: The Scientific Basis. Contribution of Working Group I to the Third Assessment Report of the Intergovernmental Panel on Climate Change.

Jacobson, M.C., Hansson, H.C., Noone, K.J., Charlson, R.J., 2000. Organic atmospheric aerosols: Review and state of the science. Rev. Geophys. 38, 267–294.

Jaffrezo, J.L., Aymoz, G., Delaval, C., Cozic, J., 2005. Seasonal variations of the water soluble organic carbon mass fraction of aerosol in two valleys of the French Alps. Atmos. Chem. Phys. 5, 2809–2821.

Kanakidou, M., Seinfeld, J.H., Pandis, S.N., Barnes, I., Dentener, F.J., Facchini, M.C., Van Dingenen, R., Ervens, B., Nenes, A., Nielsen, C.J., Swietlicki, E., Putaud, J.P., Balkanski, Y., Fuzzi, S., Horth, J., Moortgat, G.K., Winterhalter, R., Myhre, C.E.L., Tsigaridis, K., Vignati, E., Stephanou, E.G., Wilson, J., 2005. Organic aerosol and global climate modelling: a review. Atmos. Chem. Phys. 5, 1053–1123.

Kaufman, Y.J., Tanre, D., Boucher, O., 2002. A satellite view of aerosols in the climate system. Nature 419, 215–223.

Keeler, C., Kelly, E.F., Maciel, G.E., 2006. Chemical–structural information from solid-state 13C NMR studies of a suite of humic materials from a lower montane forest soil, Colorado, USA. Geoderma 130, 124–140.

Khare, P., Baruah, B.P., Rao, P.G., 2011. Water-soluble organic compounds (WSOCs) in PM2.5 and PM10 at a subtropical site of India. Tellus Ser. B-Chemical Phys. Meteorol. 63, 990–1000.

Kim, K.H., Sekiguchi, K., Furuuchi, M., Sakamoto, K., 2011. Seasonal variation of carbonaceous and ionic components in ultrafine and fine particles in an urban area of Japan. Atmos. Environ. 45, 1581–1590.

Kiss, G., Gelencser, A., Hoffer, A., Krivacsy, Z., Meszaros, E., Molnar, A., Varga, B., 2000. Chemical characterization of water soluble organic compounds in tropospheric fine aerosol. Nucleation Atmos. Aerosols 534, 761–764.

Kiss, G., Tombacz, E., Varga, B., Alsberg, T., Persson, L., 2003. Estimation of the average molecular weight of humic-like substances isolated from fine atmospheric aerosol. Atmos. Environ. 37, 3783–3794.

Kiss, G., Varga, B., Galambos, I., Ganszky, I., 2002. Characterization of water-soluble organic matter isolated from atmospheric fine aerosol. J. Geophys. Res. 107, Doi 10.1029/2001jd000603.

Kivilompolo, M., Hyötyläinen, T., 2007. Comprehensive two-dimensional liquid chromatography in analysis of Lamiaceae herbs: Characterisation and quantification of antioxidant phenolic acids. J. Chromatogr. A 1145, 155–164.

Kleindienst, T.E., Jaoui, M., Lewandowski, M., Offenberg, J.H., Lewis, C.W., Bhave, P. V, Edney, E.O., 2007. Estimates of the contributions of biogenic and anthropogenic hydrocarbons to secondary organic aerosol at a southeastern US location. Atmos. Environ. 41, 8288–8300.

Kondo, Y., Miyazaki, Y., Takegawa, N., Miyakawa, T., Weber, R.J., Jimenez, J.L., Zhang, Q., Worsnop, D.R., 2007. Oxygenated and water-soluble organic aerosols in Tokyo. J. Geophys. Res. 112.

Krivacsy, Z., Gelencser, A., Kiss, G., Meszaros, E., Molnar, A., Hoffer, A., Meszaros, T., Sarvari, Z., Temesi, D., Varga, B., Baltensperger, U., Nyeki, S., Weingartner, E., 2001a. Study on the chemical character of water soluble organic compounds in fine atmospheric aerosol at the Jungfraujoch. J. Atmos. Chem. 39, 235–259.

Krivacsy, Z., Hoffer, A., Sarvari, Z., Temesi, D., Baltensperger, U., Nyeki, S., Weingartner, E., Kleefeld, S., Jennings, S.G., 2001b. Role of organic and black carbon in the chemical composition of atmospheric aerosol at European background sites. Atmos. Environ. 35, 6231–6244.

Krivacsy, Z., Kiss, G., Ceburnis, D., Jennings, G., Maenhaut, W., Salma, I., Shooter, D., 2008. Study of water-soluble atmospheric humic matter in urban and marine environments. Atmos. Res. 87, 1–12.

Krivacsy, Z., Kiss, G., Varga, B., Galambos, I., Sarvari, Z., Gelencser, A., Molnar, A., Fuzzi, S., Facchini, M.C., Zappoli, S., Andracchio, A., Alsberg, T., Hansson, H.C., Persson, L., 2000. Study of humic-like substances in fog and interstitial aerosol by size-exclusion chromatography and capillary electrophoresis. Atmos. Environ. 34, 4273–4281.

Krivácsy, Z., Molnár, Á., 1998. Size distribution of ions in atmospheric aerosols. Atmos. Res. 46, 279–291.

Lambert, J., Lankes, U., 2002. Structural Investigations: Application of Nuclear Magnetic Resonance Spectroscopy to Structural Investigations of Refractory Organic Substances – Principles and Definitions. In: Frimmel, F.H., Abbt-Braun, G., Heumann, K.G., Hock, B., Lüdemann, H.-D., Spiteller, M. (Eds.), Refractory Organic Substances in the Environment. Wiley-VCH, pp. 89–95.

Limbeck, A., Kulmala, M., Puxbaum, H., 2003. Secondary organic aerosol formation in the atmosphere via heterogeneous reaction of gaseous isoprene on acidic particles. Geophys. Res. Lett. 30, n/a–n/a.

Lin, Y.C., Cheng, M.T., Chio, C.P., Kuo, C.Y., 2009. Carbonaceous Aerosol Measurements at Coastal, Urban, and Inland Sites in Central Taiwan. Environ. Forensics 10, 7–17.

MADRP-Direcção de Unidade de Defesa da Floresta, 2011. Relatório anual de áreas ardidas e ocorrências 2010. Portugal.

Maimone, F., Turpin, B.J., Solomon, P., Meng, Q.Y., Robinson, A.L., Subramanian, R., Polidori, A., 2011. Correction Methods for Organic Carbon Artifacts When Using Quartz-Fiber Filters in Large Particulate Matter Monitoring Networks: The Regression Method and Other Options. J. Air Waste Manage. Assoc. 61, 696–710.

Malcolm, R.L., 1989. Applications of solid-state 13C-NMR spectroscopy to geochemical studies of humic substances. In: Hayes, M.H.B., MacCarthy, P., Malcolm, R.L., Swift, R.S. (Eds.), Humic Substances II: In Search of Structure. Wiley, Chichester, pp. 340–372.

Maria, S.F., Russell, L.M., Turpin, B.J., Porcja, R.J., 2002. FTIR measurements of functional groups and organic mass in aerosol samples over the Caribbean. Atmos. Environ. 36, 5185–5196.

Matos, J.T. V, Duarte, R.M.B.O., Duarte, A.C., 2012. Trends in data processing of comprehensive two-dimensional chromatography: State of the art. J. Chromatogr. B 910, 31–45.

Matos, J.T. V, Duarte, R.M.B.O., Duarte, A.C., 2013. A simple approach to reduce dimensionality from comprehensive two-dimensional liquid chromatography coupled with a multichannel detector. Anal. Chim. Acta 804, 296–303.

Mayol-Bracero, O.L., Guyon, P., Graham, B., Roberts, G., Andreae, M.O., Decesari, S., Facchini, M.C., Fuzzi, S., Artaxo, P., 2002. Water-soluble organic compounds in

biomass burning aerosols over Amazonia - 2. Apportionment of the chemical composition and importance of the polyacidic fraction. J. Geophys. Res. 107, Doi 10.1029/2001jd000522.

Mazzoleni, L.R., Ehrmann, B.M., Shen, X.H., Marshall, A.G., Collett, J.L., 2010. Water-Soluble Atmospheric Organic Matter in Fog: Exact Masses and Chemical Formula Identification by Ultrahigh-Resolution Fourier Transform Ion Cyclotron Resonance Mass Spectrometry. Environ. Sci. Technol. 44, 3690–3697.

McDonald, S., Bishop, A.G., Prenzler, P.D., Robards, K., 2004. Analytical chemistry of freshwater humic substances. Anal. Chim. Acta 527, 105–124.

McKnight, D.M., Boyer, E.W., Westerhoff, P.K., Doran, P.T., Kulbe, T., Andersen, D.T., 2001. Spectrofluorometric characterization of dissolved organic matter for indication of precursor organic material and aromaticity. Limnol. Oceanogr. 46, 38–48.

McMurry, P.H., 2000. A review of atmospheric aerosol measurements. Atmos. Environ. 34, 1959–1999.

Miller, J.N., Miller, J.C., 2005. Statistics and Chemometrics for Analytical Chemistry, Fifth. ed. England: Pearson - Prentice Hall.

Mircea, M., Facchini, M.C., Decesari, S., Fuzzi, S., Charlson, R.J., 2002. The influence of the organic aerosol component on CCN supersaturation spectra for different aerosol types. Tellus B 54, 74–81.

Miyazaki, Y., Kondo, Y., Takegawa, N., Komazaki, Y., Fukuda, M., Kawamura, K., Mochida, M., Okuzawa, K., Weber, R.J., 2006. Time-resolved measurements of water-soluble organic carbon in Tokyo. J. Geophys. Res. 111.

Mkoma, S.L., Chi, X.G., Maenhaut, W., 2010. Characteristics of carbonaceous aerosols in ambient PM10 and PM2.5 particles in Dar es Salaam, Tanzania. Sci. Total Environ. 408, 1308–1314.

Mladenov, N., Alados-Arboledas, L., Olmo, F.J., Lyamani, H., Delgado, A., Molina, A., Reche, I., 2011. Applications of optical spectroscopy and stable isotope analyses to organic aerosol source discrimination in an urban area. Atmos. Environ. 45, 1960–1969.

Mladenov, N., Reche, I., Olmo, F.J., Lyamani, H., Alados-Arboledas, L., 2010. Relationships between spectroscopic properties of high-altitude organic aerosols and Sun photometry from ground-based remote sensing. J. Geophys. Res. Biogeosciences 115, G00F11.

Nakajima, H., Okada, K., Kuroki, Y., Nakama, Y., Handa, D., Arakaki, T., Tanahara, A., 2008. Photochemical formation of peroxides and fluorescence characteristics of the water-soluble fraction of bulk aerosols collected in Okinawa, Japan. Atmos. Environ. 42, 3046–3058.

Navrátil, T., Hladil, J., Strnad, L., Koptíková, L., Skála, R., 2012. Volcanic ash particulate matter from the 2010 Eyjafjallajökull eruption in dust deposition at Prague, central Europe. Aeolian Res.

Park, S.S., Cho, S.Y., 2011. Tracking sources and behaviors of water-soluble organic carbon in fine particulate matter measured at an urban site in Korea. Atmos. Environ. 45, 60–72.

Parlanti, E., Wörz, K., Geoffroy, L., Lamotte, M., 2000. Dissolved organic matter fluorescence spectroscopy as a tool to estimate biological activity in a coastal zone submitted to anthropogenic inputs. Org. Geochem. 31, 1765–1781.

Peltier, R.E., Weber, R.J., Sullivan, A.P., 2007. Investigating a liquid-based method for online organic carbon detection in atmospheric particles. Aerosol Sci. Technol. 41, 1117–1127.

Pereira, A.S., David, F., Vanhoenacker, G., Sandra, P., 2009. The acetonitrile shortage: Is reversed HILIC with water an alternative for the analysis of highly polar ionizable solutes? J. Sep. Sci. 32, 2001–2007.

Peuravuori, J., Koivikko, R., Pihlaja, K., 2002a. Characterization. differentiation and classification of aquatic humic matter separated with different sorbents: synchronous scanning fluorescence spectroscopy. Water Res. 36, 4552–4562.

Peuravuori, J., Lehtonen, T., Pihlaja, K., 2002b. Sorption of aquatic humic matter by DAX-8 and XAD-8 resins: Comparative study using pyrolysis gas chromatography. Anal. Chim. Acta 471, 219–226.

Peuravuori, J., Pihlaja, K., 1997. Molecular size distribution and spectroscopic properties of aquatic humic substances. Anal. Chim. Acta 337, 133–149.

Pio, C.A., Alves, C.A., Duarte, A.C., 2001. Identification, abundance and origin of atmospheric organic particulate matter in a Portuguese rural area. Atmos. Environ. 35, 1365–1375.

Pio, C.A., Legrand, M., Alves, C.A., Oliveira, T., Afonso, J., Caseiro, A., Puxbaum, H., Sanchez-Ochoa, A., Gelencsér, A., 2008. Chemical composition of atmospheric aerosols during the 2003 summer intense forest fire period. Atmos. Environ. 42, 7530–7543.

Pól, J., Hohnová, B., Jussila, M., Hyötyläinen, T., 2006. Comprehensive two-dimensional liquid chromatography–time-of-flight mass spectrometry in the analysis of acidic compounds in atmospheric aerosols. J. Chromatogr. A 1130, 64–71.

Poschl, U., 2005. Atmospheric aerosols: Composition, transformation, climate and health effects. Angew. Chemie-International Ed. 44, 7520–7540.

Putaud, J.-P., Van Dingenen, R., Alastuey, A., Bauer, H., Birmili, W., Cyrys, J., Flentje, H., Fuzzi, S., Gehrig, R., Hansson, H.C., Harrison, R.M., Herrmann, H., Hitzenberger, R., Hüglin, C., Jones, A.M., Kasper-Giebl, A., Kiss, G., Kousa, A., Kuhlbusch, T.A.J., Löschau, G., Maenhaut, W., Molnar, A., Moreno, T., Pekkanen, J., Perrino, C., Pitz, M., Puxbaum, H., Querol, X., Rodriguez, S., Salma, I., Schwarz, J., Smolik, J., Schneider, J., Spindler, G., ten Brink, H., Tursic, J., Viana, M., Wiedensohler, A., Raes, F., 2010. A European aerosol phenomenology – 3: Physical and chemical

characteristics of particulate matter from 60 rural, urban, and kerbside sites across Europe. Atmos. Environ. 44, 1308–1320.

Ram, K., Sarin, M.M., 2010. Spatio-temporal variability in atmospheric abundances of EC, OC and WSOC over Northern India. J. Aerosol Sci. 41, 88–98.

Reemtsma, T., 2009. Determination of molecular formulas of natural organic matter molecules by (ultra-) high-resolution mass spectrometry Status and needs. J. Chromatogr. A 1216, 3687–3701.

Remoundaki, E., Papayannis, A., Kassomenos, P., Mantas, E., Kokkalis, P., Tsezos, M., 2012. Influence of Saharan Dust Transport Events on PM2.5 Concentrations and Composition over Athens. Water, Air, Soil Pollut. 224, 1–14.

Rogge, W.F., Hildemann, L.M., Mazurek, M.A., Cass, G.R., Simoneit, B.R.T., 1998. Sources of fine organic aerosol. 9. Pine, oak and synthetic log combustion in residential fireplaces. Environ. Sci. Technol. 32, 13–22.

Saarikoski, S., Sillanpaa, M., Sofiev, M., Timonen, H., Saarnio, K., Teinela, K., Karppinen, A., Kukkonen, J., Hillamo, R., 2007. Chemical composition of aerosols during a major biomass burning episode over northern Europe in spring 2006: Experimental and modelling assessments. Atmos. Environ. 41, 3577–3589.

Saarikoski, S., Timonen, H., Saarnio, K., Aurela, M., Jarvi, L., Keronen, P., Kerminen, V.M., Hillamo, R., 2008. Sources of organic carbon in fine particulate matter in northern European urban air. Atmos. Chem. Phys. 8, 6281–6295.

Salma, I., Ocskay, R., Chi, X.G., Maenhaut, W., 2007. Sampling artefacts, concentration and chemical composition of fine water-soluble organic carbon and humic-like substances in a continental urban atmospheric environment. Atmos. Environ. 41, 4106–4118.

Salma, I., Ocskay, R., Varga, I., Maenhaut, W., 2006. Surface tension of atmospheric humic-like substances in connection with relaxation, dilution, and solution pH. J. Geophys. Res. 111, -.

Samara, C., Voutsa, D., 2005. Size distribution of airborne particulate matter and associated heavy metals in the roadside environment. Chemosphere 59, 1197–1206.

Samburova, V., Zenobi, R., Kalberer, M., 2005. Characterization of high molecular weight compounds in urban atmospheric particles. Atmos. Chem. Phys. 5, 2163–2170.

Sannigrahi, P., Sullivan, A.P., Weber, R.J., Ingall, E.D., 2006. Characterization of water-soluble organic carbon in urban atmospheric aerosols using solid-state C-13 NMR spectroscopy. Environ. Sci. Technol. 40, 666–672.

Santos, E.B.H., Duarte, A.C., 1998. The influence of pulp and paper mill effluents on the composition of the humic fraction of aquatic organic matter. Water Res. 32, 597–608.

Santos, E.B.H., Duarte, R.M.B.O., Filipe, O.S., Duarte, A.C., 2000. Structural characterisation of the coloured organic matter from an eucalyptus pleached Kraft pulp mill effluent. Int. J. Environ. Anal. Chem. 78, 333–342.

Santos, E.B.H., Filipe, O.M.S., Duarte, R.M.B.O., Pinto, H., Duarte, A.C., 2001. Fluorescence as a tool for tracing the organic contamination from pulp mill effluents in surface waters. Acta Hydrochim. Hydrobiol. 28, 364–371.

Santos, P.S.M., Duarte, R.M.B.O., Duarte, A.C., 2009. Absorption and fluorescence properties of rainwater during the cold season at a town in Western Portugal. J. Atmos. Chem. 62, 45–57.

Schmitt-Kopplin, P., Gelencsér, A., Dabek-Zlotorzynska, E., Kiss, G., Hertkorn, N., Harir, M., Hong, Y., Gebefügi, I., 2010. Analysis of the Unresolved Organic Fraction in Atmospheric Aerosols with Ultrahigh-Resolution Mass Spectrometry and Nuclear Magnetic Resonance Spectroscopy: Organosulfates As Photochemical Smog Constituents†. Anal. Chem. 82, 8017–8026.

Seinfeld, J.H., 1986. Atmospheric chemistry and physics of air pollution. John Wiley & Sons, Inc., New York, EUA.

Seinfeld, J.H., Pandis, S.N., 1998. Atmospheric Chemistry and Physics: From Air Pollution to Climate Change. John Wiley & Sons, Inc., New York, EUA.

Seinfeld, J.H., Pandis, S.N., 2006. Atmospheric Chemistry and Physics: From Air Pollution to Climate Change., 2nd ed. John Wiley & Sons, Canada.

Seinfeld, J.H., Pankow, J.F., 2003. Organic atmospheric particulate material. Annu. Rev. Phys. Chem. 54, 121–140.

Sempére, R., Kawamura, K., 1994. Comparative distributions of dicarboxylic acids and related polar compounds in snow, rain and aerosols from urban atmosphere. Atmos. Environ. 28, 449–459.

Senesi, N., Miano, T.M., Provenzano, M.R., Brunetti, G., 1991. Characterization, differentiation, and classification of humic substances by fluorescence spectroscopy. Soil Sci. 152, 259–271.

Simoneit, B.R.T., Rogge, W.F., Mazurek, M.A., Standley, L.J., Hildemann, L.M., Cass, G.R., 1993. Lignin pyrolysis products, lignans, and resin acids as specific tracers of plant classes in emissions from biomass combustion. Environ. Sci. Technol. 27, 2533–2541.

Simoneit, B.R.T., Schauer, J.J., Nolte, C.G., Oros, D.R., Elias, V.O., Fraser, M.P., Rogge, W.F., Cass, G.R., 1999. Levoglucosan, a tracer for cellulose in biomass burning and atmospheric particles. Atmos. Environ. 33, 173–182.

Simpson, A.J., 2001. Multidimensional solution state NMR of humic substances: A practical guide and review. Soil Sci. 166, 795–809.

Simpson, A.J., Simpson, M.J., 2009. Nuclear Magnetic Resonance Analysis of Natural Organic Matter. In: Senesi, N., Xing, B., Huang, P.. (Eds.), Biophysico-Chemical Processes Involving Natural Nonliving Organic Matter in Environmental Systems. John Wiley & Sons, Inc., New Jersey, pp. 589–650.

Smith, D.M., Chughtai, A.R., 1995. The surface structure and reactivity of black carbon. Colloids Surfaces A Physicochem. Eng. Asp. 105, 47–77.

Snyder, D.C., Rutter, A.P., Collins, R., Worley, C., Schauer, J.J., 2009. Insights into the Origin of Water Soluble Organic Carbon in Atmospheric Fine Particulate Matter. Aerosol Sci. Technol. 42, 1099–1107.

Stoll, D.R., Li, X., Wang, X., Carr, P.W., Porter, S.E.G., Rutan, S.C., 2007. Fast, comprehensive two-dimensional liquid chromatography. J. Chromatogr. A 1168, 3–43.

Stone, E.A., Hedman, C.J., Sheesley, R.J., Shafer, M.M., Schauer, J.J., 2009. Investigating the chemical nature of humic-like substances (HULIS) in North American atmospheric aerosols by liquid chromatography tandem mass spectrometry. Atmos. Environ. 43, 4205–4213.

Subbalakshmi, Y., Patti, A.F., Lee, G.S.H., Hooper, M.A., 2000. Structural characterisation of macromolecular organic material in air particulate matter using Py-GC-MS and solid state C-13-NMR. J. Environ. Monit. 2, 561–565.

Subramanian, R., Khlystov, A.Y., Cabada, J.C., Robinson, A.L., 2004. Positive and Negative Artifacts in Particulate Organic Carbon Measurements with Denuded and Undenuded Sampler Configurations Special Issue of Aerosol Science and Technology on Findings from the Fine Particulate Matter Supersites Program. Aerosol Sci. Technol. 38, 27–48.

Sullivan, A.P., Weber, R.J., 2006. Chemical characterization of the ambient organic aerosol soluble in water: 1. Isolation of hydrophobic and hydrophilic fractions with a XAD-8 resin - art. no. D05314. J Geophys Res Atmos 111, 5314.

Sullivan, A.P., Weber, R.J., Clements, A.L., Turner, J.R., Bae, M.S., Schauer, J.J., 2004. A method for on-line measurement of water-soluble organic carbon in ambient aerosol particles: Results from an urban site. Geophys. Res. Lett. 31, -.

Sun, Y., Zhang, Q., Zheng, M., Ding, X., Edgerton, E.S., Wang, X., 2011. Characterization and Source Apportionment of Water-Soluble Organic Matter in Atmospheric Fine Particles (PM2.5) with High-Resolution Aerosol Mass Spectrometry and GC–MS. Environ. Sci. Technol. 45, 4854–4861.

Takahama, S., Schwartz, R.E., Russell, L.M., Macdonald, A.M., Sharma, S., Leaitch, W.R., 2011. Organic functional groups in aerosol particles from burning and non-burning forest emissions at a high-elevation mountain site. Atmos. Chem. Phys. 11, 6367–6386.

Timonen, H., Aurela, M., Carbone, S., Saarnio, K., Saarikoski, S., Makela, T., Kulmala, M., Kerminen, V.M., Worsnop, D.R., Hillamo, R., 2010. High time-resolution chemical characterization of the water-soluble fraction of ambient aerosols with PILS-TOC-IC and AMS. Atmos. Meas. Tech. 3, 1063–1074.

Timonen, H.J., Saarikoski, S.K., Aurela, M.A., Saarnio, K.M., Hillamo, R.E.J., 2008. Water-soluble organic carbon in urban aerosol: concentrations, size distributions and contribution to particulate matter. Boreal Environ. Res. 13, 335–346.

Turpin, B.J., Huntzicker, J.J., Hering, S. V, 1994. Investigation of organic aerosol sampling artifacts in the los-angeles basin. Atmos. Environ. 28, 3061–3071.

Turpin, B.J., Lim, H.J., 2001. Species contributions to PM2.5 mass concentrations: Revisiting common assumptions for estimating organic mass. Aerosol Sci. Technol. 35, 602–610.

Turpin, B.J., Saxena, P., Andrews, E., 2000. Measuring and simulating particulate organics in the atmosphere: problems and prospects. Atmos. Environ. 34, 2983–3013.

Varga, B., Kiss, G., Ganszky, I., Gelencser, A., Krivacsy, Z., 2001. Isolation of water-soluble organic matter from atmospheric aerosol. Talanta 55, 561–572.

Viana, M., Chi, X., Maenhaut, W., Cafmeyer, J., Querol, X., Alastuey, A., Mikuska, P., Vecera, Z., 2006a. Influence of sampling artefacts on measured PM, OC, and EC levels in Carbonaceous aerosols in an urban area. Aerosol Sci. Technol. 40, 107–117.

Viana, M., Chi, X., Maenhaut, W., Querol, X., Alastuey, A., Mikuska, P., Vecera, Z., 2006b. Organic and elemental carbon concentrations in carbonaceous aerosols during summer and winter sampling campaigns in Barcelona, Spain. Atmos. Environ. 40, 2180–2193.

Viana, M., Maenhaut, W., ten Brink, H.M., Chi, X., Weijers, E., Querol, X., Alastuey, A., Mikuška, P., Večeřa, Z., 2007. Comparative analysis of organic and elemental carbon concentrations in carbonaceous aerosols in three European cities. Atmos. Environ. 41, 5972–5983.

Viidanoja, J., Sillanpaa, M., Laakia, J., Kerminen, V.M., Hillamo, R., Aarnio, P., Koskentalo, T., 2002. Organic and black carbon in PM2.5 and PM10: 1 year of data from an urban site in Helsinki, Finland. Atmos. Environ. 36, 3183–3193.

Wang, Y., Chiu, C., Westerhoff, P., Valsaraj, K.T., Herckes, P., 2013. Characterization of atmospheric organic matter using size-exclusion chromatography with inline organic carbon detection. Atmos. Environ. 68, 326–332.

Weber, R.J., Orsini, D., Daun, Y., Lee, Y.-N., Klotz, P.J., Brechtel, F., 2001. A Particle-into-Liquid Collector for Rapid Measurement of Aerosol Bulk Chemical Composition. Aerosol Sci. Technol. 35, 718–727.

Weber, R.J., Sullivan, A.P., Peltier, R.E., Russell, A., Yan, B., Zheng, M., de Gouw, J., Warneke, C., Brock, C., Holloway, J.S., Atlas, E.L., Edgerton, E., 2007. A study of secondary organic aerosol formation in the anthropogenic-influenced southeastern United States. J. Geophys. Res. Atmos. 112, D13302.

Wozniak, A.S., Bauer, J.E., Sleighter, R.L., Dickhut, R.M., Hatcher, P.G., 2008. Technical Note: Molecular characterization of aerosol-derived water soluble organic carbon using ultrahigh resolution electrospray ionization Fourier transform ion cyclotron resonance mass spectrometry. Atmos. Chem. Phys. 8, 5099–5111.

Yamashita, Y., Tanoue, E., 2003. Chemical characterization of protein-like fluorophores in DOM in relation to aromatic amino acids. Mar. Chem. 82, 255–271.

Yang, H., Xu, J., Wu, W., Wan, C.H., Yu, J.Z., 2004. Chemical Characterization of Water-Soluble Organic Aerosols at Jeju Island Collected During ACE-Asia. Environ. Chem. 1, 13–17.

Yoon, Y.J., Ceburnis, D., Cavalli, F., Jourdan, O., Putaud, J.P., Facchini, M.C., Decesari, S., Fuzzi, S., Sellegri, K., Jennings, S.G., O'Dowd, C.D., 2007. Seasonal characteristics of the physicochemical properties of North Atlantic marine atmospheric aerosols. J. Geophys. Res. Atmos. 112, D04206.

Yu, L.E., Shulman, M.L., Kopperud, R., Hildemann, L.M., 2004. Characterization of Organic Compounds Collected during Southeastern Aerosol and Visibility Study: Water-Soluble Organic Species. Environ. Sci. Technol. 39, 707–715.

Zappoli, S., Andracchio, A., Fuzzi, S., Facchini, M.C., Gelencser, A., Kiss, G., Krivacsy, Z., Molnar, A., Meszaros, E., Hansson, H.C., Rosman, K., Zebuhr, Y., 1999. Inorganic, organic and macromolecular components of fine aerosol in different areas of Europe in relation to their water solubility. Atmos. Environ. 33, 2733–2743.

Zhang, F., Zhao, J., Chen, J., Xu, Y., Xu, L., 2011. Pollution characteristics of organic and elemental carbon in PM2.5 in Xiamen, China. J Env. Sci 23, 1342–1349.

Zhang, Q., Alfarra, M.R., Worsnop, D.R., Allan, J.D., Coe, H., Canagaratna, M.R., Jimenez, J.L., 2005a. Deconvolution and Quantification of Hydrocarbon-like and Oxygenated Organic Aerosols Based on Aerosol Mass Spectrometry. Environ. Sci. Technol. 39, 4938–4952.

Zhang, Q., Worsnop, D.R., Canagaratna, M.R., Jimenez, J.L., 2005b. Hydrocarbon-like and oxygenated organic aerosols in Pittsburgh: insights into sources and processes of organic aerosols. Atmos. Chem. Phys. 5, 3289–3311.

Zhang, Y.Y., Müller, L., Winterhalter, R., Moortgat, G.K., Hoffmann, T., Pöschl, U., 2010. Seasonal cycle and temperature dependence of pinene oxidation products, dicarboxylic acids and nitrophenols in fine and coarse air particulate matter. Atmos. Chem. Phys. 10, 7859–7873.

Annexes

Annex A

Table A. 1. Sampling details of the intensive field campaign II.

Sample	Sampling Period		Observations
AVE 1	23-11-2009 10:45	30-11-2009 10:45	
AVE 2	30-11-2009 11:05	07-12-2009 11:05	
AVE 3	07-12-2009 11:26	14-12-2009 11:30	
AVE 4	14-12-2009 12:00	21-12-2009 12:00	
AVE 5	21-12-2009 12:30	28-12-2009 10:10	Field blank
AVE 6	28-12-2009 10:30	04-01-2010 11:27	Field blank
AVE 7	11-01-2010 10:10	18-01-2010 10:10	
AVE 8	18-01-2010 10:45	25-01-2010 10:45	Field blank
AVE 9	26-01-2010 11:15	02-02-2010 11:15	
AVE 10	02-02-2010 11:35	09-02-2010 11:35	
AVE 11	09-02-2010 11:58	12-02-2010 09:40	Engine failure of the sampler
AVE 12	15-02-2010 10:11	22-02-2010 09:52	Field blank
AVE 13	22-02-2010 10:15	01-03-2010 10:00	Field blank
AVE 14	08-03-2010 14:25	15-03-2010 14:25	
AVE 15	15-03-2010 14:44	22-03-2010 10:00	Engine failure of the sampler
AVE 16	30-03-2010 10:00	06-04-2010 10:05	
AVE 17	06-04-2010 10:20	13-04-2010 10:18	
AVE 18	13-04-2010 10:45	20-04-2010 10:45	
AVE 19	20-04-2010 11:05	27-04-2010 11:15	
AVE 20	27-04-2010 11:32	04-05-2010 11:26	
AVE 21	04-05-2010 11:47	11-05-2010 11:45	
AVE 22	11-05-2010 12:13	18-05-2010 12:45	
AVE 23	18-05-2010 12:35	25-05-2010 12:45	
AVE 24	25-05-2010 13:15	01-06-2010 10:45	Field blank
AVE 25	01-06-2010 11:50	08-06-2010 11:43	
AVE 26	08-06-2010 12:09	15-06-2010 10:35	Field blank
AVE 27	15-06-2010 11:40	22-06-2010 10:46	
AVE 28	22-06-2010 11:07	29-06-2010 10:47	
AVE 29	29-06-2010 11:14	30-06-2010 10:05	Engine failure of the sampler
AVE 30	05-07-2010 10:54	12-07-2010 10:42	
AVE 31	12-07-2010 11:00	19-07-2010 11:00	
AVE 32	19-07-2010 11:09	26-07-2010 11:00	
AVE 33	26-07-2010 11:20	02-08-2010 11:24	
AVE 34	02-08-2010 11:45	09-08-2010 11:46	
AVE 35	09-08-2010 12:11	16-08-2010 12:18	
AVE 36	16-08-2010 12:35	19-08-2010 09:46	Engine failure of the sampler
AVE 37	19-08'2010 12:00	26-08-2010 12:00	Field blank
AVE 38	06-09-2010 11:20	13-09-2010 11:15	
AVE 39	13-09-2010 11:36	20-09-2010 11:30	
AVE 40	20-09-2010 11:43	27-09-2010 12:05	
AVE 41	27-09-2010 12:21	04-10-2010 12:25	
AVE 42	04-10-2010 12:47	11-10-2010 12:48	
AVE 43	11-10-2010 13:11	18-10-2010 13:15	
AVE 44	18-10-2010 13:40	22-10-2010 23:30	Engine failure of the sampler
AVE 45	25-10-2010 09:15	01-11-2010 09:30	Field blank
AVE 46	02-11-2010 10:15	09-11-2010 10:28	
AVE 47	09-11-2010 10:45	16-11-2010 11:10	
AVE 48	16-11-2010 11:28	23-11-2010 11:45	
AVE 49	23-11-2010 12:02	30-11-2010 12:05	
AVE 50	30-11-2010 12:25	07-12-2010 12:58	
AVE 51	07-12-2010 13:20	13-12-2010 11:30	Engine failure of the sampler
AVE 52	13-12-2010 14:50	20-12-2010 10:25	Field blank

Table A. 2. Sampling details of the intensive field campaign II (Cont.).

Sample	Sampling Period		Observations
AVE 53	20-12-2010 13:10	27-12-2010 10:15	
AVE 54	27-12-2010 10:36	03-01-2011 10:50	
AVE 55	03-01-2011 11:10	07-01-2011 01:30	Engine failure of the sampler
AVE 56	11-01-2011 10:45	18-01-2011 10:45	
AVE 57	18-01-2011 11:00	25-01-2011 10:59	
AVE 58	25-01-2011 11:15	01-02-2011 11:25	
AVE 59	01-02-2011 11:40	08-02-2011 11:54	Engine failure of the sampler
AVE 60	08-02-2011 12:15	15-02-2011 10:26	Field blank
AVE 61	15-02-2011 11:00	22-02-2011 10:50	
AVE 62	22-02-2011 11:10	01-03-2011 11:02	
AVE 63	01-03-2011 11:18	08-03-2011 11:45	
AVE 64	08-03-2011 12:20	15-03-2011 11:30	
AVE 65	15-03-2011 11:45	22-03-2011 12:05	
AVE 66	22-03-2011 12:26	29-03-2011 12:08	

Annex B

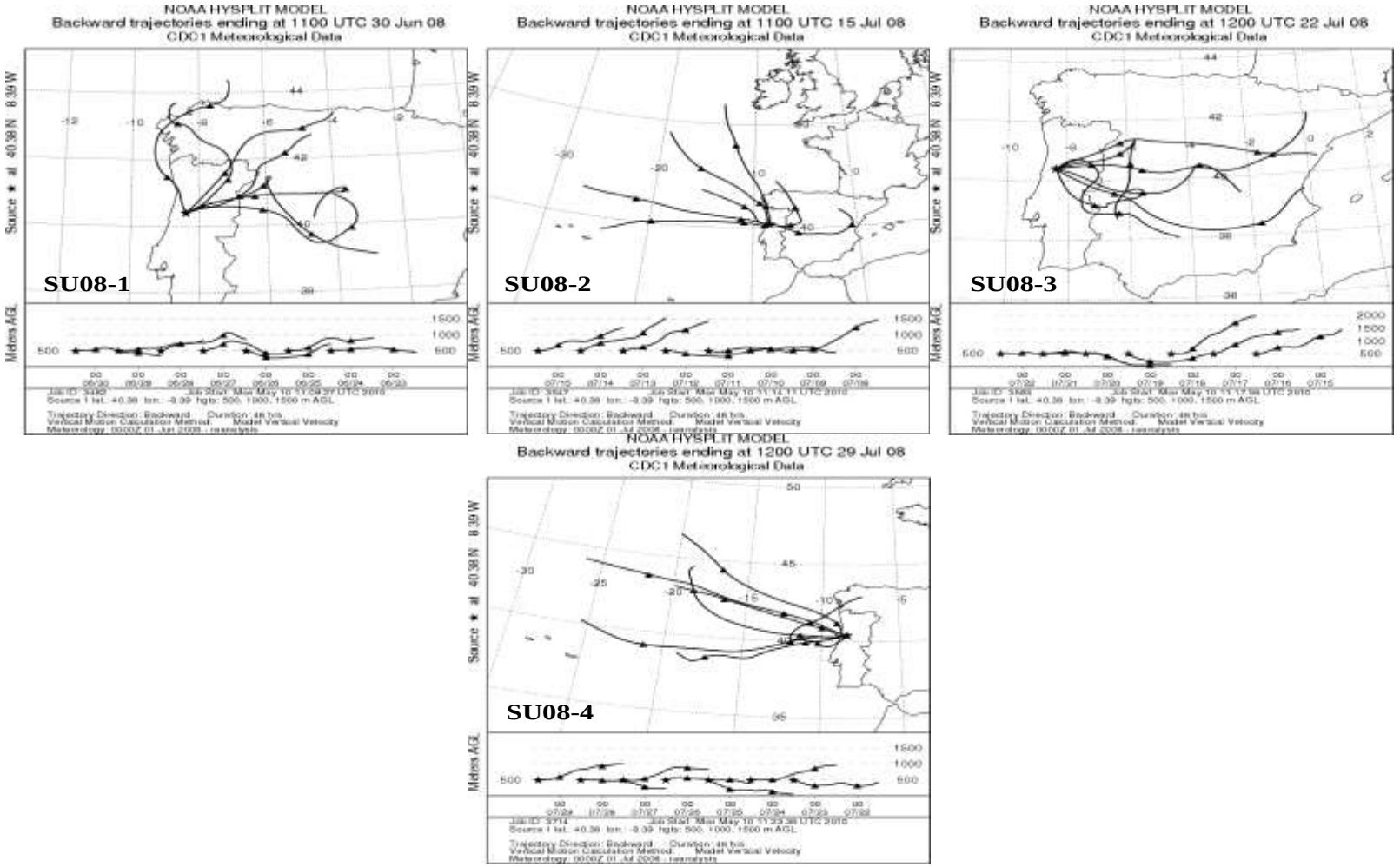

Fig. B. 1. Air mass backward trajectories ending at Aveiro at distinct altitudes (>500 m a.g.l.) during each week in Summer 2008 (SU08-1 – SU08-4), Spring 2009 (SP09-1 – SP09-4) and Summer 2009 (SU09-1 – SU09-4).

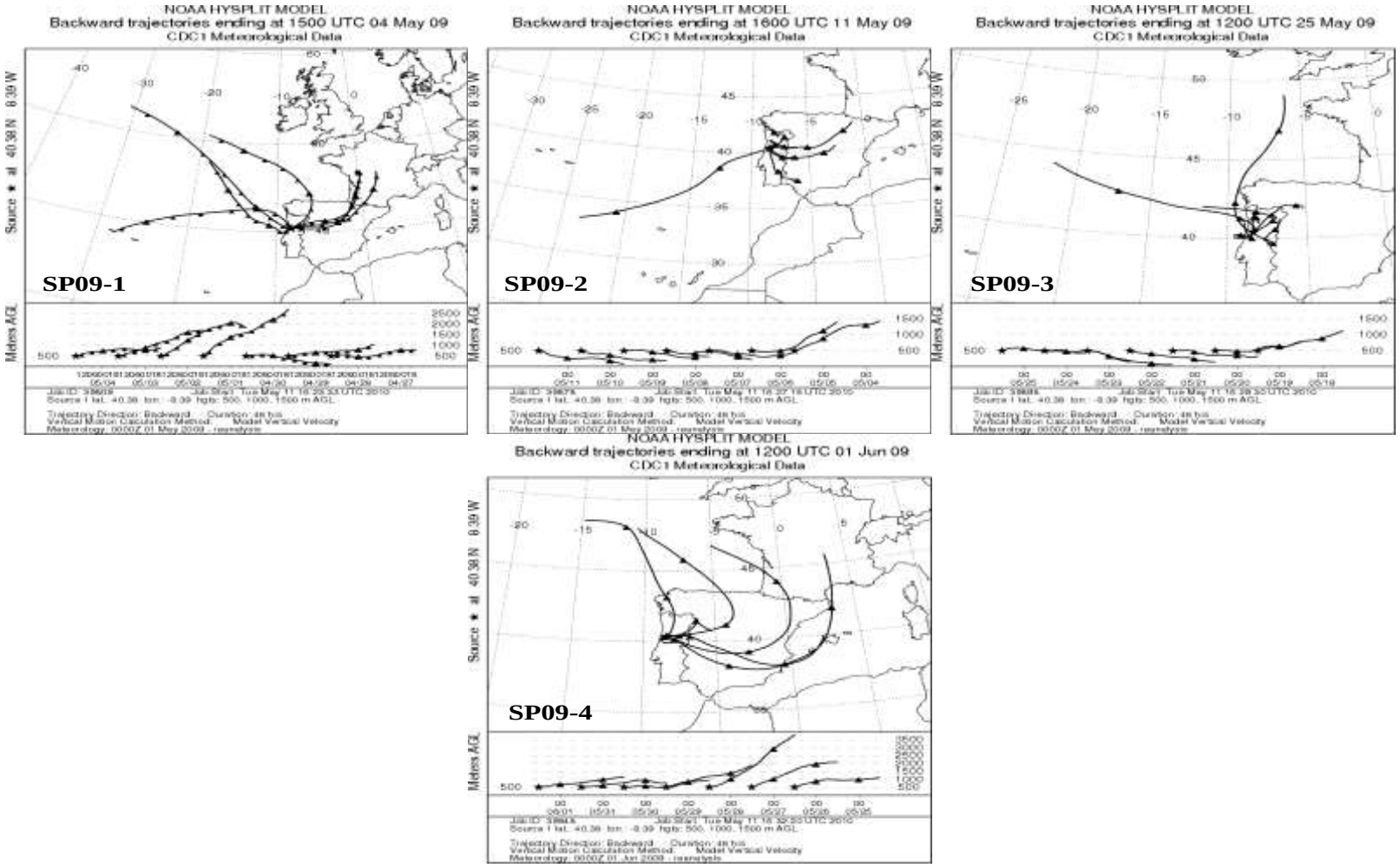

Fig. B. 1. *Continued.*

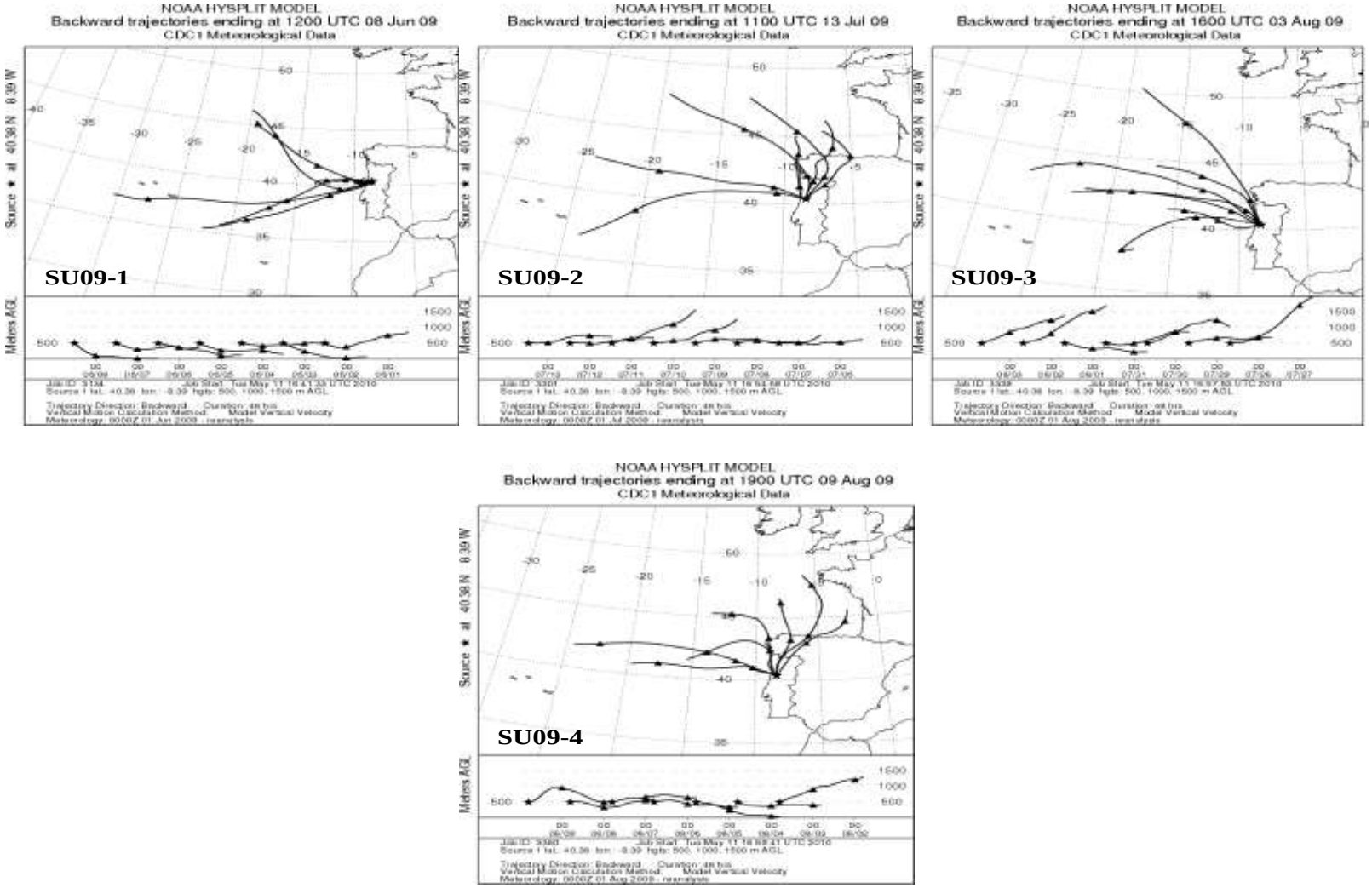

Fig. B. 1. *Continued.*

Annex C

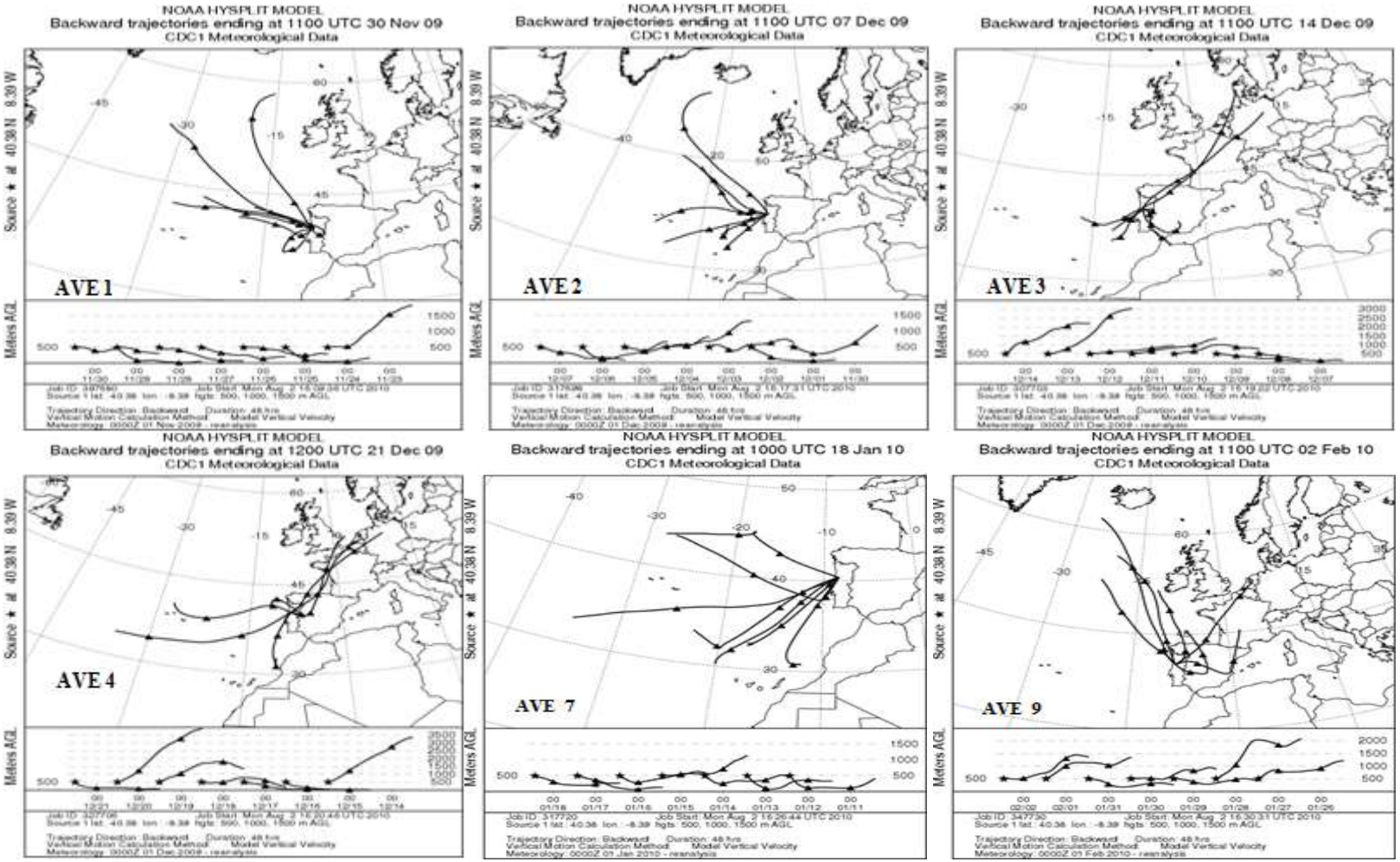

Fig. C. 1. Air mass backward trajectories ending at Aveiro at distinct altitudes (>500 m a.g.l.) during each week in Autumn 2009 (AVE 1 – AVE 4), Winter 2010 (AVE 7 – AVE 14), Spring 2010 (AVE 16 – AVE 27), Summer 2010 (AVE 28 – AVE 39), Autumn 2010 (AVE 40 – AVE 50), Winter (AVE 53 – AVE 65), and Spring 2011(AVE 66) seasons.

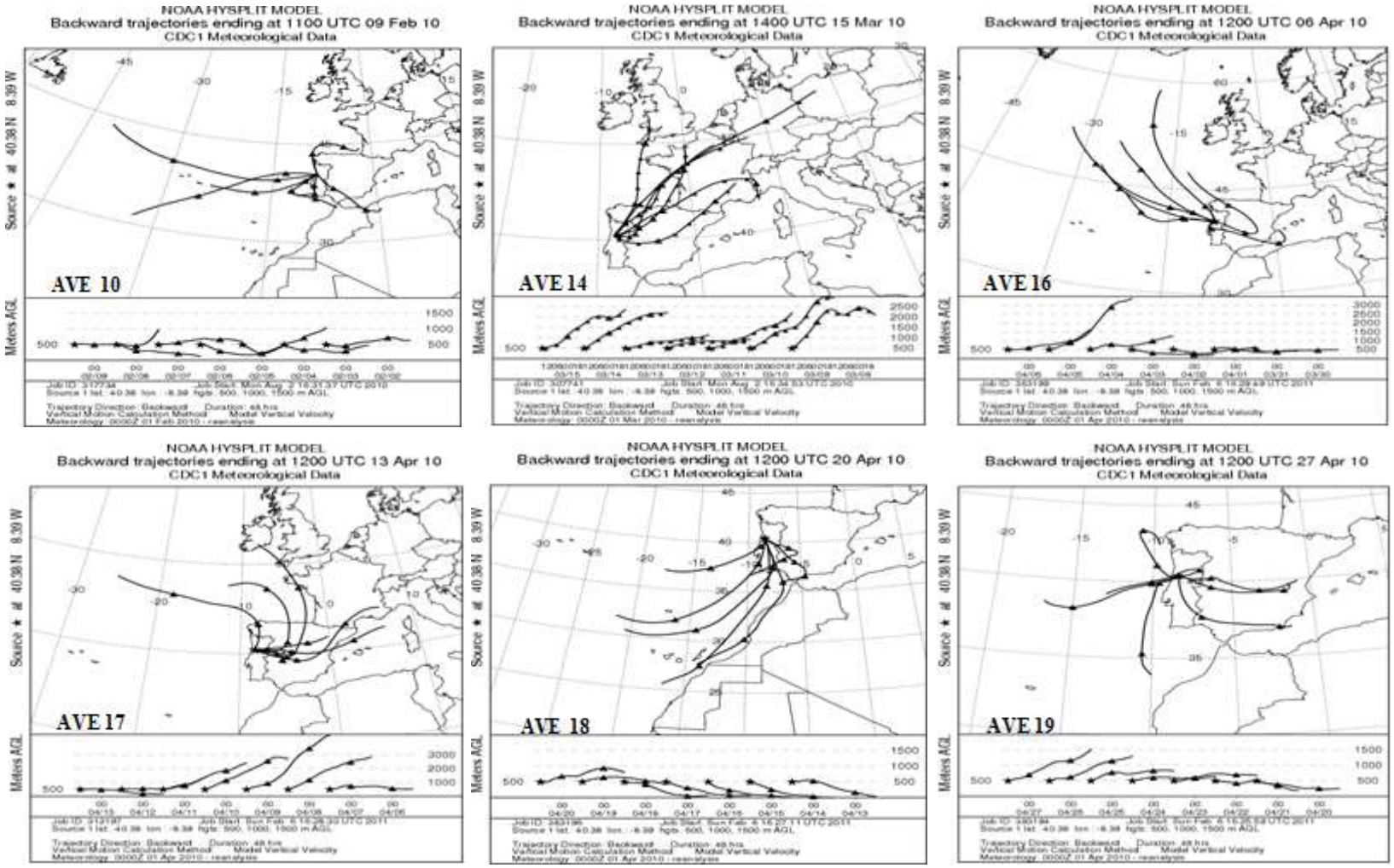

Fig. C. 1. *Continued.*

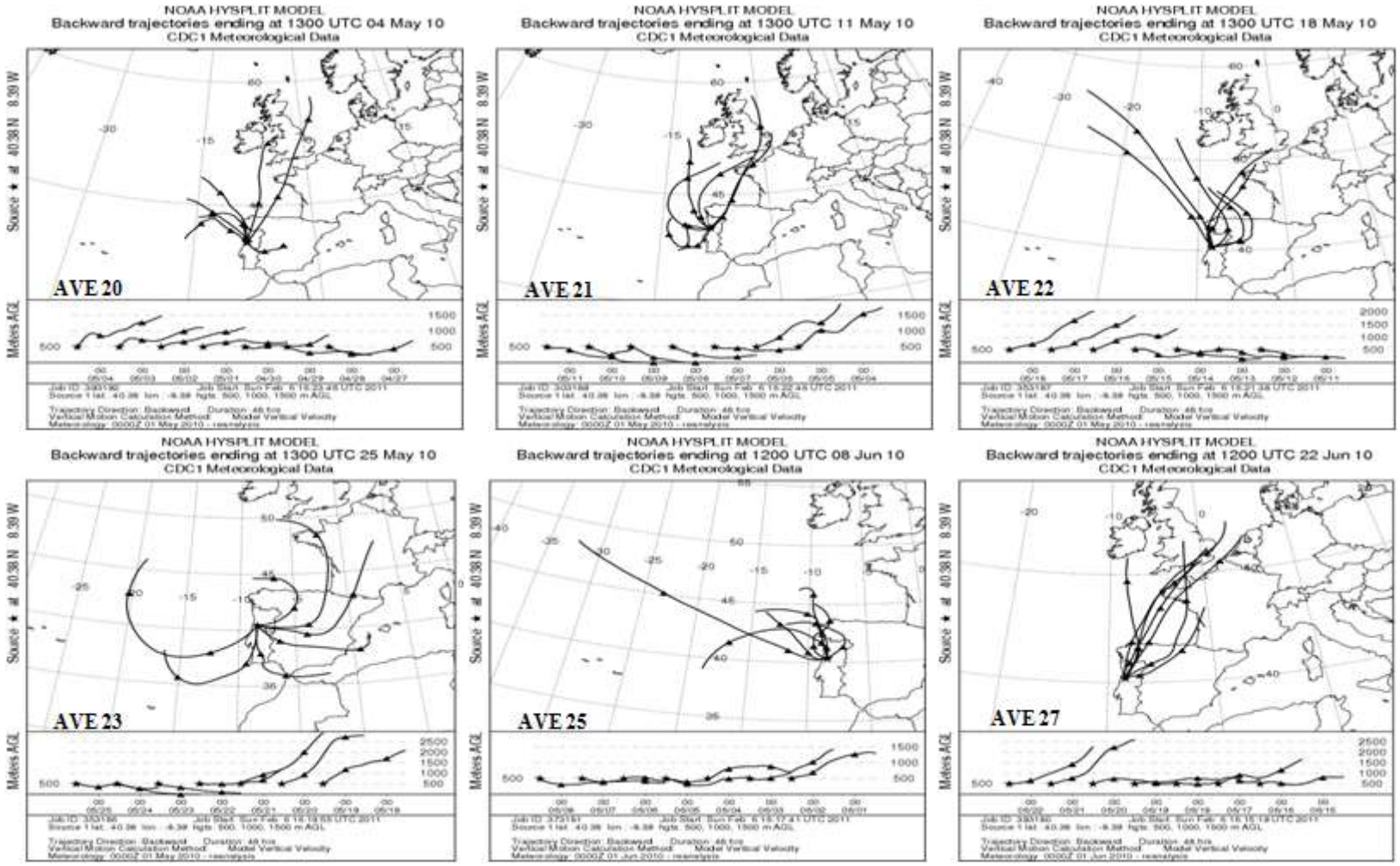

Fig. C. 1. *Continued.*

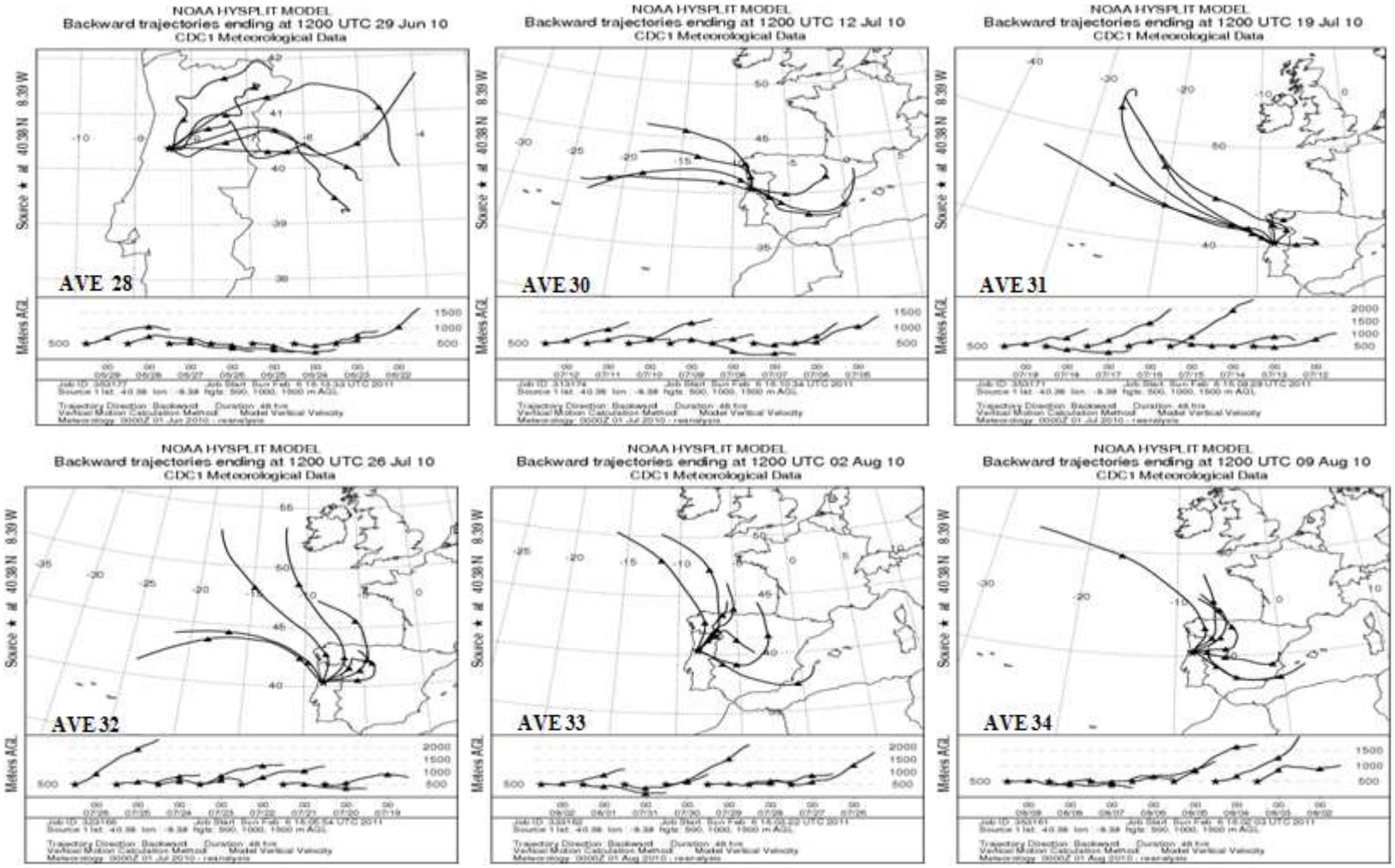

Fig. C. 1. *Continued.*

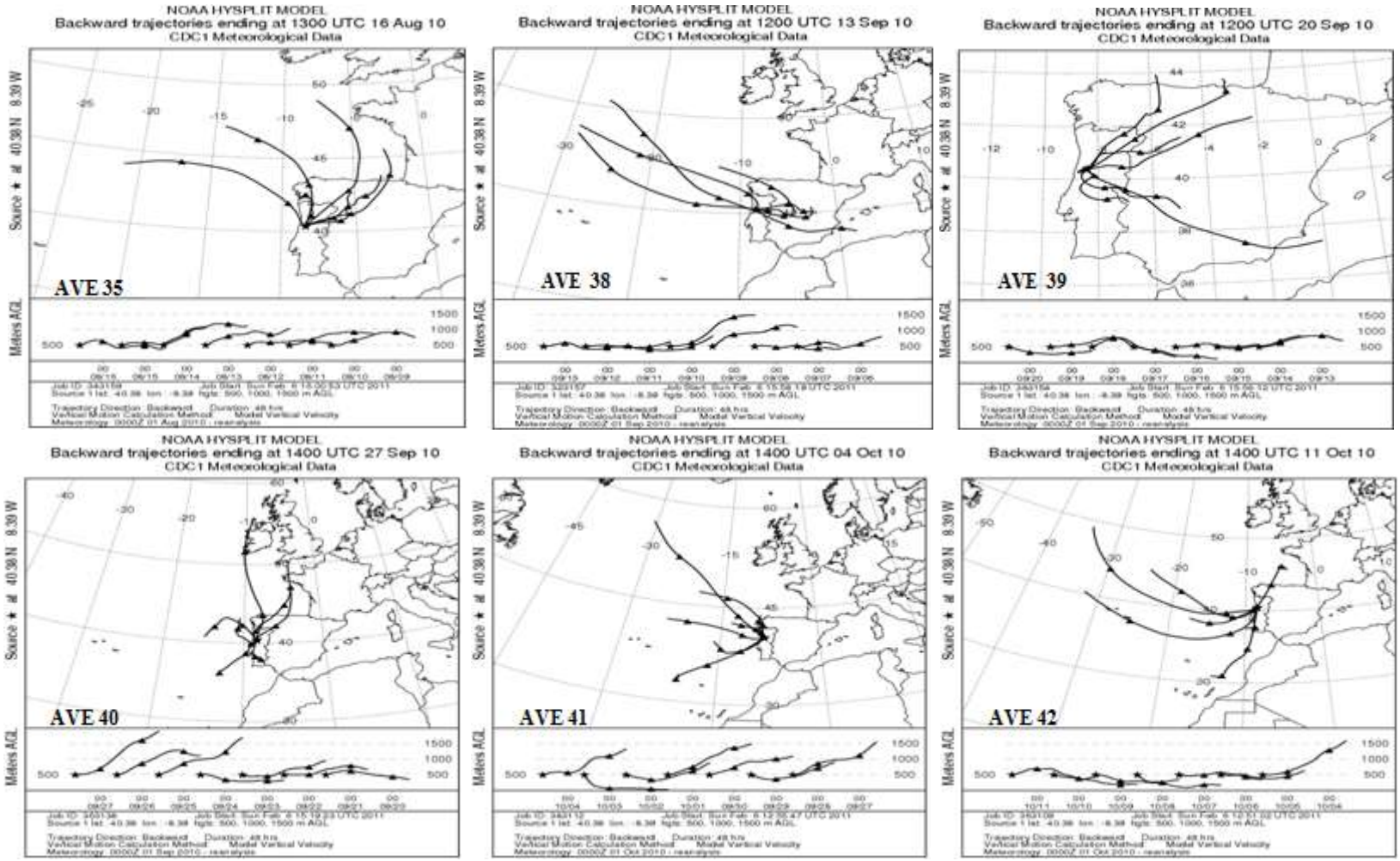

Fig. C. 1. *Continued.*

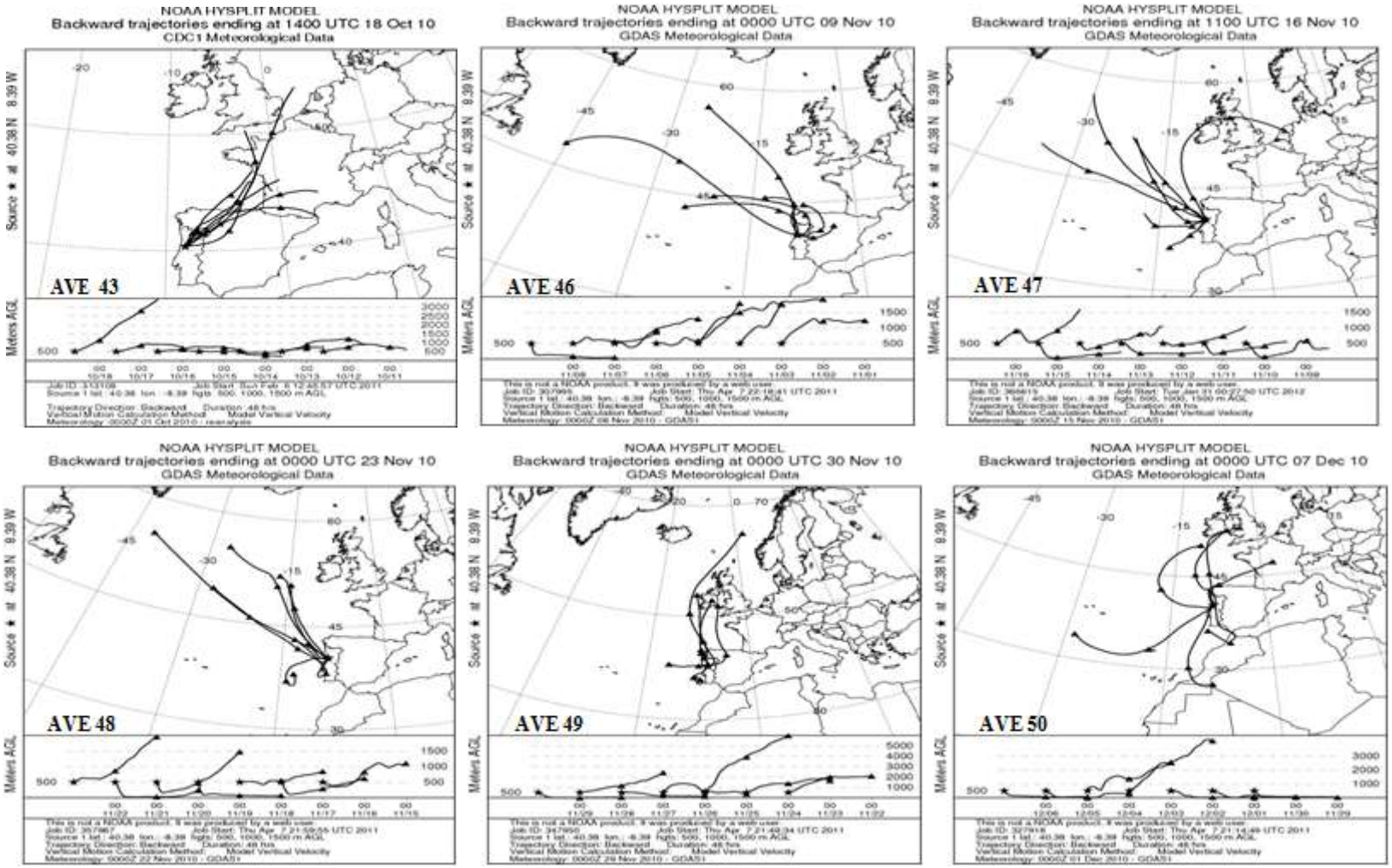

Fig. C. 1. *Continued.*

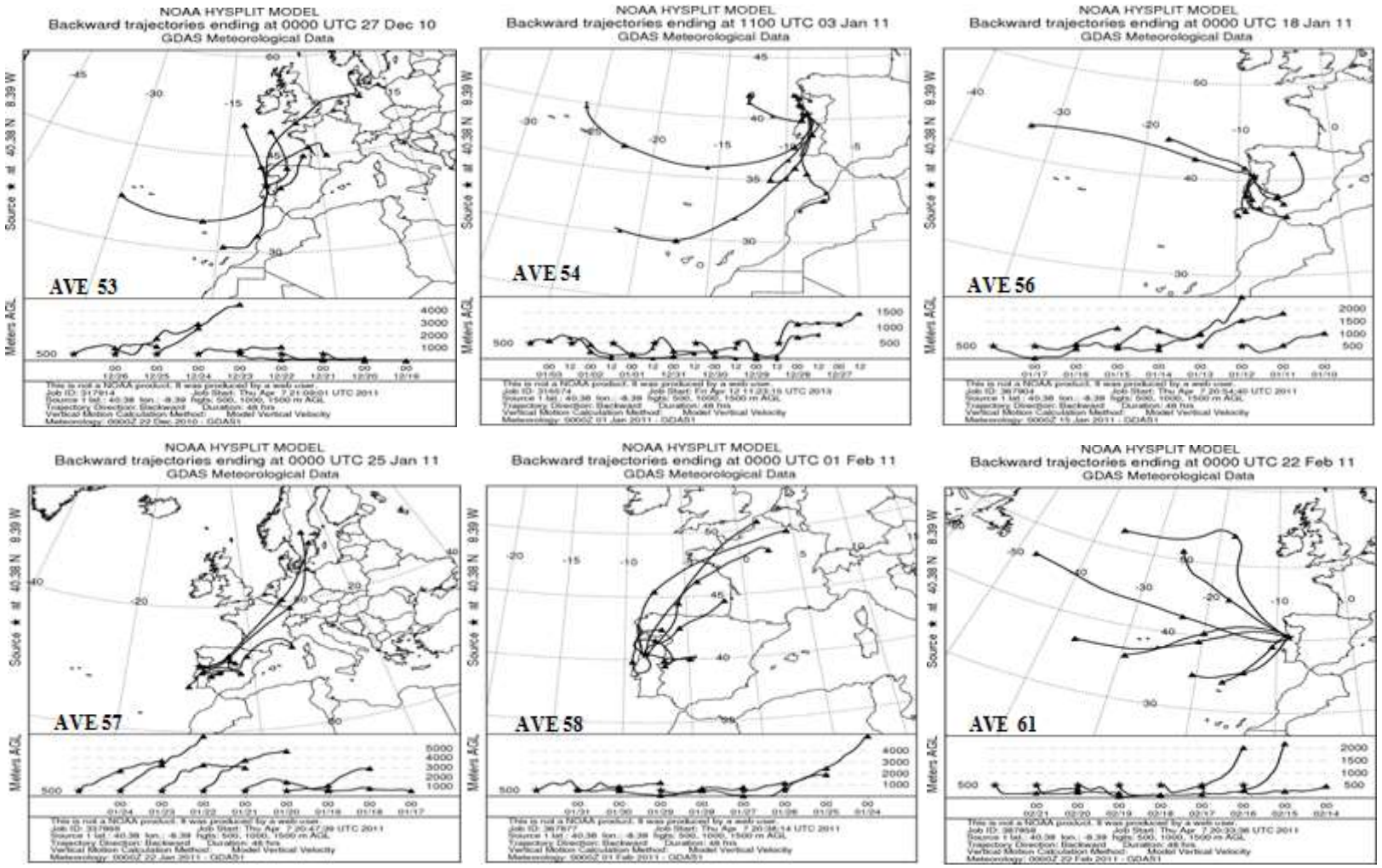

Fig. C. 1. *Continued.*

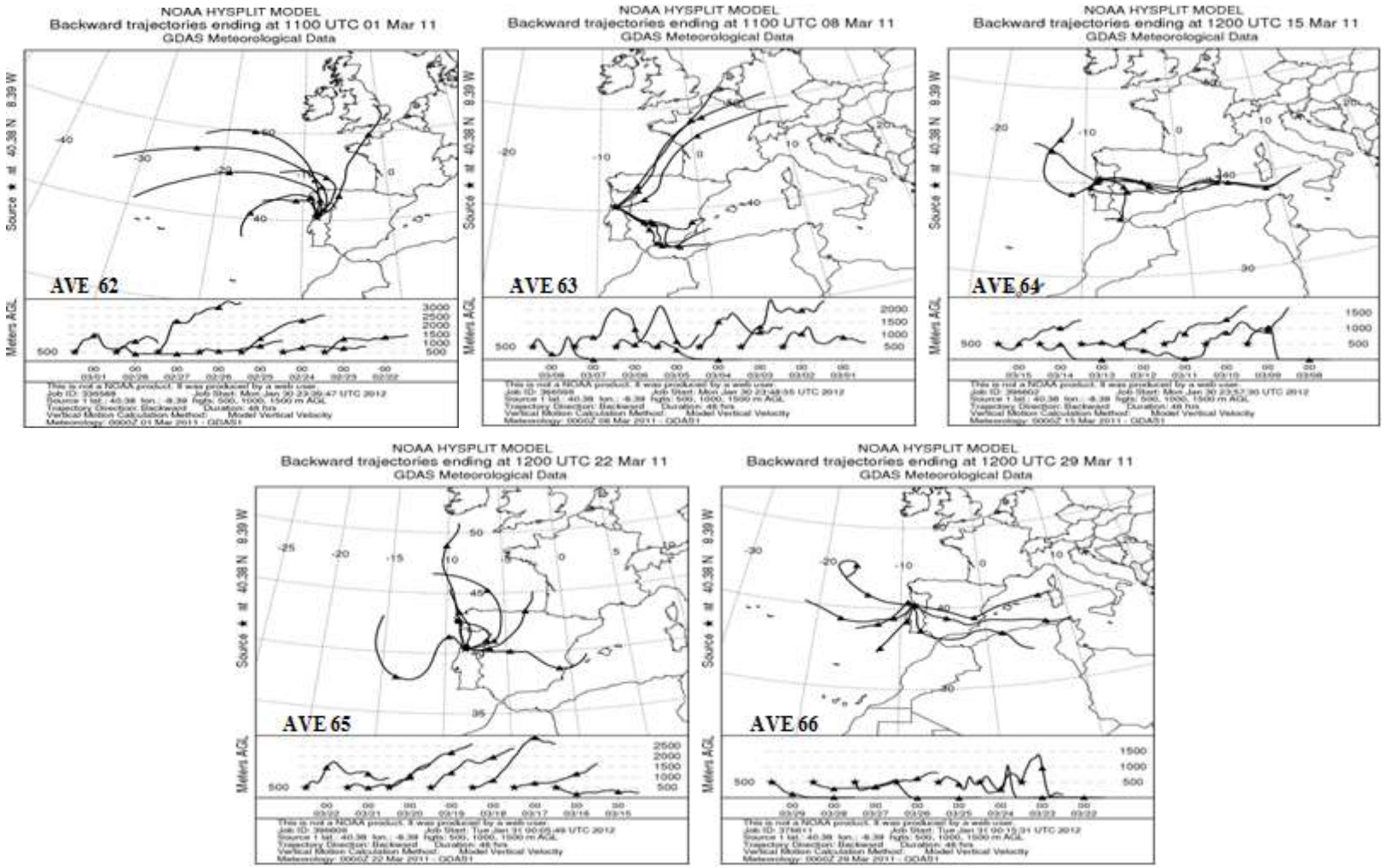

Fig. C. 1. *Continued.*

Annex D

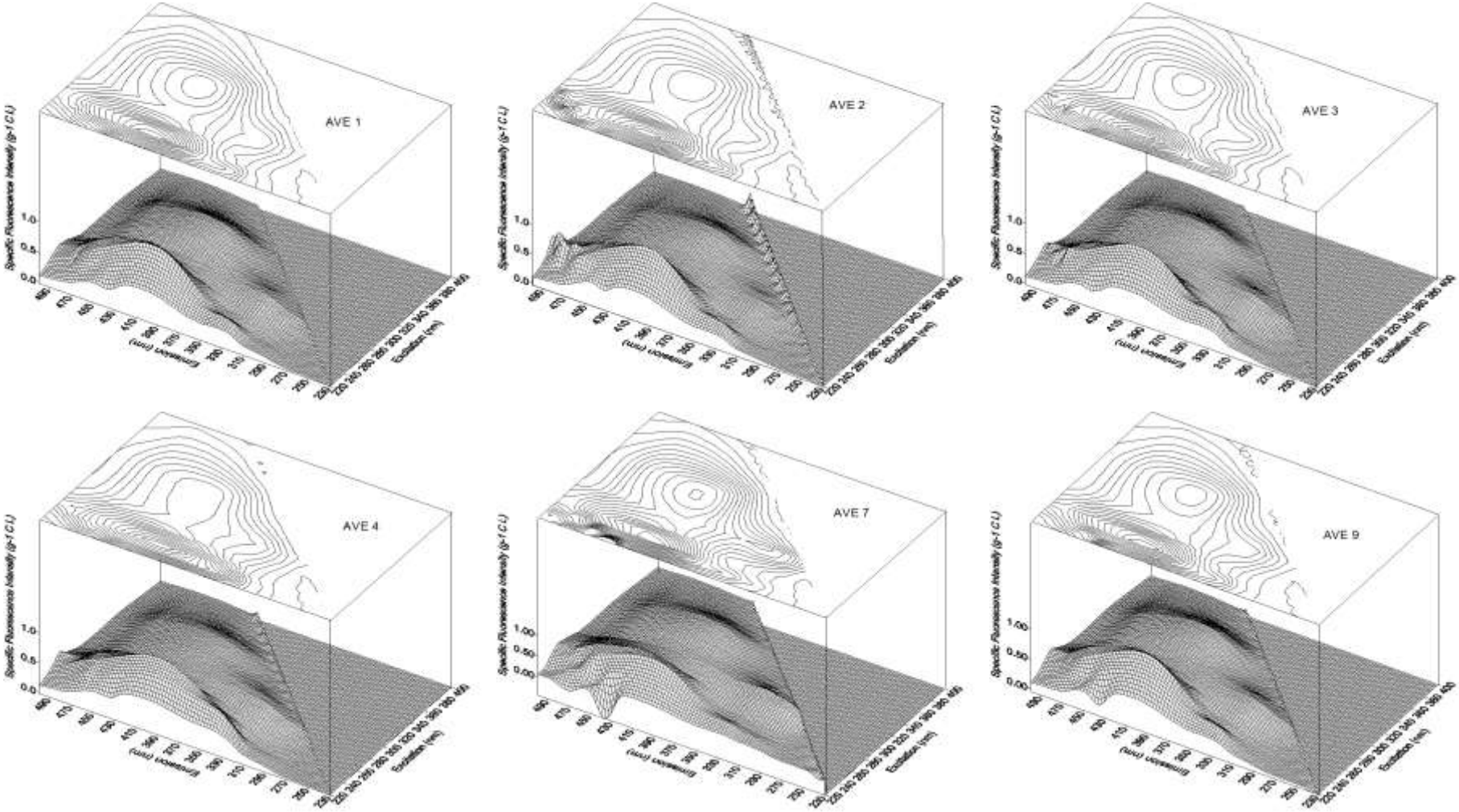

Fig. D. 1. EEM spectra (specific fluorescence intensity (g^{-1} C L) versus excitation and emission wavelengths (nm)) of the WSOC fractions extracted from the aerosol samples collected in each week during Autumn 2009 (AVE 1 – AVE 4), Winter 2010 (AVE 7 – AVE 14), Spring 2010 (AVE 16 – AVE 27), Summer 2010 (AVE 28 – AVE 39), Autumn 2010 (AVE 40 – AVE 50), Winter (AVE 53 – AVE 65), and Spring 2011(AVE 66) seasons.

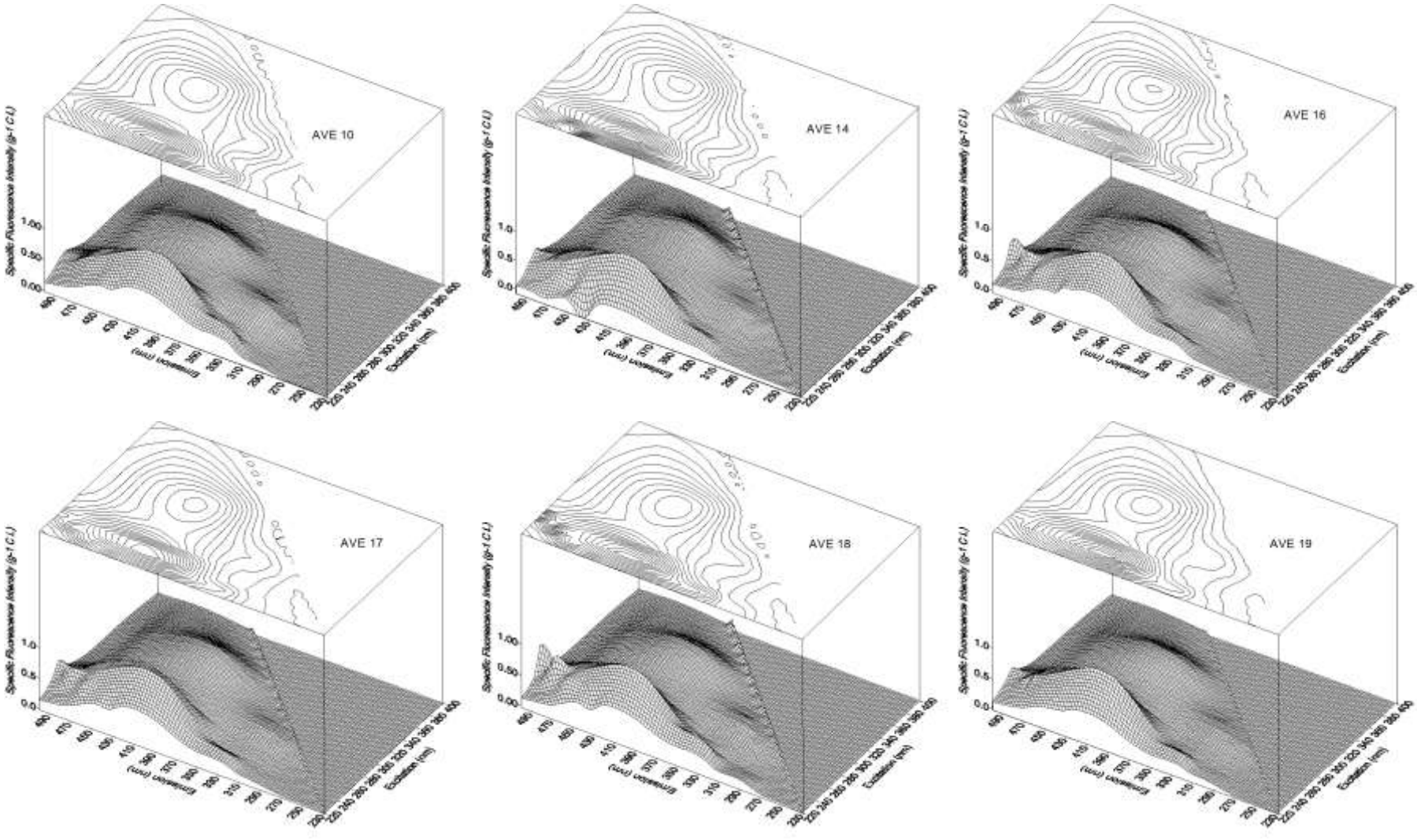

Fig. D. 1. *Continued.*

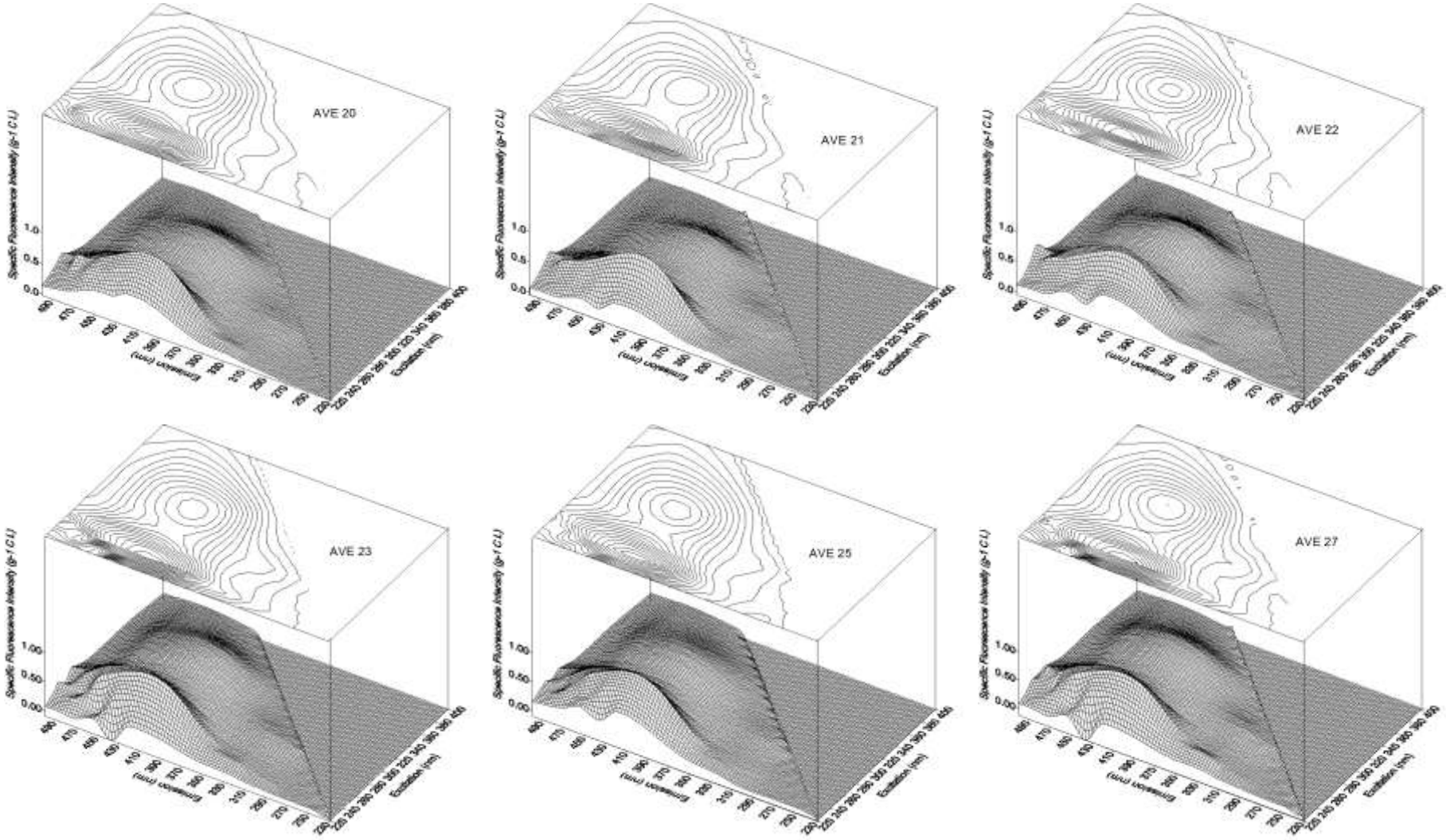

Fig. D. 1. *Continued.*

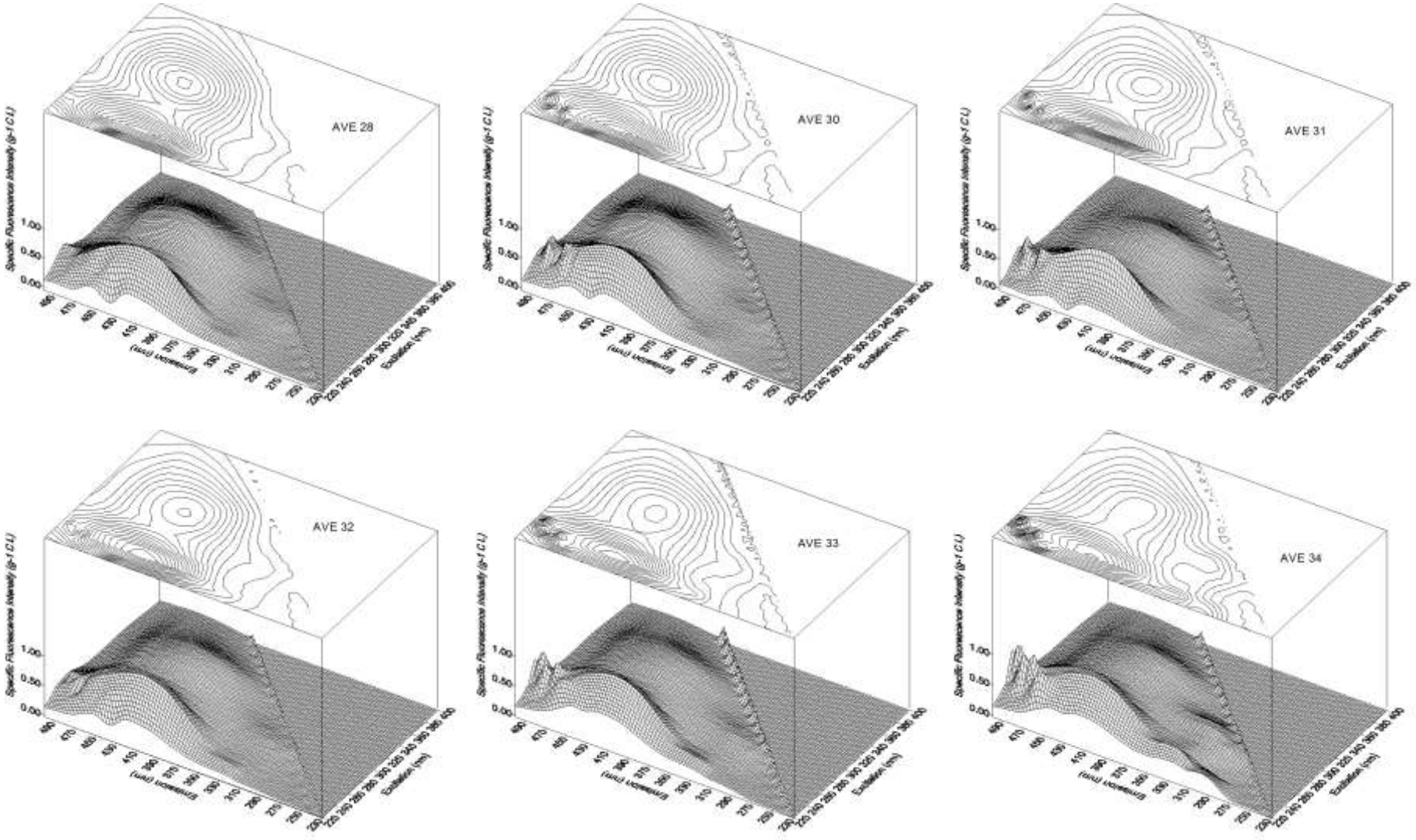

Fig. D. 1. *Continued.*

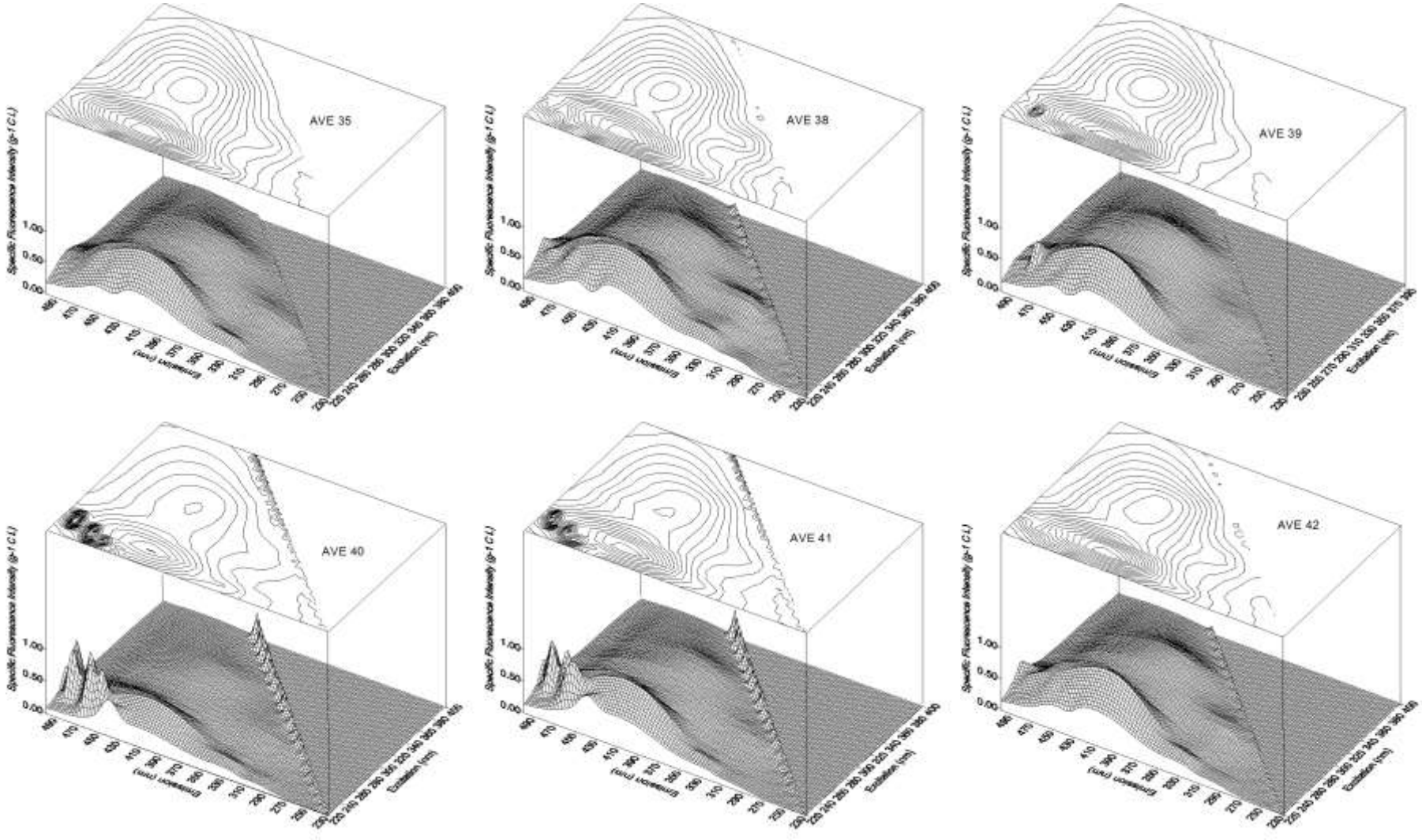

Fig. D. 1. *Continued.*

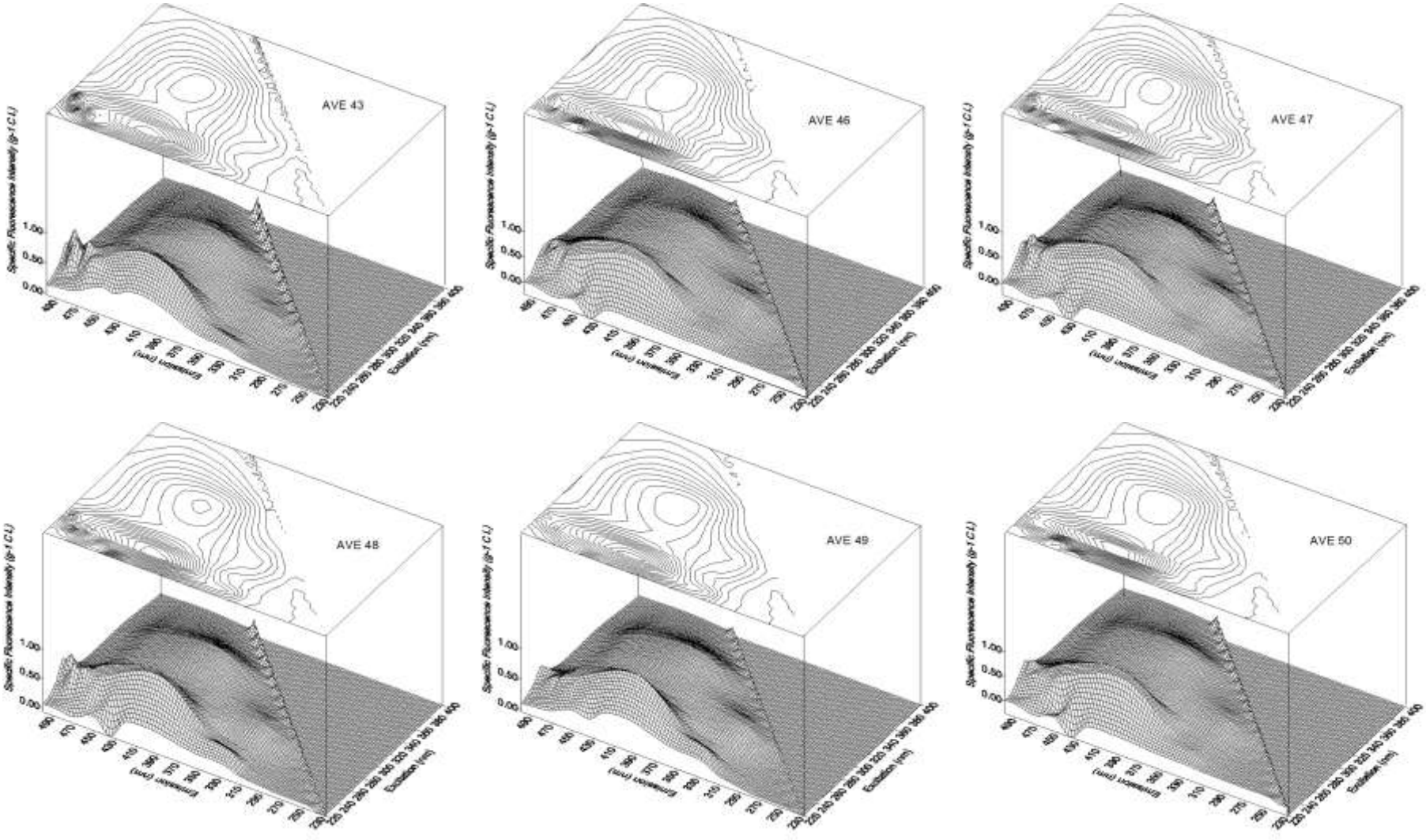

Fig. D. 1. *Continued.*

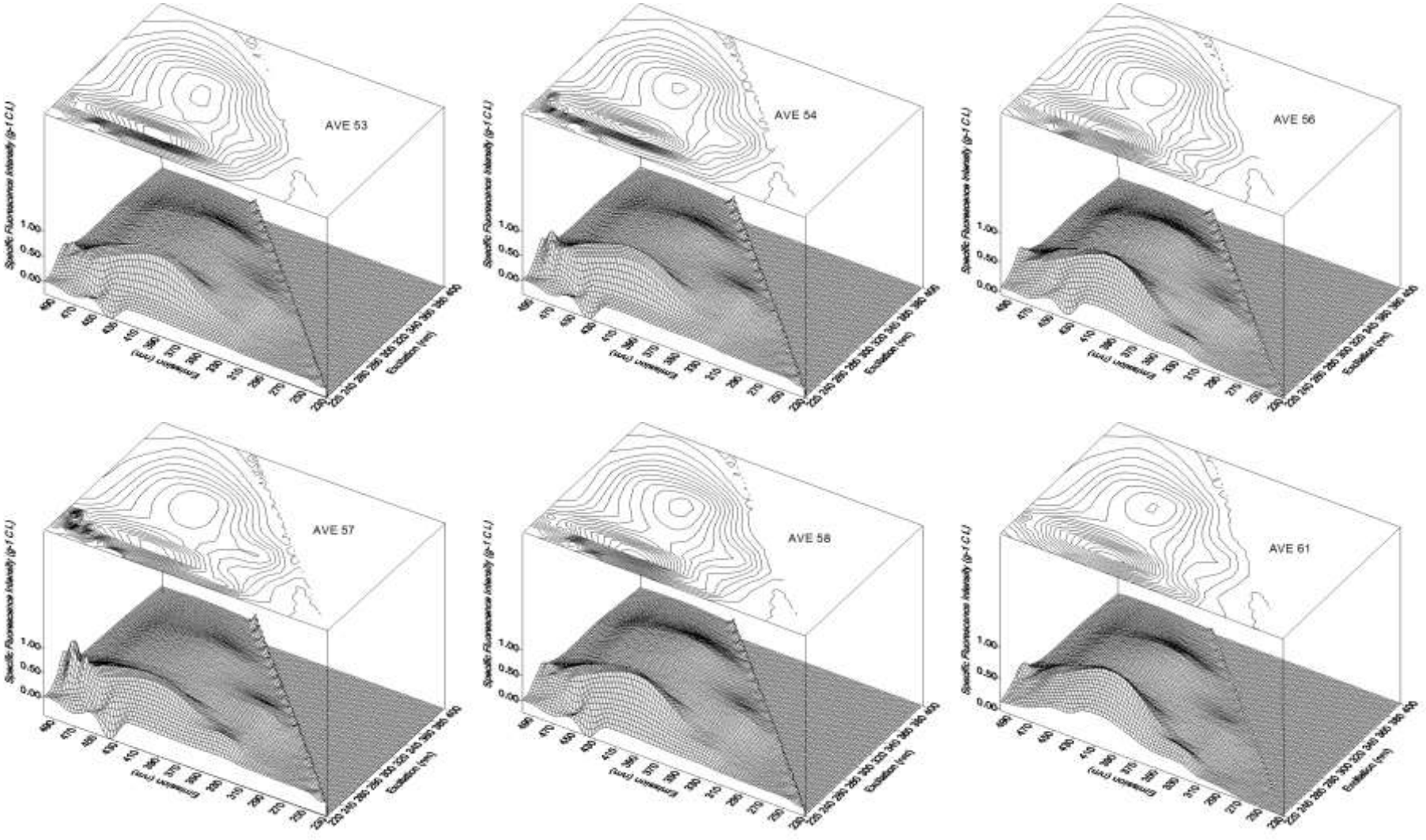

Fig. D. 1. *Continued.*

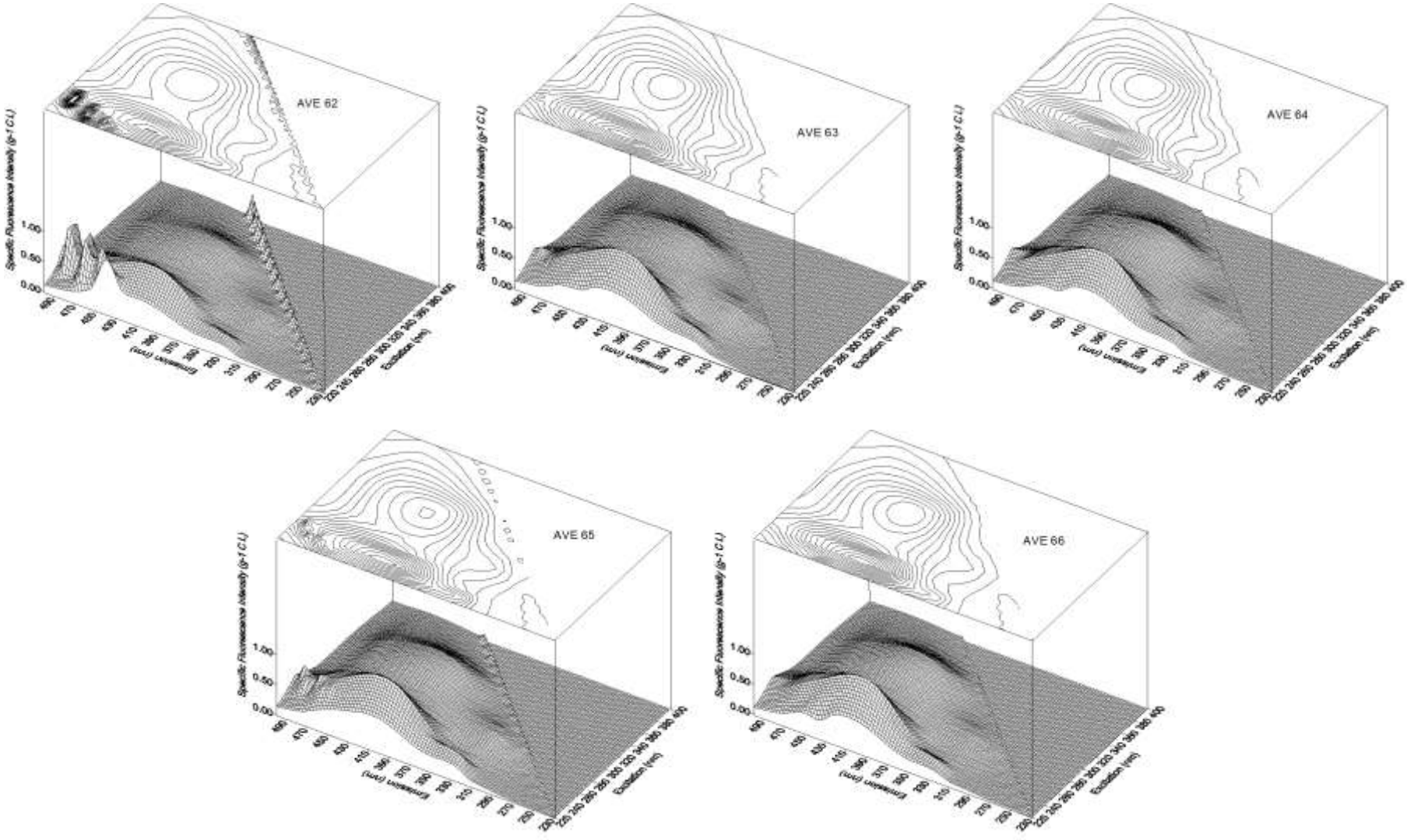

Fig. D. 1. *Continued.*